Johannes Zschocke
Matthias Baumgartner
Eva Morava
Marc Patterson
Shamima Rahman
Verena Peters *Editors*

JIMD Reports

Volume 24

SSIEM

Springer

JIMD Reports
Volume 24

Johannes Zschocke
Editor-in-Chief

Matthias Baumgartner · Eva Morava ·
Marc Patterson · Shamima Rahman
Editors

Verena Peters
Managing Editor

JIMD Reports
Volume 24

Springer

SSIEM

ISSN 2192-8304 ISSN 2192-8312 (electronic)
JIMD Reports
ISBN 978-3-662-48226-1 ISBN 978-3-662-48227-8 (eBook)
DOI 10.1007/978-3-662-48227-8

Springer Heidelberg New York Dordrecht London

Printed on acid-free paper

Springer-Verlag GmbH Berlin Heidelberg is part of Springer Science+Business Media (www.springer.com)

Contents

Part II Case & Research Reports

Part I
Reports on Alkaptonuria

JIMD Reports
DOI 10.1007/8904_2014_380

RESEARCH REPORT

Analysis of HGD Gene Mutations in Patients with Alkaptonuria from the United Kingdom: Identification of Novel Mutations

Jeannette L. Usher • David B. Ascher • Douglas E.V. Pires • Anna M. Milan • Tom L. Blundell • Lakshminarayan R. Ranganath

Received: 09 September 2014 / Revised: 23 October 2014 / Accepted: 03 November 2014 / Published online: 15 February 2015

Abstract Alkaptonuria (AKU) is a rare autosomal recessive disorder with incidence ranging from 1:100,000 to 1:250,000. The disorder is caused by a deficiency of the enzyme homogentisate 1,2-dioxygenase (HGD), which results from defects in the *HGD* gene. This enzyme converts homogentisic acid to maleylacetoacetate and has a major role in the catabolism of phenylalanine and tyrosine. To elucidate the mutation spectrum of the *HGD* gene in patients with alkaptonuria from 42 patients attending the National Alkaptonuria Centre, 14 exons of the *HGD* gene and the intron–exon boundaries were analysed by PCR-based sequencing. A total of 34 sequence variants was observed, confirming the genetic heterogeneity of AKU. Of these mutations, 26 were missense substitutions and four splice site mutations. There were two deletions and one duplication giving rise to frame shifts and one substitution abolishing the translation termination codon (no stop). Nine of the mutations were previously unreported novel variants. Using computational approaches based on the 3D structure, these novel mutations are predicted to affect the activity of the protein complex through destabilisation of the individual protomer structure or through disruption of protomer–protomer interactions.

Communicated by: Viktor Kožich

Competing interests: None declared

Electronic supplementary material: The online version of this chapter (doi:10.1007/8904_2014_380) contains supplementary material, which is available to authorized users.

J.L. Usher (✉) · A.M. Milan · L.R. Ranganath
Department of Clinical Biochemistry and Metabolic Medicine, Royal Liverpool and Broadgreen University Hospital Trust, Duncan Building, Liverpool L7 8XP, UK
e-mail: jeanette.usher@rlbuht.nhs.uk

D.B. Ascher · D.E.V. Pires · T.L. Blundell
Department of Biochemistry, University of Cambridge, Sanger Building, 80 Tennis Court Road, Cambridge CB2 1GA, UK

Introduction

Alkaptonuria (AKU) [OMIM #203500] was the first inborn error of metabolism described by Garrod, in 1902 (Garrod 1908). It is a rare autosomal recessive disorder, which results from mutations in the homogentisate 1,2-dioxygenase (*HGD*) gene. These mutations disrupt HGD [E.C.1.13.11.5] enzyme activity (La Du et al. 1958). The resulting deficiency of HGD activity leads to accumulation of homogentisic acid (HGA), a product of the tyrosine degradation pathway. The incidence of AKU is 1:100,000 to 1:250,000 with higher incidence in Slovakia and the Dominican Republic (1:19,000) (Phornphutkul et al. 2002; Srsen et al. 2002). Oxidation of HGA results in the formation of benzoquinones, which polymerise and bind to cartilage and connective tissue proteins leading to ochronotic pigmentation (Helliwell et al. 2008; Keller et al. 2005; Ranganath et al. 2013; Taylor et al. 2012). This deposition leads to degenerative premature arthritis and cardiac valve deterioration, leading AKU patients to experience considerable pain, incapacity and disability. The same reaction causes the urine of patients to darken upon standing, usually the first visible symptom of the disease (Fernandez-Canon et al. 1996).

The *HGD* gene has been mapped to chromosome 3q21-q23 (Pollak et al. 1993) with potential disruptive mutations identified in AKU patients and their families. The *HGD* genes carrying the AKU-associated mutations were then

expressed and assayed demonstrating the loss of enzyme activity (Fernandez-Canon et al. 1996). The enzymatic defect in HGD is autosomal recessive, due to homozygosity or compound heterozygosity for mutations within the *HGD* gene. While AKU is not very common, a wide variety of causative mutations and polymorphisms have been reported (http://hgddatabase.cvtisr.sk).

The X-ray crystal structure of the wild-type protein revealed that the active enzyme consists of six protomers that form a dimer of trimers. Each protomer contains an N-terminal domain of 280 residues with a central β-sandwich and a C-terminal domain of 140 residues that sits aside a straddle formed by the N-terminal domain. The active site of the enzyme binds iron that is coordinated by the side chains of His335, Glu341 and His371 (Titus et al. 2000). Many non-covalent intra- and intermolecular interactions are essential to maintain the intricate structures of the protomer, trimer and hexamer. The complex structure of HGD, and hence its enzyme activity, can be easily disrupted by mutations.

In 2012, the NHS National Special Services Commissioning Group established the Robert Gregory National Alkaptonuria Centre (NAC) at the Royal Liverpool University Hospital in 2012. To date, 42 patients with confirmed AKU have attended for clinical assessments, with a national register establishing 75 patients in the UK with AKU, thus far. These patients have received trial therapy with nitisinone with subsequent metabolic investigations to monitor the safety and efficacy of the treatment. This study details the genetic analysis undertaken on all 42 patients who have been attending the NAC. Each patient has had genetic screening for small-scale mutations within the 14 exons of the *HGD* gene and in the intron–exon boundaries.

Material and Methods

Subjects

The 42 patients with AKU were diagnosed by clinical evaluation of their symptoms and by measurement primarily of urine homogentisic acid by liquid chromatography tandem mass spectrometry (Hughes et al. 2014). Classically, AKU patients excrete HGA in mmol/L quantities (normal reference range <0.29 mmol/mol creatinine) (Davison et al. 2014). The patient population included 34 non-related probands, three pairs of affected siblings and a father and son who were both affected. There were 24 males and 18 females who ranged from 20 to 74 years of age. The cohort included seven patients of non-Caucasian origin.

Mutation Analysis of the HGD Gene

Genomic DNA was extracted from whole blood using the QIAamp DNA blood mini kit (Qiagen Ltd, Crawley, West Sussex). Sequence variation was studied by amplification of the *HGD* coding regions and intron–exon boundaries by PCR and direct sequencing of the PCR products. Sequence variation was detected by comparison of the sample sequences with the genomic reference sequence of the *HGD* gene (NG_011957). The position of mutations was described with reference to the mRNA sequence (NM_000187.3) with the first base of the Met codon counted as position +1. The Mutalyzer 2.0β-8 https://mutalyzer.nl/name-generator name checker was used to check that the sequence variants were described according to the Human Genome Variation Society (HGVS) nomenclature.

Although the sequencing was performed in order to identify mutations affecting HGD enzyme function, the regions sequenced also covered the sites of some polymorphic variations. Nine single-nucleotide polymorphisms were analysed by sequencing: IVS2+35 (c.87+35A/T), H80Q (c.240T/A), IVS5+25 (c.342+25T/C), IVS6+16 (c.434+16C/T), IVS6+46 (c.434+46C/A), IVS7+24 (c.469+24C/A), IVS9+31 (c.549+31G/A), IVS9+39 (c.549+39T/G) and IVS11+18 (c.879+18A/G) (Supplementary Table 1)

The effects of missense mutations identified in the coding regions were analysed and predicted using the bioinformatics programs PolyPhen2 http://genetics.bwh.harvard.edu/pph2/ and SIFT http://sift.jcvi.org/ (Ramensky et al. 2002; Ng and Henikoff 2003). The PolyPhen server uses the UniProt entry, which is annotated for function, to check the site of the substitution and to identify homologous proteins. The resulting multiple alignment is used to calculate a profile matrix and a PSIC (position-specific independent counts) score. High values of this difference may indicate that the studied substitution is rarely or never observed in the protein family and could be potentially deleterious. The missense variations were also submitted to the SIFT (Sorting Intolerant from Tolerant) program, PROVEAN (Protein Variation Effect Analyzer) http://provean.jcvi.org/seq_submit.php (Choi et al. 2012) and SNAP (screening for non-acceptable polymorphisms) https://rostlab.org/services/snap/submit (Bromberg and Rost 2007). These are able to predict the consequences of the changes to the protein structure and function.

We also used mCSM (Pires et al. 2014a) and DUET (Pires et al. 2014b) in order to predict the effects of the novel missense mutations on a structural basis. These approaches are novel machine-learning algorithms that use the three-dimensional structure in order to predict quantitatively the effects of point mutations on protein stability and

protein–protein and protein–nucleic acid affinities. Two crystal structures of human HGD have been published and were used in this analysis (PDB code 1EY2 and 1EYB) (Titus et al. 2000). The effects of the mutations were assessed in the context of the molecular interactions of the wild-type residue and using mCSM (Pires et al. 2014a) and DUET (Pires et al. 2014b) to predict the effects of the mutations on protomer and hexamer thermal stability and mCSM-PPI (Pires et al. 2014a) to predict the effects of the mutations on the affinity of the protomers to interact with each other.

Computer programs are also available for the analysis of more complex splice site, deletion and no-stop mutations which are all likely to be pathogenic. For splice site mutations, the Berkley Drosophila Genome Project (BDGP) fruit fly splice site predictor http://www.fruitfly.org/seq_tools/splice.html and the Net2Gene splice site predictor were used http://www.cbs.dtu.dk/services/NetGene2/ (Reese et al. 1997; Brunak et al. 1991) in order to predict the location of alternative splice sites. Both programs use artificial neural networks to predict splice sites with high levels of confidence. Most splicing mutations are found to eliminate the GT or AG dinucleotides that define the 5′ and 3′ ends of introns (Kralovicova and Vorechovsky 2007).

Splice site mutations cause either exon skipping of the respective exon or activation of pre-existing splice sites; the CRYP-SKIP utility found at http://www.dbass.org.uk/cryp-skip was developed to distinguish between these two outcomes and uses a multivariate discrimination procedure to predict which is the most likely (Divina et al. 2009).

The protein effect of either cryptic splice site activation or exon skipping can be described by the Mutalyzer 2.0 β-8 program which was primarily designed to assist in checking the nomenclature of variants using the Human Genome Sequence Variation Society (HGVS) standard human sequence variant guidelines and using annotated genomic reference sequences (Wildeman et al. 2008).

Once the position and nature of a sequence change has been established, the sequence change is analysed by a set of tools for the prediction of the variant effect on transcription and RNA processing such as splicing and translation.

Results and Discussion

A total of 34 mutations were identified in the 42 UK patients with AKU, including nine novel and 25 previously reported mutations (Table 1). The mutations from five patients included in this study have been previously reported (Zatkova et al. 2011). There were eleven recurrent mutations that have been identified in the *HGD* mutation database (Zatkova et al. 2011). The *HGD* mutation database currently lists 620 variants, from which almost eighty percent are missense substitutions. The remainder are deletions, duplications, insertions, indels or unknown. In their report of 72 AKU patients and review of previously reported mutations, Vilboux et al. (2009) described 91 variants, 62 missense, 10 frameshift, 13 splice site, 5 nonsense and one no-stop mutation. The results from the UK cohort mirror these findings; 26 of the 34 mutations identified were missense with the remaining eight mutations falling into the other categories. Fifteen of the subjects were homozygous for eleven different variants, six of these were common European variants, two were previously reported variants and three were novel.

In four of the subjects, only one mutation was identified in the *HGD* gene, in these cases there may be mutations in the unsequenced regulatory regions of the gene, or there could be large-scale deletions that have gone undetected by the sequencing method used. There were 26 missense mutations, 24 of these were predicted as damaging by PolyPhen2 and 25 were predicted to affect protein function by SIFT and all 26 were predicted deleterious by PROVEAN. Twenty of the missense mutations were predicted as non-neutral and five as neutral by SNAP. The E13K and D18N mutations were predicted as damaging by PolyPhen2 and damaging by SIFT and PROVEAN but as neutral by SNAP. One mutation (F169L) was predicted "benign" by PolyPhen2 and "tolerated" by SIFT, deleterious by PROVEAN and neutral by SNAP (Table 2). One mutation (M172T) was predicted as benign by PolyPhen2, damaging by SIFT, deleterious by PROVEAN and non-neutral by SNAP.

The disparities between the predictions made by the prediction tools used may reflect the variations in performance between them. The maximum level of accuracy achieved is around 83% (SIFT), and the sensitivity and specificity vary considerably.

The commonly observed European mutation, M368V, was predicted as possibly damaging by PoyPhen2, deleterious by SIFT and PROVEAN and non-neutral by SNAP. The M368 residue is involved in the formation of the active site of the enzyme, and the effect of the M368V mutation is to disrupt interaction at the subunit interfaces (Titus et al. 2000).

The complex structure of the enzyme can be disrupted by mutations in many different ways. Some will affect the assembly of the hexamer, others will affect the stability of the protomer and some will interfere with the active site of the enzyme. Additionally, the majority of patients carry two

Table 1 The *HGD* gene mutations identified in the 42 AKU patients

Patient ID	Variant 1	Protein	Variant 2	Protein	Other remarks
001 sib of 022	c.359G>T	C120F	c.589A>G	R197G	Compound heterozygous
002	c.481G>A	G161R	c.674G>A	R225H	Compound heterozygous
003	c.342+1G>T	L95_S114del	c.470-479del25G>T	V157fs	Compound heterozygous
004	c.343G>C	G115R	c.1282_1292 del GAGCCACTCAA	K431fs	Compound heterozygous
005	c.125A>C	E42A	c.125A>C	E42A	Homozygous
006	Unknown	Unknown	c.899T>G	V300G	Unknown
007	c.688C>T	P230S	c.688C>T	P230S	Homozygous
008	c.359G>T	C120F	c.359G>T	E42A	Compound heterozygous
009 sib of 013	c.125A>C	E42A	c.1102A>G	M368V	Compound heterozygous
010	c.125A>C	E42A	c.125A>C	E42A	Homozygous
011	c.481G>A	G161R	c.481G>A	G161R	Homozygous
012	c.808G>A	G270R	c.1120G>C	D374H	Compound heterozygous
013 sib of 009	c.125A>C	E42A	c.1102A>G	M368V	Compound heterozygous
014	Unknown	Unknown	c.367G>A	G123R	Unknown
015	c.16-1G>A	ivs1-1G>A	c.1102A>G	M368V	Compound heterozygous
016	c.828G>C	K276N	c.1081G>A	G361R	Compound heterozygous
017	c.828G>C	K276N	c.828G>C	K276N	Homozygous
018	c.469+2T>C	ivs7+2T>C	c.507T>G	F169L	Compound heterozygous
019	c.359G>T	C120F	c.1079G>C	G360R	Compound heterozygous
020	c.158G>A	R53Q	c.515T>C	M172T	Compound heterozygous
021	c.656A>G	N219S	c.656A>G	N219S	Homozygous
022 sib of 001	c.359G>T	C120F	c.589A>G	R197G	Compound heterozygous
023	c.367G>A	G123R	c.1075C>T	P359L	Compound heterozygous
024	c.175delA	S59fs	c.175delA	S59fs	Homozygous
025 sib of 034	c.158G>A	R53Q	c.158G>A	R53Q	Homozygous
026	c.175delA	S59fs	c.175delA	S59fs	Homozygous
027	c.175delA	S59fs	c.899T>G	V300G	Compound heterozygous
028	c.688C>T	P230S	c.899T>G	V300G	Compound heterozygous
029 father of 036	c.674G>C	R225P	c.674G>C	R225P	Homozygous
030	c.52G>A	D18N	c.175delA	S59fs	Compound heterozygous
031	c.359G>T	C120F	c.359G>T	C120F	Homozygous
032	Unknown	Unknown	c.664_674dupGCCAATCCTCG	D226PfsX7	Unknown
033	c.37G>A	E13K	c.733G>T	V245F	Compound heterozygous
034 sib of 025	c.158G>A	R53Q	c.158G>A	R53Q	Homozygous
035	c.125A>C	E42A	c.481G>A	G161R	Compound heterozygous
036 son of 029	c.674G>C	R225P	c.674G>C	R225P	Homozygous
037	c.343G>C	G115R	c.1102A>G	M368V	Compound heterozygous
038	Unknown	Unknown	c.125A>C	E42A	Unknown
039	c.1009A>G	N337D	c.1009A>G	N337D	Homozygous
040	c.125A>C	E42A	c.899T>G	V300G	Compound heterozygous
041	c.347T>C	L116P	c.674G>C	R225P	Compound heterozygous
042	c.513G>T	K171N	c.513G>T	K171N	Homozygous

different mutations, and the combined effects of these on enzyme structure and function are difficult to predict. The protomer interfaces are non-isologous, and heterozygous hexamers appear likely to be as or more disruptive than the homozygous complex. The novel mutations are spread throughout the structure of HGD: with four buried within the protomer structure (D18N, M172T, V245F, G361R) and four located at the interface between two protomers (E13K,

Table 2 The effects of the missense mutations in the NAC patients as predicted by PolyPhen2, SIFT, PROVEAN and SNAP

Protein effect	Nucleotide change NM_000187.3	PolyPhen2 prediction	SIFT score/prediction	PROVEAN score/ prediction	SNAP
E13K	c.37G>A	0.842 possibly damaging	0.01 affect protein function	−2.959 deleterious	Neutral
D18N	c.52G>A	1.00 probably damaging	0.01 affect protein function	−2.758 deleterious	Neutral
E42A	c.125 A>C	1.00 probably damaging	0.0 affect protein function	−5.639 deleterious	Non-neutral
R53Q	c.158G>A	1.00 probably damaging	0.0 affect protein function	−3.724 deleterious	Non-neutral
H80Q	c.240T>A	0.01 benign	0.65 tolerated	1.231 neutral	Neutral
G115R	c.343G>C	0.998 probably damaging	0.0 affect protein function	−7.013 deleterious	Non-neutral
C120F	c.359G>T	0.984 probably damaging	0.0 affect protein function	−8.373 deleterious	Non-neutral
G123R	c.367G>A	1.00 probably damaging	0.0 affect protein function	−7.547 deleterious	Non-neutral
G161R	c.481G>A	1.00 probably damaging	0.0 affect protein function	−7.957 deleterious	Non-neutral
F169L	c.507T>G	0.097 benign	0.80 tolerated	−4.260 deleterious	Neutral
K171N	c.513G>T	0.744 possibly damaging	0.01 affect protein function	−3.283 deleterious	Neutral
M172T	c.515T>C	0.446 benign	0.0 affect protein function	−4.492 deleterious	Non-neutral
R197G	c.589A>G	1.00 probably damaging	0.0 affect protein function	−6.496 deleterious	Non-neutral
N219S	c.656A>G	0.992 probably damaging	0.0 affect protein function	−4.973 deleterious	Non-neutral
R225H	c.674G>A	0.983 probably damaging	0.0 affect protein function	−4.573 deleterious	Non-neutral
R225P	c.674G>C	0.993 probably damaging	0.004 affect protein function	−6.229 deleterious	Non-neutral
P230S	c.688C>T	1.00 probably damaging	0.0 affect protein function	−7.957 deleterious	Non-neutral
V245F	c.733G>T	0.900 possibly damaging	0.004 affect protein function	−3.741 deleterious	Neutral
G270R	c.808G>A	1.00 probably damaging	0.0 affect protein function	−7.957 deleterious	Non-neutral
K276N	c.828G>C	1.00 probably damaging	0.0 affect protein function	−4.973 deleterious	Non-neutral
V300G	c.899T>G	0.999 probably damaging	0.0 affect protein function	−6.879 deleterious	Non-neutral
N337D	C.1009A>G	1.00 probably damaging	0.0 affect protein function	−4.891 deleterious	Non-neutral
P359L	c.1075C>T	0.999 probably damaging	0.0 affect protein function	−9.037 deleterious	Non-neutral
G360R	c.1078G>C	1.00 probably damaging	0.0 affect protein function	−7.572 deleterious	Non-neutral
G361R	c.1081G>A	0.995 probably damaging	0.0 affect protein function	−7.338 deleterious	Non-neutral
M368V	c.1102 A>G	0.596 possibly damaging	0.0 affect protein function	−3.652 deleterious	Non-neutral
D374H	c.1120G>C	0.994 probably damaging	0.0 affect protein function	−6.861 deleterious	Non-neutral

DNA variant numbering is based on cDNA (NM_000187.3), +1 corresponding to the A of the AGT
Protein effect numbering is based on NP_000178.2. The Uniprot ID Q93099 was used for submission of queries to PolyPhen
PolyPhen PSIC profile scores are based on sequence annotation and then multiple alignment to compute the absolute values of the difference between profile scores of both allelic variants in the position of the substitution and then map it to the known 3D protein structure. Based on this data, it predicts one of the four outcomes, PSIC <0.5 benign, >1–1.5 either possibly damaging or probably damaging dependent on the substitutions structural properties and >2.0 probably damaging. Larger PSIC values indicate that the substitution is rarely or never observed in the protein family

R53Q, R225P, N337D). The effects of mutations on the HGD structure were quantitatively analysed from two perspectives: changes on affinity between protomer interfaces and the effects on protomer stability. To assess the effects of the mutations on the affinity between subunits, we used mCSM-PPI (Pires et al. 2014a), a machine-learning method that uses graph-based signatures to predict the effects of the mutations on protein–protein affinity. To evaluate the effects of the mutations on the stability of the monomeric units, we used DUET (Pires et al. 2014b), an approach that combines the graph-based signatures of mCSM (Pires et al. 2014a) with the statistical potential energy function of SDM (Worth et al. 2011) to estimate the change in Gibbs free energy of folding caused by the mutation. The structural analysis of the novel mutations revealed that they affect either protomer stability and/or hexamer formation (Fig. 1 and Table 3). The majority of the variants were predicted by mCSM-PPI to reduce the affinity of protomers to interact, destabilising the hexameric structure.

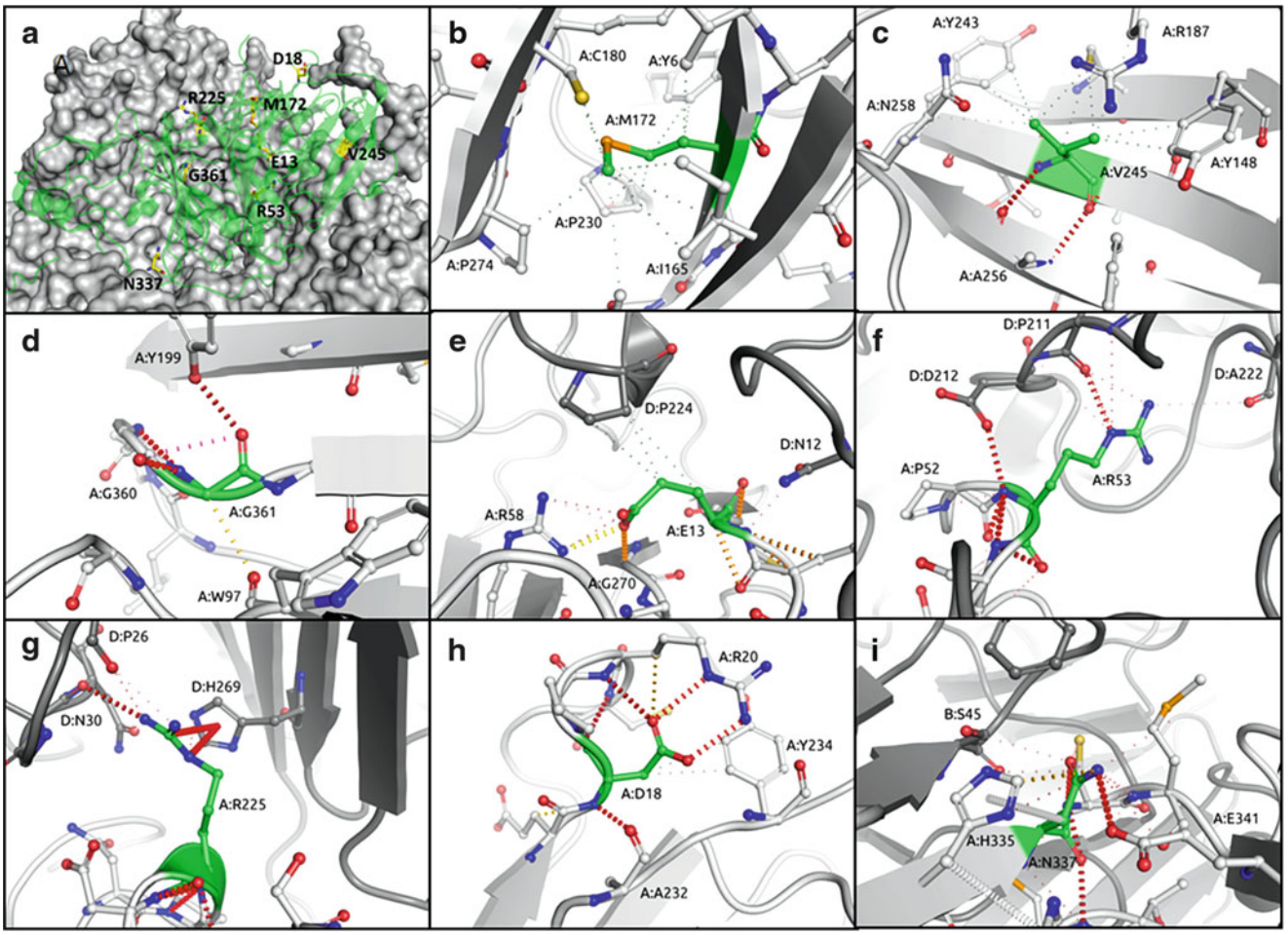

Fig. 1 Analysis of wild-type interactions made by the novel AKU mutations. The novel mutations (*yellow*) are located throughout the protomer structure (*green*), with the other protomers shown as a grey surface (**a**). Mutation of M172 (**b**), V245 (**c**) and G361 (**d**) is expected to decrease the stability of the protomer through disruption of the intramolecular hydrophobic (*grey dashes*) and hydrogen bonds (*red dashes*). Mutation of E13 (**e**), R53 (**f**) or R225 (**g**) is expected to disrupt intermolecular interactions and decrease the stability of the hexamer. Mutation of D18 (**h**) or N337 (**i**) is predicted by mCSM to destabilise the structure of both the protomer and hexamer. The sites of the novel mutations are shown in green, while partner protomer chains are shown in *dark grey*

Mutations that affect the production of active HGD enzyme through destabilisation of the protomer structure typically perturb the local secondary structure through the introduction of energetically unfavourable mutations, disrupting the wild-type interactions. For example, M172 and V245 both make strong intramolecular hydrophobic interactions. While M172T results in the loss of these interactions, V245F disrupts the local secondary structure by introducing a steric clash. G361 is a buried residue that adopts a positive phi angle, which would usually be energetically unfavourable for non-glycine amino acids. Furthermore, mutation to arginine would introduce a steric clash, destabilising the protomer.

Mutations that disrupt the network of intermolecular interactions typically lower the stability of the 3–2 symmetrical homohexameric structure. Disruption of the intricate hexameric structure of HGD is also expected to affect enzyme activity. E13 is located along a protomer interaction interface, making intra- and intermolecular interactions. Mutation to lysine reverses the local charge and is predicted to destabilise the hexamer. R53 makes intra- and intermolecular polar interactions and side-chain to main-chain hydrogen bonds. Mutation to glutamine results in the loss of the intermolecular interactions, consistent with the prediction that it would destabilise the hexamer. R225 is also located on an interface between protomers, where it makes polar hydrogen bonds and nitrogen-pi and carbon-pi intermolecular interactions. In addition to altering the backbone geometries, mutation to proline will reduce the affinity of this interaction and is predicted to destabilise the hexamer.

A few mutations were predicted by mCSM-PPI and DUET to be highly disruptive to both the protomer (predicted to reduce the free energy of folding by a factor

Table 3 The analysis of the novel UK *HGD* gene mutations

Patient ID	DNA	Protein	PolyPhen2	SIFT	PROVEAN	DUET (ΔΔG Kcal/mol)	mCSM-PPI (ΔΔG Kcal/mol)	Proposed effect
033	c.37G>A	E13K	0.842 possibly damaging	0.01 affect protein function	−2.959 deleterious	0.7	−1.562	Decreased protomer–protomer affinity
030	c.52G>A	D18N	1.00 probably damaging	0.01 affect protein function	−2.758 deleterious	−1.55	−1.004	Decreased protomer stability and protomer–protomer affinity
034	c.158G>A	R53Q	1.00 probably damaging	0.0 affect protein function	−3.724 deleterious	0.245	−3.348	Decreased protomer–protomer affinity
020	c.515T>C	M172T	0.446 benign	0.0 affect protein function	−4.492 deleterious	−2.569	−0.309	Decreased protomer stability
036	c.674G>C	R225P	0.993 probably damaging	0.004 affect protein function	−6.229 deleterious	0.289	−2.216	Decreased protomer–protomer affinity
032	c.664_674dup GCCAATCCTGC	D226PfsX7	–	–	–			
033	c.733G>T	V245F	0.900 possibly damaging	0.004 affect protein function	−3.741 deleterious	−1.797	−0.431	Decreased protomer stability
039	c.1009A>G	N337D	1.00 probably damaging	0.0 affect protein function	−4.891 deleterious	−1.205	−1.772	Decreased protomer stability and protomer–protomer affinity
016	c.1081G>A	G361R	0.995 probably damaging	0.0 affect protein function	−7.338 deleterious	−0.448	−2.173	Decreased protomer stability

greater than 1.2 kcal/mol) and hexamer structures (predicted to reduce the free energy of association by a factor greater than 1 kcal/mol), highlighting the essential nature of the wild-type residues. D18 is a buried residue located near the interaction interface for a loop from a companion protomer that fits into a deep groove. D18 makes a network of strong intramolecular hydrogen bonds. Mutation to asparagine disrupts these interactions and is predicted to destabilise the protomer and disrupt hexamer formation. N337 forms intermolecular polar and carbon-pi interactions at the interface between two protomers. Mutation to aspartic acid will introduce a repulsive intramolecular force which is predicted to destabilise both the protomer and hexamer.

The splice site mutations can give rise either to exon skipping or to the activation of alternative splice sites; frameshift mutations either cause truncation or extension of the protein (Table 4).

The effects of the splice site and frameshift mutations were expected to cause large-scale alterations to the protein structure. It is likely that these changes would either result in nonsense-mediated decay and in a null allele or introduce unfavourable steric contacts and disrupt the assembly of the subunits which is critical to the formation of the active site of the enzyme.

Conclusion

The *HGD* gene analysis of the NAC patients found mutations in 12 of the 14 exons; none were observed in exon 1 or 4. The mutations were not evenly distributed; the largest numbers of variants were found in exons 3, 6, 8, 10 and 13 (Supplementary Table 2). Exon 13 carries the residues that bind HGA in the active site, and there were ten mutated alleles identified in this exon in the UK cohort.

The mutations most commonly found in this study were E42A, R53Q, S59fs, C120F, R225P, V300G and M368V. Five of these can be found in the *HGD* mutation database; the notable exceptions were R53Q and R225P which were both novel mutations. R53Q was found in three patients, two of these were siblings and they were homozygotes. The R225P mutation was seen in two patients who were siblings, and these were also homozygotes.

Nine single-nucleotide polymorphisms in the *HGD* gene were identified including the H80Q polymorphism in exon 4. The identification of the novel mutations and studying the distribution of AKU mutations in the United Kingdom demonstrate the genetic heterogeneity of this rare disease. The analysis of AKU mutations using mCSM and DUET provides further insight into their effects on the structure and function of the defective enzyme and provides a useful source of data for making genotype–phenotype correlations.

Table 4 A summary of the analysis of the splice site, frameshift and no-stop mutations

HGD exon	Short name	Nucleotide change	Protein change	CrypSkip prediction	BDGP splice sites prediction	Net2Gene splice sites prediction	Mutalyzer protein effect prediction	Effect
01i	IVS1-1G>A	c.16-1G>A	p.(Tyr6_Gln29del)	0.16 exon skipping strongly favoured	1 alternative acceptor site	No acceptable acceptor sites above threshold		
3	S59fs	c.175delA	p.Ser59Alafsx52	–	–	–	Severely truncated protein 52 novel amino acids	Frameshift
5	IVS5+1G>T	c.342+1G>T	Uncertain (p.Leu95_Ser114del) *	0.42 cryptic splice site activation	2 alternative donor sites	2 alternative donor sites	No change in protein (if exon is skipped deletion of 20 amino acids)	Aberrant splicing
7	IVS7+2T>C	c.469+2T>C	p.Arg154SerfsX22	0.01 exon skipping strongly favoured	No alternative donor splice sites	No alternative donor splice sites	No change in protein	Exon skipping aberrant splicing
8	IVS8-1G>T (V157fs)	c.470-1_494del25	p.Val157Glufsx11 or if exon skipped p.Pro 158Thr fsx25	0.12 exon skipping strongly favoured	Acceptor splice site is abolished by the deletion	One alternative acceptor site	If skipped, a severely truncated protein with novel 10 residues + stop or a truncated protein with novel 24 residues + stop	Exon skip and frameshift
10	D226PfsX7	c.664_674dup GCCAATCCTCG	p.(Asp226Profs*7)	–	–	–	Severely truncated protein 7 novel amino acids	Frameshift
14	K431fs	c.1282-1292del11	p.Lys431Hisfsx52	–	–	–	Truncated protein with novel 10 residues + stop	Deletion causing frameshift
14	X446ext	c.1336G>C	p.X446ArgxtX24	–	–	–	Extended protein with additional 24 residues + stop	Extension

DNA variant numbering is based on cDNA (NM_000187.3), +1 corresponding to the A of the ATG. Protein effect numbering is based on NP_000178.2

Acknowledgements DBA is supported by a CJ Martin Fellowship from the National Health and Medical Research Council (NHMRC; GNT1072476). DEVP is funded by the Brazilian agency Conselho Nacional de Desenvolvimento Científico e Tecnológico (CNPq). TLB receives funding from the University of Cambridge and the Wellcome Trust.

Compliance with Ethics Guidelines

Jeannette Usher declares that she has no conflict of interest.

Anna Milan declares that she has no conflict of interest.

Lakshminarayan Ranganath declares that he has no conflict of interest.

David Ascher declares that he has no conflict of interest.

Douglas Pires declares that he has no conflict of interest.

Tom Blundell declares that he has no conflict of interest.

Informed Consent

All procedures followed were in accordance with the ethical standards of the responsible committee on human experimentation (institutional and national) and with the Helsinki Declaration of 1975, as revised in 2000 (5). Informed consent was obtained from all patients for being included in the study.

This article does not contain studies with animal subjects performed by any of the authors.

Details of the Contributions of Individual Authors

JU performed the sequence analysis of the *HGD* gene mutations, the analysis of the mutations with the freely available bioinformatics programs and the initial writing of the manuscript.

DA and DP performed the computation modelling by MCSM and DUET and the interpretation of the results.

AMM and LRR assisted with data interpretation and writing of the manuscript.

TB reviewed the result interpretation.

All authors contributed to reviewing of the manuscript.

References

Bromberg Y, Rost B (2007) SNAP: predict effect of non-synonymous polymorphisms on function. Nucleic Acids Res 35 (11):3823–3835

Brunak S, Engelbrecht J, Knudsen S (1991) Prediction of human mRNA donor and acceptor sites from the DNA sequence. J Mol Biol 220(1):49–65

Choi Y, Sims GE, Murphy S, Miller JR, Chan AP (2012) Predicting the functional effects of amino acid substitutions and indels. PLoS One 7(10):e46688

Davison AS, Milan AM, Hughes AT, Dutton JJ, Ranganath LR (2014) Serum concentrations and urinary excretion of homogentisic acid and tyrosine in normal subjects. Clin Chem Lab Med. doi:10.1515/cclm-2014-0668

Divina P, Kvitkovicova A, Buratti E, Vorechovsky I (2009) Ab initio prediction of mutation-induced cryptic splice-site activation and exon skipping. Eur J Hum Genet 17:759–765

Fernandez-Canon JM, Granadino B, Beltran-Valero de Bernabe D et al (1996) The molecular basis of alkaptonuria. Nat Genet 14:19–24

Garrod AE (1908) The Croonian lectures on inborn errors of metabolism. Lecture II. Alkaptonuria. Lancet 2:73–79

Helliwell TR, Gallagher JA, Ranganath L (2008) Alkaptonuria - a review of surgical and autopsy pathology. Histopathology 53 (5):503–512

Hughes AT, Milan AM, Christensen P et al (2014) Urine homogentisic acid and tyrosine: simultaneous analysis by liquid chromatography tandem mass spectrometry. J Chromatogr B 963:106–112

Keller JM, Macaulay W, Ohannes A et al (2005) New developments in ochronosis: review of the literature. Rheumatol Int 25(2):81–85

Kralovicova J, Vorechovsky I (2007) Global control of aberrant splice-site activation by auxiliary splicing sequences: evidence for a gradient in exon and intron definition. Nucleic Acids Res 5 (19):6399–6413

La Du BN, Zannoni VG, Laster L et al (1958) The nature of the defect in tyrosine metabolism in alkaptonuria. J Biol Chem 230:251–260

Ng PC, Henikoff S (2003) SIFT: predicting amino acid changes that affect protein function. Nucleic Acids Res 31(13):3812–3814

Phornphutkul C, Introne WJ, Perry MB et al (2002) Natural history of alkaptonuria. N Engl J Med 347:2111–2121

Pires DE, Ascher DB, Blundell TL (2014a) mCSM: predicting the effects of mutations in proteins using graph-based signatures. Bioinformatics 30:335–342

Pires DE, Ascher DB, Blundell TL (2014b) DUET: a server for predicting effects of mutations on protein stability using an integrated computational approach. Nucleic Acids Res 42(W1):W314–W319

Pollak MR, Chou YH, Cerda JJ et al (1993) Homozygosity mapping of the gene for alkaptonuria to chromosome 3q2. Nat Genet 5:201–204

Ramensky V, Bork P, Sunyaev S (2002) Human non-synonymous SNPs: server and survey. Nucleic Acids Res 30(17):3894–3900

Ranganath LR, Jarvis JC, Gallagher JA (2013) Recent advances in management of alkaptonuria. J Clin Pathol 66:367–373

Reese MG, Eeckman FH, Kulp D, Haussler D (1997) Improved splice site detection in genie. J Comp Biol 4(3):311–323

Srsen S, Muller CR, Fregin A et al (2002) Alkaptonuria in Slovakia: thirty-two years of research on phenotype and genotype. Mol Genet Metab 75(4):353–359

Taylor AM, Preston AJ, Paulk NK et al (2012) Ochronosis in a murine model of alkaptonuria is synonymous to that in the human condition. Osteoarthritis Cartilage 20(8):880–886

Titus GP, Mueller CR, Burgner J et al (2000) Crystal structure of human homogentisate dioxygenase. Nat Struct Biol 7:542–546

Vilboux T, Kayser M, Introne W et al (2009) Mutation spectrum of homogentisic acid oxidase (HGD)in alkaptonuria. Hum Mutat 30 (12):1611–1619

Wildeman M, van Ophuizen E, den Dunnen JT, Taschner PE (2008) Improving sequence variant descriptions in mutation databases and literature using the MUTALYZER sequence variation nomenclature checker. Hum Mutat 29(1):6–13

Worth CL, Preissner R, Blundell TL (2011) SDM - a server for predicting effects of mutations on protein stability and malfunction. Nucleic Acids Res 39:W215–W222

Zatkova A, Sedlackova T, Radvansky J et al (2011) Identification of 11 novel homogentisate 1,2 dioxygenase variants in alkaptonuria patients and establishment of a novel LOVD-based HGD mutation database. JIMD Rep 4:455–465

JIMD Reports
DOI 10.1007/8904_2014_403

RESEARCH REPORT

Metabolic Effects of Increasing Doses of Nitisinone in the Treatment of Alkaptonuria

Ilya Gertsman · Bruce A. Barshop · Jan Panyard-Davis · Jon A. Gangoiti · William L. Nyhan

Received: 28 October 2014 / Revised: 12 December 2014 / Accepted: 23 December 2014 / Published online: 10 February 2015

Abstract Alkaptonuria is an autosomal recessive disease involving a deficiency of the enzyme homogentisate dioxygenase, which is involved in the tyrosine degradation pathway. The enzymatic deficiency results in high concentrations of homogentisic acid (HGA), which results in orthopedic and cardiac complications, among other symptoms. Nitisinone (NTBC) has been shown to effectively treat alkaptonuria by blocking the conversion of 4-hydroxyphenylpyruvate to HGA, but there have been concerns that using doses higher than about 2 mg/day could cause excessively high levels of tyrosine, resulting in crystal deposition and corneal pathology. We have enrolled seven patients in a study to determine whether higher doses of NTBC were effective at further reducing HGA levels while maintaining tyrosine at acceptable levels. Patients were given varying doses of NTBC (ranging from 2 to 8 mg/day) over the course of between 0.5 and 3.5 years. Urine HGA, plasma tyrosine levels, and plasma NTBC were then measured longitudinally at various doses. We found that tyrosine concentrations plateaued and did not reach significantly higher levels as NTBC doses were increased above 2 mg/day, while a significant drop in HGA continued from 2 to 4 mg/day, with no significant changes at higher doses. We also demonstrated using untargeted metabolomics that elevations in tyrosine from treatment resulted in proportional elevations in alternative tyrosine metabolic products, that of *N*-acetyltyrosine and γ-glutamyltyrosine.

Abbreviations

3,4-DPA	3,4-Dihydroxyphenylacetate
4-HPPD	4-Hydroxyphenylpyruvate dioxygenase
ACN	Acetonitrile
FA	Formic acid
HGA	Homogentisic acid
LC-MS-Q-TOF	Liquid chromatography-quadrupole-time of flight mass spectrometry
mg/d	Milligrams per day
NTBC	Nitisinone

Introduction

Alkaptonuria (OMIM 203500) is an autosomal recessive disease that leads to ochronosis, joint deterioration, and cardiac valve disease, generally presenting in adulthood. The late-onset clinical manifestations are a result of a defective enzyme in the tyrosine degradation pathway, homogentisate dioxygenase, that prevents the metabolism of the intermediate homogentisic acid (HGA) to maleylacetoacetate (Pollak et al. 1993; Janocha et al. 1994; Fernandez-Canon et al. 1996). The result is a high concentration of HGA that polymerizes after oxidation to the benzoquinone form (Milch 1961; Zannoni et al. 1962, 1969). The polymers deposit in the connective tissue and are responsible for the bulk of the symptoms. The most effective treatment for lowering HGA in this disease is the drug nitisinone (Orfadin^{R}), which is also the most common and effective form of treatment for type I

Communicated by: Feillet, MD, PhD

Competing interests: None declared

Electronic supplementary material: The online version of this chapter (doi:10.1007/8904_2014_403) contains supplementary material, which is available to authorized users.

I. Gertsman · B.A. Barshop (✉) · J. Panyard-Davis · J.A. Gangoiti · W.L. Nyhan
Biochemical Genetics and Metabolomics Laboratory, University of California, San Diego, 9500 Gilman Drive, La Jolla, CA 92093, USA
e-mail: bbarshop@ucsd.edu

tyrosinemia (Anikster et al. 1998; Suwannarat et al. 2005; Introne et al. 2011; Schlune et al. 2012). NTBC blocks the enzyme 4-hydroxyphenylpyruvate dioxygenase that produces HGA from 4-hydroxyphenylpyruvate (Ellis et al. 1995; Kavana and Moran 2003).

The reduction of HGA and its corresponding polymers with NTBC treatment may have potential in reducing complications associated with alkaptonuria, including the progression of aortic valve disease (Introne et al. 2011), a correlation that still requires further study. NTBC doses of 0.5–2 mg/day were shown to reduce HGA levels nearly 95%, but the three-year study was not able to show a change in the progression of symptoms, including joint deterioration (Introne et al. 2011). There has been caution about using higher doses out of concern that high tyrosine levels associated with NTBC treatment will lead to corneal crystal deposits and ocular complications, though several studies have shown that high tyrosine itself does not appear correlated to ocular problems and that some patients are able to tolerate plasma tyrosine levels of over 1,000 μM (Ney et al. 1983; Holme and Lindstedt 1998; Gissen et al. 2003).

As previous studies have not reported patient outcomes when increasing NTBC doses higher than 2 mg/day, we set out to investigate whether using NTBC at doses between 4 and 8 mg/day would further reduce HGA levels, while keeping tyrosine levels below critically high levels, as established for tyrosinemia type 1 patients who are also using NTBC. The seven patients who were enrolled in the study were not placed on diet restriction, but did receive an amino acid supplement called Tyrex-2® (Abbott Laboratories, Columbus, Ohio), which lacks tyrosine and phenylalanine. The hypothesis for using this supplement was that, given a formula with all amino acids except tyrosine and phenylalanine, the natural process of anabolism would consume the endogenous pools, as observed in treatment of maple syrup urine disease with an amino acid mixture lacking branched-chain amino acids (Saudubray et al. 1984; Nyhan et al. 1991). In addition to measuring the levels of HGA, tyrosine, and NTBC over the course of 0.5–3.5 years during this longitudinal study, we further explored the biochemical consequence of high plasma tyrosine using untargeted metabolomics methods (LC-MS-Q-TOF) to compare the plasma metabolome from patients prior to NTBC treatment with their posttreated samples and potentially identify unknown biochemical implications of excessive tyrosine and NTBC treatment.

Methods

Patient Enrollment

The protocol is an IRB-approved open-label study (listed in clinicaltrials.gov# NCT01390077), which was approved by the UCSD Human Research Protections Program. Patients of any age with the diagnosis of alkaptonuria and documented increased excretion of homogentisic acid were eligible; exclusion criteria included significant laboratory abnormalities unrelated to alkaptonuria or significant comorbidities. Eight patients were enrolled (two women and six men), though only seven have participated in treatment. Age at enrollment ranged from 31 years to 61 years. All patients had arthritic joint damage with resulting pain. Four patients had experienced arthroscopic debridement or replacement surgeries of one or more joints. Echocardiograms, radiographs, eye examination, and routine laboratory panels were obtained. Treatment with 2 mg/day NTBC (once daily) was initiated, and plasma tyrosine levels were measured one week and one month after. Routine chemistry and hematology analyses were obtained at month 3 and then annually. Plasma tyrosine, trough NTBC, and 12-hour urine HGA measurements were obtained at months 3 and 6 and then every 6 months, more often if the NTBC dose was changed. Patients 1–3 have been monitored over the course of 3–3.5 years, while patients 4–7 have been monitored between 0.5 and 1 year (Table 1). Patient 3 spent the majority of the study at a 2 mg/day NTBC dosage, while patients 1 and 2 have been on 4 mg/day NTBC or higher for the majority of the study. No changes were made to ongoing medications or dietary intake, though five of the patients (patients 3–7) took a supplement of Tyrex-2® (35 g, twice daily) approximately 1 month after starting treatment. Patient 1 began taking Tyrex-2® 6 months after starting NTBC treatment, while patient 2 began ten months after treatment initiation. Patient 3 discontinued Tyrex-2® several months after starting supplement, while several of the other patients had discontinued taking supplement for only portions of the study (patients 1, 2, and 4).

Sample Storage

Urine and plasma samples were stored in −80°C freezer. Urine samples were extracted and analyzed within 1–3 months after sample collection. HGA is known to be unstable in alkaline conditions (Hughes et al. 2014). We tested stability under our own storage times and conditions by comparing the HGA concentration from five different urine samples extracted shortly after collection, compared to aliquots of the same samples stored for 3 months at −80°C prior to extraction and analysis (Supplementary Table 1). We separately acidified three urine samples within the same day of sample acquisition (using a final concentration of either 250 mM final perchloric acid or 3% sulfosalicylic acid) and compared their endogenous HGA levels (normalized to a 3,4-DPA internal standard) with sample aliquots that were stored at −80°C for a month prior to acidification. The relatively small change in HGA between these sample sets was within the acceptable

Table 1 Tyrosine and HGA (in parentheses) concentrations are shown in μM for the seven different patients following treatment at different dose levels of NTBC. The time in months (m) that each patient remained on the respective dose level is shown below these values. At dose levels where multiple measurements were taken (time between repeat measurements varied for the seven patients and ranged from 1 to 6 months between measurements), the standard deviation is displayed. The total time that each patient has been monitored in the study is shown below the patient number in parenthesis

	Pre-NTBC	1 mg NTBC	2 mg NTBC	4 mg NTBC	6 mg NTBC	8 mg NTBC
Patient 1 (3.5 years)	56 (1,046)		460 ± 48 (42) 8 m	465 ± 24 (20) 8 m	510 ± 113 (30 ± 13) 16 m	413 (19 ± 4) 8 m
Patient 2 (3.5 years)	57 (1,465)	869 6 m	850 ± 269 (126) 6 m	793 (48) 12 m	736 ± 73 (34 ± 13) 18 m	
Patient 3 (3 years)	51 (1,025)		646 ± 127 (101 ± 28) 36 m	734 (42) 1 m		
Patient 4 (1 year)	44 (1,251)		694 (121 ± 6) 4 m	775 ± 60 (40 ± 13) 4 m	654 (32) 1 m	
Patient 5 (1 year)	35 (2,192)		704 (22) 2 m	749 (16) 10 m		
Patient 6 (6 months)	47 (1,645)		664 (143) 3 m	706 (38) 3 m		
Patient 7 (6 months)	82 (2,357)		663 (238) 6 m			

analytical variation of the method (<15% CV) (Supplementary Table 2).

Sample Preparation

Prior to extraction of urine samples, the concentration of creatinine was determined in each sample, and an aliquot was transferred to a fresh reaction tube and diluted to 100 μL with H_2O/0.1% formic acid at a final concentration of 1 mM creatinine. The Jaffe method for creatinine determination was used, as preferred for alkaptonuria study (Loken et al. 2010). Diluted urine aliquots were extracted with a final concentration of 80% cold methanol. For the quantitation of HGA, an internal standard of 3,4-dihydroxyphenylacetate ((3,4-DPA) ring-$^2H_3$, 2,2-$^2H_2$, Cambridge Isotope) was added to each extraction at a final concentration of 1 μM. 3,4-DPA was used for its chemical, chromatographic (Supplementary Fig. 1), and ionization similarities to HGA. Samples were vortexed for 30 s, left at −20°C for an hour, and centrifuged at 16 kg at 4°C for 15 min. The supernatant was removed and dried in a SpeedVac (Thermo Fisher) coupled with a lyophilizer (Labconco). Dried supernatants were resuspended in 300 μL of 5% acetonitrile (ACN)/0.1% formic acid (FA).

For plasma samples analyzed by mass spectrometry, 100 μL of each sample was treated as reported previously (Gertsman et al. 2014). In this method, a stable isotopic mixture of 50 compounds is spiked into each sample extraction, permitting absolute quantification of many intermediates in major metabolic energy pathways and enabling potential normalization of chemically similar analytes discovered by untargeted analysis. In addition, the internal standard mesotrione (Sigma-Aldrich) was added to each extraction (final concentration of 2.4 μM/sample extraction) for the quantitation of NTBC, which was previously used for NTBC quantitation by LC-MS/MS (Sander et al. 2011).

Sample Acquisition Methods

An LC-MS/MS method was developed to enable quantification of HGA, tyrosine, and nitisinone from urine in a single run, though only the urine HGA values are reported in the current study. An 8-pt calibration curve and three levels of quality control samples containing freshly prepared HGA were processed and run with each batch of urine samples. A control urine sample that had no detectable HGA (<1 μM based on a comparison with an LLOQ sample containing an additional 3 μM of spiked HGA) was used as the matrix for all standard curve and QC samples. Analytical validation for four days measuring intra- and inter-day accuracy and precision was performed and reported in Supplementary Fig. 1. We used a Kinetex pentafluorophenyl (PFP) stationary phase column (150 x 2.1 mm, 2.6 micron particle diameter, Phenomenex, Torrance, CA) in-line with an API 4000 mass spectrometer for this analysis (AB SCIEX, with Agilent 1200 HPLC and Leap Technologies autosampler). We used the following LC method: 0% mobile phase B (mobile phase A 0.1% FA, mobile phase B 100% ACN/0.1% FA) for 3 min, a gradient from 0% to 45% B over 1 min, 2 min of isocratic flow at 45% B, a gradient from 45% to 70% B over 1 min, 3 min of isocratic flow at 70% B, a gradient from 70% to 100% B over 1 min, followed by a 5-min isocratic flow of 100% B, and finally re-equilibration at 0% B for 10 min. A flow rate of 300 μL/min was used, and 5 μL of each sample resuspension was injected per run. The parent to daughter ion (MRM) transition of 167 → 123 was

used for HGA, while a transition of 172 → 128 was monitored for 3,4-DPA. The run was acquired in negative ionization mode using −4,500 V for the cone voltage and a collision energy of −20 V. The nebulizing gas pressure was set to 30 psi, and the heating gas pressure was 70 psi at a temperature of 300°C. Curtain gas was set to 15 psi. Declustering potential was set to −80 V and a dwell time of 0.15 s for each transition.

Plasma tyrosine levels reported in the manuscript were measured using a Biochrom 30 ion exchange automated amino acid analyzer with ninhydrin detection (Shapira et al. 1989). A hybrid targeted/untargeted metabolomics method using LC-MS-Q-TOF (AB SCIEX 5600 mass spectrometer with Shimadzu Prominence UFLC) and a C18-PFP (MAC-MOD Analytical, Inc.) was used for untargeted analyte profiling while also quantifying NTBC and tyrosine. This method was previously validated for the quantification of tyrosine (Gertsman et al. 2014), but these values are not reported here for purposes of consistency, as not all of the plasma samples had been quantified by LC-Q-TOF, while all were evaluated by the Biochrom 30 system. The C18-PFP column exhibited suitable linearity for the quantification of NTBC in the range of 0.5–20 μM as well (6- to 8-pt calibration curves were prepared and run along with each batch, with correlation coefficients of linear regression exceeding 0.99).

Statistical Analysis

Quantification from mass spectrometry runs was performed using MultiQuant Software (AB SCIEX). Untargeted analysis from Q-TOF runs was performed using Marker-View Software (AB SCIEX). Runs from pre-NTBC treated samples along with post-NTBC treated samples were aligned, integrated, and statistically compared between these two distinct cohorts. Unpaired *t*-test analysis of all aligned peaks was evaluated to find statistically significant changes corresponding to NTBC treatment. Statistical correction for multicomponent null hypothesis testing using the Q-value software was applied to limit false discovery (Storey and Tibshirani 2003). Analytes of interest were initially identified by MS/MS matching with existing database entries. Standards for γ-glutamyltyrosine and glu-tyr dipeptide were purchased (Sigma-Aldrich) and analyzed to confirm analyte identity.

Results

HGA in Urine

Aliquots from pooled 12-hour (overnight) urine samples were evaluated for HGA and normalized to creatinine concentrations from the same sample. Values reported in Table 1 for all patients are reported in μM HGA/mM creatinine from each patient's pooled 12-h sample. The average decrease in HGA following a 2 mg/day dosage of NTBC was 93% (pre-NTBC: 1538 ± 483 μM, 2 mg/day NTBC: 110 ± 70 μM). Six of the seven enrolled patients were further evaluated at a 4 mg dose and showed an additional 2.7-fold decline in mean HGA concentrations (p-value <0.05 from paired t-test analysis (Fig. 1a)). Three patients had doses increased to 6 mg/day, and one of those patients later had her dose increased further to 8 mg. As shown in Figure 1, though the HGA levels dropped significantly from a 2 mg to 4 mg/day NTBC dosage, there was no significant change when increasing to 6–8 mg/day NTBC in the three patients taking those higher doses. Plasma NTBC concentrations and NTBC dose levels were correlated to urine HGA in Fig. 1c, d.

Tyrosine and NTBC in Plasma

As reported in previous studies, the levels of tyrosine dramatically increase during treatment with NTBC (Suwannarat et al. 2005; Introne et al. 2011). There was a mean 13-fold increase in tyrosine from pretreated plasma to samples following 2 mg of NTBC treatment. However, as patient doses were increased to 4 mgs, there was not a significant change in tyrosine levels, as shown in Fig. 2a (1.1 mean fold change, p-value >0.05 following paired t-test analysis). Though there were only three patients in whom tyrosine levels were measured at NTBC doses >4 mg/day, tyrosine levels were not further elevated in those samples.

Four of the seven patients in the study have had tyrosine levels measured with and without taking the supplement Tyrex-2® while on the same NTBC dose level. Several of these patients showed a decrease in plasma tyrosine using the supplement, while for others the reverse was measured, with no overall statistical significance to the change in this limited sampling (Supplementary Fig. 2). Patient 3 spent the majority of the study without taking the supplement and did not show further elevations in tyrosine following discontinuation. Further studies are required to determine if Tyrex-2® can reduce tyrosine levels, which may also require diet restriction for a pronounced effect.

Untargeted Metabolomics Analysis

From untargeted metabolomics comparison of pretreated to NTBC-treated patient plasma samples, a number of different metabolite changes were detected, including metabolites of tyrosine, products of NTBC metabolism, and a class of indolic compounds (described in a separate manuscript currently under review). Here we report the identified compounds relevant to the study, which include *N*-acetyltyrosine and γ-glutamyltyrosine (MS/MS analysis

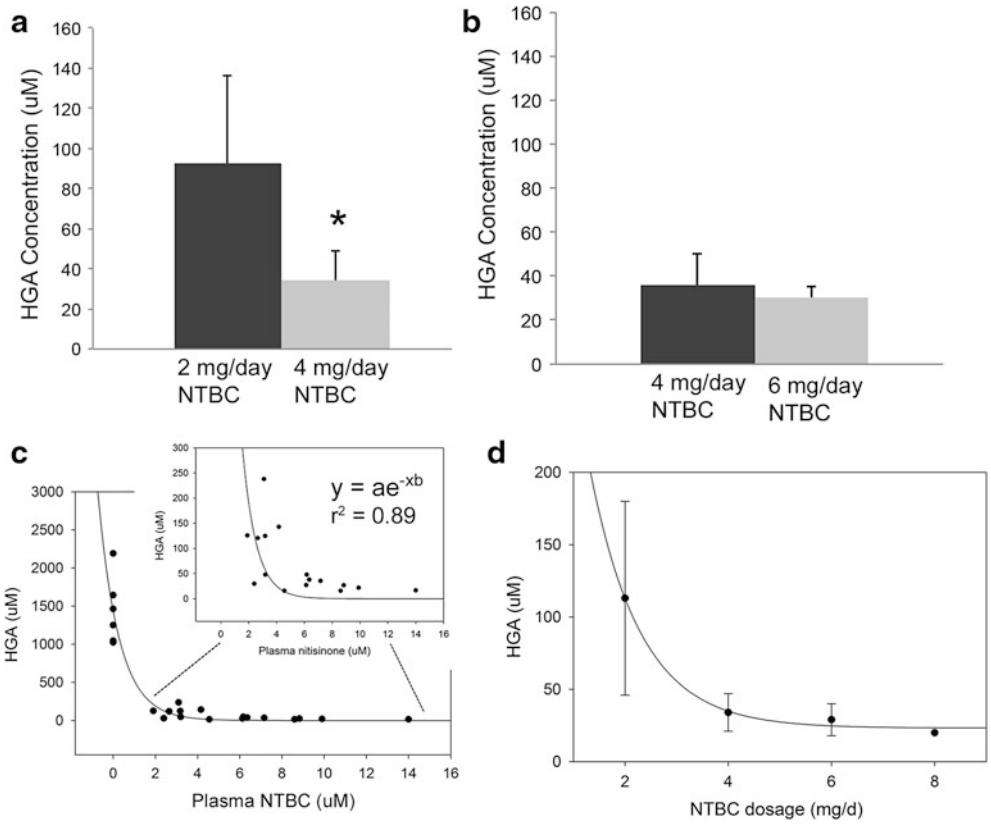

Fig. 1 HGA concentrations measured in urine. (**a**) Comparison of mean HGA levels of six patients evaluated at both 2 and 4 mg/day NTBC. The average fold change in HGA concentration was 2.7-fold (* indicates *p*-value of 0.01 from paired *t*-test analysis). (**b**) Urine HGA comparison between 4 and 6 mg/day NTBC dosage (fails null hypothesis testing, *p*-value >0.05). (**c**) Urine HGA concentrations plotted versus NTBC plasma concentration and fit to a single exponential decay curve. Plasma was acquired from the same day as the 12-h urine collection. The region of the graph corresponding to values of samples acquired after NTBC treatment is shown zoomed in. (**d**) Mean urine HGA concentrations plotted versus NTBC dosage. Standard deviations are depicted by error bars

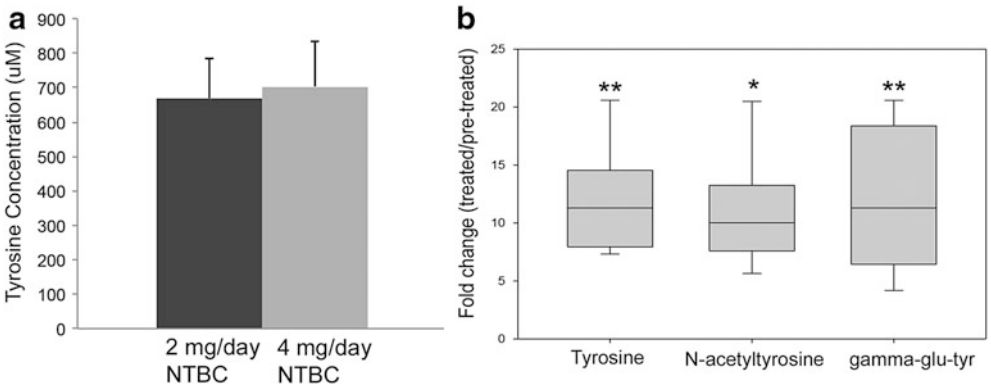

Fig. 2 Plasma tyrosine and associated metabolites. (**a**) Plasma tyrosine concentrations compared following treatment with either 2 or 4 mg/day NTBC (1.1-fold change, not statistically significant). (**b**) Tyrosine conjugates discovered by untargeted metabolomics. The *graph* shows fold changes in normalized peak intensities of tyrosine, *N*-acetyltyrosine, and γ-glutamyltyrosine between NTBC-treated and untreated patient plasma samples (12.5-fold, 11.5-fold, and 11.6-fold, respectively). Peak areas were normalized by the stable isotope internal standard $^{2}H_{4}$-tyrosine, which was spiked into all extraction reactions for improved inter-batch comparisons. *Note*: * indicates $p < 0.01$, and ** indicates $p < 0.001$ from paired *t*-test analysis of untreated versus NTBC-treated metabolite levels

shown in Supplementary Fig. 3). These compounds were determined to be significantly altered after unpaired *t*-test and further analysis of *Q*-value (*Q*-value < 0.05 for both). Their peak areas were normalized to a $^{2}H_{4}$-(ring)-tyrosine internal standard, which was spiked into all extraction reactions and which demonstrated consistent linear proportionality to these

compounds in negative ionization mode. These compounds are conjugates of tyrosine and are elevated proportionally to the increased plasma tyrosine levels. We show that N-acetyltyrosine and γ-glutamyltyrosine had an 11.5- and 11.6-fold normalized peak area changes when comparing NTBC-treated to untreated patients (Fig. 2b). The presence of these compounds reveals alternative pathways for tyrosine metabolism/diversion when the oxidative pathway is blocked.

Patient Symptoms

Quantitative measurements of joint mobility, ochronosis, and other symptoms have not been evaluated in the study, though all patients completed short form health surveys (SF-36) for assessment of overall health, pain (Brief Pain Inventory), and life interference (Ware et al. 1981; Ware and Sherbourne 1992). Patient 1 reported significant improvement in ochronosis of the fingers, while patient 2 has had significant improvement in shoulder joint pain that allowed the cancellation of surgery. No patients reported worsening of the three categories in the SF-36 survey, while five of the seven patients reported improvements in at least one of these categories following treatment. The reported complications included ocular irritation in two patients. Specifically, patient 3 had a blood spot tyrosine of 1,180 μM shortly after starting NTBC treatment, and described eye discomfort, while patient 2 had a recurrence of blurry vision, but did not have tyrosine measured during this episode. Both patients were temporarily placed on lower NTBC doses as well as Tyrex-2® and showed no further complications or tyrosine levels higher than 800 μM. A third patient (patient 1) experienced abdominal discomfort at 8 mg/day NTBC, which resolved upon returning to 6 mg/day.

Discussion

NTBC, a drug that has been widely used for the treatment of tyrosinemia type 1, has been more recently used for the treatment of alkaptonuria. NTBC reduces toxic levels of HGA in patients with alkaptonuria, but, by inhibiting the 4-hydroxyphenylpyruvate dioxygenase (4-HPPD), causes a significant elevation in 4-hydroxyphenylpyruvate and tyrosine. This high elevation in tyrosine has been a concern for physicians in their choice of NTBC doses administered to patients. In this study, we demonstrate that there was a negligible change in plasma tyrosine concentrations in patients who are given a 4 mg/day as compared to a 2 mg/day dose of NTBC, while the HGA further decreased an additional 2.7-fold. In the three patients who were given doses of 6 mg/day or higher, however, there was little further change in HGA levels, and tyrosine levels continued to remain virtually unchanged. Though we have monitored a limited patient cohort, the data suggest that though there was additional utility in prescribing 4 mg/day NTBC, there was little or no benefit to higher doses in achieving HGA reduction.

There was no major change in plasma tyrosine concentrations in the six patients who had doses of NTBC increased from the initial 2 mg/day dose. Increased levels of tyrosine (>1,000 μM) have been reported in patients from previous NTBC dose studies, but the tyrosine fluctuation has not previously been reported beyond a 2 mg/day dose. Untargeted metabolomics uncovered two previously unreported products of excess tyrosine in alkaptonuria patients, *N*-acetyltyrosine and γ-glutamyltyrosine, which had similar peak intensity fold changes as tyrosine itself following NTBC treatment. The presence of *N*-acetyltyrosine has been identified in the urine of type II tyrosinemia patients (Macsai et al. 2001), but γ-glutamyltyrosine has never previously been reported in disorders of tyrosine metabolism. It is likely formed by γ-glutamyl transpeptidase, an enzyme critical to glutathione catabolism and regulation of cellular redox (Griffith et al. 1979; Zhang and Forman 2009). These findings help explain nontraditional pathways for the metabolism of excess tyrosine. The data show that there is no equilibrium shift between tyrosine and the concentrations of these derivative forms as plasma tyrosine levels increase, as their fold changes are nearly identical. Ocular complications have been associated with high tyrosine concentrations, but some studies have shown that high tyrosine itself does not appear correlated to ocular problems (Holme and Lindstedt 1998; Gissen et al. 2003), so it may be pertinent to investigate these and possibly other nontraditional metabolites of tyrosine in relation to the phenotype.

NTBC is known to bind tightly in the 4-HPPD-inhibitor complex, with a very slow dissociation rate (Ellis et al. 1995; Kavana and Moran 2003) and a mean half-life of 54 hours in humans (Hall et al. 2001). Therefore, the concentration of plasma NTBC should never drop below ~20% of the peak concentration in patients taking a daily dose, and at a dose of 2 mg/day, the 4-HPPD enzyme-inhibitor complex appears to approach saturation, reflected by a nearly 93% reduction of HGA. With an increase in dosage from 2 to 4 mg/day, it does appear that there is additional enzymatic inhibition, with an additional 2.4% mean decrease in HGA from pretreatment levels. Since 4-HPPD is nearly completely inhibited with 4 mg/day NTBC, it was not surprising that there was no significant additional decrease of HGA observed at higher doses. These data indicate that there may be limited rationale to utilize doses >4 mg/day. The fact that HGA levels were never measured below 15 μM in any of the patients could be attributed to a basal amount of newly synthesized enzyme that functions

prior to the initial slow binding reaction with NTBC or potentially to an inability for NTBC to reach all affected tissues. Following this line of reasoning, only variations in dietary tyrosine should impact the levels of plasma tyrosine when treating with NTBC doses above this point of saturated 4-HPPD inhibition.

Acknowledgments We would like to thank Gabrielle Golden for helping with the organization of the study and sample acquisition. We would like to thank Kasie Auler for the tyrosine analysis by the amino acid analyzer. We would like to thank Swedish Orphan Biovitrum for the supply of NTBC used in the study and Abbott Laboratories for the supply of Tyrex-2.

Synopsis

Treatment of alkaptonuria with nitisinone doses greater than 2 mg/day significantly lowers homogentisic acid levels while tyrosine levels remain unchanged.

Compliance with Ethics Guidelines

Conflicts of Interest

Ilya Gertsman has no conflict of interest to declare.
Bruce Barshop has no conflict of interest to declare.
Jan Panyard-Davis has no conflict of interest to declare.
Jon Gangoiti has no conflict of interest to declare.
William Nyhan has no conflict of interest to declare.

Informed Consent

All procedures followed were in accordance with the ethical standards of the responsible committee on human experimentation (institutional and national) and with the Helsinki Declaration of 1975, as revised in 2000. Informed consent was obtained from all patients for being included in the study.

Author Contributions

IG: Developed methods for analysis, analyzed the data collected, principal author of the manuscript

BAB: Assisted in the design of chemometric analyses and identification of target compounds, contributed substantially to writing the manuscript

JP-D: Planned and coordinated patient treatment regimens, reviewed the manuscript

JAG: Developed chemometric methodology, reviewed the manuscript

WLN: Conceived of patient treatment regimens, contributed to writing of the manuscript

References

Anikster Y, Nyhan WL, Gahl WA (1998) NTBC and alkaptonuria. Am J Hum Genet 63:920–921

Ellis MK, Whitfield AC, Gowans LA et al (1995) Inhibition of 4-hydroxyphenylpyruvate dioxygenase by 2-(2-nitro-4-trifluoromethylbenzoyl)-cyclohexane-1,3-dione and 2-(2-chloro-4-methanesulfonylbenzoyl)-cyclohexane-1,3-dione. Toxicol Appl Pharmacol 133:12–19

Fernandez-Canon JM, Granadino B, Beltran-Valero de Bernabe D et al (1996) The molecular basis of alkaptonuria. Nat Genet 14:19–24

Gertsman I, Gangoiti J, Barshop B (2014) Validation of a dual LC–HRMS platform for clinical metabolic diagnosis in serum, bridging quantitative analysis and untargeted metabolomics. Metabolomics 10:312–323

Gissen P, Preece MA, Willshaw HA, McKiernan PJ (2003) Ophthalmic follow-up of patients with tyrosinaemia type I on NTBC. J Inherit Metab Dis 26:13–16

Griffith OW, Bridges RJ, Meister A (1979) Transport of gamma-glutamyl amino acids: role of glutathione and gamma-glutamyl transpeptidase. Proc Natl Acad Sci U S A 76:6319–6322

Hall MG, Wilks MF, Provan WM, Eksborg S, Lumholtz B (2001) Pharmacokinetics and pharmacodynamics of NTBC (2-(2-nitro-4-fluoromethylbenzoyl)-1,3-cyclohexanedione) and mesotrione, inhibitors of 4-hydroxyphenyl pyruvate dioxygenase (HPPD) following a single dose to healthy male volunteers. Br J Clin Pharmacol 52:169–177

Holme E, Lindstedt S (1998) Tyrosinaemia type I and NTBC (2-(2-nitro-4-trifluoromethylbenzoyl)-1,3-cyclohexanedione). J Inherit Metab Dis 21:507–517

Hughes AT, Milan AM, Christensen P et al (2014) Urine homogentisic acid and tyrosine: simultaneous analysis by liquid chromatography tandem mass spectrometry. J Chromatogr B Analyt Technol Biomed Life Sci 963:106–112

Introne WJ, Perry MB, Troendle J et al (2011) A 3-year randomized therapeutic trial of nitisinone in alkaptonuria. Mol Genet Metab 103:307–314

Janocha S, Wolz W, Srsen S et al (1994) The human gene for alkaptonuria (AKU) maps to chromosome 3q. Genomics 19:5–8

Kavana M, Moran GR (2003) Interaction of (4-hydroxyphenyl) pyruvate dioxygenase with the specific inhibitor 2-[2-nitro-4-(trifluoromethyl)benzoyl]-1,3-cyclohexanedione. Biochemistry 42:10238–10245

Loken PR, Magera MJ, Introne W et al (2010) Homogentisic acid interference in routine urine creatinine determination. Mol Genet Metab 100:103–104

Macsai MS, Schwartz TL, Hinkle D, Hummel MB, Mulhern MG, Rootman D (2001) Tyrosinemia type II: nine cases of ocular signs and symptoms. Am J Ophthalmol 132:522–527

Milch RA (1961) Studies of alcaptonuria: mechanisms of swelling of homogentisic acid-collagen preparations. Arthritis Rheum 4:253–267

Ney D, Bay C, Schneider JA, Kelts D, Nyhan WL (1983) Dietary management of oculocutaneous tyrosinemia in an 11-year-old child. Am J Dis Child 137:995–1000

Nyhan WL, Rice-Asaro M, Acosta P (1991) Advances in the treatment of amino acid and organic acid disorders. In: Treatment of genetic diseases. Churchill Livingstone, New York

Pollak MR, Chou YH, Cerda JJ et al (1993) Homozygosity mapping of the gene for alkaptonuria to chromosome 3q2. Nat Genet 5:201–204

Sander J, Janzen N, Terhardt M et al (2011) Monitoring tyrosinaemia type I: Blood spot test for nitisinone (NTBC). Clin Chim Acta 412:134–138

Saudubray JM, Ogier H, Charpentier C et al (1984) Hudson memorial lecture. Neonatal management of organic acidurias. Clinical update. J Inherit Metab Dis 7(Suppl 1):2–9

Schlune A, Thimm E, Herebian D, Spiekerkoetter U (2012) Single dose NTBC-treatment of hereditary tyrosinemia type I. J Inherit Metab Dis 35:831–836

Shapira E, Blitzer MG, Miller JB, Affrick DK (1989) Biochemical genetics: a laboratory manual. Oxford University, USA

Storey JD, Tibshirani R (2003) Statistical significance for genome-wide studies. Proc Natl Acad Sci U S A 100:9440–9445

Suwannarat P, O'Brien K, Perry MB et al (2005) Use of nitisinone in patients with alkaptonuria. Metabolism 54:719–728

Ware JE Jr, Sherbourne CD (1992) The MOS 36-item short-form health survey (SF-36). I. Conceptual framework and item selection. Med Care 30:473–483

Ware JE Jr, Brook RH, Davies AR, Lohr KN (1981) Choosing measures of health status for individuals in general populations. Am J Public Health 71:620–625

Zannoni VG, Malawista SE, La Du BN (1962) Studies on ochronosis. II. Studies on benzoquinoneacetic acid, a probable intermediate in the connective tissue pigmentation of alcaptonuria. Arthritis Rheum 5:547–556

Zannoni VG, Lomtevas N, Goldfinger S (1969) Oxidation of homogentisic acid to ochronotic pigment in connective tissue. Biochim Biophys Acta 177:94–105

Zhang H, Forman HJ (2009) Redox regulation of gamma-glutamyl transpeptidase. Am J Respir Cell Mol Biol 41:509–515

JIMD Reports
DOI 10.1007/8904_2015_412

RESEARCH REPORT

Relationship Between Serum Concentrations of Nitisinone and Its Effect on Homogentisic Acid and Tyrosine in Patients with Alkaptonuria

Birgitta Olsson • Trevor F Cox • Eftychia E Psarelli • Johan Szamosi • Andrew T Hughes • Anna M Milan • Anthony K Hall • Jozef Rovensky • Lakshminarayan R Ranganath

Received: 27 November 2014 / Revised: 21 January 2015 / Accepted: 22 January 2015 / Published online: 13 March 2015

Abstract *Background*: Alkaptonuria (AKU) is a serious genetic disease due to a defect in tyrosine metabolism, leading to increased serum levels of homogentisic acid (HGA). Nitisinone decreases HGA in AKU, but the concentration–response relationship has not been previously reported.

Objectives: To determine the relationship between serum concentrations of nitisinone and the effect on both HGA and tyrosine; secondly to determine steady-state pharmacokinetics of nitisinone in AKU patients.

Method: Thirty-two patients with AKU received either 1, 2, 4, or 8 mg nitisinone daily. Urine and serum HGA and serum tyrosine and nitisinone were measured during 24 h at baseline (before first dose) and after 4 weeks of treatment.

Results: Nitisinone pharmacokinetics (area under the curve [AUC] and maximum concentrations [C_{max}]) were dose proportional. The median oral clearance determined in all patients, irrespective of dose, was 3.18 mL/h·kg (range 1.6–6.7).

Nitisinone decreased urinary excretion of HGA in a concentration-dependent manner, with a maximum effect seen at average nitisinone concentrations of 3 μmol/L. The association between nitisinone and tyrosine concentrations was less pronounced. Serum levels of HGA at Week 4 were below the limit of quantitation in 65% of samples, which prevented determination of the relationship with nitisinone concentrations.

Conclusion: Nitisinone exhibits dose-proportional pharmacokinetics in the studied dosage interval. Urinary excretion of HGA decreases in a concentration-dependent manner, while the increase in tyrosine is less clearly related to nitisinone concentrations.

Communicated by: Ertan Mayatepek, MD

Competing interests: None declared

Electronic supplementary material: The online version of this chapter (doi:10.1007/8904_2015_412) contains supplementary material, which is available to authorized users.

B. Olsson (✉) · J. Szamosi
Swedish Orphan Biovitrum AB (publ), Tomtebodavägen 23A, SE-112 76 Stockholm, Sweden
e-mail: birgitta.olsson@sobi.com

T.F. Cox · E.E. Psarelli
Cancer Research UK Liverpool Cancer Trials Unit, University of Liverpool, 1-3 Brownlow Street, Liverpool L69 3GL, UK

A.T. Hughes · A.M. Milan · L.R. Ranganath
Department of Clinical Biochemistry and Metabolic Medicine, Royal Liverpool University Hospital Trust, Prescot Street, Liverpool L7 8XP, UK

A.K. Hall
Cudos BV, Planetenweg 5, 2132 HN Hoofddorp, The Netherlands

J. Rovensky
National Institute of Rheumatic Diseases, Nabrezie, Ivana Krasku 4, SK-921 01 Piešťany, Slovakia

Introduction

Alkaptonuria (AKU, OMIM reference 203500) is a rare autosomal recessive disorder caused by a deficiency in homogentisate 1,2-dioxygenase (HGD, EC 1.13.11.5), the third enzyme in the tyrosine metabolism pathway (Fig. 1). It converts homogentisic acid (HGA, 2,5-dihydroxyphenylacetic acid) to 4-maleylacetoacetic acid. Inability to metabolize HGA leads to urinary excretion of at least 90% of the compound, or 3–6 g per day, in patients with AKU (Garrod

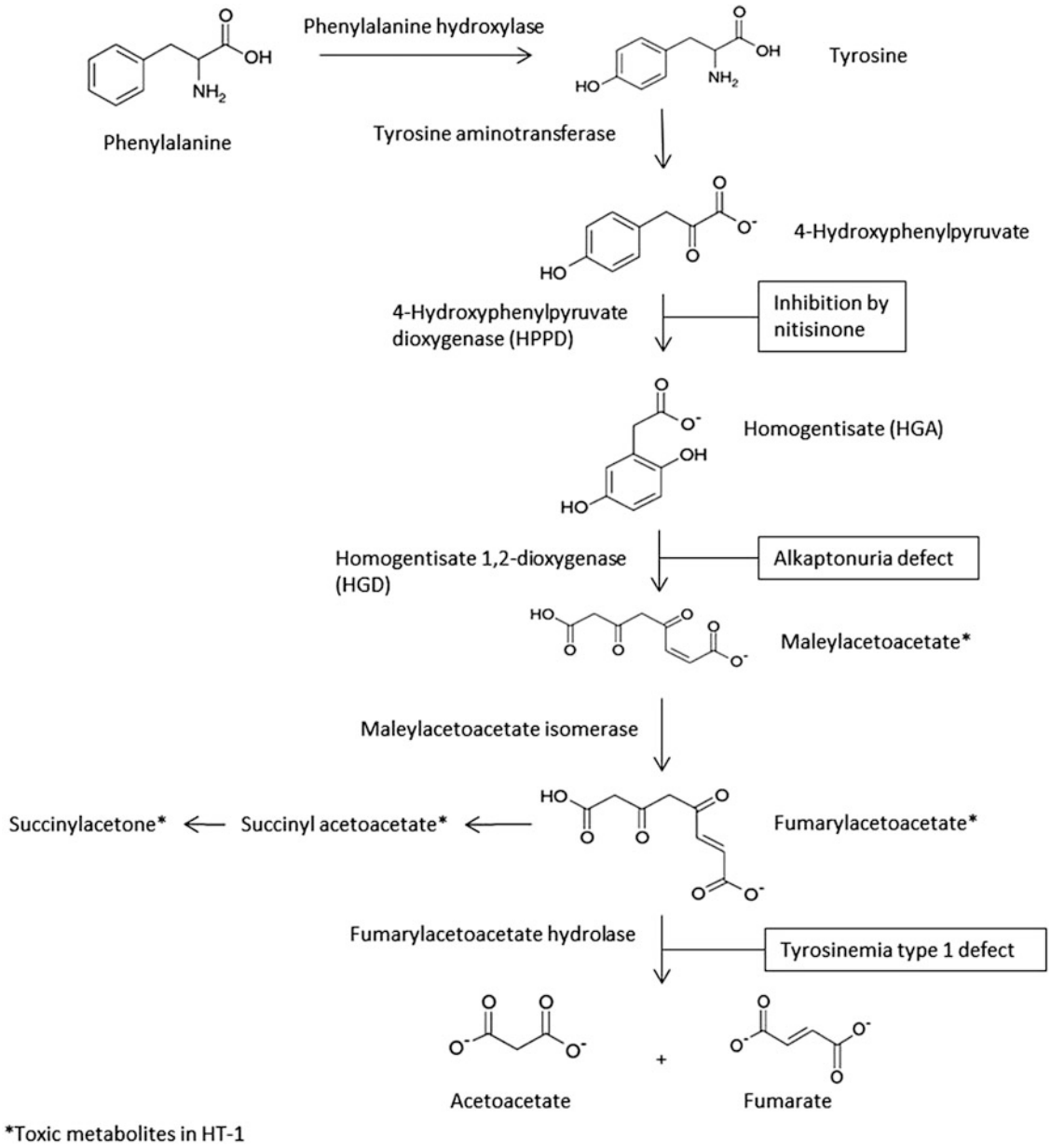

Fig. 1 Schematic presentation of tyrosine metabolism, with AKU and HT-1 defects, and nitisinone site of action

1902; Lustberg et al. 1969; Introne et al. 2011). Despite this pronounced renal elimination, some HGA is oxidized to a melanin-like polymeric pigment via benzoquinone acetic acid. The pigment is deposited in connective tissue, especially in cartilage, a process called ochronosis (Zannoni et al. 1969). This leads to early onset arthritis of the spine and synovial joints and other debilitating symptoms (O'Brien et al. 1963; Ranganath et al. 2013). There is currently no approved pharmacological treatment for AKU.

Nitisinone (also known as NTBC, an abbreviation of its full chemical name), a potent competitive inhibitor of the enzyme 4-hydroxyphenyl-pyruvate dioxygenase (HPPD) (Fig. 1), has been proposed as a treatment for AKU (Anikster et al. 1998; Lock et al. 2014). This drug is registered in several countries for the treatment of hereditary tyrosinemia type I (HT-1, OMIM reference 276700) which is caused by a defect further downstream in the tyrosine metabolism pathway compared to AKU. In HT-1, nitisinone prevents the formation of the highly toxic metabolites maleylacetoacetate, fumarylacetoacetate, and succinylacetone (Lindstedt et al. 1992), and in combination with a tyrosine-restricted diet, it serves as a successful therapeutic intervention. In AKU, nitisinone can effectively reduce HGA and prevent ochronosis in mice (Suzuki et al.

1999; Preston et al. 2013) and reduce HGA in patients (Introne et al. 2011).

A 4-week dose–response study ("SONIA 1") in patients with AKU to investigate the effect of nitisinone on 24-hour urinary excretion of HGA (u-HGA_{24}), and serum concentrations of HGA and tyrosine, as well as the safety of this treatment has been performed and recently reported (Ranganath et al. 2014). In short, u-HGA_{24} decreased in a dose-dependent manner, with the highest dose (8 mg) reducing u-HGA by more than 98%. The fasting predose serum concentrations of HGA (s-HGA) also decreased, and predose serum tyrosine increased with increasing doses. All doses were well tolerated by the patients.

Previous studies with nitisinone have not determined its pharmacokinetics (PK) after repeated dosing nor the relationship between serum exposure and pharmacological effect. Therefore, the SONIA 1 study also aimed at determining nitisinone PK at steady state and to test for PK dose proportionality, as well as describing the relationship between serum concentrations and the effect on HGA and tyrosine in patients with AKU.

Materials and Methods

Patients

Patients with AKU were verified by increased urine HGA excretion and *HGD* gene mutation identification and were eligible for participation. Detailed inclusion and exclusion criteria have been presented earlier (Ranganath et al. 2014).

Study Design and Treatments

SONIA 1 was an international, multicenter, open-label, parallel-group, randomized study in 40 AKU patients, of which 32 (8 per dose group) received nitisinone in doses of either 1, 2, 4, or 8 mg nitisinone once daily for 4 weeks, administered as an oral suspension containing 4 mg nitisinone per milliliter. Another eight patients served as an untreated control group (data not included).

Measurements

Measurement of serum nitisinone, s-HGA, and tyrosine was performed over 24 h after 4 weeks of treatment (Week 4). The first sample was collected after breakfast, just prior to administration of the last dose of nitisinone. Subsequent postdose samples at 0.5, 1, 2, 3, 4, 6, 8, 10, 12, 15, 18, and 24 h were taken. Full s-HGA and tyrosine profiles were also determined at baseline, before administration of the first dose of study medication.

Measurement of u-HGA_{24} was performed at baseline and at Weeks 2 and 4 (see details in Ranganath et al. 2014). Only baseline and Week 4 data are discussed here, since no 24-hour serum profiles were collected at Week 2.

The urine and serum samples were analyzed according to the liquid chromatography–mass spectrometry methods described by Hughes et al. (2014, 2015).

Calculations and Statistics

Based on nitisinone serum concentrations, the following PK variables were calculated using Phoenix WinNonlin 6.3 (Certara L.P., St. Louis, MO, USA): maximum and minimum concentrations (C_{max}, C_{min}), the area under the 24-hour concentration vs. time curve (AUC_{24}, calculated by the linear trapezoidal rule), and oral clearance (CL/F, calculated as dose/AUC_{24}). The same software was used to determine C_{max} and AUC_{24} for s-HGA and serum tyrosine.

The average concentrations during 24 h (C_{av}) were calculated as $AUC_{24}/24$ for nitisinone, s-HGA, and tyrosine.

The dose proportionality of nitisinone AUC_{24} and C_{max}, respectively, was evaluated using a power model (Gough et al. 1995).

Results

Demographics

Demographics for all 40 patients in SONIA 1 have previously been presented (Ranganath et al. 2014). The 32 patients who were treated with nitisinone, and are included in this report of the exposure–response relationships, had a mean age of 47.5 years (range 19–62 years), mean body weight of 79.9 kg (59–112 kg), and mean height of 168.0 cm (164–180 cm). Twenty-three of these 32 patients (72%) were male.

Nitisinone Pharmacokinetics

The AUC_{24} and C_{max} data indicate that exposure to nitisinone is dose proportional within the studied dose range, as indicated by the 95% confidence intervals for the regression coefficients, 0.90–1.26 for AUC_{24} and 0.85–1.21 for C_{max} (Table 1). The oral clearance was similar across the dose groups and ranged from 1.6 to 6.7 mL/h·kg with an overall median of 3.18 mL/h·kg.

The median C_{max}/C_{min} ratio for all patients was 1.80, ranging from 1.3 to 3.8 in individual patients (data not shown). Mean serum concentration profiles for the four doses are shown in Supplementary Figure S1.

Table 1 Dose proportionality of nitisinone PK parameters

	Estimate (beta)	95% CI lower	95% CI upper
AUC_{24} (μmol · h/L)	1.08	0.90	1.26
C_{max} (μmol/L)	1.03	0.85	1.21

AUC_{24} area under the 24-hour serum concentration profile, *CI* confidence interval, *C_{max}* maximum serum concentration

Relationship Between Nitisinone Exposure and the Effect on HGA and Tyrosine

At baseline, u-HGA_{24} ranged from 14 400 to 69 500 μmol across all dose groups (Ranganath et al. 2014). At Week 4, u-HGA_{24} decreased in relation to nitisinone concentrations up to a C_{av} of about 3 μmol/L, with no further decrease in u-HGA_{24} above this level (Fig. 2). In the seven patients with concentrations above 3 μmol/L (all receiving 8 mg nitisinone), median u-HGA_{24} was 135.7 μmol (range 83–213 μmol). The change in u-HGA_{24} from baseline was 99.4–99.7% in these patients.

Serum concentrations of HGA at Week 4 were below the lower limit of quantification (LLOQ, 3.1 μmol/L) in 65% of all samples from treated patients, and only four patients (three on 1 mg and one on 2 mg nitisinone) had HGA above the LLOQ in all samples. The number of patients with s-HGA below the LLOQ increased with increasing nitisinone dose, and therefore, no analysis of individual s-HGA data vs. nitisinone concentrations has been performed. However, for all patients on 1 mg, C_{av} could be reasonably well estimated, and a comparison of the median results at baseline and Week 4 (Table 2) indicates that a dose of 1 mg nitisinone decreased s-HGA by approximately 88%.

Median C_{av} values for serum tyrosine increased in relation to dose (Table 2), but no clear relationship between nitisinone exposure and individual tyrosine data could be seen (Fig. 2). At the highest nitisinone serum concentrations, above 5 μmol/L, daily average tyrosine concentrations were in the range of 800–1,000 μmol/L. However, all treated patients had daily tyrosine averages above 500 μmol/L, and values above 800 μmol/L were seen at nitisinone concentrations as low as 0.7 μmol/L and a dose of 1 mg.

Similar profiles were seen for serum tyrosine and HGA at baseline. After intake of breakfast (time = 0), mean serum tyrosine concentrations decreased from 58 μmol/L right after breakfast to 50 μmol/L at 4 h, thereafter to increase to a maximum of 65 μmol/L at 12 h. The s-HGA profile followed the tyrosine profile, except that it showed a slight increase between 0 and 2 h. Mean s-HGA concentrations after breakfast ($t = 0$) were 29 μmol/L, and maximum concentrations at 12 h were 47 mmol/L (Supplementary Figure S2).

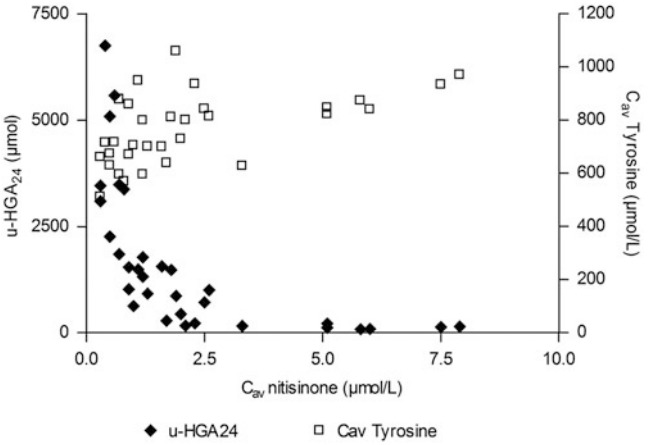

Fig. 2 Individual urinary excretion of HGA and daily average serum tyrosine concentrations vs. daily average serum nitisinone concentrations at Week 4 in AKU patients treated with nitisinone ($N = 32$)

Discussion

The nitisinone serum concentrations increased in proportion to dose, as shown by the power model analysis of AUC and C_{max} data and supported by the similar clearance in all dose groups The median oral clearance in all 32 patients, 3.2 mL/h·kg, is in reasonable accordance with the data in HT-1 patients; 4.0 mL/h·kg (0.0956 L/kg · day). The fluctuation in nitisinone serum concentrations (C_{max}/C_{min} ratio) was relatively low, supporting previous reports of a long half-life (Hall et al. 2001).

We found that nitisinone decreased urinary excretion of HGA in a concentration-dependent manner, up to nitisinone serum concentrations of about 3 μmol/L. This concentration was reached with a dose of 8 mg daily in seven of the eight patients in that dose group, and these had a reduction in u-HGA_{24} from baseline of at least 99.4%. Despite this near 100% decrease in u-HGA, the amount excreted at the highest nitisinone concentrations, or dose, is still about 50 times higher than the highest amount (2.92 μmol/24 h) found in a recent study in 22 normal subjects, using the same analytical method as in our study (Davison et al. 2014). It is therefore possible that even higher doses and concentrations of nitisinone could lead to a complete normalization, which would correspond to a decrease in u-HGA from baseline of 99.98–100.00% in individual patients.

Assuming that the reduction in u-HGA reflects the degree of inhibition of HPPD, the results indicate that the enzyme is almost completely inhibited at a nitisinone concentration of 3 μmol/L. Nitisinone is extensively bound to serum albumin with a free fraction of about 4.5% at

Table 2 Serum concentration data (median and range) for HGA, tyrosine, and nitisinone in patients with AKU treated with nitisinone ($N = 8$ per dose group)

	Time	1 mg	2 mg	4 mg	8 mg
Nitisinone					
C_{av} (μmol/L)	Week 4	0.47 (0.3–0.8)	1.04 (0.7–1.6)	1.94 (1.3–2.6)	5.49 (2.3–7.9)
C_{min} (μmol/L)	Week 4	0.30 (<0.2–0.5)	0.70 (0.5–1.2)	1.40 (1.0–2.3)	4.55 (1.5–6.2)
C_{max} (μmol/L)	Week 4	0.70 (0.4–1.1)	1.55 (0.9–1.9)	2.50 (1.9–3.0)	7.30 (3.3–9.7)
CL/F (mL/h·kg)	Week 4	2.80 (1.8–6.7)	3.49 (1.7–4.6)	3.49 (1.9–5.2)	2.27 (1.6–5.0)
HGA					
C_{av} (μmol/L)	Baseline	32.96 (22.5–44.1)	34.21 (25.1–29.1)	37.69 (28.9–49.9)	38.61 (25.2–47.7)
	Week 4	3.93 (0.5–7.3)	3.32 (<3.1–5.8)	<1.3 (<1.3–1.3)	<0.4 (<0.4–0.4)
C_{max} (μmol/L)	Baseline	51.30 (40.8–69.9)	52.85 (39.8–72.9)	61.70 (48.4–88.3)	57.05 (38.8–78.2)
	Week 4	6.60 (4.3–10.7)	5.10 (<3.1–7.5)	3.40 (<3.1–4.7)	<3.1 (<3.1–3.2)
Tyrosine					
C_{av} (μmol/L)	Baseline	56.0 (50–61)	62.6 (46–79)	58.0 (47–75)	59.3 (50–82)
	Week 4	667.3 (511–879)	702.1 (596–948)	805.9 (639–1,059)	860.0 (627–970)
C_{max} (μmol/L)	Baseline	71.0 (57–113)	77.5 (59–100)	80.5 (57–114)	75.0 (62–120)
	Week 4	721.0 (594–978)	835.5 (662–1,010)	889.0 (696–1,155)	984.0 (715–1,066)

C_{av} average serum concentration during the 24-hour dosing interval ($C_{av} = AUC_{24}/24$), C_{min} minimum serum concentration, C_{max} maximum serum concentration, *CL/F* oral clearance

normal serum albumin concentrations (unpublished data). Thus, a total concentration of 3 μmol/L corresponds to an unbound concentration of approximately 135 nmol/L. This is in agreement with the maximum inhibition of HPPD by nitisinone seen in vitro (Ellis et al. 1995).

The results indicate a dose–response relationship between s-HGA and nitisinone, as the number of patients with s-HGA below the LLOQ increased with dose. An analysis of the relationship between C_{av} for s-HGA and nitisinone concentrations could not be performed due to the nonquantifiable s-HGA values. The decrease in s-HGA, from baseline to Week 4, which could be estimated for the 1-mg dose (approximately 88%), is in line with the previously reported decrease in u-HGA_{24} for that dose (Ranganath et al. 2014).

The s-HGA profile at baseline shows the expected increase with feeding due to a continuous supply of tyrosine. The circulating concentrations of both HGA and tyrosine show a fall after the last meal and true fasting late in the evening and night, reaching a nadir prior to feeding in the morning.

At baseline, serum tyrosine was normal in the AKU patients, despite the defect in HGD. Normal, non-AKU subjects had fasting serum tyrosine concentrations up to 88 μmol/L (Davison et al. 2014). The maximum daily average in AKU patients at baseline was 82 μmol/L.

In patients with AKU, renal clearance of HGA is 4–5 times creatinine clearance suggesting active secretion of HGA (Lustberg et al. 1969). An ongoing study of proximal tyrosine metabolites in samples from SONIA 1 may throw more light on this issue, but such data are as yet unavailable. The importance of a normal renal function has also been illustrated in an AKU patient with renal failure. He had exacerbated ochronosis and s-HGA levels about twice those of other AKU patients. After a renal transplant, the levels decreased to those normally seen in AKU, and u-HGA increased by 2–3 g per day (Introne et al. 2002).

Inhibiting HPPD leads to pronounced tyrosinemia even at low nitisinone doses. High serum concentrations of tyrosine are known to cause eye lesions in some patients due to high concentrations in the aqueous humor (Hanhart 1947; Lock et al. 2014). In the treatment of HT-1 with nitisinone, it is therefore recommended that serum tyrosine be kept below 400–500 μmol/L, by using a diet low in tyrosine and phenylalanine (Mayorandan et al. 2014; SmPC for Orfadin). Even the lowest dose in our study, 1 mg daily, resulted in tyrosine levels above this limit in every patient, indicating that diet restrictions may be required also if treating AKU patients with nitisinone, at least if such patients would develop eye symptoms due to tyrosinemia.

In conclusion, nitisinone exhibits dose-proportional pharmacokinetics in the studied dosage interval. Urinary excretion of HGA decreases in a concentration-dependent manner, while the increase in tyrosine is less clearly related to nitisinone concentrations.

Acknowledgements We wish to thank Jean Devine and Jeannette Usher in the Clinical Biochemistry and Metabolic Medicine for the handling of the serum and urine samples. We also want to thank Helen Bygott, Emily Luangrath-Nicholson, Richard Fitzgerald, and Asad Ullah at the Clinical Trials Units in Royal Liverpool University Hospital and Oľga Lukačová, Eva Vrtíková, and Vanda Mlynariková in the National Institute of Rheumatic Disease in Piešťany for the diligence shown in carrying out the study.

This study was part of the DevelopAKUre program, which received funding from the European Commission 7th Framework Program (FP7).

Synopsis (Take-Home Message)

In patients with alkaptonuria, nitisinone decreases urinary excretion of HGA in a concentration-dependent manner, while the increase in serum tyrosine is less clearly related to nitisinone concentrations.

Compliance with Ethics Guidelines

All procedures followed were in accordance with the ethical standards of the responsible committee on human experimentation (institutional and national) and with the Helsinki Declaration of 1975, as revised in 2008 (6).

Informed consent was obtained from all patients before being included in the study.

Animal rights: Not applicable for this clinical study.

The study EudraCT number is 2012-005340-24 and is registered at ClinicalTrials.gov with number NCTO1828463 and the title "Dose Response Study of Nitisinone in Alkaptonuria (SONIA1)."

Conflict of Interest

B Olsson and J Szamosi are Sobi employees and shareholders. All other authors declare that they have no conflict of interest.

Contributors

BO, LRR, AKH, TFC, JR contributed to the study design.

LRR, JR undertook medical procedures.

ATH, AMA developed analytical methods and analyzed study samples.

TFC, EEP, JS, BO contributed to the statistical analyses including PK calculations.

BO drafted the first version of the manuscript.

All authors contributed to the interpretation of data and writing and revision of the manuscript.

All authors approved the manuscript for publication.

References

Anikster Y, Nyhan WL, Gahl WA (1998) NTBC and alkaptonuria. Am J Hum Genet 63:920–921

Davison AS, Milan AM, Hughes AT et al (2014) Serum concentrations and urinary excretion of homogentisic acid and tyrosine in normal subjects. Clin Chem Lab Med. doi:10.1515/cclm-2014-0668

Ellis MK, Whitfield AC, Gowans LA et al (1995) Inhibition of 4-hydroxyphenylpyruvate dioxygenase by 2-(2-nitro-4-trifluoromethylbenzoyl)-cyclohexane-1,3-dione and 2-(2-chloro-4-methanesulfonylbenzoyl)-cyclohexane-1,3-dione. Toxicol Appl Pharmacol 133:12–19

Garrod AE (1902) About alkaptonuria. Med Chir Trans 85:69–78

Gough K, Hutchison M, Keene O et al (1995) Assessment of dose proportionality: report from the statisticians in the pharmaceutical industry/pharmaceutics UK joint working party. Drug Inf J 29:1039–1048

Hall MG, Wilks MF, Provan WM et al (2001) Pharmacokinetics and pharmacodynamics of NTBC (2-(2-nitro-4-fluoromethylbenzoyl)-1,3-cyclohexanedione) and mesotrione, inhibitors of 4-hydroxyphenyl pyruvate dioxygenase (HPPD) following a single dose to healthy male volunteers. Br J Clin Pharmacol 52:169–177

Hanhart E (1947) Neue sonderformen von keratosis palmo-plantaris, u.a. eine regelmässig-dominante mit systematisierten lipomen, ferner 2 einfach-rezessive mit schwachsinn und z.T. mit hornhautveränderungen des auges (ektodermalsyndrom). Dermatologica 94:286–308

Hughes AT, Milan AM, Christensen P et al (2014) Urine homogentisic acid and tyrosine: simultaneous analysis by liquid chromatography tandem mass spectrometry. J Chromatogr B Analyt Technol Biomed Life Sci 963:106–112. doi:10.1016/j.jchromb.2014.06.002

Hughes AT, Milan AM, Davison AS et al (2015) Serum markers in alkaptonuria: simultaneous analysis of homogentisic acid, tyrosine and nitisinone by liquid chromatography tandem mass spectrometry. Ann Clin Biochem pii:0004563215571969

Introne WJ, Phornphutkul C, Bernardini I et al (2002) Exacerbation of the ochronosis of alkaptonuria due to renal insufficiency and improvement after renal transplantation. Mol Genet Metab 77:136–142

Introne WJ, Perry MB, Troendle J et al (2011) A 3-year randomized therapeutic trial of nitisinone in alkaptonuria. Mol Genet Metab 103:307–314

Lindstedt S, Holme E, Lock EA et al (1992) Treatment of hereditary tyrosinaemia type I by inhibition of 4-hydroxyphenylpyruvate dioxygenase. Lancet 340:813–817

Lock E, Ranganath LR, Timmis O (2014) The role of nitisinone in tyrosine pathway disorders. Curr Rheumatol Rep 16:457

Lustberg TJ, Schulman JD, Seegmiller JE (1969) Metabolic fate of homogentisic acid-1–14 C (HGA) in alkaptonuria and effectiveness of ascorbic acid in preventing experimental ochronosis. Arthritis Rheum 12:678

Mayorandan S, Meyer U, Gokcay G et al (2014) Cross-sectional study of 168 patients with hepatorenal tyrosinaemia and implications for clinical practice. Orphanet J Rare Dis 9:107

O'Brien WM, La Du BN, Bunim JJ (1963) Biochemical, pathologic and clinical aspects of alcaptonuria, ochronosis and ochronotic arthropathy: review of world literature (1584–1962). Am J Med 34:813–838

Preston AJ, Keenan CM, Sutherland H et al (2013) Ochronotic osteoarthropathy in a mouse model of alkaptonuria, and its inhibition by nitisinone. Ann Rheum Dis 73(1):284–289

Ranganath LR, Jarvis JC, Gallagher JA (2013) Recent advances in management of alkaptonuria (invited review; best practice article). J Clin Pathol 66:367–373

Ranganath LR, Milan AM, Hughes AT (2014) Suitability of nitisinone in alkaptonuria 1 (SONIA 1): an international, multicenter, randomized, open-label, no-treatment controlled, parallel-group, dose–response study to investigate the effect of once daily nitisinone on 24-hour urinary homogentisic acid excretion in patients with alkaptonuria after 4 weeks of treatment. Ann Rheum Dis 1–6. doi:10.1136/annrheumdis-2014-206033

SmPC for Orfadin capsules. http://www.ema.europa.eu/docs/en_GB/document_library/EPAR_-_Product_Information/human/000555/WC500049195.pdf

Suzuki Y, Oda K, Yoshikawa Y et al (1999) A novel therapeutic trial of homogentisic aciduria in a murine model of alkaptonuria. J Hum Genet 44:79–84

Zannoni VG, Lomtevas N, Goldfinger S (1969) Oxidation of homogentisic acid to ochronotic pigment in connective tissue. Biochim Biophys Acta 177:94–105

JIMD Reports
DOI 10.1007/8904_2015_430

RESEARCH REPORT

Investigating the Robustness and Diagnostic Potential of Extracellular Matrix Remodelling Biomarkers in Alkaptonuria

F. Genovese • A.S. Siebuhr • K. Musa • J.A. Gallagher • A.M. Milan • M.A. Karsdal • J. Rovensky • A.C. Bay-Jensen • L.R. Ranganath

Received: 28 November 2014 / Revised: 09 February 2015 / Accepted: 23 February 2015 / Published online: 19 March 2015

Abstract *Background and aim*: Alkaptonuria (AKU) clinical manifestations resemble severe arthritis. The Suitability of Nitisinone in Alkaptonuria 1 (SONIA 1) study is a dose-finding trial for nitisinone treatment of AKU patients. We tested a panel of serum and urinary biomarkers reflecting extracellular matrix remodelling (ECMR) of cartilage, bone and connective tissue in SONIA 1 patients to identify non-invasive and diagnostic biomarkers of tissue turnover in AKU.

Methods: Fasted serum and urine were retrieved from 40 SONIA 1 patients and 44 healthy controls. Established biomarkers of bone remodelling (CTX-I, P1NP, OC), cartilage remodelling (CTX-II, C2M, AGNx1) and inflammation (CRPM) as well as exploratory biomarkers of ECMR (C6M, VCANM, MIM, TIM) were measured at baseline in serum and urine by means of enzyme-linked immunosorbent assays (ELISAs) or automated systems (Elecsys 2010).

Results: The levels of bone resorption (CTX-I) and cartilage degradation (C2M) were elevated in AKU patients as compared to controls ($p > 0.0001$ and $p = 0.03$, respectively). Also tissue inflammation (CRPM) was elevated in AKU patients ($p = 0.01$). In addition all four exploratory biomarkers of ECMR (C6M, VCANM, MIM, TIM) were elevated in AKU patients compared to healthy controls. CTX-II was the only biomarker to be reduced in AKU patients. TIM was the only marker that showed a higher concentration than the normal assay range in AKU patients.

Conclusions: We have identified new potential biomarkers for assessment of cartilage, bone and cardiovascular remodelling in AKU and demonstrated the robustness of the assays used to measure the biomarker concentration in biological fluids.

Communicated by: Verena Peters

Competing interests: None declared

Electronic supplementary material: The online version of this chapter (doi:10.1007/8904_2015_430) contains supplementary material, which is available to authorized users.

F. Genovese (✉) · A.S. Siebuhr · K. Musa · M.A. Karsdal · A.C. Bay-Jensen
Nordic Bioscience, Herlev Hovedgade 205, 2730, Herlev, Denmark
e-mail: fge@nordicbioscience.com

J.A. Gallagher · A.M. Milan · L.R. Ranganath
Department of Musculoskeletal Biology, Institute of Ageing and Chronic Disease, University of Liverpool, Liverpool L69 3GE, UK

A.M. Milan · L.R. Ranganath
Department of Clinical Biochemistry and Metabolic Medicine, Royal Liverpool University Hospital Trust, Prescot Street, Liverpool L7 8XP, UK

J. Rovensky
National Institute of Rheumatic Diseases, Nabrezie, Ivana Krasku 4, 921 01 Piešťany, Slovakia

Introduction

Alkaptonuria (AKU, OMIM disorder accession number 203500) is an ultra orphan autosomal recessive disorder caused by the deficiency of the enzyme homogentisate 1,2-dioxygenase (HGO). HGO is responsible for the breakdown of homogentisic acid (HGA) into 4-maleylacetoacetate during the tyrosine and phenylalanine catabolism. Accumulated HGA can be oxidised to a melanin-like polymeric pigment via benzoquinone acetic acid (BQA), which in turn is deposited in connective tissues in a process termed ochronosis. Cartilage appears to be a preferred site for ochronosis, and one of the earliest and most severe

clinical manifestations is a premature osteoarthropathy resembling osteoarthritis, which begins to occur around the age of 30 years. Progressive arthritic pain affects the spine and weight-bearing joints, which develops into kyphoscoliosis, impaired spinal and thoracic mobility disc disease/prolapse and vertebral and long bone fractures. Hearing loss, cardiac arrhythmias and congestive cardiac failure also occur in 40, 40 and 10%, respectively of all AKU patients (Ranganath et al. 2013). AKU has an incidence of 1:250,000–1,000,000, which increases to 1:19,000 in restricted communities, e.g. in Slovakia (Zatkova 2011). AKU is diagnosed by urine homogentisic acid measurement following clinical suspicion in case of symptoms such as dark urine, staining of nappies in babies and pigmentation in the ears and eyes.

Because of the similarities and the differences of joint destruction in AKU and osteoarthritis and the rapid progression of joint disease in AKU, we decided to investigate biomarkers previously tested in arthritis in AKU. Several protease-dependent ECM remodelling biomarkers (neo-epitope) of cartilage degradation and bone resorption have been described in arthritis-related literature; the most characterised and validated are CTX-II (matrix metalloproteinase (MMP)-dependent type II collagen degradation) indicating subchondral remodelling (Dam et al. 2009a) and CTX-I (cathepsin K-dependent type I collagen degradation) and OC (osteocalcin) indicating bone resorption and formation, respectively (Garnero et al. 2003; Rosenquist et al. 1995). Other cartilage and bone biomarkers have shown promising results in arthritis, such as AGNxI (aggrecanase-mediated aggrecan degradation), C2M (MMP-mediated type II collagen degradation) (Siebuhr et al. 2014; Dorleijn et al. 2014; Bay-Jensen et al. 2014) and P1NP (type I collagen formation) (Siebuhr et al. 2012). Moreover, since the pathology of ochronosis may involve the cardiac cartilage, with clinical manifestations such as cardiac arrhythmias and congestive cardiac failure, our interest was to investigate also potential biomarkers of cardiac and vascular remodelling. TIM (MMP-mediated titin degradation) is a biomarker for cardiac remodelling (Vassiliadis et al. 2012), and VCANM (MMP-mediated versican degradation) and MIM (MMP-mediated mimecan degradation) were previously associated with atherosclerosis (Barascuk et al. 2013; Barascuk et al. 2011). The biomarker for MMP-mediated type VI collagen remodelling C6M and the inflammatory biomarker CRPM (MMP-mediated degradation of C-reactive protein) (Veidal et al. 2011; Skjot-Arkil et al. 2012) were also considered as possible AKU diagnostic biomarkers. Type VI collagen is a prominent component of articular cartilage (Soder et al. 2002), and CRPM was shown as a biomarker for local inflammation in another articular disease, ankylosing spondylitis (Skjot-Arkil et al. 2012).

The currently available treatment is mostly palliative, with lifelong analgesia and joint surgery. Suitability of Nitisinone in Alkaptonuria 1 (SONIA 1) is a randomised clinical study for nitisinone dose selection to treat AKU patients (Ranganath et al. 2014). Nitisinone is a competitive inhibitor of the enzyme 4-hydroxyphenylpyruvate dioxygenase, which metabolises 4-hydroxyphenylpyruvate to HGA, which therefore prevents HGA formation. A recent study has demonstrated that nitisinone blocks the formation of the ochronotic pigment in a mouse model of AKU (Preston et al. 2014). Here we analysed the mentioned biomarkers of extracellular matrix remodelling in the serum and urine of SONIA 1 patients, in order to identify possible biomarkers of disease status.

Methods

Clinical Cohort

SONIA 1 is a randomised, open-label, parallel-group study with a no-treatment control group. The study was conducted at two sites, Liverpool (United Kingdom) and Piešťany (Slovakia).

Patients were recruited if they were 18 years and older, with proven increased homogentisic acid excretion in the urine. Ochronosis was not a requirement for participation; however, 80% of the patients presented observable signs of ochronosis in the ears, eyes or skin at enrolment. Forty AKU patients were randomised into five groups (eight patients per group) to receive either 1, 2, 4 or 8 mg nitisinone once daily or no treatment (control) for 4 weeks. Serum and urine (first morning void) were collected at baseline, 2 weeks and 4 weeks. Detailed information on the study has previously been published (Ranganath et al. 2014). Forty-four healthy individuals were used as a control group. Serum and urine (first morning void, 40 samples) were collected in Denmark from healthy volunteers and elderly women enrolled in a variety of studies at CCBR, Ballerup (Dam et al. 2009b). Demographics of the patients enrolled in the study that were considered for this work and of healthy controls are detailed in Table 1.

Measurements

Selected biomarkers for extracellular matrix remodelling were measured in the serum and urine of AKU patients (SONIA 1 baseline) and healthy controls to detect which of the biomarkers had increased concentration in AKU in order to profile the turnover of cartilage and bone in AKU patients. Established biomarkers of bone formation and resorption and cartilage remodelling were measured together with more exploratory biomarkers for extracellular

Table 1 Demographics of SONIA 1 population and controls

Parameter	AKU pts Liverpool	AKU pts Piestany	Controls (serum)	Controls (urine)
Number	15	25	44	40
Age (mean; min–max)	48.3; 32–60	47.1; 19–63	58.6; 22–79	46.9; 22–68
Gender (male/female)	12/3	15/10	3/41	6/34
BMI (mean; min–max)	27.6; 19.6–40.3	28.0; 21.3–42.3	–	–

Table 2 Biomarkers measured in the SONIA 1 study

Biomarker	Matrix	Specification	Indication	References
AGNx1	Serum	Aggrecan degradation mediated by aggrecanase	Cartilage remodelling	Wang et al. (2009)
C2M	Serum	Collagen type II degradation mediated by MMPs	Cartilage remodelling	Bay-Jensen et al. (2011)
CTX-II	Urine	C-telopeptide of collagen type II	Cartilage remodelling	Dam et al. (2009a)
C6M	Serum	Collagen type VI degradation mediated by MMPs	Cartilage remodelling	Veidal et al. (2011)
P1NP	Serum	Collagen type I pro-peptide	Bone formation	Leeming et al. (2010)
OC	Serum	Osteocalcin	Bone formation	Rosenquist et al. (1995)
CTX-I	Serum and urine	Collagen type I degradation mediated by cathepsin K and cross-linking	Bone resorption	Garnero et al. (2003)
CRPM	Serum	C-reactive protein degradation mediated by MMPs	Local inflammation	Skjot-Arkil et al. (2012)
MIM	Serum	Mimecan degradation mediated by MMPs	Cardiovascular remodelling	Barascuk et al. (2011)
TIM	Serum	Titin degradation mediated by MMPs	Cardiovascular remodelling	Vassiliadis et al. (2012)
VCANM	Serum	Versican degradation mediated by MMPs	Cardiovascular remodelling	Barascuk et al. (2013)

matrix remodelling. The biomarkers measured in the study and the bibliographic references for the corresponding assays are listed in Table 2. All commercial assays were run following manufacturer's instructions. β-CrossLaps Elecsys 2010 was used for the measurement of CTX-I, U-CartiLaps ELISA for the measurement of CTX-II, N-MID Osteocalcin Elecsys 2010 for the measurement of OC and P1NP Elecsys 2010 for the measurement of P1NP. All other assays (C2M, AGNx1, C6M, CRPM, TIM, VCANM, MIM) were competitive ELISAs developed at Nordic Bioscience and performed according to the protocols detailed in the indicated references. CTX-II was measured in the urine, and CTX-I was measured in both the serum and urine. The concentration of the urinary biomarkers was normalised for urine creatinine. All other biomarkers were measured only in the serum.

Robustness Analysis

The robustness of the biomarkers in this cohort was evaluated by observing their dependence from demographic parameters, such as age, gender and BMI, from collection site and from collection time. To explore this last point, we used repeated samples from six SONIA 1 patients collected over 24 h: two baseline samples, two samples after 1 month of treatment with 8 mg/day nitisinone and two samples after 1 month in the non-treated arm. The variation is shown as % change from time 0. A % change <20% was considered in the limits of intrinsic variation of the assay. This evaluation was performed in serum assays only, since the 24 h collection of urine was done by acidifying the urine and this procedure was incompatible with the assays used. The concentration range of normal samples (normal range) specified in the ELISA protocols was used as standard to compare the values of the biomarkers measured in the study.

Creatinine Assessment

The urinary biomarkers were normalised for levels of urine creatinine. Since AKU patients have high levels of homogentisic acid (HGA) in their urine, the possibility that HGA could interfere with the enzymatic creatinine assay was explored. In order to assess the possible interference of HGA with the creatinine assessment, the creatinine levels measured by a creatininase-based reaction assay and by a Jaffé-based reaction assay were compared. Creatinine was assessed in first void morning urine of AKU patients using two different commercial assays. Urine creatinine was measured on the Siemens Advia 1800 analyser, using an

enzymatic creatinine assay, based upon the conversion of creatinine to glycine, formaldehyde and hydrogen peroxide, catalysed by creatininase and sarcosine oxidase. Urine creatinine was also measured using the creatinine Jaffé method on the COBAS 701 analyser where creatinine forms a yellow-orange complex with picrate at an alkaline pH.

Assessment of HGA Interference with Hydroxyperoxidase-Based ELISAs

To assess the possible interference of HGA with the peroxidase-based detection system in the ELISAs, three serum samples (one with no HGA, one with low HGA and one with high HGA) and three urine samples (one with no HGA, one with low HGA and one with high HGA) were spiked with twofold diluted HGA starting from 20 mM. The recovery of the analyte was investigated in the CRPM ELISA for serum and in the U-CartiLaps ELISA (CTX-II) for urine, taken as representative assays for serum and urine measurements, considering as 100% the concentration of the sample without HGA added.

Results

Robustness Analysis of the Biomarkers

P1NP, N-MID and VCANM showed a good stability over 24 h, presenting an average variation <10%. C6M, CRPM and TIM presented an average variation <20%, but they presented outliners that showed a higher variation. AGNx1, CTX-I, C2M and MIM showed an average variation >20% during the day. None of the biomarkers were age dependent. Only CTX-II/creatinine was significantly more elevated in the urine of female AKU patients than male. The same trend was observable in the control group although the difference was not significant ($p = 0.06$). Only CTX-I measured in the serum was significantly lower in obese patients compared to patients with normal weight. A similar tendency, although not significant, was observed in urine levels of CTX-I. Urine CTX-I and serum TIM levels were significantly different in patients enrolled in Liverpool and in Piešťany. The results of the robustness analysis are summarised in Fig. S1 and Table S1 of the supplementary data.

Interference of HGA with Enzyme-Based Assays

Figure S2 of the supplementary data shows the correlation between the creatinine concentration obtained using the two assays for creatinine measurement in urine samples with HGA/creatinine levels >600 μmol/mmol and in urine samples with HGA/creatinine <600 μmol/mmol. While the creatinine levels measured in the two assays were strongly correlated in samples containing HGA at very low levels (Fig. S2b), the creatininase-based assay underestimated the concentration of creatinine in samples with high HGA content (Fig. S2a). The Jaffé-based reaction assay was then used in the assessment of urine creatinine used to normalise the urinary marker CTX-II.

Table S2 and S3 show the recovery of analyte concentration in the assay for urinary CTX-I and serological CRPM. The average recovery was within the accepted values in the presence of decreasing concentrations of HGA spiked in the samples. This was particularly valid in alkaptonuric patient samples, in which HGA was already present. The initial concentration of 20 mM represents the maximum concentration present in the urine of AKU patients.

Diagnostic Markers of ECM Remodelling in AKU

As summarised in Table 3, the biomarkers for cartilage degradation C2M and C6M, for bone resorption CTX-I, for chronic inflammation CRPM and for cardiovascular remodelling MIM, TIM and VCANM were significantly more elevated in SONIA 1 patients than in healthy controls. The biomarker for subchondral cartilage remodelling CTX-II was less concentrated in the urine of SONIA 1 patients than in healthy urine. TIM was the biomarker that showed the best separation between the two groups, with an area under the receiving operating curve close to 0.9 (Fig. 1). All biomarker concentration was within the concentration range indicated in the assay protocol, which is based on measurement on serum and urine from the normal population (Table 3), except TIM in SONIA 1 patients, which was markedly more elevated than the highest concentration range.

None of the biomarkers changed following 1 month of treatment with nitisinone at any dose (Table S4).

Discussion

This is the first study exploring the protease-dependent cartilage and bone extracellular matrix remodelling in AKU patients. We have observed the basal levels of ECM turnover in patients with AKU enrolled in the SONIA 1 clinical study. We could not detect any change in the levels of the biomarkers following treatment, probably due to the short observation period; however, we were able to identify some promising diagnostic biomarkers, which can describe ochronosis features with respect to bone and cartilage remodelling.

To investigate the robustness of our biomarkers for their use in clinical studies, we evaluated the possible dependence of the biomarkers from age, BMI, gender and site of sample collection. The biomarkers were not different in

Table 3 Concentration of the serological and urinary biomarkers in SONIA 1 patients (baseline levels) and in healthy controls. Normal range of the biomarkers in serum and urine samples according to the assay protocol and statistical difference among the two groups calculated by Mann–Whitney test

Biomarker (measured in)[a]	AKU	Controls	Normal range	*p*-value	AUROC (cut-off)
AGNx1 (serum)	11.04 (12.68)	8.14 (7.13)	2.3–37	0.21	
C2M (serum)	0.30 (0.17)	0.24 (0.08)	0.16–0.94	0.03	0.632 (>0.21)
C6M (serum)	12.75 (5.04)	9.24 (4.22)	6.0–25.4	0.001	0.755 (>8.6)
CRPM (serum)	10.30 (2.72)	8.92 (2.22)	4.8–11.7	0.01	0.663 (>9.9)
CTX-I (serum)	0.52 (0.20)	0.31 (0.12)	0.025–1.008	<0.0001	0.837 (>0.35)
CTX-I/Cre (urine)	2.94 (3.15)	2.34 (1.51)	–	0.28	
CTX-II/Cre (urine)	0.51 (0.48)	0.78 (0.70)	0.65–1.17	0.05	0.643 (≤0.6)
MIM (serum)	25.27 (13.06)	12.48 (4.17)	4.58–32.76	<0.0001	0.880 (>13.4)
OC (serum)	26.99 (10.49)	24.53 (7.01)	11–46	0.22	
P1NP (serum)	68.85 (29.31)	57.72 (18.75)	15.13–73.87	0.047	
TIM (serum)	231.21 (63.37)	133.23 (56.81)	111–197	<0.0001	0.898 (>161.9)
VCANM (serum)	1.51 (0.32)	1.38 (0.24)	0.94–1.52	0.043	0.633 (>1.5)

[a] Biomarkers measured in ng/ml except CTX-I/Cre and CTX-II/Cre, µg/mmol creatinine

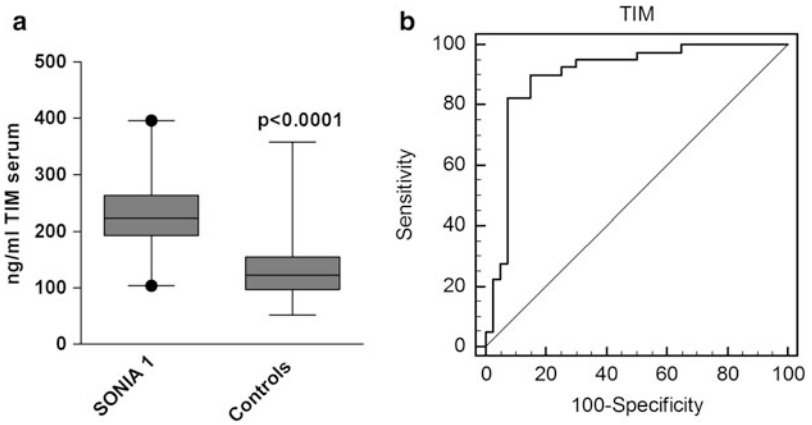

Fig. 1 Diagnostic potential of TIM. (**a**) Concentration levels in the serum of SONIA 1 patients and healthy controls; (**b**) AUROC for TIM (cut-off: 161.9 ng/ml)

various age and gender groups. CTX-I, a biomarker for bone resorption, was decreased in obese patients, suggesting that obese AKU patients present a reduced bone remodelling. Urinary levels of CTX-I were reduced, and serological levels of TIM were increased in patients enrolled in Liverpool compared to patients enrolled in Piešťany. The patients enrolled in Liverpool came from different European nations, and it is therefore not possible to identify a common trait in different lifestyle and eating habits that could explain the difference in the biomarkers. We evaluated the circadian variation of the biomarkers and showed that most of the serum biomarkers had little to none variation in the serum of SONIA 1 patients in 24 hours. The only biomarkers which showed a variation not imputable to the assay normal variation were AGNx1, CTX-I, C2M and MIM. This information is novel for the exploratory biomarkers MIM and for AGNx1 and C2M, but this tendency has already been demonstrated and discussed for CTX-I (Karsdal et al. 2008). It is possible to conclude that such variation did not affect the present study, since the sampling was performed at the same time in all patients and in all visits, but it must be taken into consideration in case of different study designs.

As part of the robustness analysis, we also investigated, following indications from previous literature (Curtis et al. 2014), whether the presence of high concentration of HGA in the urine of AKU patients could interfere with the enzymatic reaction of the creatininase used in the creatinine

assay and of the peroxidase used in the ELISAs. The correlation analysis of the creatinine levels measured with a creatininase-based assay and a Jaffé-based assay, which is not influenced by HGA, demonstrated that high urinary HGA levels interfere with the creatininase, leading to a lower signal and an underestimation of creatinine concentration. Therefore, a Jaffé-based assay is to be used for a correct estimation of urine creatinine in AKU patients, especially pre-nitisinone when urine HGA is greatest. On the contrary the peroxidase-based serum and urine assays seemed not to be affected by high levels of HGA, as demonstrated by the spiking experiment.

In AKU it is commonly held that cartilage is the predominantly affected tissue, whereas unbalanced bone remodelling is limited. However, recent evidences suggest that changes within the bone compartment occur in AKU patients (Taylor et al. 2012a). Furthermore, these changes in bone were more frequent in AKU (100%) than OA (70%) (Taylor et al. 2012a). CTX-I and OC have been heavily studied as a measure of bone balance in arthritis. In ankylosing spondylitis CTX-I and OC separately were shown to be associated with disease duration, and an association between the biomarkers indicated the skewed turnover of bone in ankylosing spondylitis (Arends et al. 2012). CTX-I alone was studied in RA numerous times and was associated with disease progression and disease activity (Syversen et al. 2009). However, in OA the results on CTX-I were contrary (Karsdal et al. 2010). In arthritis CTX-II was shown to be related to joint erosions and revealed a predictive value for radiographic progression (Hashimoto et al. 2009). In addition, CTX-II was associated with disease activity of ankylosing spondylitis (Pedersen et al. 2011) and correlated with inflammation (Vosse et al. 2008). The cartilage biomarker, C2M, was shown to be able to discriminate between early responders and nonresponders in RA patients treated with tocilizumab (Bay-Jensen et al. 2014).

In SONIA 1 patients' serum CTX-I was elevated when compared to healthy control and the biomarker could separate efficiently the two groups (AUROC: 0.837). The levels of the biomarker in SONIA 1 patients were the same as previously observed in RA patients (data not shown). P1NP, a biomarker for bone formation, was elevated in AKU patients compared to controls despite the magnitude of the difference was not as elevated as for CTX-I. These results support the histological findings that pathological bone turnover is a feature of AKU. Nevertheless, OC was not elevated in this population, which is consistent with the focal uncoupling of resorption and formation in subchondral trabecular bone. Among the cartilage degradation biomarkers, C2M and CTX-II levels were significantly different between AKU patients and controls. C2M increased in AKU patients, with levels comparable to those observed in noninflammatory OA and early RA, but lower than those observed in inflammatory OA and severe RA (data not shown). The same observation can be done regarding the levels of CRPM, a biomarker for local chronic inflammation which, despite being more elevated in AKU patients than in the controls, presented lower levels than in other rheumatologic disease such as inflammatory OA and RA (data not shown). The urinary levels of CTX-II were on the contrary lower in SONIA 1 patients. This is likely to be related to the extensive pigmentation of cartilage making it resistant to proteolytic degradation. Histological studies on joints obtained from AKU patients at arthroplasty (Taylor et al. 2011), and from AKU mice (Preston et al. 2014; Taylor et al. 2012b), have in fact revealed that the earliest deposition of ochronotic pigment is in isolated chondrons in calcified cartilage. Subsequently the pigmentation proliferates into the hyaline articular cartilage and eventually to the articular surface. Pigmentation makes the cartilage stiff and resistant to proteolysis. Once the cartilage is extensively pigmented, there are severe focal changes in bone remodelling possibly as a result of stress shielding from the stiffened ochronotic cartilage. The subchondral plate can be completely resorbed by osteoclastic action (Taylor et al. 2011), and there is a focal uncoupling of resorption resulting in the formation of trabecular excrescences (Taylor et al. 2012a). However, a limitation of this study lies in the different ratio of female/male in the AKU group compared to the control group. Due to limitation in sample availability, the control cohort included mostly females, while SONIA 1 patients were prevalently males. This could have led to a misinterpretation of the CTX-II results, since this marker is the only one affected by gender, being higher in the urine of females. The higher mean values of CTX-II in the control group could then potentially be a consequence of such difference in the two groups. Moreover, despite it is not known whether females have different ochronosis levels, it is known that generally females develop arthropathy later than males. This has been taken into account by having an older control cohort for the serum marker measurements, but not for the urine measurements, and this could further have affected the CTX-II results. Another limitation lies in the use of controls and patients from different nations. Given the differences in some markers in patients enrolled in the two study sites, it is not possible to exclude that cultural differences, such as dietary habits, could influence the marker levels in serum and urine also in the control cohort.

A longitudinal study including measurements of disease severity will be required to investigate the burden of disease and prognostic potential of these biomarkers and observe similarity and differences with other rheumatic diseases.

Cardiovascular implications have been described in AKU for more than 20 years (Kenny et al. 1990). The working hypothesis is that the deposition of the pigment could lead to injury to the vascular endothelium causing formation of atheroma (Lok et al. 2013). The versican fragment VCANM was associated with the remodelling of the atherosclerotic plaque in patients with cardiovascular diseases (Barascuk et al. 2013). MIM, a fragment reflecting the MMP-mediated degradation of the proteoglycan mimecan, was also preliminarily associated with the cardiovascular remodelling in a mouse model of atherosclerosis (Barascuk et al. 2011). Therefore, the elevation of these biomarkers in the serum of SONIA 1 patients can reflect the atheroma remodelling occurring in AKU. TIM is a biomarker for heart remodelling, and it was found elevated in patients with coronary calcifications and other cardiovascular morbidities (Vassiliadis et al. 2012). We observed an elevation of this biomarker in the serum of AKU patients, and this finding is in accordance with previous reports of calcifications in the cardiac valves due to the accumulation of the ochronotic pigment and presence of inflammatory cells (Millucci et al. 2014a; Millucci et al. 2014b), which may produce the proteases responsible for the cleavage of the titin fragment identified by the TIM assay.

Conclusions

In this study we have presented robust and well-characterised tools to measure the levels of pathological extracellular matrix turnover related to bone, cartilage and cardiovascular remodelling in ochronotic patients. The biomarkers that showed an elevation in SONIA 1 patients may be used in a successive clinical study investigating the suitability of nitisinone treatment for a longer period. Such longitudinal study would allow identifying possible biomarkers of treatment efficacy and biomarkers for disease progression, to be used for personalised healthcare and patient management in the future.

Acknowledgements This study was funded by the European Union Seventh Framework Programme (project 304985) and by the Danish Research Fund ("Den Danske Forskningsfond").

Synopsis

Robust assays for non-invasive assessment of extracellular matrix turnover biomarkers can be used to describe the cartilage, bone and cardiovascular remodelling in alkaptonuria patients.

Compliance with Ethics Guidelines

Conflict of Interests

Federica Genovese is a full-time employee at Nordic Bioscience.

Anne Sofie Siebuhr is a full-time employee at Nordic Bioscience.

Kishwar Musa is a full-time employee at Nordic Bioscience.

Morten Karsdal is a full-time employee and holds shares at Nordic Bioscience.

Anne-Christine Bay-Jensen is a full-time employee and holds shares at Nordic Bioscience.

James Gallagher, Anna Milan, Jozef Rovensky and Lakshminarayan Ranganath declare that they have no conflict of interest.

Informed Consent

All procedures followed were in accordance with the ethical standards of the responsible committee on human experimentation (institutional and national) and with the Helsinki Declaration of 1975, as revised in 2000. Informed consent was obtained from all patients for being included in the study.

Details of the Contributions of Individual Authors

Federica Genovese, Anne-Christine Bay-Jensen, Morten Karsdal, Jozef Rovensky and Lakshminarayan Ranganath conceived and designed the study; Kishwar Musa and Anna Milan performed the analysis; Federica Genovese, Anna Milan, Anne Sofie Siebuhr and Anne-Christine Bay-Jensen interpreted the data; Federica Genovese, Anne Sofie Siebuhr, James Gallagher, Anna Milan and Anne-Christine Bay-Jensen drafted the manuscript; and Anne-Christine Bay-Jensen, James Gallagher and Morten Karsdal revised the manuscript critically for important intellectual content.

References

Arends S, Spoorenberg A, Houtman PM, Leijsma MK, Bos R, Kallenberg CG, Groen H, Brouwer E, van der V (2012) The effect of three years of TNFalpha blocking therapy on markers of bone turnover and their predictive value for treatment discontinuation in patients with ankylosing spondylitis: a prospective longitudinal observational cohort study. Arthritis Res Ther 14:R98

Barascuk N, Vassiliadis E, Zheng Q, Wang Y, Wang W, Larsen L, Rasmussen LM, Karsdal MA (2011) Levels of circulating

MMCN-151, a degradation product of mimecan, reflect pathological extracellular matrix remodeling in apolipoprotein E knockout mice. Biomark Insights 6:97–106

Barascuk N, Genovese F, Larsen L, Byrjalsen I, Zheng Q, Sun S, Hosbond S, Poulsen TS, Diederichsen A, Jensen JM, Mickley H, Register TC, Rasmussen LM, Leeming DJ, Christiansen C, Karsdal MA (2013) A MMP derived versican neo-epitope is elevated in plasma from patients with atherosclerotic heart disease. Int J Clin Exp Med 6:174–184

Bay-Jensen AC, Liu Q, Byrjalsen I, Li Y, Wang J, Pedersen C, Leeming DJ, Dam EB, Zheng Q, Qvist P, Karsdal MA (2011) Enzyme-linked immunosorbent assay (ELISAs) for metalloproteinase derived type II collagen neoepitope, CIIM–increased serum CIIM in subjects with severe radiographic osteoarthritis. Clin Biochem 44:423–429

Bay-Jensen AC, Platt A, Byrjalsen I, Vergnoud P, Christiansen C, Karsdal MA (2014) Effect of tocilizumab combined with methotrexate on circulating biomarkers of synovium, cartilage, and bone in the LITHE study. Semin Arthritis Rheum 43:470–478

Curtis SL, Roberts NB, Ranganath LR (2014) Interferences of homogentisic acid (HGA) on routine clinical chemistry assays in serum and urine and the implications for biochemical monitoring of patients with alkaptonuria. Clin Biochem 47:640–647

Dam EB, Byrjalsen I, Karsdal MA, Qvist P, Christiansen C (2009a) Increased urinary excretion of C-telopeptides of type II collagen (CTX-II) predicts cartilage loss over 21 months by MRI. Osteoarthritis Cartilage 17:384–389

Dam EB, Loog M, Christiansen C, Byrjalsen I, Folkesson J, Nielsen M, Qazi AA, Pettersen PC, Garnero P, Karsdal MA (2009b) Identification of progressors in osteoarthritis by combining biochemical and MRI-based markers. Arthritis Res Ther 11:R115

Dorleijn DM, Luijsterburg PA, Bay-Jensen AC, Siebuhr AS, Karsdal MA, Rozendaal RM, Bos PK, Bierma-Zeinstra SM (2014) Association between biochemical cartilage markers and clinical symptoms in patients with hip osteoarthritis: cohort study with 2-year follow-up. Osteoarthritis Cartilage 23:57–62

Garnero P, Ferreras M, Karsdal MA, Nicamhlaoibh R, Risteli J, Borel O, Qvist P, Delmas PD, Foged NT, Delaisse JM (2003) The type I collagen fragments ICTP and CTX reveal distinct enzymatic pathways of bone collagen degradation. J Bone Miner Res 18:859–867

Hashimoto J, Garnero P, van der HD, Miyasaka N, Yamamoto K, Kawai S, Takeuchi T, Yoshikawa H, Nishimoto N (2009) A combination of biochemical markers of cartilage and bone turnover, radiographic damage and body mass index to predict the progression of joint destruction in patients with rheumatoid arthritis treated with disease-modifying anti-rheumatic drugs. Mod Rheumatol 19:273–282

Karsdal MA, Byrjalsen I, Riis BJ, Christiansen C (2008) Investigation of the diurnal variation in bone resorption for optimal drug delivery and efficacy in osteoporosis with oral calcitonin. BMC Clin Pharmacol 8:12

Karsdal MA, Byrjalsen I, Bay-Jensen AC, Henriksen K, Riis BJ, Christiansen C (2010) Biochemical markers identify influences on bone and cartilage degradation in osteoarthritis–the effect of sex, Kellgren-Lawrence (KL) score, body mass index (BMI), oral salmon calcitonin (sCT) treatment and diurnal variation. BMC Musculoskelet Disord 11:125

Kenny D, Ptacin MJ, Bamrah VS, Almagro U (1990) Cardiovascular ochronosis: a case report and review of the medical literature. Cardiology 77:477–483

Leeming DJ, Larsen DV, Zhang C, Hi Y, Veidal SS, Nielsen RH, Henriksen K, Zheng Q, Barkholt V, Riis BJ, Byrjalsen I, Qvist P, Karsdal MA (2010) Enzyme-linked immunosorbent serum assays (ELISAs) for rat and human N-terminal pro-peptide of collagen type I (PINP)–assessment of corresponding epitopes. Clin Biochem 43:1249–1256

Lok ZS, Goldstein J, Smith JA (2013) Alkaptonuria-associated aortic stenosis. J Card Surg 28:417–420

Millucci L, Ghezzi L, Paccagnini E, Giorgetti G, Viti C, Braconi D, Laschi M, Geminiani M, Soldani P, Lupetti P, Orlandini M, Benvenuti C, Perfetto F, Spreafico A, Bernardini G, Santucci A (2014a) Amyloidosis, inflammation, and oxidative stress in the heart of an alkaptonuric patient. Mediators Inflamm 2014:258471

Millucci L, Ghezzi L, Braconi D, Laschi M, Geminiani M, Amato L, Orlandini M, Benvenuti C, Bernardini G, Santucci A (2014b) Secondary amyloidosis in an alkaptonuric aortic valve. Int J Cardiol 172:e121–e123

Pedersen SJ, Sorensen IJ, Garnero P, Johansen JS, Madsen OR, Tvede N, Hansen MS, Thamsborg G, Andersen LS, Majgaard O, Loft AG, Erlendsson J, Asmussen K, Jurik AG, Moller J, Hasselquist M, Mikkelsen D, Skjodt T, Lambert R, Hansen A, Ostergaard M (2011) ASDAS, BASDAI and different treatment responses and their relation to biomarkers of inflammation, cartilage and bone turnover in patients with axial spondyloarthritis treated with TNFalpha inhibitors. Ann Rheum Dis 70:1375–1381

Preston AJ, Keenan CM, Sutherland H, Wilson PJ, Wlodarski B, Taylor AM, Williams DP, Ranganath LR, Gallagher JA, Jarvis JC (2014) Ochronotic osteoarthropathy in a mouse model of alkaptonuria, and its inhibition by nitisinone. Ann Rheum Dis 73:284–289

Ranganath LR, Jarvis JC, Gallagher JA (2013) Recent advances in management of alkaptonuria (invited review; best practice article). J Clin Pathol 66:367–373

Ranganath LR, Milan AM, Huges AT (2014) Suitability of nitisinone in alkaptonuria 1 (SONIA 1): an international, multicenter, randomized, open-label, no-treatment controlled, parallel-group, dose–response study to investigate the effect of once daily nitisinone on 24-hour urinary homogentisic acid excretion in patients with alkaptonuria after 4 weeks of treatment. Ann Rheum Dis 0:1–6

Rosenquist C, Qvist P, Bjarnason N, Christiansen C (1995) Measurement of a more stable region of osteocalcin in serum by ELISA with two monoclonal antibodies. Clin Chem 41:1439–1445

Siebuhr AS, Wang J, Karsdal M, Bay-Jensen AC, Jin Y, Zheng Q (2012) Matrix metalloproteinase-dependent turnover of cartilage, synovial membrane, and connective tissue is elevated in rats with collagen induced arthritis. J Transl Med 10:195

Siebuhr AS, Petersen KK, Rendt-Nielsen Z, Egsgaard LL, Eskehave T, Christiansen C, Simonsen O, Hoeck HC, Karsdal MA, Bay-Jensen AC (2014) Identification and characterisation of osteoarthritis patients with inflammation derived tissue turnover. Osteoarthritis Cartilage 22:44–50

Skjot-Arkil H, Schett G, Zhang C, Larsen DV, Wang Y, Zheng Q, Larsen MR, Nawrocki A, Bay-Jensen AC, Henriksen K, Christiansen C, Alexandersen P, Leeming DJ, Karsdal MA (2012) Investigation of two novel biochemical markers of inflammation, matrix metalloproteinase and cathepsin generated fragments of C-reactive protein, in patients with ankylosing spondylitis. Clin Exp Rheumatol 30:371–379

Soder S, Hambach L, Lissner R, Kirchner T, Aigner T (2002) Ultrastructural localization of type VI collagen in normal adult and osteoarthritic human articular cartilage. Osteoarthritis Cartilage 10:464–470

Syversen SW, Goll GL, van der HD, Landewe R, Gaarder PI, Odegard S, Haavardsholm EA, Kvien TK (2009) Cartilage and bone biomarkers in rheumatoid arthritis: prediction of 10-year radiographic progression. J Rheumatol 36:266–272

Taylor AM, Boyde A, Wilson PJ, Jarvis JC, Davidson JS, Hunt JA, Ranganath LR, Gallagher JA (2011) The role of calcified

cartilage and subchondral bone in the initiation and progression of ochronotic arthropathy in alkaptonuria. Arthritis Rheum 63:3887–3896

Taylor AM, Boyde A, Davidson JS, Jarvis JC, Ranganath LR, Gallagher JA (2012a) Identification of trabecular excrescences, novel microanatomical structures, present in bone in osteo-arthropathies. Eur Cell Mater 23:300–308

Taylor AM, Preston AJ, Paulk NK, Sutherland H, Keenan CM, Wilson PJ, Wlodarski B, Grompe M, Ranganath LR, Gallagher JA, Jarvis JC (2012b) Ochronosis in a murine model of alkaptonuria is synonymous to that in the human condition. Osteoarthritis Cartilage 20:880–886

Vassiliadis E, Rasmussen LM, Byrjalsen I, Larsen DV, Chaturvedi R, Hosbond S, Saabye L, Diederichsen AC, Genovese F, Duffin KL, Zheng Q, Chen X, Leeming DJ, Christiansen C, Karsdal MA (2012) Clinical evaluation of a matrix metalloproteinase-12 cleaved fragment of titin as a cardiovascular serological biomarker. J Transl Med 10:140

Veidal SS, Karsdal MA, Vassiliadis E, Nawrocki A, Larsen MR, Nguyen QH, Hagglund P, Luo Y, Zheng Q, Vainer B, Leeming DJ (2011) MMP mediated degradation of type VI collagen is highly associated with liver fibrosis–identification and validation of a novel biochemical marker assay. PLoS One 6:e24753

Vosse D, Landewe R, Garnero P, van der HD, van der LS, Geusens P (2008) Association of markers of bone- and cartilage-degradation with radiological changes at baseline and after 2 years follow-up in patients with ankylosing spondylitis. Rheumatology (Oxford) 47:1219–1222

Wang B, Chen P, Jensen AC, Karsdal MA, Madsen SH, Sondergaard BC, Zheng Q, Qvist P (2009) Suppression of MMP activity in bovine cartilage explants cultures has little if any effect on the release of aggrecanase-derived aggrecan fragments. BMC Res Notes 2:259

Zatkova A (2011) An update on molecular genetics of Alkaptonuria (AKU). J Inherit Metab Dis 34:1127–1136

JIMD Reports
DOI 10.1007/8904_2015_431

RESEARCH REPORT

Age-Related Deviation of Gait from Normality in Alkaptonuria

Gabor J. Barton · Stephanie L. King · Mark A. Robinson · Malcolm B. Hawken · Lakshminarayan R. Ranganath

Received: 28 November 2014 / Revised: 24 February 2015 / Accepted: 25 February 2015 / Published online: 19 March 2015

Abstract Alkaptonuria is a rare metabolic disease leading to systemic changes including early and severe arthropathy which affects mobility. For unknown reasons, the onset of degenerative changes is delayed to around 30 years of age when both objective and subjective symptoms develop. In order to complement description of the structural changes in alkaptonuria with measures of movement function, clinical gait analysis was added to the list of assessments in 2013. The aim of this study was to describe the deviation of gait from normality as a function of age in patients with alkaptonuria. Three-dimensional movement of reflective markers attached to joints were captured during walking in 39 patients and 10 controls. Subsequent to processing the data to emphasise the shape of marker trajectories, the mean Movement Deviation Profile was generated for all participants. This single number measure gives the deviation of a patient's gait from a distributed definition of gait normality. Results showed that gait deviation roughly follows a sigmoid profile with minimal increase of gait deviations in a younger patient group and an abrupt large increase around the second half of the 4th decade of life. Larger variations of gait deviations were found in the older group than in the younger group suggesting a complex interaction of multiple factors which determine gait function after symptoms manifest. Continued gait analysis of adults with AKU, extended to younger adults and children with AKU, is expected to complete understanding of both the natural history of alkaptonuria and how interventions can affect movement function.

Communicated by: Michael J Bennett, PhD

Competing interests: None declared

G.J. Barton (✉) · S.L. King · M.A. Robinson · M.B. Hawken
Research Institute for Sport and Exercise Sciences, Liverpool John Moores University, Byrom Street, Liverpool L3 3AF, UK
e-mail: g.j.barton@ljmu.ac.uk

L.R. Ranganath
National Alkaptonuria Centre, Royal Liverpool University Hospital, Prescot Street, Liverpool L7 8XP, UK

Introduction

Alkaptonuria (OMIM #203500) is an ultrarare autosomal recessive metabolic disease with an estimated incidence of 1:250,000–1:1,000,000 in the USA (Introne and Gahl 2003). A defect of homogentisate 1,2-dioxygenase (EC 1.13.11.5) blocks the catabolism of phenylalanine and tyrosine resulting in elevated levels of homogentisic acid. After its oxidation, a melanin-like polymer is produced which binds to virtually all fibrous connective tissues including cartilage, leading to ochronosis (Ranganath et al. 2013). While alkaptonuria begins at conception, there is only anecdotal evidence of joint pain in younger patients followed by a rapid increase of symptoms around 30 years of age (Introne and Gahl 2003; Ranganath and Cox 2011). Among various degenerative changes affecting the cardiovascular and renal systems, a characteristic of the disease is early and severe arthropathy (Abimbola et al. 2011). Despite mounting information about structural changes in alkaptonuria, little is known about the functional effects of arthritic changes on movement. A prospective randomised clinical trial showed that nitisinone reduced homogentisic acid levels by 95%, but the total hip range of motion, spinal flexion, functional reach, timed get up and go and 6-minute walk test did not improve (Introne et al. 2011). In order to better understand how movement degenerates in alkaptonuria, in 2013 we started performing gait analysis on adults who visit the National Alkaptonuria Centre in Liverpool.

Gait analysis is a routine noninvasive procedure which allows the collection of objective and quantitative information in order to identify abnormalities, postulate their causes and propose treatments for those with walking problems (Davis 2004). Body segment motion is captured by infrared cameras which track reflective markers attached to the legs and pelvis, and ground reaction forces are recorded by force platforms embedded in a walkway over which the participant walks. Dynamic joint angles, moments and powers are calculated in all anatomical planes over several strides. Interpretation of the results by gait analysts can uncover reasons for gait changes, allowing specific anatomical structures to be targeted for interventions.

The traditional interpretation of gait results has recently been complemented by the successful derivation of simplified measures of gait deviation, often represented by a single number. Notable and widely used examples are the Gait Deviation Index (GDI, Schwartz and Rozumalski 2008) and the Gait Profile Score (GPS, Baker et al. 2009). The Movement Deviation Profile (MDP, Barton et al. 2012; Barton et al. 2015) is a single curve generated by an artificial neural network model which shows quantitatively how much a patient's gait deviates from normal gait. A summary measure of the MDP, the MDP_{mean}, has demonstrated advantages over the GDI and GPS while showing good agreement with the GDI (Barton et al. 2012). The MDP_{mean} offers a simple and effective means of quantitatively describing disease progression in alkaptonuria. The aim of this study was to examine the development of gait deviations in a cross-sectional sample of adults with alkaptonuria with a view to employing our method of objective assessment of gait function to monitor disease progression and responses to treatment.

Participants and Methods

A group of 40 patients with alkaptonuria (AKU) and 10 unimpaired controls underwent clinical gait analysis at Liverpool John Moores University between May 2013 and October 2014. One patient refused consent for the use of their data in the following analysis. Thirty-two of the patients were receiving 2 mg/day nitisinone treatment (13 of them started treatment within 3 days of testing) which is expected to slow progression of the disease, but not to reverse the effects. Eighteen of the patients had had one or more joints replaced. Table 1 shows descriptive statistics together with duration of nitisinone treatment and any joint replacements.

The gait analysis procedure followed the guidelines of the Clinical Movement Analysis Society of UK and Ireland. Fifteen reflective markers were attached to the skin or tight fitting clothes over the feet, lower legs, thighs and the pelvis according to the Helen-Hayes model (Davis et al. 1991). Several walks were performed at self-selected speed on a 10 m long walkway, while the 3D coordinates of markers were captured by a 10 camera Qualisys Oqus or 16 camera Vicon T10/T160 motion capture system. The first three clean walks (without marker dropouts or measurement artefacts) of each patient and the first two walks of each control were selected for analysis.

Table 1 Characteristics of patients with alkaptonuria (AKU) and unimpaired controls

	AKU	Controls
N	39	10
Male/female	23/16	4/6
Age[a] (years)	46.5 (12.7)	34.2 (13.1)
Height[a] (m)	1.66 (0.10)	1.66 (0.08)
Mass[a] (kg)	74.1 (18.2)	69.5 (11.6)
Body mass index[a] (kg/m^2)	26.8 (5.4)	24.3 (4.7)
Nitisinone use		
On nitisinone for 1 year	19	n/a
On nitisinone for 1–3 days[b]	13	n/a
No nitisinone treatment	7	n/a
Joint replacement		
Knee or hip	14	n/a
Knee only	9	n/a
Knee and hip	5	n/a
Other	6	n/a

[a] Mean (standard deviation)
[b] Not included in "Nitisinone" group
n/a not applicable

The MDP (together with the GDI and GPS) was validated using three-dimensional joint angles, but there is no universally accepted way to describe spatial joint angles given the mathematically equivalent but effectively very different 16 Euler rotation sequences (Baker 2006; Lees et al. 2010). To circumvent the uncertainties attached to selecting one particular Euler rotation sequence over others without clear justification, we used marker positions directly to describe movement as suggested by Federolf et al. (2013). Marker coordinates attached to body segments are used to calculate joint angles and so the information contained in 3D angles is also contained in marker coordinates.

Processing of the X, Y and Z coordinates of the 15 markers involved subtraction of each marker from a calculated straight line fitted onto the progression of the centre of the pelvis during one gait cycle (means of the X, Y and Z coordinates of the two ASIS markers and the sacrum marker), followed by subtracting its mean from each of the X, Y and Z coordinates of the 15 markers and division by their respective standard deviation. The mean

correction and normalisation to unit standard deviation equalised the differences between the different amplitudes of markers attached to proximal and distal segments, thereby placing the emphasis on the shape of the marker trajectories as opposed to their amplitudes.

The processed marker coordinate data (X, Y and Z of 15 markers) was resampled to 101 values over one gait cycle and then concatenated into a single column with $3 \times 15 \times 101 = 4{,}545$ rows. Repeated gait cycles of each participant (two for controls and three for patients) were then added as further columns, giving two sets of numerical data, one for controls and one for patients. A model of normal gait was created by passing the data of controls to the self-organising neural network for training in the MDP freeware program (Barton et al. 2012). MDP_{mean} values for the patients were then derived by the program using the trained neural network model and processed further in MATLAB.

To summarise, the mean deviation from normal for each patient and control was calculated by averaging the MDP_{mean} values from the three walks of patients and two walks of controls and plotted against age. As there was considerable scatter in the data, explorative median filtering was applied in order to investigate the possibility of a transitional increase in deviation from normal gait over a small age range. Median filters, under the right circumstances, preserve transitions better than more common linear filters (Huang and Lee 2006).

Results

Preliminary examination of the values of MDP_{mean} plotted against age (Fig. 1) showed that they increase significantly with age; however, the linear association is not particularly strong ($p = 0.005$, $R^2 = 0.193$). Further examination suggested that there might be an abrupt change around ages 35–40. This pattern becomes more obvious when overlaying the series of median filtered data (with filter points ranging between 5 and 9) which suggests a sigmoid profile. The upper half of the relationship (above 35–40 years) showed more variability than the lower half (under 35–40 years).

Based on the effect of median filtering, individual regressions over (a) age <35 and (b) age >40 were fitted to the patient data and showed no significant variation with age. An appropriate sigmoid curve was fitted to the data ("R P" 2014) using starting and ending values from the regressions at the end of (a) and at the start of (b), respectively. The fitted curve showed a discontinuity with its 50% point around age 37, providing support for the conjecture suggested by the median filtering. Adjusting the start and end of the respective regressions to 37 years and making minor adjustments to the start and end values of the sigmoid curve from the revised regressions produced an almost identical sigmoid curve (Fig. 2) which was used to model the change of gait deviation as a function of age in our AKU sample.

All AKU patients under 37 years show some level of gait deviation as their MDP_{mean} values are greater than the mean of controls. The majority of AKU patients over 37 years (28 out of 30) demonstrated more gait deviations than the mean + 1SD of controls (1.88), but only 23 out of 30 were above the 95% confidence interval of the control group (2.159).

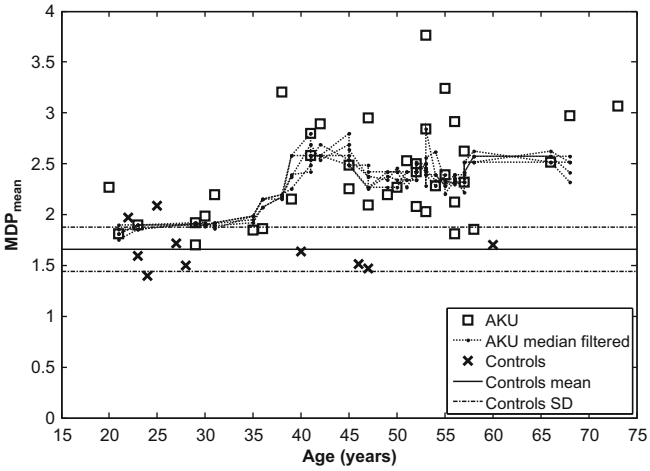

Fig. 1 Deviation of gait from normality (MDPmean) as a function of age in patients with alkaptonuria (AKU) compared to unimpaired controls (individuals and their mean ± standard deviation). A series of median filtered curves of the AKU group indicates an abrupt increase around 35–40 years of age

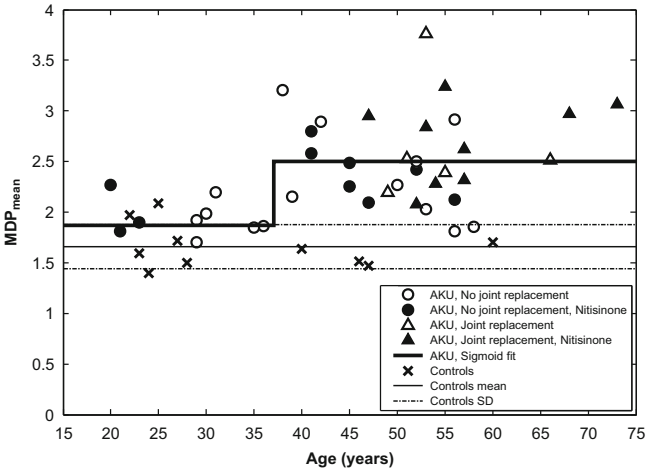

Fig. 2 Subsets of AKU patients with and without joint replacement and with and without nitisinone treatment shown against controls. A sigmoid curve fitted on the AKU group confirmed the discontinuity of gait deviation around 37 years of age

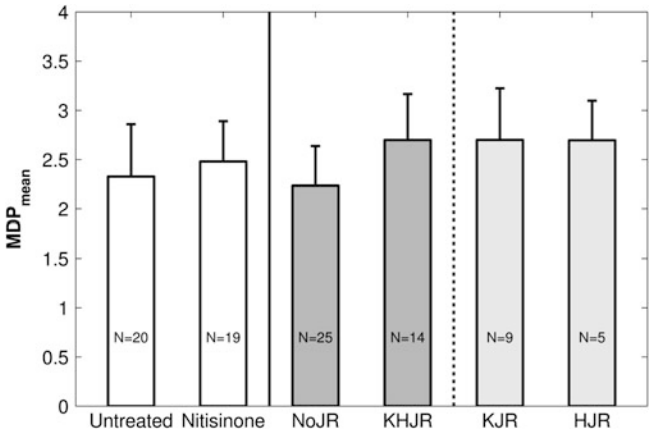

Fig. 3 A comparison of subsets of AKU patients (group means and SD with the size of group indicated on each bar). *Untreated* (no nitisinone, no joint replacement), *Nitisinone* (on nitisinone with or without joint replacement), *NoJR* (no joint replacement, with or without nitisinone), *KHJR* (knee or hip joint replacement, with or without nitisinone), *KJR* (knee joint replacement only, with or without nitisinone) and *HJR* (hip joint replacement, all five with knee replacement, with and without nitisinone)

Only patients above 47 years had joint replacements (red empty and filled triangles in Fig. 1), and their gait deviation was greater (2.70 ± 0.47, $N = 14$) than that of patients without joint replacements (2.24 ± 0.4, $N = 25$, red empty and filled circles in Fig. 1). There are 8 AKU patients in the age range 37–47 years without joint replacements but considerable deviations from normal gait.

In an attempt to clarify the association of gait deviations with nitisinone treatment and joint replacements, the MDP_{mean} of subgroups of AKU patients were plotted in Fig. 3. While clear cause-effect mechanisms cannot be established without longitudinal data of individual patients, nevertheless the comparisons of subgroups revealed some interesting findings. The 19 patients under nitisinone treatment showed higher deviations of gait from normality than the 20 patients without nitisinone treatment. Similarly, the gait of 14 patients with knee or hip joint replacements is further away from normality than those 25 without any joint replacements. Comparing the effects of knee and/or hip replacement on gait normality showed negligible differences. Nine AKU patients had a single knee replacement and an additional five had hip and knee replacements.

Discussion

An objective measure of gait function, the MDP_{mean}, showed a pattern of deterioration in alkaptonuria similar to other indices of disease severity (Ranganath and Cox 2011). Our data suggests a non-linear deterioration of gait function in the second half of the 4th decade which differs somewhat from the findings of Ranganath and Cox (2011) who described a gradual change in the 3rd decade followed by an accelerated progression of the disease in the 5th and 6th decades of life using clinical measures and patient questionnaires. Considering that AKU is an ultrarare disease, gait-related measures of 39 patients can be regarded as a large pool of data, but certainly this particular sample of patients might have influenced the fit; therefore, caution is advisable with setting a firm age threshold. Although the regression line in the AKU group over 37 years has a low slope (0.0026 units of MDP_{mean}/year) indicating minimal change as a function of age, there are considerable interindividual differences in their gait deviations. An interaction of several factors which may influence gait function (causing gait variability) justifies individualised clinical assessment for patients in this group in order to identify their specific problems which can then be targeted with appropriate treatment.

Adults with AKU under 37 years of age show some movement deviations although their MDP_{mean} is only one standard deviation away from normality. Our youngest patient was 20 years of age, and so we have no information about the gait function of even younger patients and children with AKU. Early detection of movement problems may trigger focused management in order to prevent cumulative deterioration. Especially in case of children, treatment with nitisinone may have to be delayed to prevent any potential side effects (Bendadi et al. 2014). Evidence of gait deviations in the young would support earlier intervention (either nitisinone or alternatives, e.g. physiotherapy), and conversely a lack of movement problems would support delaying nitisinone treatment to a later time when the chance of side effects is minimal.

Adults older than 37 years of age with AKU show more deviation from normal gait than the younger group. Nevertheless, if our method based on the MDP_{mean} was used to decide if a patient moved away from normality, then the sensitivity/specificity would likely be low with false positives given that 23% of AKU patients fall within the 95% confidence interval of the control group. Further evaluation of the MDP_{mean} as a method to separate a patient with AKU from controls is necessary using a larger sample.

Patients with AKU and joint replacements were all above 47 years, and their gait deviations were higher than those of the group without joint replacements. The higher age of this group likely reflects clinical decisions of when a joint replacement is indicated. Gait does not easily return to normality; in osteoarthritis, gait was shown not to return to normal until about 11 months after total hip arthroplasty (Beaulieu et al. 2010). Potential mechanisms underlying slow recovery are: unnecessary but continued pain avoidance strategies and persistent muscle weakness due to disuse, both of which may hinder not only the affected but

the contralateral side too. Persisting gait abnormality following joint replacement in AKU is likely to be due to the systemic nature of the disease which affects anatomical structures beyond the joint itself. AKU potentially affects all joints including their related ligaments, tendons and muscles, and this might explain why repairing a single joint may not lead to a rapid recovery.

Deviation of controls from normality, as measured by the MDP_{mean}, shows minimal increase as a function of age. This might be explained by the self-organising neural network's method of operation underlying the MDP method. Subsequent to defining an internal model of gait normality based on the gait of controls, the deviation from the closest matching variant of normal gait is calculated (Barton et al. 2012). As the control group included older individuals (40, 46, 47 and 60 years of age), the MDP_{mean} of AKU patients could reflect the deviation from this subgroup of controls with altered gait due to their age. In order to determine if the gait of the older control subgroup affected the calculation of the MDP_{mean}, a separate neural network model was generated by training with the younger group of controls and then calculating the MDP_{mean} of the older control group. The similar MDP for the older control group ($MDP_{mean} = 1.82$) compared to younger controls (22–28 years, $MDP_{mean} = 1.67$) indicates that only minimal gait deviations occur as a result of ageing. As such the increased MDP_{mean} of the older individuals with AKU is referenced to a rather coherent definition of gait normality regardless of age. Increased gait deviations therefore were due to genuine deterioration of gait related to AKU together with other factors like joint replacements and nitisinone treatment. More in-depth subgroup analyses will be required to differentiate between these factors.

A limitation of our method is that on its own the single number MDP_{mean} can only be used to flag an increased deviation of gait from normality. This should then be followed up by establishing the specific gait problems which eventually is expected to lead to improved clinical decision-making and treatment. Movement of body-attached markers was used to quantify deviation of gait, but this approach can be complemented by including the forces acting on the body at each joint. Such an extension of the method may offer further advantages due to its focus on joint loading which is the ultimate cause of pain in alkaptonuria. An inevitable limitation of our study was the low number of participants and the cross-sectional nature of gait data.

Conclusions

This was the first attempt to evaluate gait function in patients with alkaptonuria using a summary measure of gait deviation (the MDP). Patients with AKU showed minimally increased gait deviations between 20 and 37 years, followed by an accelerated increase around the second half of the 4th decade of life. The older group of patients was characterised by elevated and varied levels of gait deviation. Together with continued gait analysis of adults with AKU, evaluation of gait deviations in younger adults and children with AKU is necessary to complete and refine our understanding of disease progression moderated by the influence of interventions including joint replacements and nitisinone treatment.

Acknowledgements We gratefully acknowledge the support of participants in our study and the continued help and assistance by the AKU Society. We also thank Kimberley Lewin for performing gait analysis on the very first group of patients at Liverpool John Moores University.

Take-Home Message

Deviation of gait from normality shows an abrupt increase in the second half of the 4th decade of life in alkaptonuria.

Compliance with Ethics Guidelines

Conflict of interests

Gabor Barton received a grant from the National Alkaptonuria Centre.

Stephanie King is employed from the same grant income.

Mark Robinson and Malcolm Hawken are named coinvestigators in the same grant.

Lakshminarayan Ranganath is Director of the National Alkaptonuria Centre.

Informed Consent

All procedures followed were approved by the local NHS Ethics Committee (07/H1002/111 amendment 6 and 07/Q1505/29 amendment 9) and were in accordance with the ethical standards of the responsible committee on human experimentation (institutional and national) and with the Helsinki Declaration of 1975, as revised in 2000 (5). Informed consent was obtained from all patients for being included in the study.

Contributions of Individual Authors

GJB conceived the study, performed the initial analyses and was the lead author of the manuscript. SLK performed some of the data collection and parts of the data analysis

and collaborated in writing the manuscript. MAR was involved in defining the test protocol and contributed to revising the manuscript. MBH was involved in the advanced analysis of results and in writing the manuscript. LRR contributed to revising the manuscript.

References

Abimbola O, Hall G, Zuckerman JD (2011) Degenerative arthritis of the knee secondary to ochronosis. Bull NYU Hosp Jt Dis 69:331–334

Baker R (2006) Gait analysis methods in rehabilitation. J Neuroeng Rehabil 3:4

Baker R, McGinley JL, Schwartz MH et al (2009) The gait profile score and movement analysis profile. Gait Posture 30:265–269

Barton GJ, Hawken MB, Scott M et al (2012) Movement Deviation Profile: a measure of distance from normality using a self-organizing neural network. Hum Mov Sci 31:284–294

Barton GJ, Hawken MB, Holmes G et al (2015) A gait index may underestimate changes of gait: a comparison of the Movement Deviation Profile and the Gait Deviation Index. Comput Methods Biomech Biomed Engin 18:57–63

Beaulieu ML, Lamontagne M, Beaulé PE (2010) Lower limb biomechanics during gait do not return to normal following total hip arthroplasty. Gait Posture 32:269–273

Bendadi F, de Koning TJ, Visser G et al (2014) Impaired cognitive functioning in patients with tyrosinemia type I receiving nitisinone. J Pediatr 164:398–401

Davis RB (2004) The motion analysis laboratory. In: Gage J (ed) The treatment of gait problems in cerebral palsy. Mac Keith Press, London, pp 90–98

Davis RB, Ounpuu S, Tyburski D et al (1991) A gait analysis data collection and reduction technique. Hum Mov Sci 10:575–587

Federolf PA, Boyer KA, Andriacchi TP (2013) Application of principal component analysis in clinical gait research: identification of systematic differences between healthy and medial knee-osteoarthritic gait. J Biomech 46:2173–2178

Huang HC, Lee TCM (2006) Data adaptive median filters for signal and image denoising using a generalized SURE criterion. IEEE Signal Proc Let 13:561–564

Introne WJ, Gahl WA (2003) Alkaptonuria. In: NORD guide to rare disorders. Lippincott Williams & Wilkins, Philadelphia, p 431

Introne WJ, Perry MB, Troendle J et al (2011) A 3-year randomized therapeutic trial of nitisinone in alkaptonuria. Mol Genet Metab 103:307–314

Lees A, Barton G, Robinson M (2010) The influence of Cardan rotation sequence on angular orientation data for the lower limb in the soccer kick. J Sports Sci 28:445–450

"R P" (2014) Sigmoid / logistic curve fit. Matlab Central. http://uk.mathworks.com/matlabcentral/fileexchange/42641-sigmoid—logistic-curve-fit. Accessed 27 Nov 2014

Ranganath LR, Cox TF (2011) Natural history of alkaptonuria revisited: analyses based on scoring systems. J Inherit Metab Dis 34:1141–1151

Ranganath LR, Jarvis JC, Gallagher JA (2013) Recent advances in management of alkaptonuria (invited review; best practice article). J Clin Pathol 66:367–373

Schwartz MH, Rozumalski A (2008) The gait deviation index: a new comprehensive index of gait pathology. Gait Posture 28:351–357

JIMD Reports
DOI 10.1007/8904_2015_437

RESEARCH REPORT

Nitisinone Arrests but Does Not Reverse Ochronosis in Alkaptonuric Mice

Craig M Keenan • Andrew J Preston • Hazel Sutherland • Peter J Wilson • Eftychia E Psarelli • Trevor F Cox • Lakshminarayan R Ranganath • Jonathan C Jarvis • James A Gallagher

Received: 28 November 2014 / Revised: 13 February 2015 / Accepted: 24 March 2015 / Published online: 05 May 2015

Abstract Alkaptonuria (AKU) is an ultrarare autosomal recessive disorder resulting from a deficiency of homogentisate 1,2 dioxygenase (HGD), an enzyme involved in the catabolism of phenylalanine and tyrosine. Loss of HGD function prevents metabolism of homogentisic acid (HGA), leading to increased levels of plasma HGA and urinary excretion. Excess HGA becomes deposited in collagenous tissues and subsequently undergoes polymerisation, principally in the cartilages of loaded joints, in a process known as ochronosis. This results in an early-onset, devastating osteoarthropathy for which there is currently no effective treatment. We recently described the natural history of ochronosis in a murine model of AKU, demonstrating that deposition of ochronotic pigment begins very early in life and accumulates with age. Using this model, we were able to show that lifetime treatment with nitisinone, a potential therapy for AKU, was able to completely prevent deposition of ochronotic pigment. However, although nitisinone has been shown to inhibit ochronotic deposition, whether it can also facilitate removal of existing pigment has not yet been examined. We describe here that midlife administration of nitisinone to AKU mice arrests further deposition of ochronotic pigment in the tibiofemoral joint, but does not result in the clearance of existing pigment. We also demonstrate the dose-dependent response of plasma HGA to nitisinone, highlighting its efficacy for personalised medicine, where dosage can be tailored to the individual AKU patient.

Communicated by: Anita MacDonald, PhD, BSc

Competing interests: None declared

Electronic supplementary material: The online version of this chapter (doi:10.1007/8904_2015_437) contains supplementary material, which is available to authorized users.

C.M. Keenan · H. Sutherland · P.J. Wilson · L.R. Ranganath · J.A. Gallagher (✉)
Department of Musculoskeletal Biology, Institute of Ageing and Chronic Disease, University of Liverpool, Sherrington Building, Ashton Street, Liverpool L69 3GE, UK
e-mail: jag1@liverpool.ac.uk

A.J. Preston
Developmental Immunology, Paediatrics, Weatherall Institute of Molecular Medicine, University of Oxford, John Radcliffe Hospital, Oxford OX3 9DS, UK

E.E. Psarelli · T.F. Cox
Cancer Research UK Liverpool Cancer Trials Unit, University of Liverpool, 1-3 Brownlow Street, Liverpool L69 3GL, UK

L.R. Ranganath
Department of Clinical Biochemistry and Metabolism, Royal Liverpool University Hospital, Prescot Street, Liverpool L7 8XP, UK

H. Sutherland · J.C. Jarvis
School of Sport and Exercise Sciences, Liverpool John Moores University, Tom Reilly Buildings, Byrom Street, Liverpool L3 3AF, UK

Introduction

Alkaptonuria (AKU) has a unique place in the history of metabolic disease as the first disorder to be described as an "inborn error of metabolism" by distinguished English physician Sir Archibald Garrod (Garrod 1902). AKU is an ultrarare autosomal recessive disorder with a worldwide incidence of between 1 in 250,000 and 1,000,000 live births (Phornphutkul et al. 2002). AKU results from mutations in homogentisate 1,2-dioxygenase (HGD) (EC 1.13.11.5), the enzyme involved in the catabolism of phenylalanine and tyrosine (La Du et al. 1958) (Fig. 1a). Loss of HGD function results in both increased plasma levels of homogentisic acid (HGA) and HGA excretion. Urinary HGA darkens on exposure to air and is typically observed as the first symptom in patients who present with AKU.

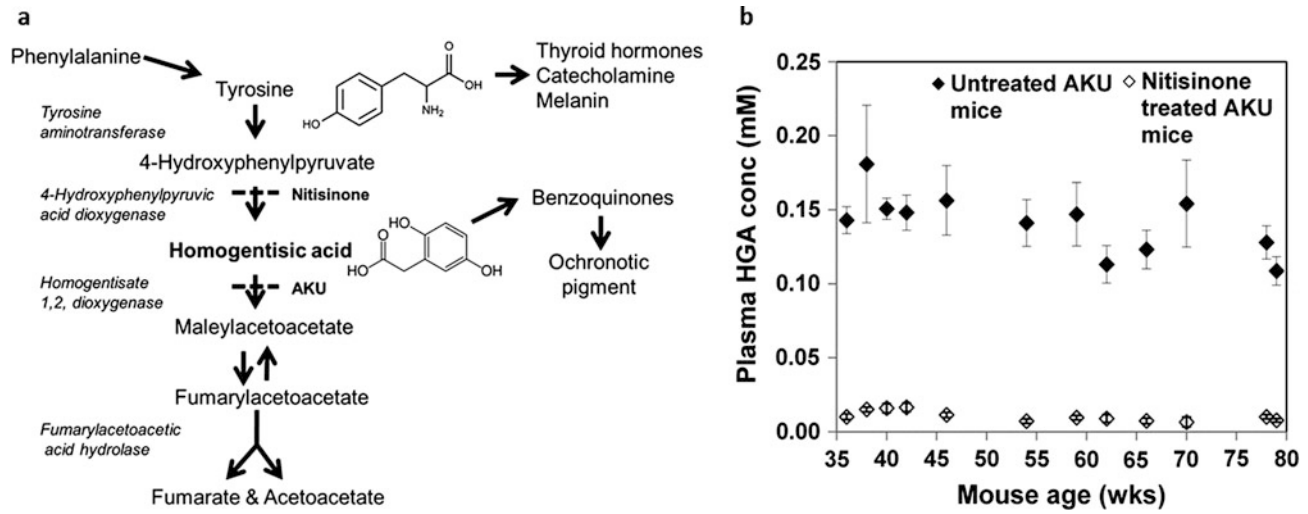

Fig. 1 (**a**) Diagram of the phenylalanine/tyrosine metabolic pathway showing the enzyme deficiency which results in AKU. The site of action of nitisinone is also *highlighted*. **(b)** The effect of midlife (34 weeks) dietary supplementation with 4 mg/L nitisinone on the plasma HGA concentration in AKU mice

Elevated levels of plasma HGA ultimately lead to the pigmentation of cartilaginous tissues, following the deposition and subsequent polymerisation of HGA in a process known as ochronosis. This results in an early-onset, devastating osteoarthropathy for which there is currently no effective treatment.

Nitisinone (2-(2-nitro-4-(trifluoromethyl)benzoyl) cyclohexane-1,3-dione) is a reversible inhibitor of 4-hydroxyphenylpyruvate dioxygenase (HPPD) (EC 1.13.11.27), the enzyme responsible for producing HGA (Fig. 1a). Originally developed as a herbicide (Schulz et al. 1993), it is routinely used for the treatment of hereditary tyrosinaemia type 1 (McKiernan 2006). Nitisinone is viewed as a potential treatment for AKU as it prevents accumulation of HGA in plasma. Ochronosis has recently been described in two murine models of AKU (Taylor et al. 2012; Preston et al. 2014). In the latter of the two models, we have described the efficacy of nitisinone in treating ochronosis in a murine model of AKU and demonstrated that lifetime administration of nitisinone reduced plasma HGA by 88% and prevented ochronotic pigment deposition in the tibiofemoral joint (Preston et al. 2014). This was the first time that inhibition of ochronosis by nitisinone had been demonstrated and highlighted the efficacy of nitisinone as a treatment for AKU.

As a large proportion of AKU patients already suffer from osteoarthropathy, it is important to determine if nitisinone's efficacy is purely prophylactic or whether it can facilitate repair and regeneration of damaged cartilage during natural metabolic turnover. Although pigmentation in AKU mice can be prevented throughout their lifetime by administration of nitisinone, there is no data on whether ochronosis is reversible. Here we describe that the midlife administration of nitisinone to AKU mice successfully arrests further deposition of ochronotic pigment in the tibiofemoral joint, but does not result in the reduction of existing pigment. We also demonstrate that the response of plasma HGA to nitisinone treatment is dose dependent, which should facilitate tailored treatment of AKU patients presenting with differing degrees of severity.

Materials and Methods

Mice

Hgd−/− (AKU) mice on a BALB/c or C57BL/6 background were used for all experiments. All mice were housed and maintained within the University of Liverpool's Biological Services Unit (BSU) in accordance with Home Office UK guidelines.

Sample Preparation

Tail bleed samples were collected into Microvettes (Sarstedt, CB 300) and stored at 4°C prior to processing within 2 h, using an adaptation of the Bory method (Bory et al. 1990). Briefly, whole blood was centrifuged at 1500×*g* for 10 min at 4°C and the plasma deproteinised by adding 5.8 M perchloric acid (Sigma, UK) equivalent to 10% of

the plasma and containing 0.1 mM 4-amino-2-chlorobenzoic acid (Sigma, UK) as the internal standard. Acidified supernatant was stored at −20°C. A 150 μL tail bleed volume yielded approximately 25 μL of deproteinised plasma.

Chromatographic Conditions

Plasma HGA concentration was determined via HPLC as described previously (Preston et al. 2014), on a Phenomenex Kinetex XB-C18 column, 2.6 μM (4.6 × 100 mm). Briefly, the initial mobile phase was 100% buffer A (12 mM orthophosphoric acid, Sigma, UK), before increasing buffer B (100% methanol, Sigma, UK) from 0 to 80% over 10 min. Detection was by UV at 290 nm.

Midlife Nitisinone Treatment

A cohort of eight BALB/c Hgd−/− mice (four males, four females) were provided with filtered water from 8 to 34 weeks of age. They were then provided with an ad libitum supply of water containing 4 mg/L of nitisinone (Shanghai Elittes Organics, China) from 34 to 81 weeks of age. The control group of 8 BALB/c Hgd−/− mice (four males, four females) was untreated over the same time period. Plasma was taken at 35 weeks and then sampled regularly by tail bleed over the mouse's lifetime. Tibiofemoral joints were taken for histological analysis at the end of study. Analysis of joint pigmentation was also performed at different ages, in either BALB/c Hgd−/− or C57BL/6 Hgd−/− mice to build up a disease progression timeline.

Nitisinone Dose–Response

Six cohorts of four age-matched C57BL/6 Hgd−/− mice (two males, two females) had their plasma sampled at 54 weeks and then were immediately treated with an ad libitum supply of water containing either 4, 1, 0.5, 0.25, 0.125 or 0 mg/L of nitisinone for 13 days. Plasma was sampled again seven and 19 days posttreatment, and its HGA concentration was determined by HPLC.

Histological Analysis

Mice were euthanised with Pentoject (sodium pentobarbitone 20% w/v) and their tibiofemoral joints harvested and stored in 10% phosphate-buffered formalin solution, pH 7.4, for a minimum of 24 h. Tissues were washed in phosphate-buffered saline before decalcification in 12% EDTA for seven days. Tibiofemoral joints were dissected free of excess muscle then paraffin embedded in the coronal plane to enable simultaneous evaluation of both the medial and lateral compartments of the joint, as recommended by the Osteoarthritis Research Society International (OARSI) histopathology initiative (Glasson et al. 2010). The first section that encompassed both the tibial plateau and femoral condyles was selected as representative of each mouse. Sections were mounted on glass slides, rehydrated and stained with H&E or Schmorl's stain, previously shown to be a sensitive method for the detection of ochronotic pigment (Tinti et al. 2011). Sections were dehydrated through graded alcohols and mounted with DPX resin (VWR International, UK) for examination by light microscopy.

Quantification of Pigmented Chondrons

The first whole section that encompassed the entire tibiofemoral joint (MTP, MFC, LTP and LFC) was selected as representative of each mouse for quantification analysis. From these sections, the total number of pigmented chondrons present in the articular cartilage and entheses of the femoral condyles and articular cartilage of the tibial plateau was assessed. Figure 2e illustrates the area quantified in a section of each tibiofemoral joint. Quantitation of each section required counting at least 36 fields. All sections were counted by a second blinded observer, and the correlation between observers was greater than 0.93.

Statistical Analyses

Comparisons in pigmentation rates between treated and untreated groups were performed using an independent sample *t*-test. Descriptive statistics are reported as mean and standard deviation (SD) as normality was achieved, while results were considered as statistically significant at the 5% level. Data analysis was undertaken using Stata 13 (StataCorp. 2013. Stata Statistical Software: Release 13. College Station, TX: StataCorp LP.).

Results

Midlife treatment with 4 mg/L nitisinone from 34 to 81 weeks of age suppressed plasma HGA concentration by approximately 15-fold, in agreement with previous work (Preston et al. 2014) (Fig. 1b). The reduction in plasma HGA following 44–46 weeks of nitisinone treatment translated into a statistically significant difference ($t = 4.645$, $p = 0.001$) in the mean number of pigmented chondrons visible in the nitisinone-treated mice at 79–81 weeks, equal to 88 (SD = 26.5) (Fig. 2b), relative to aged-matched untreated AKU mice, equal to 201.2 (SD = 48.4) (Fig. 3). The degree of pigmentation observed in nitisinone-treated BALB/c Hgd−/− mice at 79–81 weeks was considered equivalent to that observed in untreated 34-week-old BALB/c Hgd−/− mice (Fig. 2a), correspondent

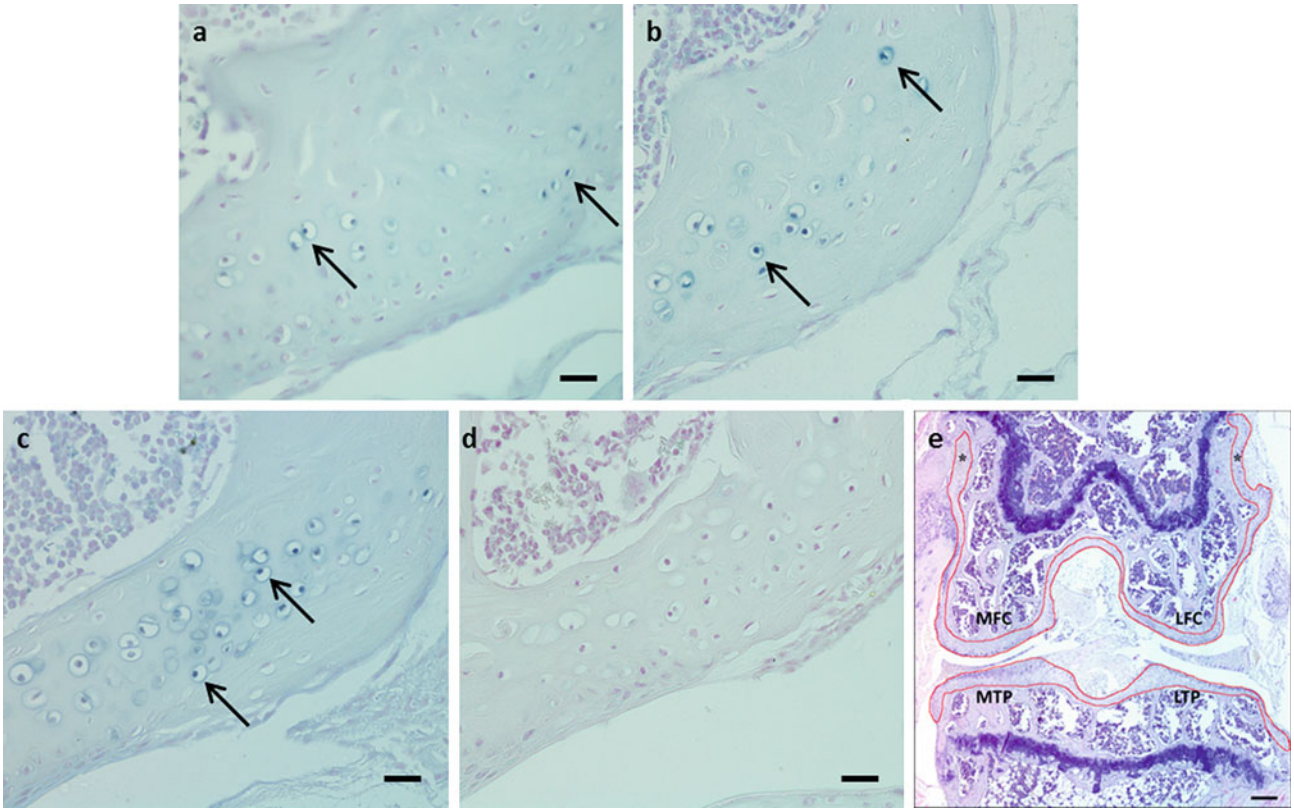

Fig. 2 (**a**) Photomicrograph displaying pigmented chondrons (*arrows*) in a 35-week-old BALB/c Hgd−/− mouse, prior to treatment with nitisinone. (**b**) Administration of nitisinone (4 mg/L) at 35 weeks prevented large-scale pigmentation of chondrons in the tibiofemoral joint. The number of pigmented chondrons (*arrows*) observed in the nitisinone-treated BALB/c Hgd−/− mice at 79–81 weeks was comparable to those seen in untreated BALB/c Hgd−/− mice at 35 weeks (Figs. 1 and 2a). (**c**) Photomicrograph of an 80-week-old untreated BALB/c Hgd−/− mouse. Large numbers of pigmented chondrons (*arrows*) were present throughout the tibiofemoral joint, highlighting the effectiveness of nitisinone when given midlife (Fig. 2b). (**d**) Lifetime treatment with nitisinone (4 mg/L) prevented any deposition of ochronotic pigment in the tibiofemoral joint. (**e**) H&E photomicrograph displaying the a section of the entire tibiofemoral joint. The *red lines* on the image highlight the boundaries of the areas where pigmented chondrons where quantified (* = entheses). Images (**a**–**d**) were all taken from the lateral femoral condyle of BALB/c Hgd−/− mice. *Bar* = 20 μm (**a**–**d**), 50 μm (**e**)

with the time at which treatment began. This demonstrated that midlife treatment with nitisinone arrested further deposition of ochronotic pigment but did not clear previously laid-down pigment, resulting in higher observable chondron pigmentation than AKU mice treated from birth (Fig. 2d). The number of pigmented chondrons observed in the untreated mice at 80 weeks (Fig. 2c) was consistent with levels previously reported in the natural history study of BALB/c Hgd−/− mice (Preston et al. 2014).

Quantification of pigmented chondrons over time (Fig. 3) confirmed that although the degree of deposition between AKU mice was highly variable (even within highly inbred mouse strains), progressive accumulation of ochronotic pigment was consistent with ageing. Nevertheless, midlife treatment with nitisinone effectively inhibited further deposition of ochronotic pigment.

Plasma HGA concentration was also highly variable in AKU mice, but was observed to respond in a dose-dependent fashion to nitisinone treatment, when plotted as a percentage of its pretreatment value (Fig. 4). Higher concentrations of nitisinone resulted in greater suppression of plasma HGA variability within cohorts, while removal of nitisinone after 13 days resulted in a rebound of plasma HGA levels.

Discussion

We have previously shown that nitisinone treatment from birth can prevent ochronosis in the adult AKU mouse (Preston et al. 2014). Here we demonstrate that beginning nitisinone treatment midway through life (34 weeks) is sufficient to arrest further disease progression. Remarkably, 44–46 weeks after treatment, the mean number of pigmented chondrons observed within the knee joint was no greater than that typical of untreated 34-week-old AKU mice, according to our disease progression timeline (Fig. 3).

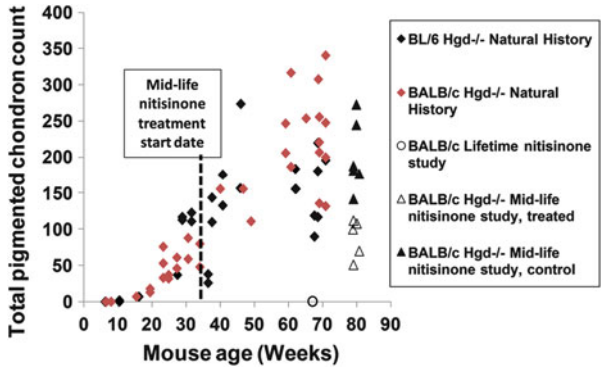

Fig. 3 Quantification of pigmented chondrons in the tibiofemoral joint of AKU mice, depicting ochronotic pigment deposition over time and the effect of treatment with 4 mg/L nitisinone when administered midlife. Treatment at 34 weeks prevented further deposition of ochronotic pigment by week 79, but did not reverse the effects of previously laid-down pigment. Quantification of pigmented chondrons was performed on a single section from each mouse and does not represent the total cell number in each mouse

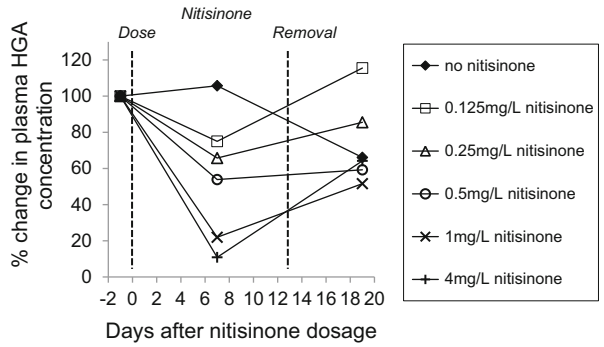

Fig. 4 The dose–response to nitisinone (as percentage change of plasma HGA concentration) in AKU mice and recovery

Unlike in mice treated with nitisinone from birth however (Fig. 2d), pigmentation could still be observed and quantified. It is evident therefore that while nitisinone can prevent further deposition of ochronotic pigment, it does not reduce pre-existing pigmentation by enabling turnover/replacement of damaged cartilage. This strongly implies that in order to minimise the irreparable joint damage typical of AKU disease progression in humans, treatment with nitisinone should begin as early as possible. Although there was no evidence that midlife treatment with nitisinone could facilitate removal of existing pigmentation, it did arrest any further deposition of ochronotic pigment which may lead to the prevention or slowing down of disease progression in patients with established ochronosis.

Establishing a minimum effective nitisinone dose is fundamental in reducing the cost of lifetime treatment and minimising potential side effects such as corneal keratopathy (Introne et al. 2011). As plasma HGA concentration in AKU patients is highly variable, we therefore examined dose–response sensitivity to nitisinone to determine the practicality of tailoring nitisinone treatment dose to the patient. A clear dose–response effect was observed between nitisinone and plasma HGA levels, which decreased consistently following increased doses of nitisinone. Treatment with 4 mg/L nitisinone reduced plasma HGA by 90% over a 13-day period when compared with baseline controls. Ranganath and colleagues recently showed a similar dose–response effect of nitisinone when analysing urinary HGA excretion over a 24 h period in AKU patients. Furthermore, they found that nitisinone was well tolerated within the studied dose range (Ranganath et al. 2014), which is consistent with our observations in mice. Both our data and that of Ranganath et al. highlight the efficacy of nitisinone in reducing the levels of circulating HGA. As excellent dose–response sensitivity was observed between differing nitisinone concentrations and plasma HGA levels, it may be possible to tailor individual treatment plans for AKU patients.

In summary, we have shown that nitisinone can effectively inhibit ochronotic deposition in an alkaptonuric mouse model and if introduced in midlife can arrest any further disease progression. Nitisinone treatment does not result in the removal of existing ochronotic pigmentation and cannot therefore be used to reverse existing joint damage. Plasma HGA concentrations display excellent sensitivity to treatment dose, facilitating the tailoring of therapy to patient disease severity.

Synopsis

Nitisinone arrests further deposition of ochronotic pigment when administered midlife, it does not reduce existing pigmentation, and it reduces the plasma HGA levels in a dose-dependent manner.

Compliance with Ethics Guidelines

Conflicts of Interest

Craig M Keenan, Andrew J Preston, Hazel Sutherland, Peter J Wilson, Eftychia E Psarelli, Trevor F Cox, Lakshminarayan R Ranganath, Jonathan C Jarvis and James A Gallagher declare they have no conflict of interest.

Animal Rights

All institutional and national guidelines for the care and use of laboratory animals were followed.

Author Contributions

CMK and AJP contributed equally and were involved in data acquisition, analysis and reporting of the work.
HS and PJW were involved in data acquisition.
EEP and TFC were involved in data analysis.
LRR, JCJ and JAG were involved in the planning of the work.
JCJ and JAG contributed equally.

References

Bory C, Boulieu R, Chantin C, Mathieu M (1990) Diagnosis of alcaptonuria: rapid analysis of homogentisic acid by HPLC. Clin Chim Acta 189(1):7–11

Garrod AE (1902) The incidence of alkaptonuria: a study in chemical individuality. Lancet ii:1616–1620

Glasson SS, Chambers MG, Van Den Berg WB et al (2010) The OARSI histopathology initiative – recommendations for histological assessments of osteoarthritis in the mouse. Osteoarthr Cartil 18(S3):S17–S23

Introne WJ, Perry MB, Troendle J et al (2011) A 3-year randomized therapeutic trial of nitisinone in alkaptonuria. Mol Genet Metab 103(4):307–314

La Du BN, Zannoni VG, Laster L, Seegmiller JE (1958) The nature of the defect in tyrosine metabolism in alcaptonuria. J Biol Chem 230(1):251–260

McKiernan PJ (2006) Nitisinone in the treatment of hereditary tyrosinaemia type 1. Drugs 66(6):743–750

Phornphutkul C, Introne WJ, Perry MB et al (2002) Natural history of alkaptonuria. N Engl J Med 347(26):2111–2121

Preston AJ, Keenan CM, Sutherland H et al (2014) Ochronotic osteoarthropathy in a mouse model of alkaptonuria, and its inhibition by nitisinone. Ann Rheum Dis 73(1):284–289

Ranganath LR, Milan AM, Hughes AT et al (2014) Suitability of nitisinone in alkaptonuria 1 (SONIA 1): an international, multicentre, randomised, open-label, no-treatment controlled, parallel-group, dose–response study to investigate the effect of once daily nitisinone on 24-h urinary homogentisic acid excretion in patients with alkaptonuria after 4 weeks of treatment. Ann Rheum Dis

Schulz A, Ort O, Beyer P, Kleinig H (1993) SC-0051, a 2-benzoyl-cyclohexane-1,3-dione bleaching herbicide, is a potent inhibitor of the enzyme p-hydroxyphenylpyruvate dioxygenase. FEBS Lett 318(2):162–166

Taylor AM, Preston AJ, Paulk NK et al (2012) Ochronosis in a murine model of alkaptonuria is synonymous to that in the human condition. Osteoarthritis Cartilage 20(8):880–886

Tinti L, Taylor AM, Santucci A et al (2011) Development of an in vitro model to investigate joint ochronosis in alkaptonuria. Rheumatology (Oxford) 50(2):271–277

JIMD Reports
DOI 10.1007/8904_2015_453

RESEARCH REPORT

The Pigment in Alkaptonuria Relationship to Melanin and Other Coloured Substances: A Review of Metabolism, Composition and Chemical Analysis

N.B. Roberts · S.A. Curtis · A.M. Milan · L.R. Ranganath

Received: 14 January 2015 / Revised: 30 April 2015 / Accepted: 04 May 2015 / Published online: 21 June 2015

Abstract The pigments found in plants, animals and humic substances are well described and classified. In humans considerable progress has been made with the main pigment melanin in defining its biochemistry, the different types and function. However, analytical techniques to show these differences in vivo are still not readily available. NMR and IR spectroscopy are relatively insensitive and reveal only major structural differences. Techniques utilising MS are useful in determining elemental content but require further studies to optimise conditions for accurate mass analysis. How the components may be structurally organised seems to be the most problematic with scanning TEM and the improved FTIR of use in this respect. As regards understanding the nature of the pigment related to HGA seen in patients with Alkaptonuria (AKU), it is still thought of as a melaninlike pigment simply because of its colour and likewise thought to be a polymer of undetermined size. It is important that detailed analysis be carried out to define more accurately this pigment. However, observations suggest it to be the same as the HGA-derived pigment, pyomelanin, produced by bacteria and containing both quinone and phenolic groups. The interesting developments in alkaptonuria will be to understand how such a polymer can cause such profound collagen and connective tissue damage and how best to reverse this process.

Communicated by: Jörn Oliver Sass

Competing interests: None declared

N.B. Roberts (✉) · S.A. Curtis · A.M. Milan · L.R. Ranganath
Department of Clinical Biochemistry and Metabolic Medicine, The Royal Liverpool and Broadgreen University Hospitals Trust, Liverpool L7 8XP, UK
e-mail: n.b.roberts@liverpool.ac.uk

Introduction

Pigmentation in humans is a well-controlled phenomenon where both structure and function of the pigment are interconnected. When control is lost, with a lack of pigmentation, albinism results and when in excess, various conditions have been described, including associated disorders of pituitary function, various inflammatory conditions as reviewed (Nordlund et al. 2006), hyperkeratosis hyperpigmentation (Figueras et al. 1993) and the rare genetic disease Alkaptonuria (AKU) (Phornphutkul et al. 2002).

AKU has been associated with many terms including black bone disease to ochronosis (yellow colouration) which suggest a process with diverse effects unlike normal pigmentation. However, the AKU pigment is still relatively poorly studied, with knowledge more than 40 years old needing updating as pigmentation is thought to be the basis for morbidity of the condition. In this review we aim to explain the nature and function of pigment material in plants, bacteria and humans and from this how we should proceed to effective analysis and classification of the pigment seen in AKU. Thus, if we can understand this pigmentation process better, it may allow further insights into the pathophysiology of AKU and yield novel therapeutic targets.

Background

In the study of pigmentation or coloured biological compounds in living matter, it is important that their nature is clearly defined in order to optimise chemical analysis. The term biological pigment is used for all coloured natural substances whose chemical structure determines the actual

colour, so if yellow (570–590 nm) by reflecting this wavelength and absorbing the remaining wavelengths of white light (375–780 nm). Obviously if a pigment is black as in the melaninlike types, all the wavelengths are absorbed and none is reflected. Distinction is usually made between a pigment, which is insoluble (resulting in a suspension), and a dye, which can be both a liquid and soluble in the respective material. The structural chemistry of dyes is well established with both conformation and specific groups producing different colours (Kassinger 2003; Venkataraman 2012). However, for pigmented tissue the final colour may be a composite of more than one component and relate to both composition and structure with specific chemical groups and if metals are involved, e.g. Fe or Cu ions. The structure and interaction with the underlying tissue may also be relevant in particular if located superficially or in deeper parts of the tissue. For example, pigment located deep within the tissue may appear as a darker shade than the superficial layers showing selective reflection and a different colouration. The actual structure of the pigments in tissue may also be more complex than any defined chemical form as a result of polymerisation and interaction with other proteins, e.g. collagen and keratin, affecting the final visual appearance.

In order to understand the structural and compositional basis of colour in human pigmentation, awareness of how other natural pigments are coloured is important. This will then help determine how analysis will be best achieved. The plant pigments comprise a variety of different kinds of molecule, including porphyrins (chlorophyll), carotenoids, anthocyanins and betalains (Delgado-Vargas et al. 2000). The carotenoids have a distinctive structure based on the 5 carbon 2-methyl-1,3-butadiene isoprene unit producing the unsaturated hydrocarbons formula $C_{40}H_x$. These are synthesised only by plants, shown as the orange pigment carotene found in carrots; lutein, a yellow pigment found in fruits and vegetables; and lycopene, the red pigment responsible for the colour of tomatoes. Anthocyanins (literally "flower blue") are water-soluble flavonoid pigments that appear red to blue according to pH and are produced from the condensation of 4-hydroxy cinnamoyl CoA with phenylalanine. They occur in all tissues of higher plants, providing colour in leaves, plant stem, roots, flowers and fruits, though not always in sufficient quantities to be noticeable. Betalains are aromatic indole derivatives synthesised from tyrosine and complexed with a sugar to give red or yellow pigments. The betalains are water-soluble compounds responsible for the deep red colour of beets and Bougainvillea bract colour and are used commercially as food-colouring agents.

These compounds have defined structures to give their overall colour and are nonprotein in nature. In contrast coloured photopigment rhodopsin is a protein opsin with a reversibly covalently bound cofactor retinal. The rhodopsin absorbs green-blue light and, therefore, appears reddish-purple, so-called visual purple (Stuart and Brige 1996).

The coloured pigments/substances in plants are thus both well characterised and chemically well defined. However, pigmentation in humans primarily associated with the production of melanin has still many unanswered questions, in particular knowledge about the chemical structure and what are the most reliable analytical procedures to describe differences (D'Ischia et al. 2013). A variety of definitions and models are found in the literature, which seems to reflect an arbitrary use of terminology as well as several assumptions and speculations that have never been proven on experimental grounds. This lack of standardised procedures (D'Ischia et al. 2013) makes identification of the pigment associated with the genetic disease alkaptonuria even more challenging.

The following is an update of melanins, their structure and how better understanding of these will help in the interpretation of the nature of the pigment seen in alkaptonuria.

Melanins

The family of melanins, related to the metabolism of tyrosine (Fig. 1), were first described as a black animal pigment and subsequently used to indicate any black or dark brown organic pigment material. A classification was proposed (Nicolaus 1969) indicating three main groups: eumelanin, pheomelanin and allomelanins. A more recent classification (Fig. 1a) of melanins comprises four main classes: (a) eumelanins, black-to-brown insoluble pigments derived from the oxidative polymerisation of L-dopa via 5,6-dihydroxyindole (DHI) intermediates; (b) pheomelanins, yellow-to-reddish brown; (c) neuromelanins, dark pigments produced within substantia nigra neurons; and (d) allomelanins (pyomelanin). These could be further classified in at least five main types according to the source: animal, plant, fungal, bacterial and synthetic melanin (Solano 2014).

Melanin is mainly synthesised in melanocytes, a heterogeneous group of cells originating from embryonic neural crest cells (Cichorek et al. 2013). The melanocytes predominate in the skin epidermis but are also found in the hair and iris where they give colour to these structures and in the inner ear, nervous system and heart (Wakamatsu et al. 2008; Takeda et al. 2007). Other cells as well as melanocytes may produce melanin, e.g. cells of pigmented epithelium of retina, epithelia of iris and ciliary body of the eye, some neurones and adipocytes (Takeda et al. 2007 and Sakamoto et al. 2005). Melanin is made within small membrane-bound packages, the melanosomes. As they

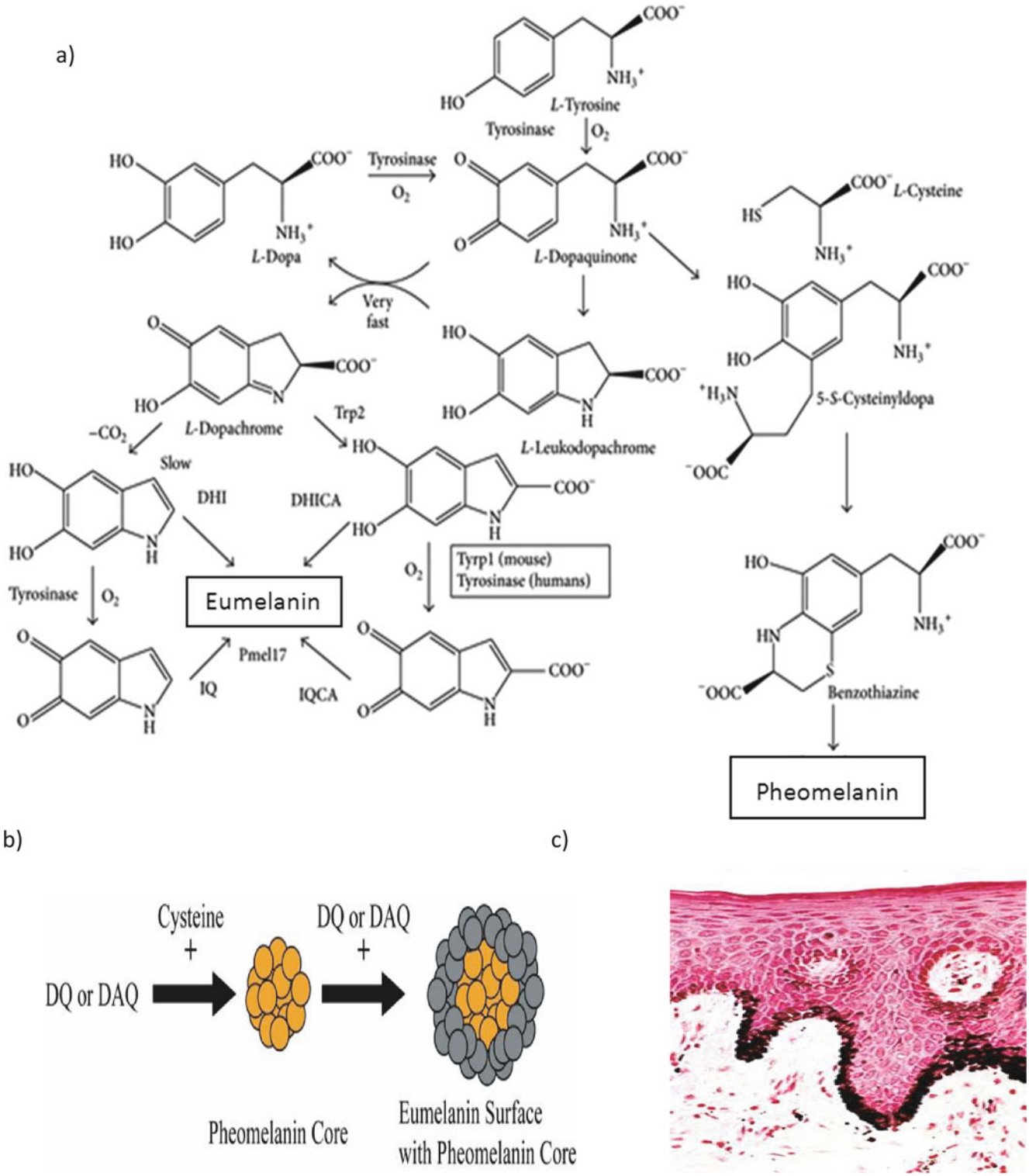

Fig. 1 (**a**) Raper–Mason pathway for eumelanin and pheomelanin formation. The initial phase until L-dopaquinone is common to pheomelanin and eumelanin through the oxidation of L-tyrosine catalysed by the two activities of tyrosinase, tyrosine hydroxylase and dopa oxidase. L-Dopa quinone is the pivotal intermediate. Addition of L-cysteine gives place to benzothiazine units and then to pheomelanins (right side of the pathway). In the absence of L-cysteine, eumelanogenesis takes place since L-dopaquinone spontaneously cycled to L-leukodopachrome. This indoline reacts with L-dopaquinone in a very fast spontaneous reaction to yield L-dopachrome. L-Dopachrome is converted to DHI and DHICA mixtures, according to Trp2 activity and decarboxylation rate. Further oxidation of these dihydroxyindoles by tyrosinase or Trp1 gives place to indolequinones, and subsequent cross-link reactions between hydroxy and quinone forms lead to the polymer (Solano 2014). (**b**) Representation of eumelanin stacking on top of a core of pheomelanin. DQ, dopaquinone, and DAQ, dopamine quinone, from Ito and Wakamatsu (2008) and Sulzer and Zecca (1999). (**c**) Fontana–Masson stain shows melanin granules by reduction of silver nitrate to metallic silver at pH 4.0, shown as accumulation of black material in the cytoplasm of skin keratinocytes

become full of melanin, they move into the melanocytes, from where they are transferred to the keratinocytes, the predominant cell in the epidermis or outer layer of the skin. Under normal conditions, melanosomes cover the upper part of the keratinocytes as a barrier to UV-associated genetic damage (Jablonski 2012).

Microphthalmia-associated transcription factor (MITF) acts as a master regulator of melanocyte development, function and survival by modulating various differentiations and cell-cycle progression genes (Levy et al. 2006). The premelanosome protein or melanocyte-specific glycoprotein Pmel17 is synthesised as an integral membrane protein of melanosomal compartments, which drives the formation of striations from within multivesicular bodies (MVBs) and is thus directly involved in the biogenesis of premelanosomes (Berson et al. 2001). The Pmel17 protein and MVBs create the unique architecture of the premelanosome where Pmel17 is enriched in the lumen of premelanosomes and where it associates with characteristic striations of unknown composition upon which melanin is deposited.

Thus, melanin is produced and stored in specialised lysosome-related organelles called melanosomes. The members of the tyrosinase-related family (tyrosinase and tyrosinase-related proteins TRP-1 (DHICAoxidase) and TRP-2, DOPAchrome tautomerase (Del Marmol and Beermann 1996) are also involved in the process of melanogenesis leading to the production of either eumelanin (brown-black) or pheomelanin (yellow-red). This difference in colour development in cell-specific pigment is regulated by MITF through transactivation of the promoters of the tyrosinase gene family (Murisier and Beermann 2006). The overall production of melanin is orchestrated by the pituitary through secretion of melanocyte-stimulating hormone and other cleavage products of a large precursor peptide proopiomelanocortin (Pritchard et al. 2002). The fragment α-MSH is the most important melanocortin for pigmentation and is a fragment of the ACTH part of the precursor molecule. In diseases with oversecretion of ACTH because of pituitary tumours or failure of cortisol production as in Addison's disease, marked increases in pigmentation (bronzing) are often a clinical presentation because of the concomitant production of α-MSH (Pritchard et al. 2002; Barber et al. 2010).

People have different skin colours, mainly because their melanocytes produce different amounts and kinds of melanin. Natural skin colour can also darken after exposure to intense sunlight as an adaptation to provide partial protection against the UV light-mediated damage to the skin cell DNA (Jablonski and Chaplin 2010).

Melanin Types

Eumelanin has two types: black and brown (Fig. 1). The associated polymers have long been thought to comprise numerous cross-links comprising 5,6-dihydroxyindole (DHI) and 5,6-dihydroxyindole-2-carboxylated acid (DHICA). A small amount of black eumelanin in the absence of other pigments causes grey hair, and brown eumelanin in the absence of other pigments causes yellow (blonde) hair. People with darker skin tones have more of eumelanin as a photo-protectant against harmful UV rays.

Pheomelanin (Fig. 1) is a reddish colour pigment, with very weak absorptive properties of UV radiation. It acts as a photosensitiser by enhancing the skin sensitivity toward sunlight and increases during the aging process. Females tend to have more of this pigment in their skin than men. It is found in particularly large quantities in red hair, lips, nipples, glands of the penis and vagina (Valverde et al. 1995).

The eumelanin-to-pheomelanin ratio determines the skin tone more eumelanin the skin looks darker dependent on the spread, size and number of melanosomes.

Neuromelanin is so called because of black/brown pigmented granules, different from melanosomes, found in the brain, particularly dopaminergic neuronal cells of the substantia nigra, causing their characteristic dark appearance. The pigment is composed of aggregates of 30-nm diameter spheres with a pheomelanin core, a eumelanin surface and a pheomelanin-to-eumelanin ratio of 3:1 of indeterminate size. The complex has been shown to bind heavy metals (Zecca et al. 2008). A recent study using proteomics of the melanin complex systems within neurones suggested the presence of endoplasmic reticulum-derived chaperones, especially the transmembrane protein calnexin, located in lysosome-related melanosomes suggested to be a melanogenic chaperone (Tribl et al. 2005).

Other cells if the necessary enzymes are present will also produce melanins, e.g. epithelia of the retina and iris, some neurones and adipocytes (Ito and Wakamatsu 2008; Murisier and Beermann 2006).

Biosynthetic Pathways of Eumelanin and Pheomelanin

The genetic mechanism behind colouration of human skin, eyes and hair shades is mainly regulated by the activity of tyrosinase which catalyses the first step of the biosynthetic pathway for both eumelanins and pheomelanins (Fig. 1a). The initial phase consists of the oxidation of L-tyrosine catalysed by the two activities of tyrosinase, tyrosine

hydroxylase and dopa oxidase with L-Dopaquinone, the key intermediate. Addition of L-cysteine gives place to benzothiazine units and then to pheomelanins. In the absence of L-cysteine, the formation of eumelanin occurs as L-dopaquinone spontaneously cycles to L-leukodopachrome. This indoline reacts with L-dopaquinone in a very fast spontaneous reaction to yield L-dopachrome.The L-dopachrome is then converted to DHI and DHICA mixtures, according to Trp2 activity and the rate of decarboxylation. Further oxidation of these dihydroxyindoles by tyrosinase or Trp1 gives place to indolequinones; subsequent cross-link reactions between hydroxy and quinone forms lead to the polymer (Solano 2014).

Thus, tyrosine is hydroxylated to L-dopa via tyrosinase and the intermediate dopaquinone can then combine with cysteine by two pathways to benzothiazines and pheomelanins:

Dopaquinone + cysteine → 5-*S*-cysteinyldopa → benzothiazine intermediate → pheomelanin
Dopaquinone + cysteine → 2-*S*-cysteinyldopa → benzothiazine intermediate → pheomelanin

The dopaquinone can also be converted to leucodopachrome (cyclo-dopa, 2-carboxy-2,3-dihydro-5,6-dihydroxyindole) and follow two more pathways to the eumelanins:

Dopaquinone → leucodopachrome → the cyclised product dopachrome(5,6-Dioxo-2,3,5,6-tetrahydro-1*H*-indole-2-carboxylic acid) → 5,6-dihydroxyindole-2-carboxylic acid → quinone → eumelanin
Dopaquinone → leucodopachrome → dopachrome → 5,6-dihydroxyindole → quinone → eumelanin

Studies of the early stages of melanogenesis (involving dopaquinone and cysteine) indicate that mixed melanogenesis proceeds in three distinct stages: the initial production of cysteinyldopas, followed by their oxidation to produce pheomelanin and finally by the production of eumelanin. A model was proposed in which a preformed pheomelanic core is covered by a eumelanic surface (Ito and Wakamatsu 2008) creating the final colour of the melanin. This was supported by kinetic studies (Bush et al. 2006) of pigments containing a mixture of pheomelanin and eumelanin, of which neuromelanin is an example, where pheomelanin formation occurs first with eumelanin formation predominantly occurring only after cysteine levels are depleted. Such a kinetic model would predict a structure with pheomelanin at the core and eumelanin at the surface (Fig. 1b).

The final reactions in forming the pigments may be nonenzymatic mediated by conditions of pH and precursor concentrations (Land et al. 2003). In this final phase of polymerisation, the Pmel17 protein located in the eumelanosome seems to have a role in the regulation and deposition of the polymer on that organelle.

The proposed structural basis for these polymers and a relationship to black appearance are shown (Fig. 2). However, the unsaturated backbone is not planar but if they form layers will result in similar light properties (Tran et al. 2006). These melanin pigments with or without nitrogen systems have defined pathways which can be found in the KEGG (Kyoto Encyclopedia of Genes and Genomes) database.

The primary function of melanin is the protection of tissues from sunburn by ultraviolet radiation, and there is a direct correlation between the geographic distribution of UV radiation (UVR) and the distribution of indigenous skin pigmentation around the world. Reducing this pigmentation can be achieved by inhibiting tyrosinase activity (Videria et al. 2013).

Pigmentation in AKU: The Nature of the Pigment

The nonnitrogenous melanin (Fig. 3), based on the oxidation of homogentisic acid and subsequent chemical modification/polymerisation, causes the ochronosis seen in the genetic disease Alkaptonuria (Ranganath et al. 2013). This is explained by a marked accumulation of HGA as a result of a defective homogentisate 1,2-dioxygenase (HGD) enzyme that is unable to metabolise HGA. The production of the precursor benzoquinone (BQA) (Zannoni et al. 1969) shown in Fig. 3 is the pivotal first step in pigment formation similar to the formation of dopaquinone in melanin synthesis (Turick et al. 2010). The oxidation product of HGA in aqueous solution was shown to be stable in acidic, neutral and weak alkaline media using cyclic voltammetry and that the subsequent chemical dimerisation is more probable for the oxidised form of HGA (Eslami et al. 2014).

The question in human metabolism relates to how this pigment forms as there is relatively low activity of tyrosinase to oxidise HGA. However, studies (Martin and Batkoff 1987) showed that homogentisic acid oxidation can occur nonenzymatically between pH 6.8 and 9.5 in the presence of oxygen, proportional to the concentration of HGA and optimal at 37°C. Formation of the oxidised product, benzoquinoneacetic acid (BQA), was inferred by decreased absorption at 290 (HGA) and increase at 250 and 315 nm, respectively. This was inhibited by the reducing agents – NADH, reduced glutathione and ascorbic acid – and accelerated by SOD and manganese pyrophosphate. These studies also indicated that the viscosity of buffered solutions of hyaluronic acid treated with homogentisic acid up to 100 μM was decreased by 40–50%, with maximal loss after 40–60 min incubation. Hyaluronic acid solutions incubated without homogentisic acid showed no change in viscosity. This may be highly relevant to the damaging

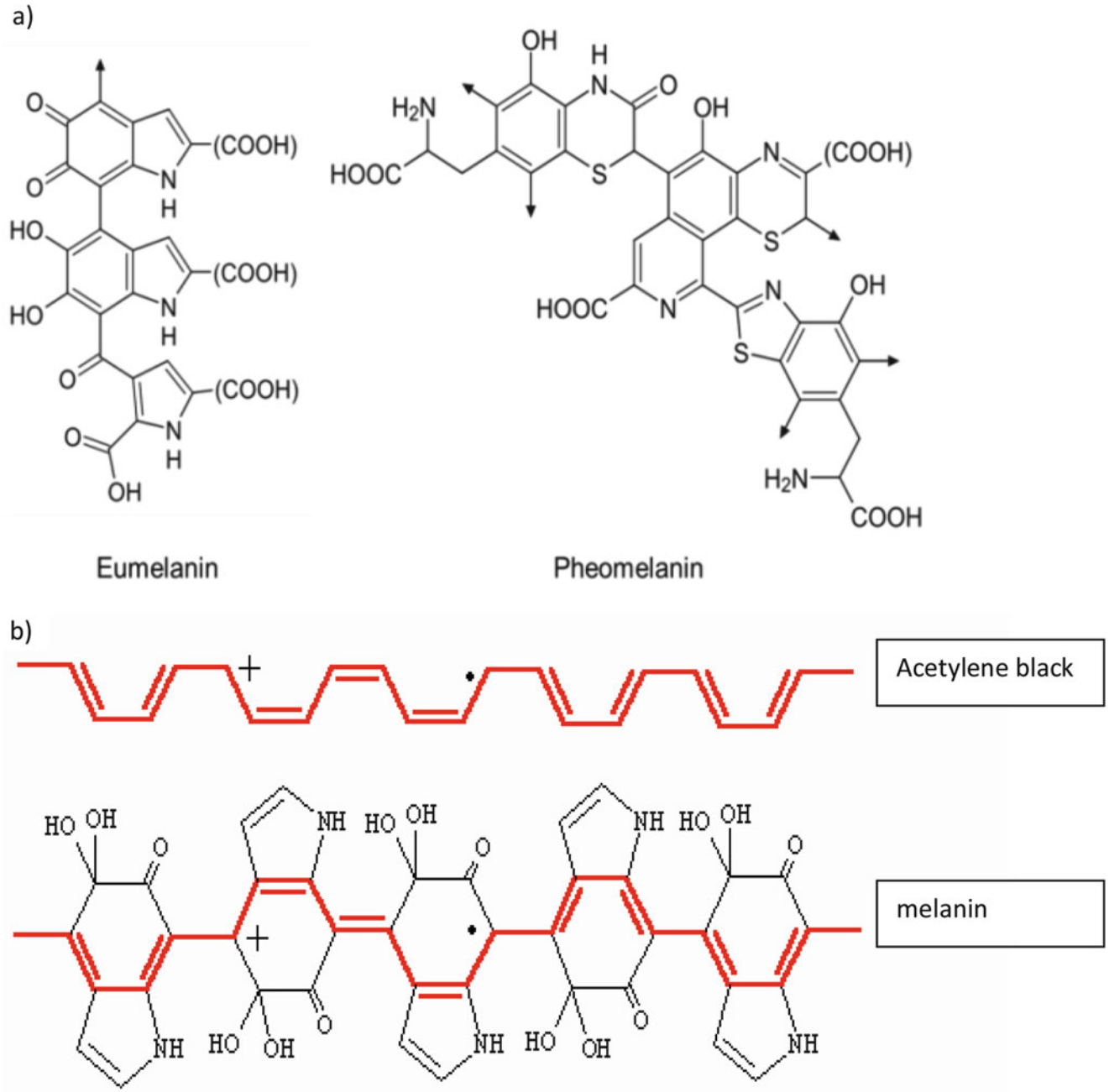

Fig. 2 (**a**) Part of the structural formula of eumelanin or pheomelanin. "(COOH)" can be COOH or H or (more rarely) other groups. The *arrow* denotes where the polymer continues. (**b**) Structure of repeating acetylene groups produces a black colour (*top*) similar to the structure of repeating units in melanin (*bottom*)

process as hyaluronic acid is the chief viscous element of synovial fluid and the backbone of cartilage collagen (Martin and Batkoff 1987). Wolff et al. (1989) were able to measure both HGA and the benzoquinone acetate (BQA) by HPLC and EC detection and indicated that ascorbic acid administration reduced the output of BQA but not HGA, suggesting the importance of vitamin C treatment as BQA was thought to be the damaging agent rather than HGA. Subsequent clinical studies on the effectiveness of vitamin C in reducing pigmentation have been inconclusive, and Forslind et al. (1984) concluded that "ascorbic acid is not effective in the treatment of symptomatic ochronosis." However, studies from an in vitro model using human serum treated with 0.33 mM HGA showed that the reducing agents, ascorbic acid (ASC) and other antioxidants including N-acetyl cysteine, were able to prevent HGA oxidation to BQA and formation of both protein adducts with the benzoquinone and the ochronotic pigment, as well

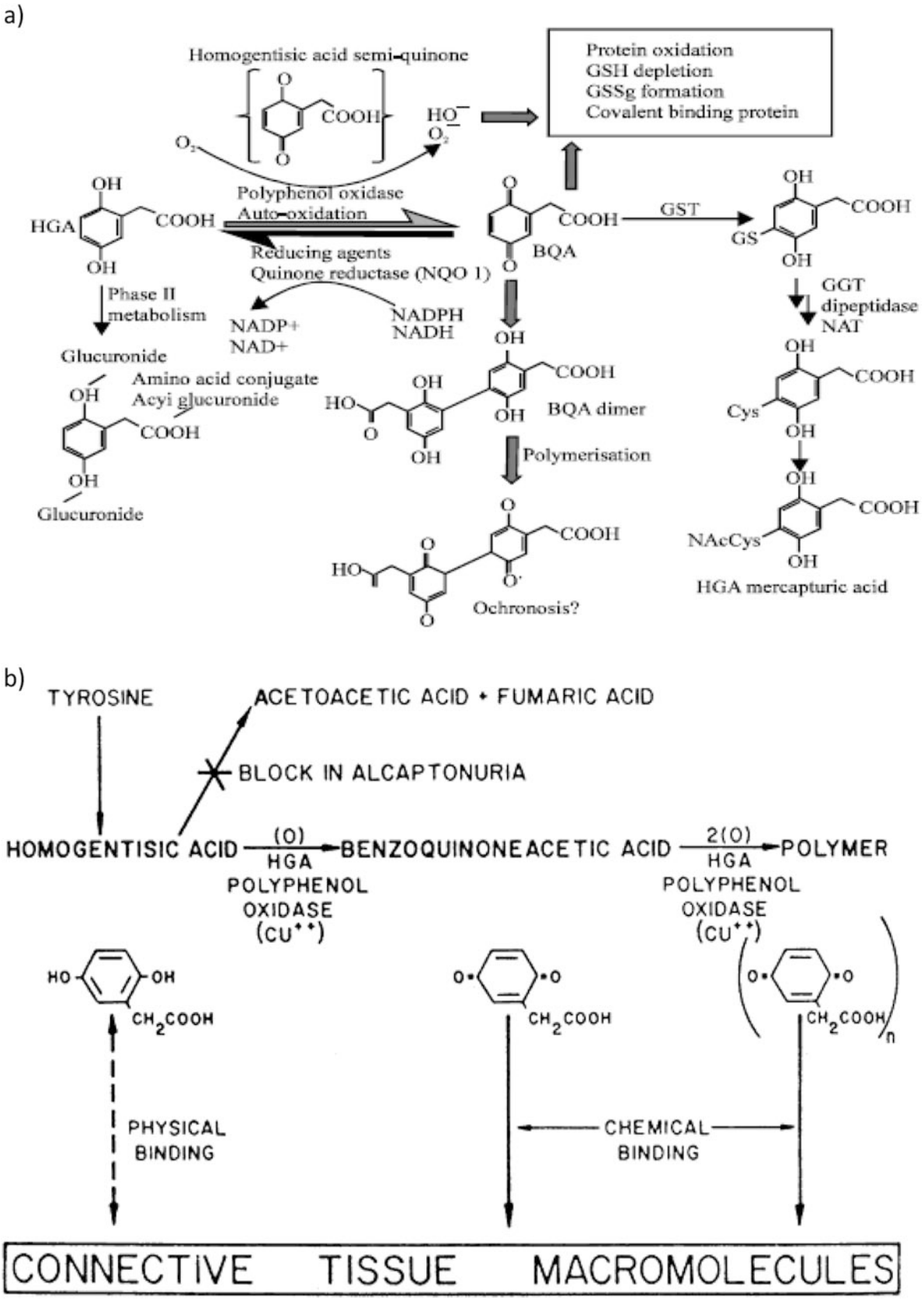

Fig. 3 Proposed pathway of the pyomelaninlike AKU pigment based on the formation of benzoquinone enzymatically or by auto-oxidation and then subsequent dimerisation as well as alternative metabolic routes to, HGA mercaptouric acid and HGA glucuronide and subsequent protein binding. NB the relative proportions of these processes are not known (Williams et al. 2012; Zannoni et al. 1969).

as reactive oxygen-mediated cell damage (Braconi et al. 2010, 2011).

Unfortunately, ASC may also auto-co-oxidise with HGA, i.e. act together as prooxidants to produce additional oxidative damage. To counteract this, a second reducing agent in combination, *N*-acetylcysteine (NAC) that specifically protects cell glutathione ,was added to reduce the negative effects of excess HGA (0.33 mM) and restore viability, proliferation and chondrocyte anabolism (Tinti et al. 2010). On the basis of these in vitro cell models, in particular the human articular primary chondrocytes, Tinti et al. (2010) suggested a possible way forward for the treatment of ochronotic arthropathy. Also further studies have shown that the combination of antioxidants vitamin C and *N*-acetylcysteine improves red cell viability during storage (Pallotta et al. 2014) and protects from indoxyl sulphate-induced oxidative stress and antiproliferative effects attributed to mitochondrial dysfunction and impaired biogenesis (Lee et al. 2015).

However, data from an acute human inflammatory model of muscle injury (Childs et al. 2001) indicated that administration of vitamin C and NAC immediately post injury may increase tissue damage and oxidative stress. In addition, because ascorbic acid serves as a cofactor for 4-hydroxyphenylpyruvate dioxygenase, the vitamin may increase production of HGA in alkaptonuria (Phornphutkul et al. 2003). Furthermore, the large doses of ascorbic acid actually used in alkaptonuria might contribute to the formation of renal oxalate stones in patients with this disorder, who are already at increased risk for kidney stones.

Thus, the antioxidant approach to treatment still seems controversial, but being able to block the formation of HGA complexes is clearly advisable as formation of plasma-soluble melanin-type complexes similar to lipofuscin were also suggested to be cytotoxic (Hegedus 2000).

Unfortunately detailed chemical analysis outlining the structure of the AKU pigment is still lacking, but similar products have been well described in bacteria and other species. In bacteria an HGA oxidase is present and the HGA-derived pigment pyomelanin can be shown in at least three clinically isolated strains of *Pseudomonas aeruginosa* (Ogunnariwo and Hamilton-Miller 1975). Similarly the pigment formed by Vibrio cholerae was related to oxidation of homogentisic acid (Ruzafa et al. 1995). A recent study (Carreira et al. 2001) showed that the organism Yarrowia lipolytica was responsible for the brown colouration of various cheeses, ewes, Camembert and gorgonzola, by the production of homogentisic acid and oxidation to form a brown pigment. The single hydroxyl acids, *p*-hydroxyphenylethanol (*p*-HEA) and *p*-hydroxyphenylacetic acid (*p*-HPAA), did not oxidise in this way, indicating that it was related to the presence of the dihydroxy form. The pigment formation was also dependent on the release of HGA from within the cell. The HGA pigment in bacteria seems to have specific functions involved in the protection from sunlight and scavenging of trace or toxic elements (Przemyslaw et al. 2006). The organism *Burkholderia cenocepacia* C5424 produces a pigment using an HGA intermediate and was shown to help protect the organism from oxidative damage by host cells (Keith et al. 2007). The loss of pigment production resulted in the generation of a *B. cenocepacia* strain that was more sensitive to oxidative stress in vitro.

In AKU the process of pigmentation seems to be relatively random being dependent on localised concentrations of HGA able to produce pigment products which then bind to tissue proteins. The exposure to the pigment increases with age and hence the severity of the condition. Linear regression analysis indicated that the radiographic score for the severity of disease began increasing after the age of 30 years, with a more rapid increase in men than in women (Phornphutkul et al. 2002). The ochronotic chondrocyte pigmentation of a mouse model was also shown to follow an age-related pattern with the first signs of pigmentation restricted to the pericellular matrix surrounding individual chondrocytes, followed by eventual progression to the intracellular compartment (Preston et al. 2014). The cartilaginous tissues and bone seem to be particularly susceptible resulting in widespread arthritis and joint destruction (Keller et al. 2005) as well as deterioration of cardiac valves (Lok et al. 2013). In fact a lack of HGD activity in human cardiac tissue was suggested as the cause of localised production of ochronotic pigment in AKU heart (Lok et al. 2013). It could be that other tissues affected by the disease with an enzyme defect have similar increased HGA and pigment production contributing to the induction of ochronotic arthropathy (Laschi et al. 2012).

The composition of ochronotic pigment was investigated by energy-dispersive X-ray spectroscopy (EDS, EDX or XEDS or energy-dispersive X-ray analysis, EDXA) micro-analyses on the dark surface of a heart valve from a patient with AKU (Millucci et al. 2014). The data revealed that pigmented areas are composed of C, O, N, S, Na and variable amount of Ca. The white solid deposits in the pigmented valves were shown to contain P and Ca,

NB the enzyme "polyphenol oxidase" cited in the figure is reported in protein database as the enzyme EC:1.10.3.1, catalysing the oxidation of ortho- but NOT *para*-diphenols. Polyphenol oxidases are enzymes generally found in plants but not in humans, as this enzyme does not exist in the sequenced human genome. An enzyme able to oxidise *p*-diphenols is the "laccase" (EC:1.10.3.2), acting both on *o*-quinols and *p*-quinols and often acting also on aminophenols and phenylenediamine

indicating the presence of hydroxyapatite and a process of endochondral ossification. The SEM images showed an active process with collagen appearing as delicate bundles of fibres with a random orientation and bone-like concretions (Millucci et al. 2014). The unexpected finding of sulphur in cardiac valve tissue pigment was thought to be related to the ability of BQA (oxidised HGA) to form adducts with protein thiols. The rapid formation of such protein complexes has been shown to be dependent on the oxidation of HGA, i.e. through production of BQA (Hegedus 2000). It is thought that products generated by HGA/BQA-induced lipid oxidation are involved in the inflammatory process present in the AKU heart valves as HGA induces SAA (secondary A-amyloid [AA]) amyloidosis and proinflammatory cytokines (Millucci et al. 2014). SAA amyloidosis is a serious complication of chronic inflammatory conditions such as rheumatoid arthritis, and its amyloid deposition process involves a cleaved product of the acute-phase protein serum amyloid A (SAA) (Momohara et al. 2008). Indeed it was suggested that alkaptonuria is a novel-type II AA amyloidosis, if so will open new important perspectives for its therapy, particularly as methotrexate treatment significantly reduced in vitro HGA-induced amyloid A aggregates (Millucci et al. 2012).

Even though this suggests evidence of an inflammatory component, the underlying chemical mechanism for the damaging effect on cartilage is still not proven, and it may be that damage has already occurred and pigmentation is a secondary consequence. The development of nitisinone [2 (2-nitro-4-trifluoromethylbenzoyl)-1,3-cyclohexanedione (NTBC), a potent inhibitor of p-hydroxyphenylpyruvate dioxygenase (which catalyses the formation of homogentisic acid from p-hydroxyphenylpyruvic acid) (Suzuki et al. 1999)], is now used to reduce circulating HGA in AKU patients (Introne et al. 2011). The subsequent effects of such treatment on pigment production and damage will need to be carefully monitored in particular if the osteoarthritis is controlled. Such a programme will need to establish the optimal dose to properly assess how reducing HGA affects pigmentation in the long term for adults (Ranganath et al. 2014). Unfortunately the drug is not yet licensed to treat children with AKU, and as a result, it will be impossible to assess how treatment might affect the development of ochronosis in the earlier years of life.

As regards the chemical structures in the AKU pigment, these are still not clearly defined but maybe represented by forms similar to melanin, i.e. with polymers of varying repeat units (Fig. 3). However, several simple compounds that have similar structures to HGA (MW 168) can result in colouration similar to ochronosis type pigmentation. The rust-coloured perspiration of the hippopotamus contains pigments, conjugated three-ring structures, the red hipposudoric acid (MW 328.3) and the orange norhipposudoric acid (MW 284.3) (Hashimoto et al. 2007). The two compounds are formed from the oxidative dimerisation of homogentisic acid (Kai et al. 2006). They absorb light in the UV–visible range (200–600 nm) and so are thought to protect the hippo's dermis from the sun. Additionally, low concentrations of hipposudoric acid inhibit the growth of bacteria. Both compounds are highly reactive and tend to polymerise when removed from the hippo and or a water source (Galasso and Pichierri 2009). An unknown agent in hippo mucus keeps the compounds from polymerising for several hours, even after the hippo sweat dries. Further examples of low-molecular-weight-coloured substances are the active ingredients of the henna plant (Lawsonia inermis) 2-hydroxy 1,4 naphthoquinone (MW 174.15) which forms yellow ochre-like prisms when pure but behaves as a red-orange dye. It absorbs UV light and can be used as a sunscreen. The plant extract has been used for over 5,000 years to dye fabrics as well as skin and hair. Another such compound is juglone or 5,hydroxyl 1,4 naphthalenedione (MW 174.2), a brown pigment found in walnuts and naturally in leaves, roots, husks and bark of plants (Juglandaceae family). It is used as a dye, food and cosmetic colourant. In other words the ochronotic pigment may not necessarily be a molecule of polymer proportion.

Analysis/Detection of the Melanin Types

The chemical composition of melanin differs at every location, and the exact information regarding the individual pathways and structures need to be evaluated accordingly. Usually the location is a key to identification, although it can be difficult to decide whether a brown/dark pigment is lipofuscin, hemosiderin or melanin. Melanin stains are Fontana–Masson (stains melanin black) and Schmorl's method based on the reduction of ferricyanide to ferrocyanide, which in the presence of ferric ions forms prussian blue (i.e. stains melanin blue green) (Bancroft and Stevens 1955). The argentaffin cells, chromaffin cells and some lipofuscins will also stain blue and the nuclei red. Prior bleaching of tissue slides with potassium permanganate or hydrogen peroxide is used to remove melanin and thus confirms the type of complex. It is worth noting that the pseudomelanin of melanosis coli caused by accumulation of lipofuscin in macrophages of the colon is periodic acid Schiff's stain (PAS) positive, i.e. stains for mucopolysaccharides and true melanin does not. The Fontana–Masson stain is useful for melanin and the "argentaffin granules" of the digestive tract. At pH4, melanin granules reduce silver nitrate to metallic silver, a histochemical reaction that shows accumulations of black material wherever melanin is located. This is seen in the cytoplasm of skin keratinocytes (Fig. 1c).

However, the stains for melanin are simply oxidising agents that are reduced by polyphenol-type reducing substances with defined colour changes and are only indicative not confirmative of melanin. Chemically, melanin is insoluble and amorphous, and it cannot be studied as a crystal form or as a solution. The understanding of the chemical composition of melanin remains limited, due to a paucity of direct measurements. However, to improve understanding of relevant structures, partial degradation processes have been devised for each component, e.g. for eumelanin fragments 5,6-dihydroxyindole (DHI) and 5,6-dihydroxyindole-2-carboxylicacid (DHCI).

Avian feathers have an unparalleled diversity of melanin-based colour mirroring their complex chemistry (Liu et al. 2014). Elucidation of the chemical composition of avian melanin samples of black, brown, grey and iridescent feathers was carried out using laser desorption synchrotron post-ionisation (synchrotron-LDPI) mass spectrometry. The post-ionisation was achieved by tunable vacuum ultraviolet (VUV) radiation to ensure that the internal energy gained during laser desorption caused minimal fragmentation of molecules. The fragment molecules detected were able to distinguish eumelanin-to-pheomelanin ratios based upon *m/z* 311, 399, 443 and 487 of various redox forms of 5,6-dihydroxyindole (DHI) and 5,6-dihydroxyindole-2-carboxylic acid (DHICA) representing eumelanin and *m/z* 284 and 383 for pheomelanin. Structures indicative of pheomelanin fragments were defined as functionalised benzothiazole, benzothiazine and pyrrole-2,3,5-tricarboxylic acid TPCA moieties (Liu et al. 2014).

Solid-state NMR spectroscopy has also been used to study the structural properties and motional behaviour of natural eumelanin and pheomelanin extracted from black and red human hair (Thureau et al. 2012). Several 1D and 2D NMR spectroscopic techniques were combined to highlight the differences between the two forms of the pigment. It was clear that not only structural features inherent in the pure pigment, but also the role of the matrix structure in defining the overall melanin supramolecular arrangement should be taken into account to explain their functions. The characterisation of eumelanin revealed subunits organised into small planar oligomeric sheets (4–8 monomers), which stack to create nanoaggregates (Fig. 1b and Littrell et al. 2003).

A recent study, using low-voltage high-resolution transmission electron microscopy (TEM), showed the existence of eumelanin protomolecules that stack to form onion-like nanostructures with intersheet spacing between 3.7 and 4.0 Å (Watt et al. 2009). The recent developments in the optimisation of Fourier transform infrared (FTIR) spectroscopy indicate the increasing potential of this technique to highlight compositional differences, in particular a unique chemical profile in the outer segments of pigmented retina compared to other retinal layers, and this profile was altered in albino animals (Levine et al. 1999). Further developments using mid-infrared beamline IRENI (InfraRed ENvironmental Imaging) enabled study of changes in saturated and unsaturated fatty acid ester content in the neuronal layers of the retina. The analysis of amyloid plaques from the model Alzheimer mice showed elevated lipids surrounding and within the dense core of amyloid plaques, suggesting processes of inflammation and aggregation in Alzheimer's disease (Kastyak-Ibrahim et al. 2011). Further improvements in software analysis (Baker et al. 2014) will hopefully enable this technique to be more applicable to unstained tissue sections, for example, from patients with Alkaptonuria.

Although pheomelanin is less widespread in nature, interest in its characterisation has grown due to its correlation susceptibility to skin cancer as a result of underexpression of "melanocortin 1 receptor" (alpha melanocyte-stimulating hormone receptor) or *MC1R* gene. This was shown to favour the production of pheomelanin rather than eumelanin and an increased sensitivity to UV radiation (Millington 2006).

Analysis of Pigment Derived from HGA

The major issue in the analysis of the pigment seen in alkaptonuria is ready access to sufficient amounts to carry out detailed structural compositional studies. The possibility of using model systems therefore to produce the pigment would be of considerable value in optimising analytical procedures. In an AKU mouse model, the presence of extensive chondrocytic pigmentation present throughout the femoral and tibial calcified cartilage was observed using Schmorl's stain (Preston et al. 2014). This study showed how such a model can represent a source of tissue pigmentation and as a result now forms part of a detailed research programme (FP7-HEALTH 2012). Other sources of pigment are possible, for example, the fungus *Cryptococcus neoformans* is able to produce eumelanin from catecholamine precursors, such as L-dopa, epinephrine and norepinephrine and importantly the ochronotic type pigment (allomelanin/pyomelanin) from HGA (Frases et al. 2007). Unlike other fungi, melanisation in *C. neoformans* occurs only when the organism is exposed to precursor compounds; thus, it is ideal as a ready supply of the different melanin types. The forms allomelanin and melanin were produced by H99 *C. neoformans* cells grown with 1 mM of HGA at 22°C for 5 days and/or L-dopa, respectively. The separate pigments were oxidised with permanganate and analysed by high-performance liquid chromatography. The chromatograms showed the presence of peaks matching those of pyrrole-2,3-dicarboxylic acid,

1,3-thiazole-2,4,5-tricarboxylic acid (TTCA) and 1,3-thiazole-4,5-dicarboxylic acid (TDCA) in HGA melanin particles. The presence of pyrrole-2,3,5-tricarboxylic acid (PTCA) was consistent with the presence of permanganate-oxidised degradation products from L-dopa melanin. These separate oxidative products therefore imply different molecular structures for HGA and L-dopa-derived melanins. The diameters and the thicknesses of the shells of the particles recovered from HGA-pigmented cells were also less and were more negatively charged than L-dopa-derived particles. Furthermore, HGA-derived particles were fluorescent when illuminated with several wavelengths, while no fluorescence was produced by similarly irradiated L-dopa particles.

HGA melanin type can also be prepared from pure solutions of HGA (Turick et al. 2009) with molecular weight ranging from 10 to 14 kDa (Turick et al. 2002) smaller than other melanin pigments. The synthetic pyomelanin has a relative greater purity and provides for a consistent structure as microbial pigments often contain metabolic residues such as proteins, amino acids and carbohydrates (David et al. 1996). The synthetic form is therefore a more suitable material for detailed analysis. Several possible polymeric structures, based on Fourier transform infrared (FTIR) spectroscopy data, indicated the presence of quinones and phenols. The FTIR analyses of pyomelanin produced from the auto-oxidation of HGA (HGA melanin) (David et al. 1996) showed absorbance peaks consistent with the OH stretch of polymeric structures, aliphatic CH bonds, aromatic C=C bonds conjugated with C=O and/or COO- groups as well as phenolic OH groups. The presence of quinones in the pyomelanin structure was then confirmed by cyclic voltammetry indicating a two-step oxidation followed by a two-step reduction (Turick et al. 2010). The electron-transfer properties of melanin polymers, including pyomelanin, also constitute a mechanism of electron transfer to solid electron acceptors like metal oxides and electrodes (Ellis and Griffiths 1974; Turick et al. 2003, 2010). This explains how staining shows the presence of reducing substances in tissues through the coupling of hydroxybenzene depigmenting-compound oxidation caused by reduction of ferricyanide (Mentner and Willis 1997).

The application of UV–visible spectral analysis of solutions of HGA and urine from patients with alkaptonuria has been well described (Chen et al. 2014; Tokuhara et al. 2014). It was suggested that such scans could offer a quick and easy procedure to indicate the presence of the ochronotic pigment (Tokuhara et al. 2014). However, we were interested in the use of this technique to test whether we could show evidence of the presence of precursors as well as the presence of pigment. Samples taken from freshly prepared HGA solutions and urine from a patient with alkaptonuria, before and after alkalinisation, show how rapidly HGA is oxidised to the benzoquinone BZQ (Fig. 4). The latter then undergoes further change to possible pigment types with a UV–visible scan similar to synthetic pyomelanin and that produced by bacteria (Fig. 4) with no clear absorption spectra in the visible range. The loss of BZQ was slowed by maintaining pH at 6.0. Unfortunately we were not able confirm the two characteristic possible pigment peaks at 406 and 430 nm observed in urine from alkaptonuria patients incubated with NaOH (Tokuhara et al. 2014). The scan data also suggest the compounds were not similar to melanin derived from dopamine (Chen et al. 2014) where peaks in the visible region of 320, 450, 600 and 700 nm were observed. However, these latter peaks decreased markedly as the complexity of the melanin increased, i.e. via formation of increasing layers of the pigment producing the typical broadband absorption profile. This spectrum is similar to the broad spectrum of eumelanin ((Tran et al. 2006) and explains why visibly it appears black/dark brown (Fig. 2). In fact it is argued that eumelanin consists of many chemically distinct species, and the broadband absorption spectrum is a result of averaging the spectra of these species. The sharp peaks due to 5,6-dihydroxyindole (DHI) and its oligomers would therefore be eliminated after this process. Whether such scans could be used for monitoring the intermediate quinone seems unlikely as conditions favour the reaction of BZQ to form complexes with amino acids, e.g. cysteine (Bender et al. 2007).

The use of MALDI ESIMS as another approach was also investigated to assess the purity of any preparation and as a measurement of molecular weight. Analysis was carried out on pyomelanin synthesised from HGA metabolising bacteria and produced from solutions of HGA stored at pH 10 for 1 week (Turick et al. 2009).The *m/z* spectra (Fig. 5), after direct injection without any matrix-modifying agent, show a range of masses from 800 to 2,300 with the majority of around 1,100. These appeared as apparently single-charged entities suggesting a mixture of different molecular weights. Similar mass ranges were found with humic substances (Peña-Méndez et al. 2005). The use of a matrix modifier showed marked differences in the spectra with alpha cyanocinnamic acid giving masses around 900 and dihydroxy benzoic acid modifier a spectra of low mass components. These differences suggest inherent problems of complex molecular breakup within the spectrometer as a result of instrument conditions (Novotny et al. 2014). This suggests that further systematic studies are required to fully utilise the use of ESIMS on the AKU pigment.

Investigation into the composition of the humic acids may give further clues as to how to proceed in the analysis of AKU pigment. These acids are formed by condensation with polyphenol quinones and carbohydrates/sugars to

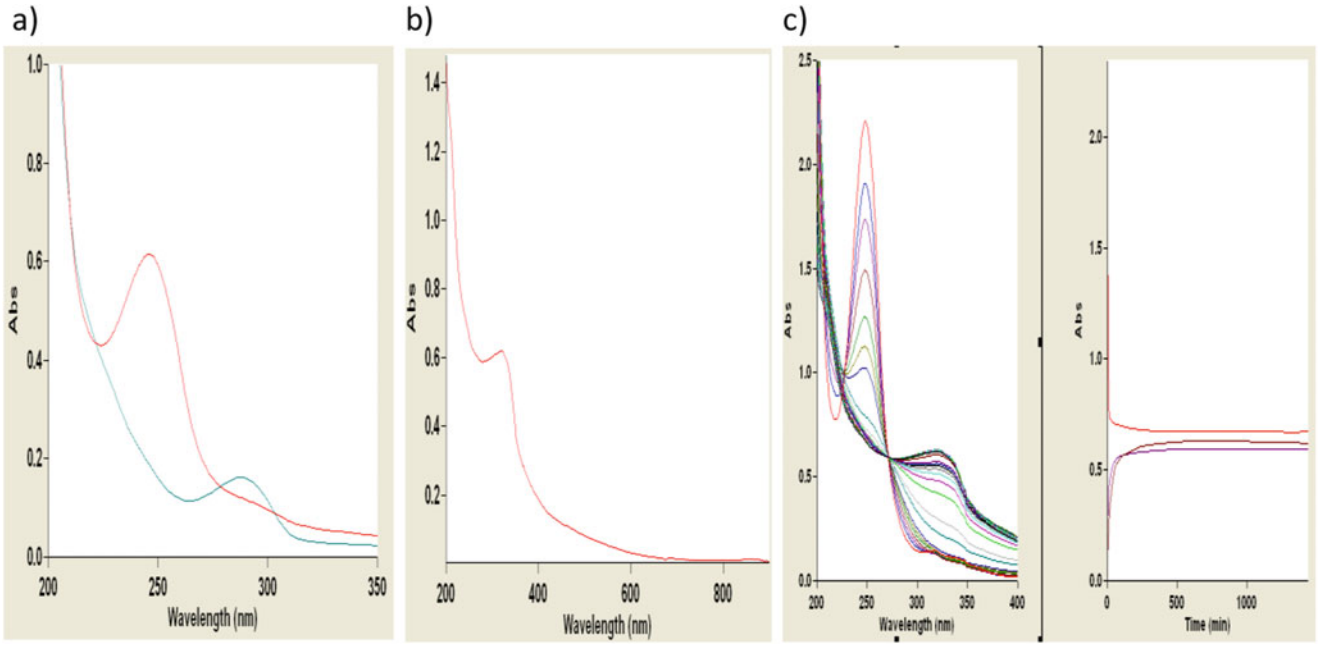

Fig. 4 Spectral scans of solutions of HGA, pigment and a urine from a patient with AKU effect of pH and time. All procedures followed were in accordance with the ethical standards of the local hospital ethics committee. Informed consent was obtained from patient(s) included in the study. (**a**) Pre- and post-alkalinisation, i.e. to pH 10 (1 pt10 M/L NaOH and 50 pts urine), of untreated AKU urine (approximately 20 mmol/L HGA): *blue line* pre and *red line* post. (**b**) HGA solution10 mmol/L scanned 24 h after alkalinisation with ammonia (20 mM/L final concentration). (**c**) A kinetic study of the alkalinisation of an HGA solution over 24 h absorbances at 250 nm (BQA=red), 290 nm (HGA=brown) and 318 nm (*purple*). Showing the rapid disappearance of BZQ peak 250 nm and slower loss of peak at 316. Scanning urine or synthetic pyomelanin at pH's 10.0, 7.0 and or 2.5 shows a similar profile with no definite peaks as in Fig. 4a (*blue line*) and **b**. However, for solution at pH 10.0 solutions, the peak at 250 nm was much less and was relatively stable at pH 6.0. Solutions/samples were diluted usually 1 pt to 100 pts of diluent deionised water or buffer solution and scanned with Cary UV−vis scanning spectrometer (Agilent, UK) giving a full scan (200–800 nm) every 1 min

produce a brown, melanin-tinted mixture of polymers, found in lignin, peat and soils (Novotny et al. 2014). Humic acid has the average chemical formula $C_{187}H_{186}O_{89}N_9S_1$ and is insoluble in strong acid (pH 1). A 1:1 hydrogen-to-carbon ratio indicates a significant presence of benzene rings in the structure, whereas a low oxygen-to-carbon ratio indicates fewer acidic functional groups than occur in fulvic acid, the other acidic organic polymer extracted from humus. Separation procedures of these compounds are available, but still more studies are required to elucidate the proposed intermolecular interactions that link humic components into supramolecular associations (Sutton and Sposito 2005) similar to the pigmentation process in AKU.

In conclusion pigments found in plants, animals and humic substances are well described and classified. In humans considerable progress has been made with the main pigment melanin in defining its biochemistry and the different types and functions. However, analytical techniques to show these differences in vivo are still not readily available. NMR and IR spectroscopy are relatively insensitive and reveal only major structural differences. Techniques utilising MS are useful in determining elemental content but require further studies to optimise conditions for accurate mass analysis. How the components may be structurally organised seems to be the most problematic, and scanning TEM as well as the improved FTIR seems to be of use in this respect. As regards understanding the nature of the pigment related to HGA seen in patients with AKU, it is still thought of as a melaninlike pigment simply because of its colour and likewise thought to be a polymer of undetermined size. It is important that detailed analysis be carried out to define more accurately this pigment. However, observations suggest it to be the same as the HGA-derived pigment pyomelanin, produced by bacteria containing both quinone and phenolic groups. The interesting developments in alkaptonuria will be to understand how such a polymer can cause such profound collagen and connective tissue damage and how best to reverse this process.

Compliance with Ethics Guidelines

All procedures reported in this review were in accordance with the ethical standards of the local hospital ethics committee and with the Helsinki Declaration of 1975, as

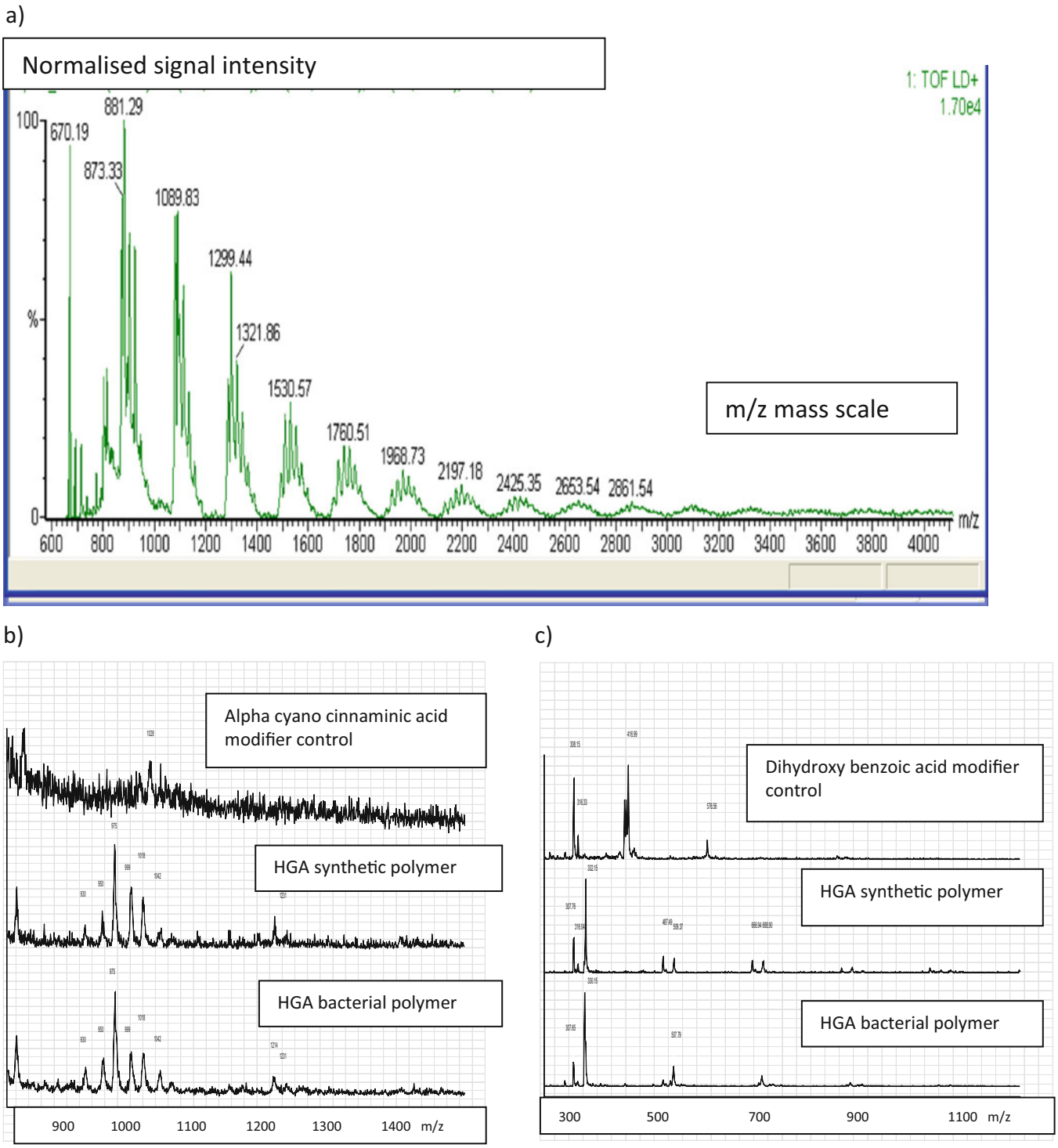

Fig. 5 (**a**) The pyomelanin was prepared from bacteria fed with increased tyrosine. Also synthetic pyomelanin was prepared from a solution of 20 mmol/L HGA at pH 10 and left for 7 days at 20°C. The samples were added to 10–15 kDa dialyser pack and dialysed against pure water for 24 h with two changes of the dialysate. The samples were then dried before analysis using a Micromass M@LDI™ linear MALDI-TOF -MS, with conditions MCP voltage 1,850, laser power 85, pulse voltage 1,500 and nitrogen UV laser 337 nM; (**a**) the *m/z* spectrum observed after straight injection into the MS with no modifier present, (**b**) MALDI MS with matrix modifier alpha cyanocinnamic acid and (**c**) MALDI MS with matrix modifier dihydroxy benzoic acid. For scans (**b**) and (**c**), top is the control matrix alone, middle synthetic and bottom bacterial pyomelanin. The pyomelanin and scans were provided by Dr CE Turick Savannah River National Laboratory, South Carolina USA

revised in 2000. Informed consent was obtained from patient(s) wherever included in this review.

Conflict of Interest

NB Roberts, SACurtis, A Milan and LR Ranganath have no conflict of interest.

NB Roberts was the main author who reviewed the literature and completed the review.

SA Curtis was responsible for the UV–visible spectra.

AM Milan, a senior colleague in the AKU group, reviewed and made corrections to the manuscript.

LR Ranganath is the director of the AKU group and was responsible for the commissioning of this review and made corrections to the manuscript.

References

Baker MJ, Trevisan J, Bassan P et al (2014) Using Fourier transform IR spectroscopy to analyze biological materials. Nature Prot 9:1771–1791

Bancroft JD, Stevens A (1955) Theory and practice of histological techniques, 2nd edn. Churchill Livingstone, New York

Barber TM, Adams E, Ansorge O, Byrne JV, Karavitaki N, Wass JAH (2010) Review Nelson's syndrome. Eur J Endo 163:495–507

Bender RP, Ham AJL, Osheroff N (2007) Quinone-induced enhancement of DNA cleavage by human topoisomerase IIα: adduction of cysteine residues 392 and 405. Biochem 46:2856–2864

Berson JF, Harper DC, Tenza D, Raposo GA, Marks MS (2001) Pmel17 initiates premelanosome morphogenesis within multivesicular bodies. Molec Biol Cell 12:3451–3464

Braconi D, Laschi M, Amato L, Bernardini G, Millucci L, Marcolongo R, Cavallo G, Spefico A, Santucci A (2010) Evaluation of anti-oxidant treatments in an in vitro model of alkaptonuric ochronosis. Rheum 49:1975–1983

Braconi D, Bianchini C, Bernardini G, Laschi M, Millucc L, Spreafico A, Santucci A (2011) Redox-proteomics of the effects of homogentisic acid in an in vitro human serum model of alkaptonuric ochronosis. J Inherit Metab Dis 34:1163–1176

Bush WD, Gargullo J, Zucca FA et al (2006) The surface oxidation potential of human neuromelanin reveals a spherical architecture with a pheomelanin core and a eumelanin surface. PNAS 103:14785–14789

Carreira A, Ferreira LM, Loureiro V (2001) Brown pigments produced by Yarrowia lipolytica result from extracellular accumulation of homogentisic acid. Appl Environ Microbiol 67:3463–3468

Chen C-T et al (2014) Excitonic effects from geometric order and disorder explain broadband optical absorption in eumelanin. Nat Commun 5:3859–3866

Childs A, Jacobs C, Kaminski T, Halliwell B, Leeuwenburgh C (2001) Supplementation with vitamin C and N-acetyl- cysteine increases oxidative stress in humans after an acute muscle induced by eccentric exercise. Free Rad Biol Med 31:745–753

Cichorek M, Wachulska M, Stasiewicz A, Tymińska A (2013) Skin melanocytes: biology and development. Postep Derm Alergol 30:30–41

D'Ischia M, Wakamatsu K, Napolitano A et al (2013) Melanins and melanogenesis: methods, standards, protocols. Pig Cell Melan Res 26:616–633

David C, Daro A, Szalai E, Atarhouch T, Mergeay M (1996) Formation of polymeric pigments in the presence of bacteria and comparison with chemical oxidative coupling-II. Catabolism of tyrosine and hydroxyphenylacetic acid by *Alcaligenes eutrophus* CH34 and mutants. Eur Polym J 32:669–697

Del Marmol V, Beermann F (1996) Tyrosinase and related proteins in mammalian pigmentation. FEBS Lett 381:165–168

Delgado-Vargas F, Jiménez AR, Paredes-López O (2000) Natural pigments: carotenoids, anthocyanins, and betalains — characteristics, biosynthesis, processing, and stability. Crit Revs Food Sci Nutr 40(3):173–289

Ellis DH, Griffiths DA (1974) The location and analysis of melanins in cell walls of some soil fungi. Canad J Micro 20:1379–1386

Eslami M, Zare HR, Namazia M (2014) The effect of solvents on the electrochemical behaviour of homogentisic acid. J Electrchem 720:76–83

Figueras LE, Rodriguez-Catellanos MA, Gonzalez-Mendoza A, Cantu JM (1993) Hyperkeratosis-hyperpigmentation syndrome: a confirmative case. Clin Genet 43(2):73–75

Forslind B, Roomans GM, Carlsson LF, Malmquist KG, Akselsson KR (1984) Elemental analysis on freeze-dried sections of human skin: studies by electron microscopy and particle induced X-ray emission analysis. Scann Elec Micro 11:755–759

FP7-HEALTH (2012) DEVELOPAKURE: clinical development of nitisinone for alkaptonuria; Project reference: 304985 Cordis.europ.eu/project/rcn/106157

Frases S, Salazar A, Dadachova E, Casadeval A (2007) *Cryptococcus neoformans* can utilize the bacterial melanin precursor homogentisic acid for fungal melanogenesis. Appl Environ Micro 73:615–621

Galasso V, Pichierri F (2009) Probing the molecular and electronic structure of norhipposudoric and hipposudoric acids from the red sweat of hippopotamus amphibius: a DFT investigation. J Phys Chem A 113(11):2534–2543

Hashimoto K, Saikawa Y, Nakata M (2007) Studies on the red sweat of the Hippopotamus amphibius. Pure Appl Chem 79 (4):507–517

Hegedus ZL (2000) The probable involvement of soluble and deposited melanins their intermediates and reactive oxygen side products in human disease and ageing. Toxic 145:85–101

Introne WJ, Perry MB, Troendle J et al (2011) A 3-year randomized therapeutic trial of nitisinone in alkaptonuria. Mol Genet Metab 103(4):307–314

Ito S, Wakamatsu K (2008) Chemistry of mixed melanogenesis–pivotal roles of dopaquinone. Photochem Photobiol 84(3): 582–592

Jablonski N (2012) Living color. University of California Press, Berkeley/Los Angeles/London

Jablonski NG, Chaplin G (2010) Colloquium paper: human skin pigmentation as an adaptation to UV radiation. PNAS 107:8962–8968

Kai M, Masanori M, Yoko S et al (2006) Properties of the enzyme responsible to the synthesis of hipposudoric acid and norhipposudoric acids, the pigments in the red sweat of the hippopotamus. Nippon Kagakkai Koen Yokoshu 86(2):1314–1318

Kassinger RG (2003) Dyes from sea snails to synthetics 21st century books. www.Millbrookpress.com

Kastyak-Ibrahim MZ, Nasse MJ, Rak M et al (2011) Biochemical label-free tissue imaging with subcellular-resolution synchrotron FTIR with focal plane array detector. Neuro Image 60 (1):376–383

Keith KE, Killip L, He P, Moran GR, Valvano MA (2007) *Burkholderia cenocepacia* C5424 produces a pigment with antioxidant properties using a homogentisate intermediate. J Bacteriol 189:9057–9065

Keller JM, Macaulay W, Nercessian OA, Jaffe IA (2005) New developments in ochronosis: review of the literature. Rheum Int 25:81–85

Land EJ, Ramsden CA, Riley PA (2003) Tyrosinase autoactivation and the chemistry of ortho-quinone amines. Acc Chem Res 36 (5):300–308

Laschi M, Tinti L, Braconi D et al (2012) Homogentisate 1,2 dioxygenase is expressed in human osteoarticular cells: implications in alkaptonuria. J Cell Physiol 227(9):3254–3257

Lee WC, Li LC, Chen JB, Chang HW (2015) Indoxyl sulfate-induced oxidative stress, mitochondrial dysfunction, and impaired biogenesis are partly protected by vitamin C and *N*-acetylcysteine. Sci World J 2015:620826

Levine N, Dorr RT, Ertl GA, Brooks C, Alberts DS (1999) Effects of a potent synthetic melanotropin, Nle^4-D-Phe^7alpha-MSH (Melanotan) on tanning: dose ranging study. J Dermatol Treat 10:127–132

Levy C, Khaled M, Fisher DE (2006) Review MITF: master regulator of melanocyte development and melanoma oncogene. Trends in Molec Med 12:406–414

Littrell KC, Gallas JM, Zajac GW, Thiyagarajan P (2003) Structural studies of bleached melanin by synchrotron small-angle X-ray scattering. Photochem Photobiol 77:115–120

Liu SY, Shawkey MD, Parkinson D, TroyTP AM (2014) Elucidation of the chemical composition of avian melanin. RSC Adv 4:40396–40399

Lok ZS, Goldstein J, Smith JA (2013) Alkaptonuria-associated aortic stenosis. J Card Surg 28:417–420

Martin JP, Batkoff B (1987) Homogentisic acid autooxidation and oxygen radical generation: implications for the etiology of Alkaptonuria arthritis. Free Rad Biol Med 3:241–250

Mentner LM, Willis I (1997) Electron transfer and photoprotective properties of melanins in solution. Pigm Cell Res 10:214–217

Millington GWM (2006) Proopiomelanocortin (POMC): the cutaneous roles of its melanocortin products and receptors. Clin Expt Dermat 31:407–412

Millucci L, Spreafico A, Tiniti A et al (2012) Alkaptonuria is a novel human secondary amyloidogenic disease. BBA Molec Basis Dis 1822:1682–1691

Millucci L, Ghezzi L, Paccagnini E et al (2014) Amyloidosis, inflammation, and oxidative stress in the heart of an alkaptonuric patient. Mediat Inflamm 12. Article ID 258471

Momohara S, Okamoto H, Yamanaka H (2008) Chondrocyte of rheumatoid arthritis serve as a source of intra-articular acute-phase serum amyloid A protein. Clin Chim Acta 398:155–156

Murisier F, Beermann F (2006) Genetics of pigment cells: lessons from the tyrosinase gene family. Histo Histopath 21(5):567–578

Nicolaus RA (1969) In: Lederer E (ed) Melanins chemistry of natural products. Hermann, Paris

Nordlund JJ, Boissy R, Hearing VJ, King RA (2006) In: Oetting W, Ortonne J-P (eds) The pigmentary system, 2nd edn. Blackwell, Oxford, 1229 pp

Novotny NR, Capley EN, Stenson AC (2014) Fact or artifact: the representativeness of ESI-MS for complex natural organic mixtures. J Mass Spect 49:316–326

Ogunnariwo J, Hamilton-Miller MT (1975) Brown and red pigmented P*seudomonas aeruginosa* differentiation between melanin and pyrorurin. J Med Microbiol 8:199–203

Pallotta V, Gevi F, D'Alessandro A, Zolla L (2014) Storing red blood cells with vitamin C and *N*-acetylcysteine prevents oxidative stress-related lesions: a metabolomics overview. Blood Transfus 12:367–387

Peña-Méndez EM, Josef Havel J, Patočka J (2005) REVIEW Humic substances compounds of still unknown structure:applications in agriculture, industry, environment, and biomedicine. J Appl Biomed 3:13–24

Phornphutkul C, Introne WJ, Perry MB et al (2002) Natural history of alkaptonuria. N Engl J Med 347:2111–2121

Phornphutkul C, IntroneWJ, Way P, William A, Gahl WA (2003) Alkaptonuria. N Engl J Med 348:1408

Preston AJ, Keenan CM, Sutherland H et al (2014) Chronotic osteoarthropathy in a mouse model of alkaptonuria, and its inhibition by nitisinone. Ann Rheum Dis 73:284–289

Pritchard LE, Turnbull AV, White A (2002) Pro-opiomelanocortin processing in the hypothalamus: impact on melanocortin signalling and obesity. J Endo 172:411–421

Przemyslaw M, Plonka L, Grabacka M (2006) Review Melanin synthesis in microorganisms – biotechnological and medical aspects. Acta Biochim Pol 53:429–443

Ranganath LR, Jarvis JC, Gallagher JA (2013) Recent advances in management of alkaptonuria (invited review, best practice article). J Clin Pathol 66(5):367–373

Ranganath LR, Milan AM, Hughes AT (2014) Suitability of nitisinone in alkaptonuria 1 (SONIA 1): an international, multicentre, randomised, open-label, no-treatment controlled, parallel-group, dose-response study to investigate the effect of once daily nitisinone on 24-h urinary homogentisic acid excretion in patients with alkaptonuria after 4 weeks of treatment. Ann Rheum Dis. doi:10.1136/annrheumdis-2014-206033

Ruzafa C, Sanchez-Amat A, Solano F (1995) Characterization of the melanogenic system in Vibrio cholerae, ATCC 14035. Pigment Cell Res 8(3):147–152

Sakamoto K, Liu C, Kasamatsu M, Pozdeyv NV, Iuvone PM, Tosini G (2005) Dopamine regulates melanopsin mRNA expression in intrinsically photosensitive retinal ganglion cells. Eur J Neurosci 22(12):3129–3136

Solano F (2014) Melanins: skin pigments and much more – types, structural models, biological functions, and formation routes. New J Sci 28. doi:10.1155/2014/498276. Article ID 498276

Stuart JA, Brige RR (1996) Characterization of the primary photochemical events in bacteriorhodopsin and rhodopsin. In: Lee AG (ed) Rhodopsin and G-protein linked receptors, part A, vol 2. JAI Press, Greenwich, pp 33–140

Sulzer D, Zecca L (1999) Intraneuronal dopamine-quinone synthesis: a review. Neurotox Res 1:181–195

Sutton R, Sposito G (2005) Molecular structure in soil humic substances: the new view. Environ Sci Technol 39(23):9009–9015

Suzuki Y, Oda K, Yoshikawa Y, Maeda Y, Suzuki T (1999) A novel therapeutic trial of homogentisic aciduria in a murine model of alkaptonuria. J Hum Genet 44(2):79–84

Takeda K, Takahashi NH, Shibahara S (2007) Neuroendocrine functions of melanocytes: beyond the skin-deep melanin maker. Tohuku J Exp Med 211(3):201–221

Thureau P, Ziarelli F, Thvand A et al (2012) Probing the motional behavior of eumelanin and pheomelanin with solid-state NMR spectroscopy: new insights into the pigment properties. Chemta Indicat Eur J 18:10689–10700

Tinti L, Spreafico A, Braconi D, Millucci L, Bernardini G, Chellini F, Cavallo G, Selvi E, Galeazzi M, Marcolongo R, Gallagher JA, Santucci A (2010) Evaluation of antioxidant drugs for the treatment of ochronotic alkaptonuria in an in vitro human cell model. J Cell Physiol 225:84–91

Tokuhara Y, Shukuya K, Tanaka M et al (2014) Detection of novel visible-light region absorbance peaks in the urine after alkalization in patients with alkaptonuria. PLoS One 9(1):e86606

Tran ML, Powell BJ, Meredith P (2006) Chemical and structural disorder in eumelanins: a possible explanation for broadband absorbance. Biophys J 90:743–752

Tribl F, Gerlach M, Marcus K et al (2005) Subcellular proteomics of neuromelanin granules isolated from the human. Brain Molec Cell Proteom 4:945–957

Turick CE, Tisa LS, Caccavo F Jr (2002) Melanin production and use as a soluble electron shuttle for Fe(III) oxide reduction and as a terminal electron acceptor by *Shewanella algae* BrY. Appl Environ Microbiol 68:2436–2444

Turick, CE, Caccavo F Jr, Tisa LS (2003) Electron transfer to Shewanella algae BrY toHFO is mediated by cell-associated melanin. FEMS Microbiol Lett 220:99–104

Turick CE, Beliaev A, Ekechukwu AA, Poppy T, Maloney A, Lowy DA (2009) The role of 4-hydroxyphenylpyruvate dioxygenase in enhancement of solid-phase electron transfer by *Shewanella oneidensis* MR-1. FEMS Microbiol Ecol 68:223–235

Turick CE, Knox AS, Becne JMl, Ekechukwu AA, Milliken CE (2010) Properties and function of pyomelanin. In: Elnashar MM (ed) Biopolymers. Sciyo Janeza Trdine, Croatia, Chap. 26

Valverde P, Healy E, Jackson I, Rees JL, Thody AJ (1995) Variants of the melanocyte – stimulating hormone receptor gene are associated with red hair and fair skin in humans. Nature Genet 11(3):328–330

Venkataraman K (ed) (2012) The chemistry of synthetic dyes. Elsevier, London

Videria IFS, Moura DFL, Magina S (2013) Mechanisms regulating melanogenesis. An Bras Dermatol 88(1):76–83

Wakamatsu K, Hu DN, McCormick SA, Ito S (2008) Characterization of melanin in human iridal and choroidal melanocytes from eyes with various colored irides. Pig Cell Melan Res 21(1):97–105

Watt AAR, Bothma JP, Meredith P (2009) The supramolecular structure of melanin. Soft Matter 5:3754–3760

Williams DP, Lawrence A, Meng X (2012) Pharmacological and toxicological considerations of homogentisic acid in alkaptonuria. Pharmacology 3:61–74

Wolff JA, Barshop B, Nyhan WL et al (1989) Effects of ascorbic acid in alkaptonuria: alterations in benzoquinone acetic acid and an ontogenic effect in infancy. Pediatr Res 26:140–144

Zannoni VG, Lomtevas N, Goldfinger SO (1969) Oxidation of homogentisic acid to ochronotic pigment in connective tissue. Biochim Biophys Acta 177:94–105

Zecca L, Bellei C, Costi P et al (2008) New melanic pigments in the human brain that accumulate in aging and block environmental toxic metals. PNAS 105:17567–17572

Part II
Case & Research Reports

JIMD Reports
DOI 10.1007/8904_2015_436

RESEARCH REPORT

Serum GDF15 Levels Correlate to Mitochondrial Disease Severity and Myocardial Strain, but Not to Disease Progression in Adult m.3243A>G Carriers

Saskia Koene · Paul de Laat · Doorlène H. van Tienoven · Gert Weijers · Dennis Vriens · Fred C.G.J. Sweep · Janneke Timmermans · Livia Kapusta · Mirian C.H. Janssen · Jan A.M. Smeitink

Received: 02 October 2014 / Revised: 02 March 2015 / Accepted: 27 March 2015 / Published online: 13 May 2015

Abstract In this observational cohort study, we examined the prognostic value of growth and differentiation factor 15 (GDF15) in indicating and monitoring general mitochondrial disease severity and progression in adult carriers of the m.3243A>G mutation.

Ninety-seven adult carriers of the m.3243A>G mutation were included in this study. The Newcastle mitochondrial disease adult scale was used for rating mitochondrial disease severity. In parallel, blood was drawn for GDF15 analysis by ELISA. Forty-nine carriers were included in a follow-up study. In a small subset of subjects of whom an echocardiogram was available from general patient care, myocardial deformation was assessed using two-dimensional speckle-tracking strain analysis.

A moderate positive correlation was found between the concentration of GDF15 and disease severity ($r = 0.59$; $p < 0.001$). The concentration of serum GDF15 was higher in m.3243A>G carriers with diabetes mellitus, cardiomyopathy, and renal abnormalities. After a 2-year follow-up, no significant correlation was found between the change in disease severity and the change in the concentration of GDF15 or between the GDF15 level at the first assessment and the change in disease severity. In the subcohort of patients of whom an echocardiogram was available, the concentration of GDF15 correlated moderately to longitudinal global strain ($r = 0.55$; $p = 0.006$; $n = 23$) but not to circumferential or radial strain.

Our results indicate that serum GDF15 is not a strong surrogate marker for general mitochondrial disease severity. Its value in indicating myocardial deformation should be confirmed in a prospective longitudinal study.

Communicated by: Shamima Rahman, FRCP, FRCPCH, PhD

Competing interests: None declared

S. Koene (✉) · P. de Laat · M.C.H. Janssen · J.A.M. Smeitink
Department of Pediatrics, Nijmegen Centre for Mitochondrial Disorders, Amalia Children's Hospital, Radboudumc, Geert Grooteplein 10, PO BOX 9101, 6500 HB, Nijmegen, The Netherlands
e-mail: Saskia.Koene@radboudumc.nl

D.H. van Tienoven · F.C.G.J. Sweep
Department of Laboratory Medicine, Radboudumc, Nijmegen, The Netherlands

G. Weijers · D. Vriens
Department of Radiology and Nuclear Medicine, Radboudumc, Nijmegen, The Netherlands

J. Timmermans
Department of Cardiology, Radboudumc, Nijmegen, The Netherlands

L. Kapusta
Department of Pediatric Cardiology, Amalia Children's Hospital, Radboudumc, Nijmegen, The Netherlands

L. Kapusta
Department of Pediatrics, Pediatric Cardiology Unit, Tel-Aviv Sourasky Medical Center, Tel Aviv, Israel

M.C.H. Janssen
Department of General Internal Medicine, Radboudumc, Nijmegen, The Netherlands

Introduction

One of the key aspects of improving the quality of clinical trials is the identification of biomarkers that are indicative of clinically relevant outcome (Pfeffer et al. 2013). The perfect biomarker, correlating closely to clinical disease severity, would make the follow-up of patients easier,

cheaper, and less invasive, both in clinical trials and in regular patient care (Mayeux 2004). Moreover, since functional measures are subject to bias (including patient factors influencing performance, report bias, and inter- and intrarater variability), measuring more objective disturbances of physiology may seem more reliable. Several tests have been used to indirectly measure the disturbed mitochondrial energy metabolism in patients with mitochondrial disease, including the determination of lactic acid concentration in the brain by magnetic resonance spectroscopy or serum and serum fibroblast growth factor 21 (FGF21) (Suomalainen 2011). Although both lactic acid and FGF21 seemed to correlate to disease severity, the concentration during follow-up did not correlate to disease progression (Koene et al. 2014; Lee et al. 2010).

A recent study reported growth and differentiation factor 15 (GDF15) as a potential new diagnostic biomarker for mitochondrial disease (Kalko et al. 2014). GDF15 was already known as a quite nonspecific biomarker for cancer, as well as cardiac, pulmonary, renal, and gynecological disease (Izumiya et al. 2014; Kempf and Wollert 2013; Trovik et al. 2014; Yang et al. 2014; Breit et al. 2012; Montoro-Garcia et al. 2012). However, the concentrations reported in these disorders are within the 1.000–7.000 pg/mL range (Dominguez-Rodriguez et al. 2014; Ho et al. 2013; Izumiya et al. 2014; Montoro-Garcia et al. 2012; Trovik et al. 2014), whereas concentrations as high as 85.252 pg/mL were reported in patients with mitochondrial disease (Kalko et al. 2014). A child with the m.3243A>G mutation, the most commonly observed mutation leading to mitochondrial disease, was reported to have a concentration of 6.999 pg/mL (reference value, 380 pg/mL (95%CI, 59–701 pg/mL)).

To evaluate the value of GDF15 as a surrogate marker for disease severity and disease progression, we examined GDF15 in a large cohort of adult carriers of the m.3243A>G mutation. Since GDF15 was previously reported as a biomarker for symptoms associated with the m.3243A>G mutation, such as cardiomyopathy (Hollingsworth et al. 2012; Xu et al. 2011), diabetes mellitus (Dominguez-Rodriguez et al. 2014), and renal failure (Emma et al. 2012; Ho et al. 2013), we assessed these symptoms and organ functions in more detail.

Methods

Patients

We determined the serum GDF15 concentration in adult carriers of the m.3243A>G mutation included in our "national inventory of patients with the m.3243A>G mutation" study. In each subject, the heteroplasmy percentage in buccal mucosa cells, urinary epithelial cells (UEC), and leukocytes was determined using pyrosequencing (de Laat et al. 2012). A heteroplasmy percentage ≥5% can be detected using this technique. Subjects with a detectable heteroplasmy percentage in either buccal mucosa cells, leukocytes, or UEC were considered to be carriers of the mutation. In this national inventory, clinical disease severity is monitored approximately 2-yearly in both symptomatic and asymptomatic subjects carrying the m.3243A>G mutation (de Laat et al. 2012). Clinical disease severity is rated using the Newcastle mitochondrial disease adult scale (NMDAS), a multidimensional clinical scale encompassing current function (patient's opinion), system-specific involvement (assessment of multisystem disease), and current clinical assessment (physical examination) (Schaefer et al. 2006). Carriers were rated as having asymptomatic (NMDAS = 0); mild (NMDAS = 1–5), moderate (NMDAS = 6–20), or severe (NMDAS >20) mitochondrial disease (cutoff values based on expert opinion). Seventy-six carriers were included in the follow-up study, and serum of 50 of these carriers was available for analysis (see Fig. 1 for a flowchart). For a more detailed description of the methods, we refer to our previous study on fibroblast growth factor 21 (FGF21) concentrations in this population (Koene et al. 2014). Patients with cancer and pregnant women were excluded since GDF15 is a known biomarker for these conditions. Since cardiomyopathy, diabetes mellitus, and renal failure – for which GDF15 is also a biomarker – are highly prevalent in carriers of the m.3243A>G mutation (de Laat et al. 2012), we also evaluated the influence of these conditions on the GDF15 concentration. Microalbuminuria was defined as an albumin-to-creatinine ratio of >2.0 g/mol for men and >2.5 g/mol for women, measured in a spot sample of urine. Decreased creatinine clearance was defined as a glomerular filtration rate <60 mL/min/1.73 m^2. Carriers were classified as having decreased creatinine clearance only, microalbuminuria only, both, or neither. The presence and severity of diabetes mellitus (DM) follows from the NMDAS (the presence of DM was rated as DM requiring diet or medication). The measurement of myocardial strain is explained in more detail later in this section.

Thirty noncarrier family members were included as a nuclear genetic and environmental matched reference population. The maternal relatives who showed no signs of diabetes mellitus, renal disease, or cardiac disease were included in the study. In these subjects, heteroplasmy percentages ≤4% (the assay's detection limit) in UEC, leukocytes, and/or buccal mucosa cells were established.

GDF15

All samples were measured in duplicate, following the instructions of the manufacturer *(R&D Biosystems, Minne-*

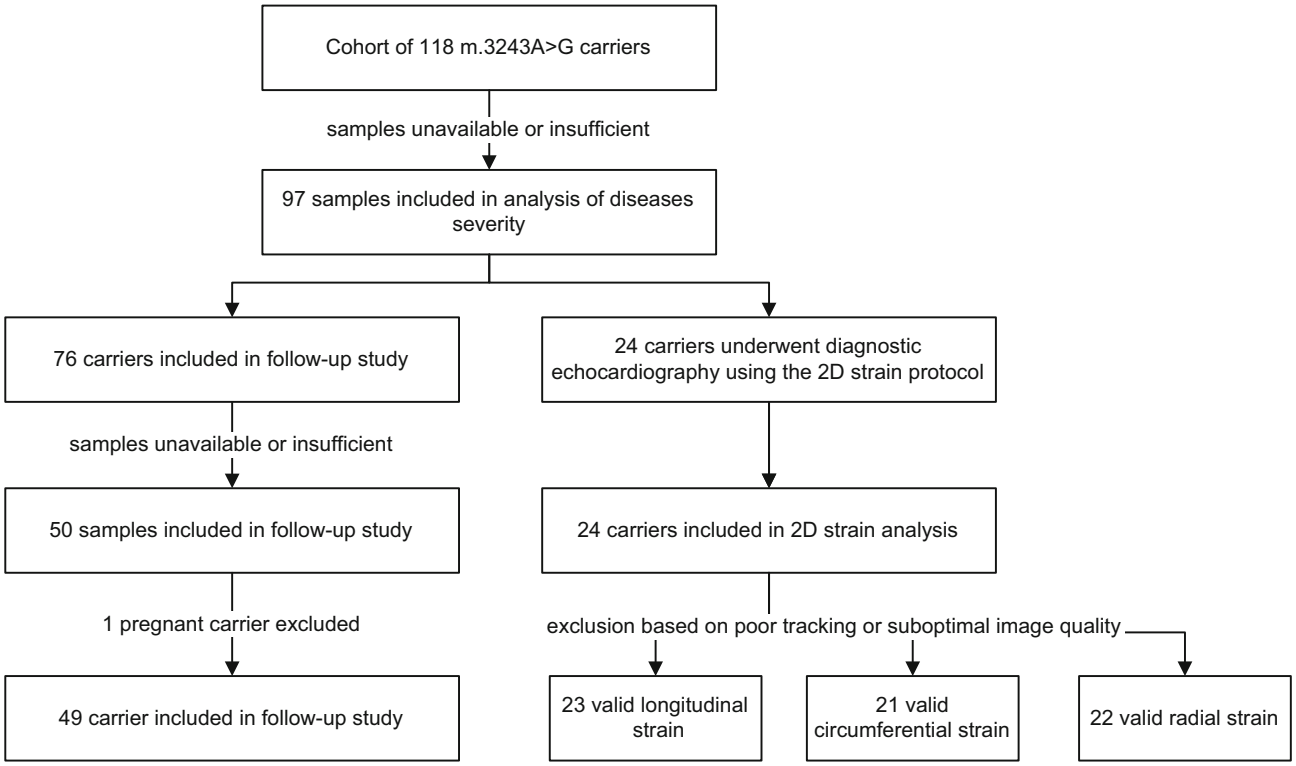

Fig. 1 Flowchart of the study cohort

apolis, USA). The inter-assay and intra-assay variability for high and low values was determined based on high and low control samples, respectively. The functional sensitivity determined at 20% covariance (CV) was 9.8 pg/mL. At a level of 1,695 pg/mL, the within-assay CV was 3.5% and the between-assay CV was 5.7%. At a level of 729 pg/mL, the within-assay CV was 3.6% and the between-assay CV was 2.2%. Samples with an initial intra-assay covariance (CV) >15% were repeated. The two values obtained from the duplicated measurements were averaged, and the mean of these two measurements was used for further analysis. Samples with a concentration higher than the highest standard value were diluted and analysis was repeated. According to the kit's manufacturer, the assay has no cross-reactivity with human GDF9 and GDF11. Age- and gender-based reference values for serum GDF15 were adopted from the Framingham Offspring Study (Ho et al. 2012) (elevated GDF15 concentration is above the 97.5th percentile matched for age and gender).

Medical Ethical Approval

This study ("national inventory of patients with the m.3243A>G mutation") was approved by the regional Medical Research Ethics Committee. All procedures followed were in accordance with the ethical standards of the responsible committee on human experimentation (institutional and national) and with the Helsinki Declaration of 1975, as revised in 2013 (World Medical Association 2013). Informed consent was obtained from all patients before being included in the study.

Myocardial Strain Measurement

As part of general patient care, carriers of the m.3243A>G mutation regularly undergo diagnostic echocardiography. Myocardial deformation was only assessed only if an echocardiogram was performed less than 1 year from an available GDF15 sampling. The myocardial strain, a measure for the deformation of the myocardium throughout the cardiac cycle, was determined using two-dimensional speckle-tracking strain analysis in accordance with a previously published protocol (Bulten et al. 2014). Since echocardiography was done as part of general patient care and 2D strain measurement can only be performed when the images are obtained following a specific protocol, only a subset of carriers was included in this part of the study.

Strain values are dimensionless and are expressed in percentages. Global longitudinal left ventricular myocardial strain was calculated by averaging the six segments of the 4-chamber long-axis view. Global radial and circumferential myocardial strain was calculated by averaging the six segments of the mid-cavity short-axis view (at the level of the papillary muscles). If less than four out of six segments

showed valid tracking of the myocardium (e.g., because of regional inferior image quality or poor tracking by the software), the strain measurement was excluded from our analyses.

Statistics

The absolute difference between two parameters was calculated by subtracting the first measurement from the second measurement. All parameters were assessed for (log)normality. To prevent non-real values for zero values of the NMDAS including its subdomains and symptom-specific items, all values were increased by 1 prior to ^{e}log transformation. The changes in GDF15 concentration and NMDAS score were increased by 3,000 and 10, respectively. Variables with a (log)normal distribution were compared using parametric tests, and the mean and 95% confidence intervals are reported. Variables that deviated strongly from a (log)normal distribution were analyzed by performing a nonparametric test, and the median and interquartile ranges are reported. In case a high number of tests were performed (5 or more), critical p-values were adjusted using the Bonferroni method (i.e., critical $p = 0.05/n$ where $n =$ number of tests). Correlation coefficients were interpreted in accordance with the guidelines provided at the BMJ website (http://www.bmj.com/about-bmj/resources-readers/publications/statistics-square-one/11-correlation-and-regression; consulted 31-Jul-2014). Thus, a correlation coefficient (r) of 0.80–1.0 is considered a very strong relationship; $r = 0.60$–0.79 is considered a strong relationship; $r = 0.40$–0.59 is considered a moderate relationship; $r = 0.20$–0.39 is considered a weak relationship; and $r = 0.00$–0.19 is considered a very weak or no relationship.

Several covariates for GDF15 are known from literature (Ho et al. 2012), including age, presence of diabetes mellitus (DM), smoking (covariates with higher estimated coefficient than 0.1), and renal failure. These, together with other possible clinical covariates (gender, body mass index (BMI), heteroplasmy percentage in urinary epithelial cells (UEC) and leukocytes, and disease severity (NMDAS)), were included as candidate predictors for GDF15. Gender, age, BMI, heteroplasmy percentage in UEC and leukocytes, and the concentration of GDF15 and FGF21 were considered candidate predictors for disease severity (NMDAS score). The influence of nominal and ordinal candidate predictors was determined by comparing between groups; the influence of continuous data was evaluated in a bilinear regression analysis. The influence of cardiomyopathy was studied in more detail in a subgroup of carriers. For the correlation between the concentration of GDF15 and strain measurements, only echocardiography examinations performed no more than 1 year from sampling were analyzed. Forward and backward iterative multivariate linear regression models were used to determine the influence of covariates and to determine the contribution of GDF15 in predicting or monitoring the disease course. Possible candidate predictors were only included for iterative multivariate modeling if they correlated to the dependent variable during univariate correlation analysis ($p < 0.1$). Standardized regression coefficients (β) are presented for each variable.

Because 38% of the variance in the concentration of GDF15 is genetically determined (Ho et al. 2012), we performed two additional analyses to correct for the effect of kinship in our analyses. First, we performed a separate analysis that included only the most severely affected patient in each family (in case two family members had the same NMDAS score, we included the youngest person with that score, assuming a relatively more severe disease in this person as age-related complaints are also included in the NMDAS). Secondly, we used generalized estimating equation models (working correlation structure: independence, with robust standard error for correction) to confirm the contribution of covariates and candidate predictors found by linear regression models, corrected for kinship.

Because genetic factors between family members are not likely to influence (intraindividual) changes in GDF15 levels during follow-up, we only used linear regression models to determine the influence of covariates on the change in disease severity and the concentration of GDF15 (longitudinal study). The (absolute) change in disease severity (i.e., NMDAS score) was used as a possible candidate predictor for the change in GDF15 concentration. Both the change in the concentration of GDF15 and the change in the concentration of FGF21 were included as candidate predictors for the change in disease severity (i.e., NMDAS score).

All analyses were performed using IBM's SPSS statistics software packages, version 20.0.0.1.

Results

Patient Characteristics

We initially included 118 adult subjects in our national inventory study. For a variety of reasons (e.g., the samples were not available or had too small remaining volume for measuring GDF15), we were unable to determine the GDF15 levels in 21 of these subjects. No data were excluded because of high intra-assay covariance of GDF15 assessment. Thus, our final cohort included 97 adult carriers of the m.3243A>G mutation (Fig. 1). The m.3243A>G mutation is not associated with a higher prevalence of cancer, and none of our subjects was known

to suffer from any form of cancer at the time of the study. One patient did have a history of acute myeloid leukemia (in remission for 8 years before samples were taken; [GDF15] 731 (baseline) and 1926 (follow-up) pg/mL). One pregnant woman was excluded ([GDF15] 43,304 pg/mL) from the follow-up cohort (Moore et al. 2000). For patient characteristics, we refer to Tables 1 and 2. Renal function at the time of the sampling (spread, 6 months) was known in 86 patients (89% of total). Seventy-one percent of the total cohort had normal renal function, 17% had microalbuminuria only, 2% had decreased creatinine clearance only, and 9% suffered from both. Three patients had had a renal transplant, two of which had moderate transplant function (GFR 24 and 50 mL/min/1.73 m^2) and one had normal transplant function (GFR >75 mL/min/1.73 m^2). The m.3243A>G carriers came from 41 distinct families (median, two subjects per family; range, 1–10 subjects per family). This cohort of adult carriers contained two asymptomatic patients (2%), 18 patients with mild mitochondrial disease (19%), 46 patients with moderate mitochondrial disease (47%), and 31 patients with severe mitochondrial disease (32%). Because sufficient material was not always available, heteroplasmy percentage in UEC is absent in two subjects; heteroplasmy percentage in leukocytes is absent for another two patients. In these four subjects, heteroplasmy levels ≥5% were established in the other available tissue (buccal mucosa cells, leukocytes, or UEC).

The Value of GDF15 as an Indicator of Clinical Disease Severity

Fifty-one carriers (53%) had an elevated concentration of GDF15 (i.e., higher than the 97.5th percentile of healthy age- and sex-matched controls) compared to the age- and gender-matched reference population from literature (Ho et al. 2012). Carriers with an elevated concentration of GDF15 had higher NMDAS scores compared to carriers with normal concentrations of GDF15 (2,440 pg/ml (95% CI, 1,097–5,431 pg/mL) versus 902 pg/mL (95%CI, 381–2,131 pg/mL); $p = < 0.001$; independent sample t-test). The correlation between the concentration of GDF15 and total NMDAS score in the cohort of m.3243A>G carriers at baseline was $r = 0.59$ ($p < 0.001$; $n = 97$; Pearson's correlation coefficient) (see Fig. 2). This correlation coefficient is not significantly higher ($p = 0.20$; Fisher r-to-z transformation) than the correlation between NMDAS score and FGF21 ($r = 0.45$; $p < 0.001$; $n = 93$; Spearman's correlation coefficient) in this cohort); 95 out of 99 patients (96%) of the current cohort are the same as in the study of FGF21 (Koene et al. 2014). No significant correlation was found between the heteroplasmy percentage in UEC and the NMDAS score nor between the heteroplasmy percentage in leukocytes and the NMDAS score. Among the 66 patients with asymptomatic, mild, or moderate disease, the correlation coefficient between the total NMDAS score and GDF15 was 0.54 ($p < 0.001$; Spearman's correlation coefficient); among the 31 patients with severe disease, we found no significant correlation between the total NMDAS score and the concentration of GDF15 (Pearson's correlation coefficient). The correlation between the heteroplasmy level in UEC and GDF15 was 0.30 ($p = 0.003$; $n = 95$; Spearman's rank coefficient). The correlation between the heteroplasmy level in leukocytes and GDF15 was 0.22 ($p = 0.031$; $n = 95$; Spearman's rank coefficient).

Since the 97 adult carriers came from 41 families, we minimized the role of kinship in these associations by analyzing only the most severely affected patient in each of the 41 families. The correlation coefficient between the total NMDAS score and GDF15 concentration in this cohort was $r = 0.46$ ($p = 0.003$; Pearson's correlation coefficient) and was similar ($p = 0.58$; Fisher r-to-z transformation) compared to the full cohort. During iterative multivariate linear modeling, the following parameters were found to be independent predictors for disease severity: concentration of GDF15, age, concentration of FGF21, and heteroplasmy percentage in UEC (β(GDF15) = 0.38 ($p < 0.001$); β(age) = 0.32 ($p < 0.001$); β(heteroplasmy UEC) = 0.24 ($p = 0.005$); β(FGF21) = 0.21 ($p = 0.033$; forward multilinear regression modeling)). When GDF15 and FGF21 were included as the only independent predictors for disease severity in a linear regression model, only GDF15 was included (β(GDF15) = 0.59 ($p < 0.001$); forward multilinear regression modeling). We found a moderate correlation between the concentration of GDF15 and the concentration of FGF21 ($r = 0.54$; $p > 0.001$; $n = 93$; Spearman's correlation coefficient).

Covariates for the Concentration of GDF15

The concentration of GDF15 was not higher in females compared to males ($p = 0.38$; general linear model). The concentration of GDF15 was not higher among smokers compared to nonsmokers ($p = 0.70$; $n = 84$; general linear model). Patients without microalbuminuria or decreased creatinine clearance had lower concentrations of GDF15 compared to patients with microalbuminuria only or both microalbuminuria or decreased creatinine clearance ($p = 0.031$ and 0.002, respectively; Tukey HSD), but not compared to patients with decreased creatinine clearance only ($p = 0.24$; Tukey HSD). The subgroups with renal abnormalities were comparable with respect to GDF15 concentrations (Tukey HSD). (see Fig. 3). The concentration of GDF15 was significantly higher in patients with any kind of renal abnormalities compared to those without renal

Table 1 Characteristics of the cohort of all adult m.3243A>G carriers at baseline and the follow-up cohort

		All carriers				Follow-up (49 carriers)				Difference at baseline	Difference from baseline
		Central value	Spread	Range	*n*	Central value	Spread	Range	*n*	*p*	*p*
Gender	% female	71			97	65				0.20	
Age (years)	Mean, 95%CI	45	17–72	18–81	97	45[a]	18–64	22–64	49	0.65	
BMI (kg/m^2)	Median, IQR	22.8	20.7–26.0	16.7–40.9	97	23.6[a]	17.6–33.2	17.6–33.1	49	0.96	
Smoking (current)	% yes	22			84	25			48	1.00	
Diabetes mellitus (prevalence)	% yes	39			97	37[a]			49	0.62	
Heteroplasmy percentage, leukocytes (%)	Median, IQR	17	8–26	2–49	95	19[a,b]	4–41	2–49	47	0.56	
Heteroplasmy percentage, UEC (%)	Median, IQR	45	27–69	4–96	95	52[a,b]	7–91	5–96	47	0.1	
NMDAS score	Mean, 95%CI	12[c]	1–67	0–56	97	14[c]	2–47	1–92	49	0.81	0.15
Domain 1	Median, IQR	4	1–9	0–23	97	6[b,c]	1–21	0–38	49	0.85	0.001
Domain 2	Median, IQR	5	3–9	0–22	97	5[b,c]	0–16	0–31	49	0.81	0.48
Domain 3	Median, IQR	3	1–6	0–20	97	3[b,c]	0–14	0–23	49	0.87	0.96
Myopathy score	Median, IQR	2	1–4	0–11	97	2[b,c]	0–12	0–14	49	0.96	0.11
Encephalopathy score	Median, IQR	2	0–3	0–12	97	1[b,c]	0–5	0–17	49	0.98	0.38
Diabetes mellitus (severity)	Median, IQR	0	0–5	0–5	97	1[b,c]	0–3	0–5	49	0.37	0.002
Cardiomyopathy (severity)	Median, IQR	0	0–1	0–5	97	0	0–5	0–5	49	0.59	0.001
Stroke-like episodes (severity)	Median, IQR	0	0–0	0–5	97	0	0–0	0–5	49	0.98	0.58
QoL mental	Median, IQR	48	41–55	25–66	97	45	39–55	14–62	47	0.11	0.63
QoL physical	Median, IQR	41	33–51	17–61	97	41	35–49	21–64	47	0.29	0.36
[GDF15] (pg/mL)	Mean, 95%CI	1,525[c]	411–5,691	333–7,421	97	1,484[d]	1,072–2,577	370–7,359	49	0.66	0.22
[FGF21] (pg/mL)	Median, IQR	263	142–534	3–1,491	93	278	117–473	56–1,776	24	0.96	0.27

Characteristics for all adult carriers (n=97) at baseline and for the patients within the follow-up cohort (n=49) at follow-up. *P*-values for the difference at baseline between the follow-up cohort and all carriers were calculated (difference at baseline; χ-square test (2 sided); Fisher's exact test (2 sided), Mann–Whitney *U* test; independent sample *t*-test). Also, *p*-values for the difference between the first and the second measurement within the follow-up cohort are shown (difference from baseline; Wilcoxon signed-rank test, paired *t*-test). The presence of diabetes mellitus was obtained from the NMDAS scale (score on diabetes mellitus item 3)

BMI body mass index, *95%CI* 95% confidence interval, *Domain 1* current function, *Domain 2* system-specific involvement, *Domain 3* current clinical assessment, *Encephalopathy score* sum of the encephalopathic symptoms of the NMDAS (psychiatric symptoms, migraine, seizure, stroke-like episodes, encephalopathy, and cognition), *GDF15* growth and differentiation factor 15, *IQR* interquartile range, *Myopathy score* sum of the myopathic symptoms of the NMDAS (exercise intolerance, respiratory muscle weakness, ptosis, external ophthalmoplegia, and myopathy), *n* number of carriers of which data were available at that specific time point, *NMDAS* Newcastle mitochondrial disease adult scale, *UEC* urinary epithelial cells

[a] At baseline

[b] Mean and 95%CI instead of median and IQR are given

[c] Lognormal distribution

[d] Median and IQR instead of mean and 95%CI are given

Table 2 Characteristics of the cohort of all adult m.3243A>G carriers and their family-matched controls

		All carriers (n = 97)				Family-matched controls (n = 30)				Difference
		Central value	Spread	Range	n	Central value	Spread	Range	n	p
Gender	% female	71			97	73			30	1.00
Age (years)	Mean, 95%CI	45	17–72	18–81	97	41	20–68	18–68	30	0.518
BMI (kg/m^2)	Median, IQR	22.8	20.7–26.0	16.7–40.9	97	24.0[a]	19.7–33.0	19–37	30	0.004
Smoking (current)	% yes	22			84	8			13	0.286
Diabetes mellitus (prevalence)	% yes	39			97	7			30	0.001
Heteroplasmy percentage, leukocytes (%)	Median, IQR	17	8–26	2–49	95	1	0–3	0–3	30	<0.001
Heteroplasmy percentage, UEC (%)	Median, IQR	45	27–69	4–96	95	1	0–2	0–2	29	<0.001
NMDAS score	Mean, 95%CI	12[a]	1–67	0–56	97	3[a]	0–17	0–22	30	<0.001
QoL mental	Median, IQR	48	41–55	25–66	97	49	33–64	31–65	30	0.314
QoL physical	Median, IQR	41	33–51	17–61	97	51	43–56	33–64	1	<0.001
[GDF15] (pg/mL)	Mean, 95%CI	1,525[a]	411–5,691	333–7,421	97	490[a]	272–1,616	236–1,687	30	<0.001
[FGF21] (pg/mL)	Median, IQR	263	142–534	3–1,491	93	13	0–444	3–1,072	25	<0.001

Characteristics for all adult carriers (n=97) at baseline and for the family-matched controls (n=30). P-values for the difference at baseline between the family-matched controls and all carriers were calculated (difference at baseline; χ-square test (2 sided); Fisher's exact test (2 sided), Mann–Whitney U test; independent sample t-test). The presence of diabetes mellitus was obtained from the NMDAS scale (score on diabetes mellitus item 3)

BMI body mass index, *95%CI* 95% confidence interval, *GDF15* growth and differentiation factor 15, *IQR* interquartile range, *n* number of carriers/controls of which data were available, *NMDAS* Newcastle mitochondrial disease adult scale, *UEC* urinary epithelial cells

[a] Lognormal distribution

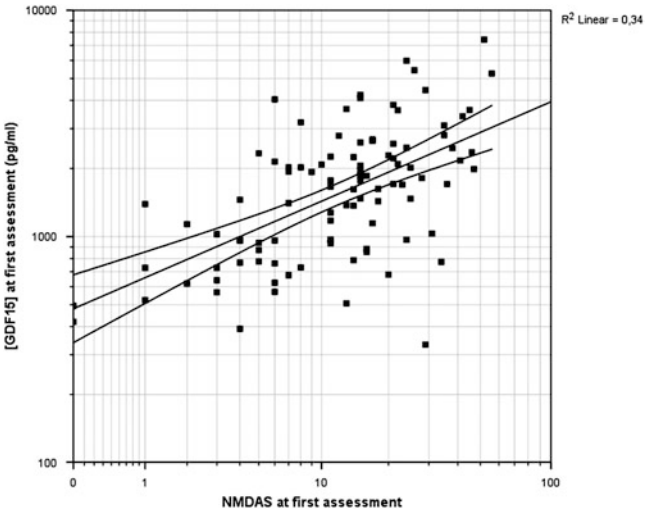

Fig. 2 Correlation between the concentration of GDF15 and disease severity in adult m.3243A>G carriers. The correlation between the concentration of GDF15 and the total NMDAS score (disease severity) is $r = 0.59$ ($p < 0.001$). Scales are loglinear

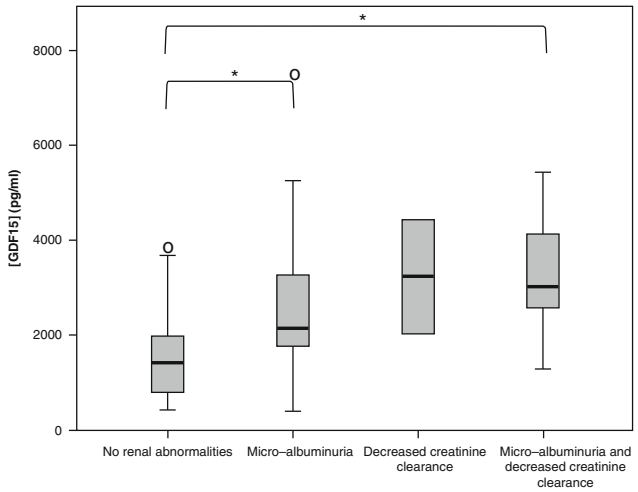

Fig. 3 GDF15 concentrations in patients with and without renal abnormalities, including decreased creatinine clearance and microalbuminuria. Significant differences between groups are flagged with an *asterisk*

abnormalities (2,515 pg/mL (95%CI, 699–9,045 pg/mL) versus 1,261 pg/mL (95%CI, 373–4,264 pg/mL; $n = 61$); $p < 0.001$; independent samples *t*-test). Carriers with microalbuminuria had higher concentrations of GDF15 compared to those without microalbuminuria (2,574 pg/mL (IQR, 1,937–4,069 pg/mL; $n = 25$) versus 1,406 pg/mL (IQR, 781–1,973 pg/mL); $p < 0.001$; Mann-Whitney *U* test). Carriers with decreased creatinine clearance had higher concentrations of GDF15 compared to carriers with normal creatinine clearance including those with microalbuminuria only (3,418 pg/mL (IQR, 2,463–4,388 pg/mL; $n = 12$) versus 1,471 pg/mL (IQR, 867–2,105 pg/mL); Mann-Whitney *U* test; $p < 0.001$).

Carriers with DM had higher concentrations of GDF15 compared to carriers without DM (1,958 pg/mL (95%CI, 579–6,620 pg/mL) versus 1,299 pg/mL (95%CI, 345–4,902 pg/mL); $p = 0.003$; independent samples *t*-test). (see Fig. 4). We found significantly higher serum GDF15 concentrations in patients with cardiomyopathy according to the NMDAS (including patients with asymptomatic ECG changes; NMDAS cardiomyopathy ≥ 1) compared to carriers without cardiomyopathy (2,574 pg/mL (998–6,638) versus 1,371 pg/mL (381–4,937); $p < 0.001$; independent samples *t*-test).

Univariate regression analysis showed that the total NMDAS score was the only significant contributor to the concentration of GDF15 (β(NMDAS) = 0.59; $p < 0.001$). In our cohort, we found no significant contribution of age and BMI to the concentration of GDF15. Generalized estimating equations confirmed the predictive value of

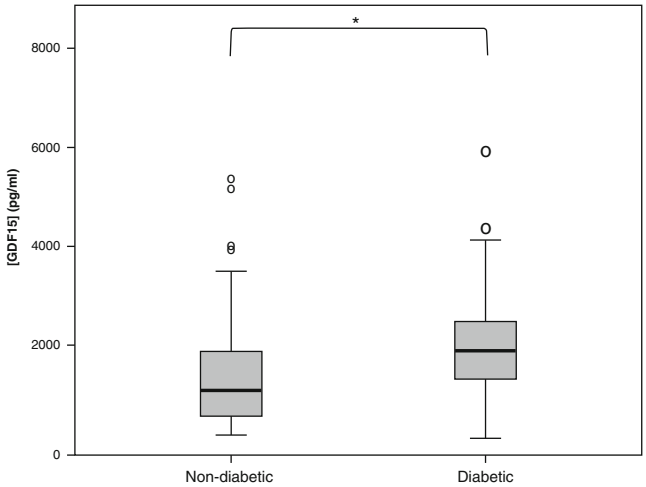

Fig. 4 GDF15 concentrations in patients with and without diabetes mellitus. Significant differences are flagged with an *asterisk*

disease severity as a significant contributor to the concentration of GDF15, after correcting for kinship clustering ($p < 0.001$; generalized estimating equations).

The Value of GDF15 in Predicting Clinical Disease Progression

Approximately 2 years after the initial assessment, the GDF15 concentration and disease severity (NMDAS score) were measured again in 76 carriers from the initial cohort of 97 carriers. Of these 76 carriers, 50 samples were available (see Fig. 1). One carrier included in the follow-up group was excluded because of pregnancy. The remaining 49 carriers in the follow-up study were similar compared to the total cohort with respect to (distribution of) gender, age, BMI, GDF15 concentration, presence and severity of DM, cardiomyopathy, stroke-like episodes, myopathy and encephalopathy, heteroplasmy percentage in UEC, heteroplasmy percentage in leukocytes, and NMDAS total and subdomain scores (independent Mann-Whitney *U* test and 2-sided chi-square test). The characteristics of the entire cohort of m.3243A>G carriers at baseline and the follow-up cohort are summarized in Tables 1 and 2. In this follow-up cohort, we found no significant correlation between the change in the NMDAS score (i.e., the change in NMDAS score between the first and second follow-up visit) and the change in the concentration of GDF15 (i.e., the change in GDF15 concentration between the first and the second follow-up visit) ($r = 0.006$; $p = 0.97$; $n = 49$; Spearman's correlation coefficient). Moreover, no significant correlation was found between GDF15 concentration at the first visit and change in the NMDAS (disease progression) during follow-up ($r = -0.19$; $p = 0.18$; $n = 49$; Spearman's correlation coefficient). Linear regression also revealed that the change in total disease severity did not contribute significantly to the change in the GDF15 concentration ($p = 0.72$; univariate linear regression). A linear regression model revealed that the change in FGF21 concentration, but not the change in GDF15 concentration contributed significantly to the change in disease severity (i.e., NMDAS score; $\beta(\text{FGF21}) = 0.45$ ($p = 0.03$; $n = 24$); forward multilinear regression modeling). There was no correlation between the change in the concentration of GDF15 and the change in the concentration of FGF21 ($r = -0.047$; $p = 0.85$; $n = 18$; Pearson's correlation coefficient).

Myocardial Strain

Twenty-four subjects underwent echocardiographies as part of clinical care within 1 year of GDF15 sampling. These subjects were similar compared to the whole group with respect to gender, age, BMI, and total NMDAS score and cardiac and DM subscores (independent Mann-Whitney *U* test and 2-sided chi-square test; see Tables 3 and 4). Qualitative descriptions of gross echocardiography findings include (not mutually exclusive): left ventricle (LV) hypertrophy ($n = 8$), LV systolic dysfunction ($n = 3$), LV diastolic dysfunction ($n = 8$), mild aortic regurgitation ($n = 2$), and mild mitral regurgitation ($n = 1$). Ten carriers had normal gross echocardiography findings.

The correlation coefficient between the global longitudinal strain and the concentration of GDF15 was 0.55 ($p = 0.006$; $n = 23$; Pearson's correlation coefficient). There was no correlation between global circumferential or radial strain and the concentration of GDF15 ($r = 0.17$; $p = 0.47$; $n = 21$ and $r = 0.20$; $p = 0.37$; $n = 22$, respectively; Spearman's correlation coefficients).

Table 3 Patient characteristics of the cohort of all adult m.3243A>G carriers of which myocardial strain was reported

		Cardiac 2D strain cohort (24 carriers)				Difference from all carriers
		Central value	Spread	Range	*n*	*p*
Gender	% female	75			24	0.80
Age (years)	Mean, 95%CI	44	25–63	24–64	24	0.80
BMI (kg/m^2)	Median, IQR	22.3	21–26	18.3–35.8	24	0.91
Smoking (current)	% yes	22			23	0.78
Diabetes mellitus (prevalence)	% yes	45			24	0.48
Heteroplasmy percentage, leukocytes (%)	Mean, 95%CI	18[a]	7–50	7–49	23	0.22
Heteroplasmy percentage, UEC (%)	Mean, 95%CI	56	24–93	23–96	24	0.078
NMDAS score	Mean, 95%CI	20	1–54	0–56	24	0.11
Domain 1	Mean, 95%CI	5[a]	0–23	0–23	24	0.11
Domain 2	Mean, 95%CI	8	0–23	0–23	24	0.015
Domain 3	Mean, 95%CI	3[a]	0–16	0–18	24	0.97
Myopathy score	Mean, 95%CI	3	0–7	0–7	24	0.57
Encephalopathy score	Median, IQR	2	1–5	0–11	24	0.25
Diabetes mellitus (severity)	Mean, 95%CI	2	0–5	0–5	24	0.31
Cardiomyopathy (severity)	Median, IQR	0	0–2	0–5	24	0.06
Stroke-like episodes (severity)	Median, IQR	0	0–0	0–5	24	0.055
QoL mental	Mean, 95%CI	44	27–61	25–61	24	0.055
QoL physical	Mean, 95%CI	38	18–59	17–60	24	0.081
[GDF15] (pg/mL)	Mean, 95%CI	1,687[a]	483–5,791	420–5,981	24	0.41
[FGF21] (pg/mL)	Median, IQR	321	252–768	4–1,491	24	0.084

Patient characteristics for those adult carriers ($n = 24$) for whom myocardial strain was measured. The difference at baseline between this cohort and all carriers was calculated (chi-square test (2 sided); Fisher's exact test (2 sided), Mann-Whitney *U* test; independent sample *t*-test). The presence of diabetes mellitus was obtained from the NMDAS scale (score on diabetes mellitus item ≥3)

BMI body mass index, *95%CI* 95% confidence interval, *Domain 1* current function, *Domain 2* system-specific involvement, *Domain 3* current clinical assessment, *Encephalopathy score* sum of the encephalopathic symptoms of the NMDAS (psychiatric symptoms, migraine, seizure, stroke-like episodes, encephalopathy, and cognition), *GDF15* growth and differentiation factor 15, *IQR* interquartile range, *Myopathy score* sum of the myopathic symptoms of the NMDAS (exercise intolerance, respiratory muscle weakness, ptosis, external ophthalmoplegia, and myopathy), *n* = number of carriers of which data were available at that specific time point, *NMDAS* Newcastle mitochondrial disease adult scale, *UEC* urinary epithelial cells

[a] Lognormal distribution

Family-Matched Controls

The family-matched controls ($n = 30$) were similar to their maternal relatives carrying the m.3243A>G mutation with respect to age ($p = 0.52$; independent sample *t*-test), gender ($p = 1.0$), and smoking ($p = 0.29$; Fisher's exact test), but not with respect to BMI ($p = 0.004$; Mann-Whitney *U* test) and the presence and severity of DM ($p = 0.001$; Fisher's exact test) (see Table 1 and 2). The mean GDF15 concentration in the family-matched control group was 490 pg/mL (95%CI, 272–1,616 pg/mL; range, 236–1,687 pg/mL), which was significantly lower than their relatives carrying the m.3243A>G mutation (1,525 pg/mL (95%CI, 411–5,691 pg/mL); range, 333–7,421 pg/mL; $p < 0.001$; independent samples *t*-test). Only one maternal family member had an elevated concentration of GDF15 (1,560 pg/mL in an 18-year-old female) compared to age- and gender-matched controls. None of the maternal relatives was pregnant or known to have cancer, renal dysfunction, or cardiac problems.

Discussion

This study explored the value of serum GDF15 in indicating and monitoring mitochondrial disease severity and disease progression in adult m.3243A>G carriers. We found that the concentration of serum GDF15 correlates moderately to disease severity but does not correlate to disease progression in m.3243A>G carriers. Analysis of

Table 4 Echocardiographic characteristics of the cohort of all adult m.3243A>G carriers of which myocardial strain was reported

Cardiac ultrasound findings	*n*	%
Normal	10	42
Left ventricular hypertrophy without systolic dysfunction	8	33
Left ventricular systolic dysfunction only	2	8
Ejection fraction <55%	3	13
Left ventricular diastolic dysfunction	8	33
Dilated left ventricle	2	8
Aortic valve insufficiency (mild)	2	8
Mitral valve insufficiency (mild)	1	4
Dilated left atrium	2	8

data obtained in general patient care indicated that GDF15 might be a surrogate biomarker of left ventricular myocardial strain.

So far, a few studies have found promising results regarding the diagnostic properties of GDF15 in patients with mitochondrial disease (Kalko et al. 2014; Yatsuga 2014). None of these studies focused on the value of GDF15 as a surrogate marker for predicting or monitoring disease progression. We found normal (age- and gender-matched (Ho et al. 2012)) concentrations of GDF15 in 47% of our carriers, including both symptomatic and asymptomatic individuals and in 97% of our family-matched controls. The family-matched controls (bearing the same nuclear genetic and environmental background as the carriers, but without the m.3243A>G detectable in UEC, leukocytes, or buccal mucosa cells) had significantly lower GDF15 concentrations compared to their maternal relatives carrying the m.3243A>G mutation.

GDF15 has also been reported as a nonspecific biomarker for many diseases, including cancer, cardiac, pulmonary, renal, and gynecological disease (Izumiya et al. 2014; Kempf and Wollert 2013; Trovik et al. 2014; Yang et al. 2014). Since several of these conditions are highly prevalent in m.3243A>G carriers (de Laat et al. 2012; Hirano et al. 2002), including kidney failure (Breit et al. 2012), diabetes mellitus (Dominguez-Rodriguez et al. 2014), and cardiomyopathy (Montoro-Garcia et al. 2012), the contribution of these conditions to the concentration of GDF15 was studied in more detail. We observed higher concentrations of GDF15 in carriers with renal abnormalities (mainly microalbuminuria) and diabetes mellitus. The myocardial strain measured in echocardiograms collected as part of general patient care with a maximum of 1 year apart from GDF15 sampling indicates that GDF15 may be a promising surrogate marker for myocardial deformity in patients with the m.3243A>G mutation. The correlation between the concentration of GDF15 and longitudinal myocardial strain, but not between the concentration of GDF15 and circumferential or radial strain (Lok et al. 2012; St John Sutton et al. 2014), might be explained by the observation that changes in longitudinal myocardial strain precede changes in ejection fraction and global longitudinal strain is now part of the recommendations in the assessment of cardiac function, e.g., in monitoring chemotherapy (Bates et al. 2013; Hollingsworth et al. 2012; Plana et al. 2014; St John Sutton et al. 2014). In summary, GDF15 is a nonspecific marker that seems to be highly influenced by several other symptoms frequently seen in this patient group.

The previously proposed biomarker FGF21 had no additional value to GDF15 in predicting and monitoring disease severity in m. 3243A>G carriers. It seems neither of the two parameters is useful as a surrogate marker for disease severity and disease progression.

Strengths of our study include the high number of carriers with different levels of the same mutation in their mitochondrial genome, resulting in a heterogeneous multisystem disease that we quantified systematically using a standardized and quantitative follow-up, enabling us to draw tentative conclusions regarding the value of GDF15 as a prognostic biomarker for monitoring disease progression. Several limitations to our study are worth mentioning. The period of follow-up is relatively short for this slowly progressive and often oscillating disease. The NMDAS used in the follow-up of disease severity is not very accurate and lacks sensitivity, making it unfit to establish subtle changes, and in this aspect the study is underpowered. The quality of the serum may have been influenced by the storage and previous use (freeze thawing) of the samples used in our study. Since the echocardiograms for 2D strain analysis were collected as part of clinical care, the level of standardization was suboptimal and samples for GDF15 analysis were not taken at the same moment as the echocardiography. Therefore, the results of this pilot study,

including the responsivity of GDF15 as a biomarker for myocardial strain, need to be confirmed in a prospective study. Finally, since only carriers of the m.3243A>G were included in this study, one may not extrapolate these findings to other causes of mitochondrial failure

The mitochondrial disease field is diligently looking for easy-to-measure biomarkers, both for diagnostic and prognostic purposes. In this study, we have demonstrated that the concentration of serum GDF15 is moderately related to disease severity, but not to disease progression. Although the current study does not focus on the diagnostic applicability of GDF15, the lack of correlation between the concentration of GDF15 and disease progression in this 2-year follow-up study makes this biomarker unsuitable as a prognostic biomarker. The moderate correlation between myocardial strain and the concentration of GDF15 is a promising starting point for finding a prognostic biomarker for myocardial deformity but warrants further confirmation, preferably in a longitudinal study including an in-depth evaluation of renal function, glucose tolerance, and the effects of pharmacological interventions.

Acknowledgments This work was partly supported by the Netherlands Organisation for Scientific Research (the NWO Centres for Systems Biology Research initiative), ZonMW (AGIKO grants Saskia Koene and Dennis Vriens), and Stichting Energy4All. We thank Inge Konijnenberg-Kramer for sample handling. Jan Smeitink is the CEO of Khondrion BV.

Take-Home Message

In adult m.3243A>G carriers, serum GDF15 levels correlate to mitochondrial disease severity and myocardial strain, but not to disease progression

Conflict of Interest

Saskia Koene received research support from the Netherlands Organisation for Scientific Research (NWO).

Paul de Laat received research support from the Stichting Energy4all.

Doorlène H. van Tienoven reports no disclosures.

Gert Weijers reports no disclosures.

Dennis Vriens received research support from the Netherlands Organisation for Scientific Research (NWO) and the Dutch Cancer Society, not related to the current study.

Prof. Fred C.G.J. Sweep reports no disclosures.

Janneke Timmermans reports no disclosures.

Livia Kapusta reports no disclosures.

Dr. Mirian C.H. Janssen reports no disclosures.

Prof. Smeitink is the founder and CEO of Khondrion and is funded by the Netherlands Organisation for Scientific Research and by ongoing Marie Curie and Eurostars grants and grants of Stichting Energy4All, none related to the current study.

This study was not industry sponsored.

Informed Consent

All procedures followed were in accordance with the ethical standards of the responsible committee on human experimentation (institutional and national) and with the Helsinki Declaration of 1975, as revised in 2013. Informed consent was obtained from all patients for being included in the study.

Details of the Contributions of Authors

Saskia Koene: manuscript preparation, study coordination, and statistical analyses

Paul de Laat: sample collection and patient inventory

Doorlène H. van Tienoven: ELISA and sample handling

Gert Weijers: strain analysis and manuscript revision

Dennis Vriens: statistical analysis, figures, and manuscript revision

Fred C.G.J. Sweep: ELISA, preparations of the analyses, and manuscript revision

Janneke Timmermans: echocardiography

Livia Kapusta: strain analyses and manuscript revision

Mirian C.H. Janssen: patient collection and manuscript revision

Jan A.M. Smeitink: manuscript preparation, study design, and manuscript revision

References

Association WM (2013) Declaration of Helsinki – ethical principles for medical research involving human subjects. 64th WMA General Assembly, Fortaleza, Brazil

Bates MG, Hollingsworth KG, Newman JH et al (2013) Concentric hypertrophic remodelling and subendocardial dysfunction in mitochondrial DNA point mutation carriers. Eur Heart J Cardiovasc Imaging 14:650–658

Breit SN, Carrero JJ, Tsai VW et al (2012) Macrophage inhibitory cytokine-1 (MIC-1/GDF15) and mortality in end-stage renal disease. Nephrol Dial Transplant 27:70–75

Bulten BF, Mavinkurve-Groothuis AM, de Geus-Oei LF et al (2014) Early myocardial deformation abnormalities in breast cancer survivors. Breast Cancer Res Treat 146:127–135

de Laat P, Koene S, van den Heuvel LP, Rodenburg RJ, Janssen MC, Smeitink JA (2012) Clinical features and heteroplasmy in blood, urine and saliva in 34 Dutch families carrying the m.3243A>G mutation. J Inherit Metab Dis 11:1059–1969

Dominguez-Rodriguez A, Abreu-Gonzalez P, Avanzas P (2014) Usefulness of growth differentiation factor-15 levels to predict diabetic cardiomyopathy in asymptomatic patients with type 2 diabetes mellitus. Am J Cardiol 2:01367–01368

Emma F, Bertini E, Salviati L, Montini G (2012) Renal involvement in mitochondrial cytopathies. Pediatr Nephrol 27:539–550

Hirano M, Konishi K, Arata N et al (2002) Renal complications in a patient with A-to-G mutation of mitochondrial DNA at the 3243 position of leucine tRNA. Intern Med 41:113–118

Ho JE, Mahajan A, Chen MH et al (2012) Clinical and genetic correlates of growth differentiation factor 15 in the community. Clin Chem 58:1582–1591

Ho JE, Hwang SJ, Wollert KC et al (2013) Biomarkers of cardiovascular stress and incident chronic kidney disease. Clin Chem 59:1613–1620

Hollingsworth KG, Gorman GS, Trenell MI et al (2012) Cardiomyopathy is common in patients with the mitochondrial DNA m.3243A>G mutation and correlates with mutation load. Neuromuscul Disord 22:592–596

Izumiya Y, Hanatani S, Kimura Y et al (2014) Growth differentiation factor-15 is a useful prognostic marker in patients with heart failure with preserved ejection fraction. Can J Cardiol 30:338–344

Kalko SG, Paco S, Jou C et al (2014) Transcriptomic profiling of TK2 deficient human skeletal muscle suggests a role for the p53 signalling pathway and identifies growth and differentiation factor-15 as a potential novel biomarker for mitochondrial myopathies. BMC Genomics 15:91

Kempf T, Wollert KC (2013) Risk stratification in critically ill patients: GDF-15 scores in adult respiratory distress syndrome. Crit Care 17:173

Koene S, de Laat P, van Tienoven DH et al (2014) Serum FGF21 levels in adult m.3243A>G carriers: clinical implications. Neurology 6:125–133

Lee SK, Kim J, Kim HD, Lee JS, Lee YM (2010) Initial experiences with proton MR spectroscopy in treatment monitoring of mitochondrial encephalopathy. Yonsei Med J 51:672–675

Lok SI, Winkens B, Goldschmeding R et al (2012) Circulating growth differentiation factor-15 correlates with myocardial fibrosis in patients with non-ischaemic dilated cardiomyopathy and decreases rapidly after left ventricular assist device support. Eur J Heart Fail 14:1249–1256

Mayeux R (2004) Biomarkers: potential uses and limitations. NeuroRx 1:182–188

Montoro-Garcia S, Hernandez-Romero D, Jover E et al (2012) Growth differentiation factor-15, a novel biomarker related with disease severity in patients with hypertrophic cardiomyopathy. Eur J Intern Med 23:169–174

Moore AG, Brown DA, Fairlie WD et al (2000) The transforming growth factor-ss superfamily cytokine macrophage inhibitory cytokine-1 is present in high concentrations in the serum of pregnant women. J Clin Endocrinol Metab 85:4781–4788

Pfeffer G, Horvath R, Klopstock T et al (2013) New treatments for mitochondrial disease-no time to drop our standards. Nat Rev Neurol 9:474–481

Plana JC, Galderisi M, Barac A et al (2014) Expert consensus for multimodality imaging evaluation of adult patients during and after cancer therapy: a report from the American Society of Echocardiography and the European Association of Cardiovascular Imaging. Eur Heart J Cardiovasc Imaging 15:1063–1093

Schaefer AM, Phoenix C, Elson JL, McFarland R, Chinnery PF, Turnbull DM (2006) Mitochondrial disease in adults: a scale to monitor progression and treatment. Neurology 66:1932–1934

St John Sutton M, Ky B, Regner SR et al (2014) Longitudinal strain in Friedreich Ataxia: a potential marker for early left ventricular dysfunction. Echocardiography 31:50–57

Suomalainen A (2011) Biomarkers for mitochondrial respiratory chain disorders. J Inherit Metab Dis 34:277–282

Trovik J, Salvesen HB, Cuppens T, Amant F, Staff AC (2014) Growth differentiation factor-15 as biomarker in uterine sarcomas. Int J Gynecol Cancer 24:252–259

Xu X, Li Z, Gao W (2011) Growth differentiation factor 15 in cardiovascular diseases: from bench to bedside. Biomarkers 16:466–475

Yang CZ, Ma J, Zhu DW et al (2014) GDF15 is a potential predictive biomarker for TPF induction chemotherapy and promotes tumorigenesis and progression in oral squamous cell carcinoma. Ann Oncol 24:24

Yatsuga S, Koga Y (2014) Growth differentiation factor 15 and fibroblast growth factor 21: novel biomarkers for mitochondrial diseases United Mitochondrial Disease Foundation Conference 2014

JIMD Reports
DOI 10.1007/8904_2015_444

RESEARCH REPORT

Novel Genetic Mutations in the First Swedish Patient with Purine Nucleoside Phosphorylase Deficiency and Clinical Outcome After Hematopoietic Stem Cell Transplantation with HLA-Matched Unrelated Donor

Nicholas Brodszki · Maria Svensson · André B.P. van Kuilenburg · Judith Meijer · Lida Zoetekouw · Lennart Truedsson · Jacek Toporski

Received: 19 February 2015 / Revised: 09 April 2015 / Accepted: 13 April 2015 / Published online: 13 May 2015

Abstract Purine nucleoside phosphorylase (PNP) is an enzyme active in the purine salvage pathway. PNP deficiency caused by autosomal recessive mutations in the *PNP* gene leads to severe combined immunodeficiency (SCID) and in two thirds of cases also to neurological effects such as developmental delay, ataxia, and motor impairment.

PNP deficiency has a poor outcome, and the only curative treatment is allogenic hematopoietic stem cell transplantation (HSCT). We present the first Swedish patient with PNP deficiency with novel mutations in the *PNP* gene and the immunological results of the HSCT and evaluate the impact of HSCT on the neurological symptoms. The patient presented early in life with neurological symptoms and suffered later from repeated serious respiratory tract infections. Biochemical tests showed severe reduction in PNP activity (1% residual activity). Genetic testing revealed two new mutations in the *PNP* gene: c.729C>G (p.Asn243Lys) and c.746A>C (p.Tyr249Cys). HSCT was performed with an unrelated donor, resulting in prompt and sustained engraftment and complete donor chimerism. There was no further aggravation of the patient's neurological symptoms at 21 months post HSCT, and appropriate developmental milestones were achieved. HSCT is curative for the immunological defect caused by PNP deficiency, and our case strengthens earlier reports that HSCT is effective as a treatment even for neurological symptoms in PNP deficiency.

Communicated by: Jerry Vockley, M.D., Ph.D.

Competing interests: None declared

N. Brodszki (✉) · J. Toporski
Childrens Hospital, Skåne University Hospital, Lasarettsgatan 48, SE-221 85 Lund, Sweden
e-mail: nicholas.brodszki@skane.se

M. Svensson
Lund University, Lund, Sweden

A.B.P. van Kuilenburg · J. Meijer · L. Zoetekouw
Academic Medical Center Lab. Genetic Metabolic Diseases, University of Amsterdam, Amsterdam, The Netherlands

L. Truedsson
Department of Laboratory Medicine, Section of Microbiology, Immunology and Glycobiology, Lund University, Lund, Sweden

Introduction

Purine nucleoside phosphorylase (PNP) is an enzyme active in purine metabolism (Fig. 1), in which it degrades guanosine, deoxyguanosine, inosine, and deoxyinosine (Bzowska et al. 2000). PNP is found in most cells of the body, but different tissues have different levels of PNP activity, with the highest expression in lymphoid tissue. Deficiency in PNP enzymatic activity leads to the accumulation of its substrates, which in turn leads to accumulation of deoxyguanosine triphosphate (dGTP) intracellularly, especially in the thymus, where high cell turnover takes place. dGTP may interfere with DNA synthesis or repair directly or by inhibition of ribonucleotide reductase activity, thereby preventing the cellular proliferation required for an immune response.

PNP deficiency is an autosomal recessive disorder and leads to a progressive form of severe combined immunodeficiency (SCID) with decreased numbers of T cells and lymphopenia (Giblett et al. 1975). Some studies have shown that B cell function can be disrupted as well (Markert 1991).

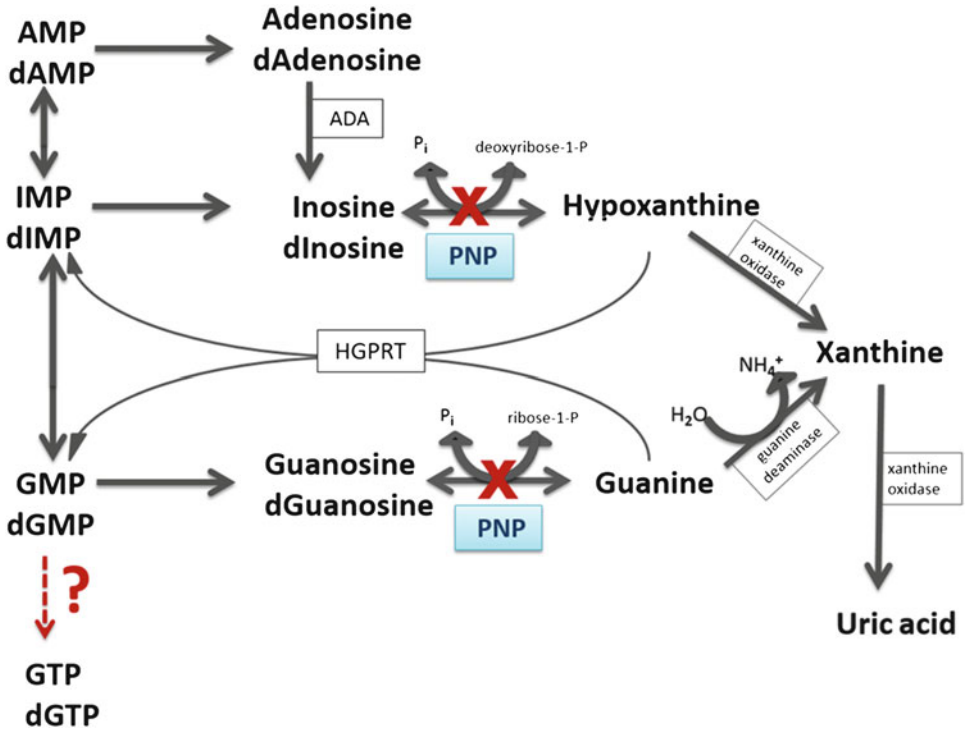

Fig. 1 Schematic presentation of the role of PNP in the degradation and salvage pathways of purine nucleosides. *ADA* adenosine deaminase, *AMP* adenosine monophosphate, *dGTP* deoxyguanosine triphosphate, *GMP* Guanine monophosphate, *IMP* inosine monophosphate, *HGPRT* hypoxanthine guanine phosphoribosyltransferase, *PNP* purine nucleoside phosphorylase, *d* deoxy

In two thirds of cases of PNP deficiency with the SCID phenotype, neurodevelopmental problems also arise (Markert 1991). Symptoms usually develop towards the end of the patient's second year of life and include ataxia, mental retardation, developmental delay, and muscle spasticity. In addition, PNP deficiency is associated with an increased risk of autoimmune disorders like autoimmune hemolytic anemia, immune thrombocytopenia, neutropenia, thyroiditis, and lupus.

Low uric acid in plasma has been suggested as a marker for PNP deficiency, but a recent study found normal uric acid in five of seven patients, suggesting that this marker is not reliable (Walker et al. 2011). If the disease is suspected, PNP enzyme activity should be measured either in a red blood cell lysate, blood spots, or in white blood cells (van Kuilenburg et al. 2010).

To confirm the diagnosis, a genetic analysis can be done. The *PNP* gene containing six exons is located on the long arm of chromosome 14 (14q13.1). Exon skipping, missense, and frameshift mutations in these six exons have been found to cause PNP deficiency, and the most common mutation is a change from A to C or G nucleotides at cDNA position 58 or 234, respectively (Alangari et al. 2009; Walker et al. 2011).

PNP deficiency has a poor prognosis, and the only successful treatment known to date is hematopoietic stem cell transplantation (HSCT). The effectiveness of this treatment on the neurological and autoimmune problems is unclear because of the small number of transplanted patients and limited number of studies (Grunebaum et al. 2013).

We present a patient with PNP deficiency with two novel mutations in the *PNP* gene. The findings of new mutations are important for future diagnostics and treatment of children with this deficiency. We also address whether the neurological defects of PNP deficiency are treatable by HSCT in order to further evaluate the usefulness of this therapy.

Patient

Our patient is the only child of Kurdish parents who are first-degree cousins. He was healthy until 9 months of age, when he was referred to a pediatric department for developmental delay and obesity. He was unable to sit up without support and had general muscular hypotonia but could hold his head stable. He measured 14 kg and 79 cm (both $\geq$3 standard deviations for age). The investigations at that age were inconclusive.

At 2 years of age, he was admitted to the local hospital with his first pneumonia. He was noted to have persistent

cough but had no significant history of infections. Neurologically, he showed trunk ataxia, areflexia of the lower extremities, and general muscular hypotonia with inability to walk independently and bilateral pes planus. Unfortunately, a more extensive neurological assessment was not done at this time. His speech development was difficult to assess at that time because his native language is not Swedish. In the following 4 months, he suffered three more pneumonias.

Investigations

Standard blood investigations showed leukopenia (2.5×10^9/L) with a low lymphocyte count ($0.3–0.8 \times 10^9$/L) and mild anemia (hemoglobin 98 g/L) with hypochromic and microcytic erythrocytes. Other laboratory tests, including electrolytes, ALT, AST, GT, pancreatic amylase, bilirubin, and thyroid hormone status, were normal.

Urine investigations showed increased purine metabolites and a low uric acid concentration at 12 μmol/L (ref: 230–480) pointing towards PNP deficiency.

Immunological investigation revealed low B and T cell counts (Table 1). Immunoglobulin levels and antibody response to tetanus vaccine were normal, while specific antibody levels to pneumococci were very low. The lymphocyte stimulation test showed almost no proliferation with T cell mitogens and low activity with T cell-dependent B cell mitogen.

T cell receptor excision circles (TRECs), a byproduct of the maturation of T cells that reflects the number of recently formed T cells in peripheral blood, have been suggested as a screening test for early detection of SCID (Chan and Puck 2005). For identification of B cell deficiencies in patients, the measurement of κ-deleting recombinant excision circles (KRECs) is used (Nakagawa et al. 2011). The retrospective analysis of KRECs on the patient's Guthrie card taken at birth was low at 4.2/μL (ref: >8), whereas TRECs were normal at 13.5/μL (ref: >10).

Genetic and Enzymatic Analysis

The analysis of the PNP enzyme activity in blood spots and the analysis of the *PNP* gene were performed by PCR amplification of all six coding exons, and flanking intronic regions of the *PNP* gene was carried out using intronic primer sets. Sequence analysis of genomic fragments amplified by PCR was carried out on an Applied Biosystems (Carlsbad, CA, USA) model 3730 automated DNA sequencer using the dye-terminator method (van Kuilenburg et al. 2010). The genetic analysis showed that the patient was compound heterozygous for two novel mutations in exon 6 of the *PNP* gene (14q13.1) c.729C>G (p.Asn243Lys) and c.746A>C (p.Tyr249Cys). The parents were carriers for the mutations.

Table 1 Lymphocyte subset levels before and 21 months after HSCT

Cell concentration ($\times 10^9$/L)	At diagnosis	21 months after HSCT	Ref interval
Lymphocytes	0.6	2.4	2.30–5.40
T cells (CD3+)	0.39	1.89	1.40–3.70
T helper cells (CD4+)	0.13	1.09	0.70–2.20
T cytotoxic cells (CD8+)	0.15	0.71	0.49–1.30
B cells (CD19+)	0.07	0.36	0.39–1.40
NK cells (CD16 + CD56+)	0.10	0.16	0.13–0.72

PNP enzyme activity was almost absent at 16 mol/h/mg (normal 823–2387), thus establishing the diagnosis of PNP deficiency.

Transplantation

Considering the low numbers of lymphocytes, the poor results of the lymphocyte functional tests, and the recurrent infections, the decision was made to perform HSCT. The parents signed a written informed consent.

Because the patient had no siblings, he underwent a 9/10 HLA loci identical female unrelated donor bone marrow transplantation (DPB1 mismatch). There was a major blood type mismatch; the patient was type 0 and the donor type B. The patient was CMV IgG positive, while the donor was negative.

According to guidelines (ESID/EBMT 2011) regarding HSCT for primary immunodeficiencies, the patient was conditioned with myeloablative regimen. This consisted of exposure-targeted i.v. busulfan given in 8 doses every 12 h, from day −6 to −3 (first day 4.9 mg/kg and then adjusted aiming for AUC day 0–4 90 ± 5 mg h/L), and fludarabine (40 mg/m^2/day, from day −6 to −3). Serotherapy with s.c. alemtuzumab (0.2 mg/kg) was administered for 5 days (day −12 to −8).

He received 5×10^6 CD34+ cells/kg body weight. The posttransplant graft vs. host disease (GvHD) prophylaxis consisted of four doses of methotrexate, cyclosporine, and steroids.

Engraftment and Immunological Reconstitution

Complete hematological recovery was achieved at day +24. Despite profound lymphocytopenia, chimerism analysis showed mixed chimerism in B cells (23% recipient origin) and T cells (35% recipient origin) and with 100% donor chimerism in all other cell lines. Two months after HSCT

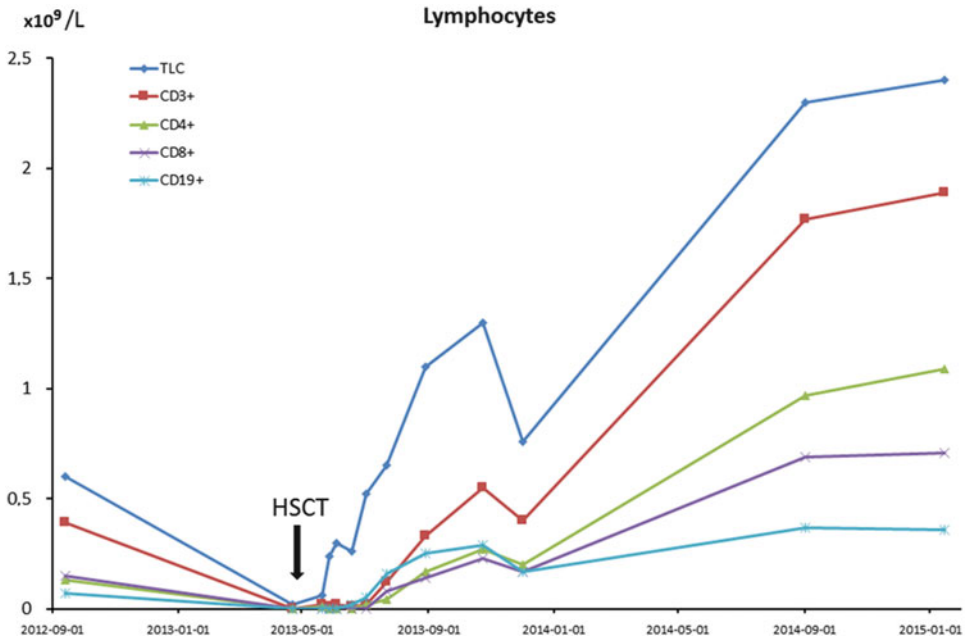

Fig. 2 Total lymphocyte count (TLC) and concentration of different lymphocyte subsets as indicated by CD positivity over time in relation to hematopoietic stem cell transplantation (HSCT). The *arrow* indicates time of HSCT. *TLC* total lymphocyte count

together with the increasing total lymphocyte count, increasing number of autologous cells were detected, 65% autologous T lymphocytes at day +70. Due to the risk of graft rejection and the persistent CMV viremia immunosuppression was discontinued. Four weeks later, the patient achieved stable 100% donor chimerism in all cell lines. IVIG supplementation was discontinued 23 weeks post HSCT. At 21 months after HSCT, the patient had a normal lymphocyte count with normal lymphocyte subsets (Table 1 and Fig. 2), and neither new nor exacerbations of preexisting infections were observed.

The earlier high levels of purine metabolites in the urine, especially inosine, were normalized as a sign of functioning PNP enzyme.

Posttransplant Morbidity

On day +10 after HSCT, he suffered from mucositis grades II–III, metapneumovirus pneumonia, and CMV reactivation with CMV enteritis. On day +15, he developed engraftment syndrome with sudden weight gain, fever, and fluid retention and was treated successfully with steroids.

Eight weeks after the discontinuation of the immunosuppressive drugs, the patient developed acute cutaneous GvHD (stage III, overall grade II) but responded to three treatments with steroids without sequelae. No chronic GvHD was observed.

Neurological Development

His neurologic development showed no further deterioration. At 55 months of age, his gross and fine motor skills corresponded to what is expected for a 3- to 4-year-old. His cognitive and social/emotional skills were close to that of a 4-year-old, while his language skills were similar to that of a 3-year-old child. He did not have spasticity but has a persisting hyporeflexia in the lower extremities. The assessment at that age concluded that he had clearly reached new developmental milestones.

Literature Review

To evaluate the neurological outcome of HSCT in our patient, we completed a literature review. We found ten articles describing 14 cases of HSCT-treated PNP deficiency (Markert 1991; Broome et al. 1996; Carpenter et al. 1996; Pannicke et al. 1996; Classen et al. 2001; Baguette et al. 2002; Myers et al. 2004; Delicou et al. 2007; Aytekin et al. 2008; Singh 2012). Of these, two articles describing six cases had no description of the neurological outcome (Markert 1991; Broome et al. 1996). In one case, the patient died 1 month following HSCT (Pannicke et al. 1996). The seven remaining cases and the case presented here were evaluated for this review.

Discussion

Only approximately 4% of all cases of SCIDs are caused by PNP deficiency. The first case was presented in 1975, and up to the end of 2014, fewer than 80 cases have been reported. A total of 24 mutations causing PNP deficiency have been described (Giblett et al. 1975; Markert 1991; Walker et al. 2011). The two new mutations in our patient, c.729C>G (p.Asn243Lys) and c.746A>C (p.Tyr249Cys), both in exon 6, resulted in a near-complete absence of the PNP activity and caused both SCID and neurological defects such as developmental delay and muscular hypotonia, but no autoimmunity. Other mutations and a nonsense and frameshift mutation causing deficiency have been identified in exon 6 of the PNP gene (Walker et al. 2011). There is marked heterogeneity in the phenotype and onset of symptoms in PNP deficiency. Thus, no certain conclusion can be drawn regarding our patient's mutations and manifestation of specific symptoms.

Typically, PNP deficiency presents with severe T cell defects, but the effects on B cells have been variable (Markert 1991). In our patient, both T and B cell counts were low when he was age 2.5 years. There was a poor response on mitogen-stimulation tests for both B and T cells. Even though immunoglobulin levels were normal, the patient's immunodeficiency clearly affected both his B and T cells.

The late onset of the immunodeficiency in PNP deficiency may allow for normal TREC and KREC levels with screening in infancy. In line with this possibility, our patient had only abnormal levels of KRECs, whereas TRECs were normal at birth. As described elsewhere (la Marca et al. 2014), we suggest tandem mass spectrometry on dried blood spots to identify PNP metabolites as a more accurate screening method.

Our patient was successfully treated with HSCT which is the only curative treatment available for SCID caused by PNP deficiency. No patient with PNP deficiency has survived longer than the second decade of life without HSCT. When treating SCID caused by deficiency in adenosine deaminase, another enzyme in the purine salvage pathway, the transplant-related mortality is 20% (Grunebaum et al. 2013). The mortality for treatment of PNP deficiency is not known because of the limited number of patients.

After HSCT, no further neurological deterioration was reported in any of the PNP-deficient patients. In most cases, neurological evaluation was done approximately 1 year after transplantation. Marked improvement was reported in two patients, while in one patient, only slight improvement was reported. For the rest of the patients, appropriate developmental milestones were reached, but some of the neurological impairment remained. Persistent spasticity or muscular hypotonia was reported in five patients.

One patient was evaluated after 24 months and another after 32 months, and in both cases, persistent neurological deficits were reported. Our patient, evaluated 21 months after HSCT, clearly belongs to the group showing obvious neurodevelopmental improvements.

The cause of the neurological impairments is not yet known, but the symptoms are similar to those of Lesch-Nyhan syndrome, a deficiency in hypoxanthine guanine phosphoribosyltransferase (HGPRT), which is the next enzyme in the purine salvage pathway (Fig. 1) (Cohen et al. 2000). Because HGPRT deficiency does not present with immunodeficiency, it has been suggested that the mechanism causing the neurological effects of PNP deficiency differs from that causing the immunological defects. Low levels of guanosine triphosphate (GTP) could be the reason for the neurological effects rather than toxic levels of dGTP. The de novo synthesis of GTP is limited in the brain, and because the GTP salvage pathway is disturbed in PNP deficiency, the result is low levels of GTP in the brain and disruption of metabolic processes.

A recent study showed smaller than average cerebellum, corpus callosum, and thalamus in PNP-deficient mice (Mansouri et al. 2012). There were also a reduced number of Purkinje cells in the cerebellum, and the existing Purkinje cells had an abnormal shape. The two patients in our review who had undergone MRI had normal results, but some reported cases had abnormal MRIs (Ozkinay et al. 2007; Madkaikar et al. 2011; Somech et al. 2013). One patient with substantial neurological impairment had an MRI late in the progress of the illness, showing atrophy of the cerebellum and the cerebral cortex with loss of white matter myelination (Ozkinay et al. 2007). Two other cases had mild to significant brain atrophy (Madkaikar et al. 2011; Somech et al. 2013). All three patients died in early childhood. These results indicate that the brain damage visible on MRI can develop late in the course of the disease.

Early treatment with PNP replacement in the studied mice prevented cerebellar damage, indicating that the time of detection and start of treatment are important for reversing the neurological damage (Mansouri et al. 2012).

In the reported cases, only one other patient in addition to our patient had detectable levels of PNP activity, and the neurological symptoms before and after HSCT did not remarkably differ from those with no detectable PNP activity. The age when HSCT was performed varied, and in this very limited number of patients, there was no correlation between improvement and age at transplantation.

In none of the cases was further neurological deterioration after HSCT reported, and improvement was even reported in some. One reason for the reduction in further neurological damage could be that after HSCT, the stem cells can differentiate into blood monocytes that can

migrate over the BBB and become microglia cells (Singh 2012). These cells can then produce the missing enzyme, halting the progress of the disease.

The improvement after HSCT is hard to evaluate. Because new developmental milestones are normally reached over time and the patients are relatively young when transplanted, it is difficult to know what the neurological progress would have been if they had not been transplanted. The oldest reported untreated patient lived to age 13 years and died after a stroke (Tam and Leshner 1995). Two more patients have been reported to have seriously deteriorated neurologically before death, one because of a viral brain infection and one because of cerebral edema following intracranial hemorrhage (Dror et al. 2004; Parvaneh et al. 2007). Most patients with PNP deficiency die from infections during the first decade of life (Markert 1991). Given that the course of the neurological decline is not known, it is hard to assess the effect of HSCT. Both in our case and the cases reported, there was no further neurological deterioration after the treatment, and some patients even showed improvement, indicating that HSCT is partly effective as a treatment for these symptoms.

Conclusion

We present a case with two novel mutations in the PNP gene, resulting in severe PNP deficiency with almost absent PNP activity. The patient had a SCID-like phenotype and showed neurological impairment. He was successfully treated with HSCT from an unrelated donor and was infection free after 21 months. He did not show worsening of the neurological symptoms and reached new developmental milestones. This case and reports in the literature on neurological improvement after HSCT indicate that this is an effective treatment even for the neurological symptoms.

Synopsis

Hematopoietic stem cell transplant is an effective treatment immunodeficiency caused by purine nucleoside phosphorylase deficiency and ameliorates neurological symptoms of the disorder.

Compliance with Ethics Guidelines

Informed Consent

All procedures followed were in accordance with the ethical standards of the Helsinki Declaration of 1975, as revised in 2000.

Upon contact with the Regional Ethical Review Board in Lund, we were advised that signed consent from the patient's parents is sufficient for publication of this case report and the consent was obtained.

Author Contributions

Nicholas Brodszki: conception, planning, collection and compiling of the clinical and laboratory data and writing the manuscript.

Maria Svensson: collection and compiling of the clinical and laboratory data and drafting the manuscript.

André B.P. van Kuilenburg: supervising enzymatic and genetic analysis, cowriting of the manuscript.

Judith Meijer: experimental analysis, cowriting of the manuscript.

Lida Zoetekouw: experimental analysis.

Lennart Truedsson and Jacek Toporski: interpretation of the results and supervising the writing of the manuscript.

All authors read and approved the final manuscript.

Conflict of Interest

Nicholas Brodszki, Maria Svensson, André B.P. van Kuilenburg, Judith Meijer, Lida Zoetekouw, Lennart Truedsson, and Jacek Toporski declare that they have no conflict of interest.

References

Alangari A, Al-Harbi A, Al-Ghonaium A, Santisteban I, Hershfield M (2009) Purine nucleoside phosphorylase deficiency in two unrelated Saudi patients. Ann Saudi Med 29:309–312

Aytekin C, Yuksek M, Dogu F et al (2008) An unconditioned bone marrow transplantation in a child with purine nucleoside phosphorylase deficiency and its unique complication. Pediatr Transplant 12:479–482

Baguette C, Vermylen C, Brichard B et al (2002) Persistent developmental delay despite successful bone marrow transplantation for purine nucleoside phosphorylase deficiency. J Pediatr Hematol Oncol 24:69–71

Broome CB, Graham ML, Saulsbury FT, Hershfield MS, Buckley RH (1996) Correction of purine nucleoside phosphorylase deficiency by transplantation of allogeneic bone marrow from a sibling. J Pediatr 128:373–376

Bzowska A, Kulikowska E, Shugar D (2000) Purine nucleoside phosphorylases: properties, functions, and clinical aspects. Pharmacol Ther 88:349–425

Carpenter PA, Ziegler JB, Vowels MR (1996) Late diagnosis and correction of purine nucleoside phosphorylase deficiency with allogeneic bone marrow transplantation. Bone Marrow Transplant 17:121–124

Chan K, Puck JM (2005) Development of population-based newborn screening for severe combined immunodeficiency. J Allergy Clin Immunol 115:391–398

Classen CF, Schulz AS, Sigl-Kraetzig M et al (2001) Successful HLA-identical bone marrow transplantation in a patient with PNP

deficiency using busulfan and fludarabine for conditioning. Bone Marrow Transplant 28:93–96
Cohen A, Grunebaum E, Arpaia E, Roifman CM (2000) Immunodeficiency caused by purine nucleoside phosphorylase deficiency. Immunol Allergy Clin North Am 20(1):143–159
Delicou S, Kitra-Roussou V, Peristeri J et al (2007) Successful HLA-identical hematopoietic stem cell transplantation in a patient with purine nucleoside phosphorylase deficiency. Pediatr Transplant 11:799–803
Dror Y, Grunebaum E, Hitzler J et al (2004) Purine nucleoside phosphorylase deficiency associated with a dysplastic marrow morphology. Pediatr Res 55:472–477
ESID/EBMT (2011) EBMT/ESID guidelines for haematopoietic stem cell transplantation for primary immunodeficiencies
Giblett ER, Ammann AJ, Wara DW, Sandman R, Diamond LK (1975) Nucleoside-phosphorylase deficiency in a child with severely defective T-cell immunity and normal B-cell immunity. Lancet 1:1010–1013
Grunebaum E, Cohen A, Roifman CM (2013) Recent advances in understanding and managing adenosine deaminase and purine nucleoside phosphorylase deficiencies. Curr Opin Allergy Clin Immunol 13:630–638
la Marca G, Canessa C, Giocaliere E et al (2014) Diagnosis of immunodeficiency caused by a purine nucleoside phosphorylase defect by using tandem mass spectrometry on dried blood spots. J Allergy Clin Immunol 134:155–159
Madkaikar MR, Kulkarni S, Utage P et al (2011) Purine nucleoside phosphorylase deficiency with a novel PNP gene mutation: a first case report from India. BMJ Case Rep 2011
Mansouri A, Min W, Cole CJ et al (2012) Cerebellar abnormalities in purine nucleoside phosphorylase deficient mice. Neurobiol Dis 47:201–209
Markert ML (1991) Purine nucleoside phosphorylase deficiency. Immunodefic Rev 3:45–81
Myers LA, Hershfield MS, Neale WT, Escolar M, Kurtzberg J (2004) Purine nucleoside phosphorylase deficiency (PNP-def) presenting with lymphopenia and developmental delay: successful correction with umbilical cord blood transplantation. J Pediatr 145:710–712
Nakagawa N, Imai K, Kanegane H et al (2011) Quantification of kappa-deleting recombination excision circles in Guthrie cards for the identification of early B-cell maturation defects. J Allergy Clin Immunol 128(223–225), e222
Ozkinay F, Pehlivan S, Onay H et al (2007) Purine nucleoside phosphorylase deficiency in a patient with spastic paraplegia and recurrent infections. J Child Neurol 22:741–743
Pannicke U, Tuchschmid P, Friedrich W, Bartram CR, Schwarz K (1996) Two novel missense and frameshift mutations in exons 5 and 6 of the purine nucleoside phosphorylase (PNP) gene in a severe combined immunodeficiency (SCID) patient. Hum Genet 98:706–709
Parvaneh N, Ashrafi MR, Yeganeh M, Pouladi N, Sayarifar F, Parvaneh L (2007) Progressive multifocal leukoencephalopathy in purine nucleoside phosphorylase deficiency. Brain Dev 29: 124–126
Singh V (2012) Cross correction following haemopoietic stem cell transplant for purine nucleoside phosphorylase deficiency: engrafted donor-derived white blood cells provide enzyme to residual enzyme-deficient recipient cells. JIMD Rep 6:39–42
Somech R, Lev A, Grisaru-Soen G, Shiran SI, Simon AJ, Grunebaum E (2013) Purine nucleoside phosphorylase deficiency presenting as severe combined immune deficiency. Immunol Res 56: 150–154
Tam DA Jr, Leshner RT (1995) Stroke in purine nucleoside phosphorylase deficiency. Pediatr Neurol 12:146–148
van Kuilenburg AB, Zoetekouw L, Meijer J, Kuijpers TW (2010) Identification of purine nucleoside phosphorylase deficiency in dried blood spots by a non-radiochemical assay using reversed-phase high-performance liquid chromatography. Nucleosides Nucleotides Nucleic Acids 29:466–470
Walker PL, Corrigan A, Arenas M, Escuredo E, Fairbanks L, Marinaki A (2011) Purine nucleoside phosphorylase deficiency: a mutation update. Nucleosides Nucleotides Nucleic Acids 30: 1243–1247

JIMD Reports
DOI 10.1007/8904_2015_445

CASE REPORT

CSF 5-Methyltetrahydrofolate Serial Monitoring to Guide Treatment of Congenital Folate Malabsorption Due to Proton-Coupled Folate Transporter (PCFT) Deficiency

A. Torres • S.A. Newton • B. Crompton • A. Borzutzky • E.J. Neufeld • L. Notarangelo • G.T. Berry

Received: 09 February 2015 / Revised: 11 April 2015 / Accepted: 16 April 2015 / Published online: 26 May 2015

Abstract Hereditary folate malabsorption is characterized by folate deficiency with impaired folate transport into the central nervous system (CNS). This disease is characterized by megaloblastic anemia of early appearance, combined immunodeficiency, seizures, and cognitive impairment. The anemia and immunologic disease are responsive but neurological signs are refractory to folic-acid treatment. We report a 7-year-old girl who has congenital folate deficiency and SLC46A1 gene mutation who is unable to transport folate from her gut to the circulatory system and consequently from the blood to the cerebrospinal fluid (CSF). As a result she developed undetectable 5-methyltetrahydrofolate levels in her plasma and CSF and became immunocompromised and quite ill. Intramuscular treatment with 5-formyltetrahydrofolate (folinic acid) was therapeutic at her presentation and has been successful preventing other signs and symptoms of hereditary folate malabsorption even at relatively low CSF levels. Although difficult, early detection and diagnosis of cerebral folate deficiency are important because folinic acid at a pharmacologic dose may normalize outcome in PCFT gene defects, as well as bypass autoantibody-blocked folate receptors and enter the cerebrospinal fluid by way of the reduced folate carrier. This route elevates the 5-methyltetrahydrofolate level within the central nervous system and can prevent the neuropsychiatric disorder. CSF levels of 5-methyltetrahydrofolate between 18 and 46 nmol/L may be sufficient to eradicate CNS disease.

Communicated by: Georg Hoffmann

Competing interests: None declared

A. Torres
Department of Pediatrics, Division of Pediatric Neurology, Boston Medical Center, Boston University Medical School, Boston, MA, USA

S.A. Newton · B. Crompton · A. Borzutzky · E.J. Neufeld · L. Notarangelo · G.T. Berry (✉)
Department of Neurology, Divisions of Hematology and Genetics and Genomics, The Manton Center for Orphan Disease Research, Boston Children's Hospital, Harvard Medical School, Boston, MA, USA
e-mail: Gerard.Berry@childrens.harvard.edu

Introduction

Hereditary folate malabsorption is a rare inborn error of metabolism, first reported by Lubby et al. in 1961 (Lubhy et al. 1961). This autosomal recessive disease is due to mutations in the SLC46A1 gene, which encodes the proton-coupled folate transporter (PCFT) (Qiu et al. 2006). It presents in early infancy with megaloblastic anemia, poor growth, diarrhea, infections, stomatitis, hypotonia, and progressive neurological deterioration including severe developmental delay and seizures that could be refractory to treatment (Diop-Bove et al. 1993–2014; Fernandes et al. 2012; Scriver et al. 1995; Zhao et al. 2012). To date 31 patients have been reported in the literature (Atabay et al. 2010; Borzutzky et al. 2009; Corbeel et al. 1985; Diop-Bove et al. 2013; Geller et al. 2002; Hansen and Blau 2005; Jebnoun et al. 2001; Kishimoto et al. 2014; Lanzkowsky et al. 1969; Lasry et al. 2008; Malatack et al. 1999; Ponz et al. 1898; Rosenblatt and Fenton 2001; Santiago-Borrero et al. 1973; Shin et al. 2011; Sofer et al. 2007; Steinschneider et al. 1990; Su 1976; Urbach et al. 1987; Wang et al. 2014; Zhao et al. 2007). It is imperative that the patients be treated very early and effectively with 5-formyltetrahydrofolate (folinic acid) in order to prevent irreversible neurological disease (Surtees 2001; Urbach et al. 1987; Wang et al. 2014; Whitehead 2006). The use of intramuscular folinic acid since infancy was reported to allow normal development and

health in a 27-year-old woman with severe disease (Min et al. 2008). The purpose of this report is to demonstrate the levels of cerebrospinal fluid (CSF) 5-methyltetrahydrofolate (5-CH3-THF) that are associated with normal neurological outcome in a child with hereditary folate malabsorption. Our goal was to use the concentration of 5-methyltetrahydrofolate in spinal fluid as a biomarker to guide treatment.

Human cells cannot synthesize folate de novo, but require folate for many metabolic functions, including the conversion of serine to glycine; the catabolism of histidine; the synthesis of thymidylate, methionine, and purine; and the DNA chromatin methylation that regulates gene expression (Cains et al. 2009). Folate is a B vitamin, essential for brain metabolism. It participates in the de novo synthesis of purines and thymidine and together with cobalamin represents an important cofactor for homocysteine remethylation and *S*-adenosylmethionine production in the brain. As with other vitamin deficiency states, folate deficiency may be the consequence of acquired or inherited disorders. Several inborn errors of metabolism can lead to defective folate transport or impaired metabolism, resulting in systemic folate deficiency and, obligatorily, 5-methyltetrahydrofolate depletion in the nervous system detectable by assay of CSF levels (Rosenblatt and Fenton 2001).

We report a child with severe systemic folate deficiency due to proton-coupled folate transporter deficiency who has done remarkably well with intramuscular administration of folinic acid and careful monitoring of CSF 5-methyltetrahydrofolate levels. Her diagnosis, hematological, and immunological rehabilitation was the subject of a previous report (Borzutzky et al. 2009).

Case Report

A 7-year-old female, born to non-consanguineous parents of Puerto Rican descent, developed frequent emesis and failure to thrive at 3 months of age. Her weight dropped from the 25th percentile to the 5th percentile. She was able to smile responsively, follow past the midline, vocalize sounds, and lift her head. At 4 months of age, she developed cough, coryza, low-grade fever, irritability, and increased emesis without diarrhea, for which she was hospitalized at another institution. Chest X-ray revealed diffuse interstitial pneumonia. Laboratory studies showed severe normocytic anemia (hemoglobin 6.7 g/dL, MCV 76 μm^3) with 0.4% reticulocyte count, mild neutropenia (1.4×10^9 cells/L) with hypersegmentation, eosinophilia (1.1×10^9 cells/L), and a normal absolute lymphocyte count (3.4×10^9 cells/L). Serum folate levels were undetectable. She was treated with antibiotics, a packed red blood cell transfusion and a single replacement dose of intravenous folinic acid (2 mg/kg) prior to transfer to Boston Children's Hospital.

Upon admission, bronchoalveolar lavage revealed *Pneumocystis jiroveci*. In addition, active cytomegalovirus (CMV) infection was documented by p65 antigenemia, PCR positivity in the bone marrow, and positive staining for CMV in endoscopic biopsies of esophagus and duodenum. Testing for HIV by ELISA was negative. Treatment was started with trimethoprim-sulfamethoxazole and ganciclovir. High-frequency ventilation was initially required due to respiratory distress, but gradual improvement allowed extubation after 12 days. The clinical course was complicated by *Klebsiella pneumoniae* bacteremia, requiring treatment with ceftriaxone.

Bone marrow aspirate performed 10 days after the initial dose of folinic acid was normal except for decreased iron staining and rare neutrophil hypersegmentation, without evidence of megaloblastic hematopoiesis. At that time, blood folate levels were still low. Continued treatment with intravenous folate resulted in normalization of plasma levels. However, 5-methyltetrahydrofolate in the CSF was undetectable. The patient was then switched to parenteral folinic acid to facilitate CSF penetration. Progressive clinical improvement, with normalization of hematological and immunological parameters was observed. The CSF 5-methyltetrahydrofolate improved to 33 nmol/L on 5 mg IM folinic acid daily. Dosing has been increased since then to 50 mg daily of IM folinic acid at 7 years of age with the goal of normalizing CSF 5-methyltetrahydrofolate. During this period, her neurological exam was only significant for hypotonia. Her brain MRI was normal at presentation, 7 months and 2 years of age. At the age of 7 years, she has had no more serious infections since infancy. She has reached all developmental milestones appropriate for her age and is doing well in school.

Her mother had a cousin diagnosed at a young age with anemia that was treated with vitamins and got better. We were unable to obtain more details. However, he has not required further treatments and is healthy.

Results

The goal of our treatment plan was to maintain CSF 5-methyltetrahydrofolate within the normal range. To that end, we adjusted the dose of folinic acid based on the measurements of 5-methyltetrahydrofolate in CSF obtained approximately every 6 months during the first few years of life considered critical for future development.

The CSF 5-methyltetrahydrofolate values are presented in Table 1. The doses shown were those the patient was taking at the time of the lumbar puncture before any adjustments were made. The samples were obtained in the fasting state early in the morning. Some samples were

Table 1 CSF 5-methyltetrahydrofolate (5-CH3-THF) levels and IM folinic acid therapy

Age (months)	6	8	13	15	18	26	34	44	53	65	84
Sample collection time	1200	0752	0728	0800	0945	0918	1100	0810	0950	0918	1030
CSF 5-CH3-THF nmol/L[a]	18	33	23	28	29	19	42	33	27	39	46
Serum folate nmol/L[b]	178	179	>261	152	113	>261	>261	>261	>261	>261	>261
Dose (mg/kg/day)	0.5	1	1.5	1.5	1.5	2	2.5	2.5	3	3	3
Total daily dose in mg	2	5	7.5	10	12.5	15	20	20	30 (15bid)	40 (20bid)	50 (30 am 20 pm)

[a] CSF 5-CH3-THF normal range: 40–187 nmol/L
[b] Serum folate normal range: 4–45 nmol/L

obtained between 1 and 4 h after the injection but the mother could not recall this information with certainty. Since it was difficult to achieve therapeutic values and the half-life of folinic acid is about 6 h, we recommended to split the dose but her compliance has not been very good with the second dose. The first 4 years IM injections were given in the legs, but since then, she has been injected in her arms too. She had no local or systemic side effects. The samples were collected and sent to the Medical Neurogenetics laboratory in Atlanta, GA, for analyses, according to the recommendations of Keith Hyland. Her current dose is 50 mg/day IM of folinic acid taken 30 mg IM in AM and 20 mg IM in PM (3 mg/kg/day). As seen in the table, we were not able to achieve parameters considered normal consistently of cerebrospinal fluid 5-methyltetrahydrofolate. Despite the fact that levels were between 18 and 46 nmol/L (mean 35 nmol/L), our patient's cognitive development and motor function are within normal limits. The CSF levels of this magnitude were associated with serum levels between 113 and >261 nmol/L.

Her weight, length, and head circumference are near the third percentile, but this most likely is familial because the measurements of weight and length are proportional and her mother has the same phenotype and similar percentiles. She currently does not have failure to thrive which has been reported in other cases of hereditary folate deficiency.

She is currently in first grade with neither motor nor cognitive problems. Her neurological, developmental, and neuropsychological evaluations showed no significant abnormalities. To evaluate her cognitive abilities, she was administered the DAS-II, Early Years, Upper Level Battery at 6.6 years of age. The DAS-II measures intelligence in terms of verbal, nonverbal, and spatial reasoning abilities. Verbal abilities were in the average range (standard score of 100, 50%). Nonverbal skills were in low average range (standard score 83, 13%). Her ability to use categorical reasoning to perceive increasingly complex similarities among stimuli was in the average range. In contrast she scored in the low average range on a task of abstract visual reasoning and pattern recognition. Visual motor skills were average (standard score of 93, 32%). Selected subtests of the Wechsler Individual Achievement Test (WIAT-III) were administered. She performed in the average range (standard score of 93, 23%) on early reading. Math problem-solving skills were low average (standard score of 89, 23%). She was also administered the Beery-Buktenica Developmental Test of Visual Motor Integration, Sixth Edition (VMI-6); Developmental Neuropsychological Assessment, Second Edition (NEPSY-2); Behavior Rating Inventory of Executive Function (BRIEF); Behavior Assessment System for Children, Second Edition, Parent Rating Scale (BASC-2-PRN); Children's Depression Inventory, Second Edition (CDI-2); and Roberts Apperception Test, Second Edition (Roberts-2) and did not show abnormalities.

Her father completed 1 year of college and is currently a singer, and her mother obtained a bachelor's degree and currently stays at home. They are both from Puerto Rico but neither of them nor their ancestry are from the Villalba region were the carrier prevalence of the SLC46A1 mutation is 6.3% compared to 0.2% of the rest of the island (Mahadeo et al. 2010).

Discussion

Levels of 5-methyltetrahydrofolate in CSF between 18 and 46 nmol/L may be sufficient to eradicate CNS disease. Folate is an essential cofactor for one-carbon methyl transfer reactions and crucial for a variety of biological processes, such as synthesis and repair of DNA (Blount et al. 1997; Kronenberg et al. 2008; Linhart et al. 2008), regulation of gene expression (Ghoshal et al. 2006; Pogribny et al. 2008), and synthesis of amino acids and neurotransmitters (Fournier et al. 2002; Shinohara et al. 2006). Since the 1940s, folate-deficient states and inborn errors of folate metabolism including defective transport have increasingly been recognized to play a role in the development of a macrocytic anemia, atherosclerosis,

thrombosis, neuropsychiatric disorders, and neural tube defects (Surtees et al. 1993). Clinical conditions associated with abnormal folate status range from malformations such as spina bifida to isolated disorders of cerebral function such as the cerebral folate deficiency (CFD) syndrome (Djukic 2007). Folate is known to occur in higher concentrations in CSF than plasma. As it is not synthesized within CNS, folate must enter the CSF against a concentration gradient from the blood (Chen and Wagner 1975; Suleiman et al. 1981). In various species, a folate binder was found in plasma membrane of choroid plexuses, suggesting a role for this protein in transport of folate to CSF and CNS (Chen and Wagner 1975; Suleiman et al. 1981). Dietary folate is taken up in the gut, metabolized to 5-methyltetrahydrofolate, and then distributed by the bloodstream. Cellular uptake of 5-methyltetrahydrofolate is mediated by the PCFT, the reduced folate carrier (RFC), and by two GPI-anchored receptors, folate receptor alpha (FRα) and beta (Frβ) (Matherly and Goldman 2003). Unlike the reduced folate carrier, PCFT has a similar affinity for reduced folate and folic acid, at pH 5.5, ambient in the upper small intestine. A loss-of-function mutation affecting the PCFT gene coding for this transmembrane protein was identified as the cause of hereditary folate malabsorption (Qiu et al. 2006; Zhao et al. 2007). However, PCFT is also expressed in many other tissues, including the brain, where it might export folate from acidified endosomes after FRα-mediated endocytosis (Zhao et al. 2009). After folate binds to the receptors, it is internalized by the epithelial cells through receptor-mediated endocytosis and, from there, passes into the brain interstitium and the cerebrospinal fluid (Henderson 1990; Holm et al. 1991; Wu and Pardridge 1999).

The PCFT plays a key role in intestinal folate absorption and folate transport into the central nervous system (Blount et al. 1997). Loss-of-function mutations in the PCFT gene lead to the rare autosomal recessive disorder, hereditary folate malabsorption, characterized by markedly reduced folate levels in blood and CSF (Blount et al. 1997; Diop-Bove et al. 1993–2014; Geller et al. 2002; Green and Miller 1999; Mahadeo et al. 2010; Qiu et al. 2006; Whitehead 2006; Zhao et al. 2007). Folic acid transport deficiency, another rare congenital metabolic defect, is presumably a recessive disorder, given that it is more prevalent in children of consanguineous matings and may simply be hereditary folate malabsorption (Lanzkowsky et al. 1969).

The initial manifestations of the condition may be agitation and insomnia, followed by deceleration of head growth, psychomotor retardation, hypotonia, and later spasticity, ataxia, dyskinesia, gait disturbances, speech, and epilepsy (Hansen and Blau 2005). The clinical manifestations are multisystemic, stressing the central role of folate in many organ systems. Manifestations in the CNS include microcephaly, seizures, and progressive neurological deterioration along with ataxia and autism. Cranial computed tomography may show calcifications (Geller et al. 2002). Manifestations in the central nervous system are explained by the involvement of folate in the synthesis of methionine and *S*-adenosylmethionine, which are essential for normal development of the central nervous system (Surtees et al. 1993). During early stages of the disease, when folate body stores are depleted but not yet exhausted, the signs are often minimal, and the only abnormality may be neutrophil hypersegmentation (Nath and Lindebaum 1979; Zittoun and Zittoun 1999). Megaloblastic anemia, and both reduced red blood cell count and cerebrospinal fluid folate, and hyperhomocysteinemia are the hallmarks of severe folate depletion. In hereditary folate malabsorption, CSF 5-methyltetrahydrofolate is very low or not detectable. Even when blood 5-methyltetrahydrofolate levels in patients with hereditary folate malabsorption are restored to, or above, the normal levels by folate supplementation, the CSF/blood 5-methyltetrahydrofolate ratio remains low (0.07–0.14) (Geller et al. 2002). Min et al has suggested CSF levels might not represent intraneural concentrations (Min et al. 2008). The variation might represent different times since last administration. The absence of control studies because of the rarity of the disease precludes definition of optimal therapy (Min et al. 2008).

Treatment with pharmacologic doses of folinic acid, most of which is enzymatically converted in vivo to the physiologically active 5-methyltetrahydrofolate (Levitt et al. 1971; Wright et al. 2003), enters the CSF by way of the reduced folate carrier on the choroid epithelial cells. Treatment of this condition with folinic acid, with a dose of 0.5–1.0 mg/kg body weight/day of a racemic mixture of the DL-form or half of this dose for the levo-form of folinic acid, has resulted in significant improvement of clinical symptoms and increased concentrations of 5-methyltetrahydrofolate in the CSF. Folinic acid is a more stable form of a metabolically active reduced folate compound, in contrast to folic acid which is an oxidized and metabolically inactive folate form. Also, the latter substance is more likely to have adverse effects such as inducing epileptic seizures (Ramaekers and Blau 2004). The starting dose ranges from 0.5 to 1.0 mg/kg/day and can be followed by monthly increments of 0.5 mg/kg/day according to the recommendations by the International Cerebral Deficiency Group (Ramaekers and Blau 2004). We have used doses up to 3 mg/kg/day and prefer to give every 12 h. An interval of 8 h would be more technically correct but is not practical with children. An alternative explanation for our patient excellent outcome might be that the half-life of the folinic acid in the brain or CSF is longer than in the blood. Because the majority of patients respond to treatment with folinic acid, physicians should remain vigilant to the possibility of deficiencies of folate and consider it before drawing any conclusions about the cryptogenic etiologies of

unexplained cases. The deleterious outcomes of untreated patients underscore the importance of making an early diagnosis (Green and Miller 1999).

Conclusion

Folinic acid supplementation is effective and should be initiated as early as possible. It may offer a life-changing therapy in patients with confirmed congenital hereditary folate deficiency. Folinic acid is therapeutic for the hematological and immunological complications, and CSF 5-methyltetrahydrofolate levels between 18 and 46 nmol/L (mean of 35 nmol/L) might be sufficient to prevent the neurological complications that, if untreated, are irreversible. Folinic acid was well tolerated in our patient without side effects. However, treatment of this condition in patients without CSF investigations is not recommended. The remaining questions about how often a lumbar puncture should be performed and what is the appropriate intramuscular dose of folinic acid necessary to prevent an irreversible neurological disorder remains to be determined.

Compliance with Ethics Guidelines

Conflict of Interest:

Alcy Torres, Stephanie A. Newton, Brian Crompton, Arturo Borzutzky, Ellis J. Neufeld, Luigi Notarangelo, and Gerard T. Berry declare that they have no conflict of interest.

Informed Consent

Informed consent was not obtained from the family as lumbar punctures for CSF testing were considered to be a part of routine care for patients with this potentially very serious encephalopathic illness.

References

Atabay B, Turker M, Ozer EA, Mahadeo K, Diop-Bove N, Goldman ID (2010) Mutation of the proton-coupled folate transporter gene (PCFT-SLC46A1) in Turkish siblings with hereditary folate malabsorption. Pediatr Hematol Oncol 27(8):614–619

Blount BC, Mack MM, Wehr CM, MacGregor JT, Hiatt RA, Wang G, Wickramasinghe SN, Everson RB, Ames BN (1997) Folate deficiency causes uracil misincorporation into human DNA and chromosome breakage: implications for cancer and neuronal damage. Proc Natl Acad Sci U S A 94:3290–3295

Borzutzky A, Crompton B, Bergamm AK, Giliani S, Baxi S, Martin M, Neufeld EJ, Notarangelo LD (2009) Reversible severe combined immunodeficiency phenotype secondary to a mutation of the proton-coupled folate transporter. Clin Immunol 133(3):287–294

Cains S, Shepherd A, Nabiuni M, Owen-Lynch PJ, Miyan J (2009) Addressing a folate imbalance in fetal cerebrospinal fluid can decrease the incidence of congenital hydrocephalus. J Neuropathol Exp Neurol 68:404–416

Chen C, Wagner C (1975) Folate transport in the choroid plexus. Life Sci 2049–2064

Corbeel L, Van den Berghe G, Jaeken J, Van Tornout J, Eeckels R (1985) Congenital folate malabsorption. Eur J Pedoatr 143(4): 284–290

Diop-Bove N, Kronn D, Goldman D (1993–2014) Gene reviews® [Internet]. University of Washington, Seattle,WA

Diop-Bove N, Jain M, Scaglia F, Goldman ID (2013) A novel deletion mutation in the proton-coupled folate transporter (PCFT; SLCA6A1) in a Nicaraguan child with hereditary folate malabsorption. Gene 527(2):673–674

Djukic A (2007) Folate-responsive neurological diseases. Pediatr Neurol 37:387–397

Fernandes J, Saudubary JM, Den Berghe V (2012) Inborn metabolic diseases. Springer, Heidelberg

Fournier I, Ploye F, Cottet-Emard JM, Brun J, Claustrat B (2002) Folate deficiency alters melatonin secretion in rats. J Nutr 132:2781–2784

Geller J, Kronn D, Jayabose S, Sandoval C (2002) Hereditary folate malabsorption: family report and review of the literature. Medicine (Baltimore) 81:51–68

Ghoshal K, Li X, Datta J, Bai S, Pogribny I, Pogribny M, Huang Y, Young D, Jacob ST (2006) A folate- and methyl-deficient diet alters the expression of DNA methyltransferases and methyl CpG binding proteins involved in epigenetic gene silencing in livers of F344 rats. J Nutr 136:1522–1527

Green R, Miller J (1999) Folate deficiency beyond megaloblastic anemia: hyperhomocysteinemia and other manifestations of dysfunctional folate status. Semin Hematol 36:47–64

Hansen FJ, Blau N (2005) Cerebral folate deficiency: life-changing supplementation with folinic acid. Mol Genet Metab 84:371–373

Henderson GB (1990) Folate-binding proteins. Annu Rev Nutr 10: 319–335

Holm J, Hansen SI, Hoier-Madsen M, Bostad L (1991) High-affinity folate binding in human choroid plexus: characterization of radioligand binding, immunoreactivity, molecular heterogeneity and hydrophobic domain of the binding protein. Biochem J 280: 267–271

Jebnoun S, Kacem S, Mokrani C, Chabchoub A, Khrouf N, Zittoun J (2001) A family study of congenital malabsorption of folate. J Inherit Metab Dis 24:749–750

Kishimoto K, Kobayashi R, Sano H, Suzuki D, Maruoka H, Yasuda K, Chida N, Yamada M, Kobayashi K (2014) Impact of folate therapy on combined immunodeficiency secondary to hereditary folate malabsorption. Clin Immunol 153(1):17–22. doi:10.1006/j.clim.2014.03.014

Kronenberg G, Harms C, Sobol RW, Cardozo-Pelaez F, Linhart H, Winter B, Balkaya M, Gertz K, Gay SB, Cox D (2008) Folate deficiency induces neurodegeneration and brain dysfunction in mice lacking uracil DNA glycosylase. J Neurosci 28:7219–7230

Lanzkowsky P, Erlandson ME, Bezan AI (1969) Isolated defect of folic acid absorption associated with mental retardation and cerebral calcification. Blood 34:452–465

Lasry I, Berman B, Straussberg R, Sofer Y, Bessler H, Sharkia M, Glaser F, Jansen F, Drori S, Assaraf YG (2008) A novel loss-of-function mutation in the proton-coupled folate transporter from a patient with hereditary folate malabsorption reveals that Arg 113 is crucial for function. Blood 112:2055–2061

Levitt M, Nixon PF, Pincus JH, Bertino JR (1971) Transport characteristics of folates in cerebrospinal fluid; a study utilizing

doubly labeled 5-methyltetrahydrofolate and 5-formyltetrahydrofolate. J Clin Invest 50:1301–1308

Linhart HG, Troen A, Bell GW, Cantu E, Chao WH, Moran E, Steine E, He T, Jaenisch R (2008) Folate deficiency induces genomic uracil misincorporation and hypomethylation but does not increase DNA point mutations. Gastroenterology 136:227–235

Lubhy AL, Eagle FJ, Roth E, Cooperman JM (1961) Relapsing megaloblastic anemia in an infant due to a specific defect in gastrointestinal absorption of folic acid. Am J Dis Child 102: 482–483

Mahadeo K, Min SH, Diop-Bove NK, Kronn D, Goldman ID (2010) Gene reviews [Internet], updated 2010 May 06. University of Washington, Seattle, WA

Malatack JJ, Moran MM, Moughan B (1999) Isolated congenital malabsorption of folic acid in a male infant: insights into treatment and mechanism of defect. Pediatrics 104(5 Pt 1):1133–1137

Matherly LH, Goldman DI (2003) Membrane transport of folates. Vitam Horm 66:403–456

Min SH, Oh SY, Karp GI, Poncz M, Zhao R, Goldman ID (2008) The clinical course and genetic defect in the PCFT gene in a 27-year-old woman with hereditary folate malabsorption. J Pediatr 153(3):435–437. doi:10.1016/j.jpeds.2008

Nath BJ, Lindebaum J (1979) Persistence of neutrophil hypersegmentation during recovery from megaloblastic granulopoiesis. Ann Intern Med 90:757–760

Pogribny IP, Karpf AR, James SR, Melnyk S, Han T, Tryndyak VP (2008) Epigenetic alterations in the brains of Fisher 344 rats induced by long-term administration of folate/methyl-deficient diet. Brain Res 1237:25–34

Ponz M, Colman L, Herbert V, Schwartz E, Cohen AR (1898) Therapy of congenital folate malabsorption. J Pediatr 98(1):76–79

Qiu A, Jansen M, Sakaris A, Min SH, Chattopadhyay S, Tsai E, Sandoval C (2006) Identification of an intestinal folate transporter and the molecular basis for hereditary folate malabsorption. Cell 127(5):917–928

Ramaekers VT, Blau N (2004) Cerebral folate deficiency. Dev Med Child Neurol 46:843–851

Rosenblatt DS, Fenton WA (2001) Inherited disorders of folate and cobalamin transport and metabolism. In: Scriver CR, Beaudet AL, Sly WS, Valle D, Childs B, Vogelstein B (eds) The metabolic and molecular bases of inherited disease. McGraw-Hill, New York, pp 3897–3933

Santiago-Borrero PJ, Santini R Jr, Perez-Santiago E, Maldonado NI (1973) Congenital isolated defect of folic acid absorption. J Pediatr 82:450–455

Scriver AL, Beaudet WS, Sly D, Valle CR (1995) The metabolic and molecular bases of inherited disease, vol 3, 7th edn. McGraw Hill, New York

Shin DS, Mahadeo K, Min SH, Diop-Bove N, Clayton P, Zhao R, Goldman ID (2011) Identification of novel mutations in the proton-coupled folate transporter (PCFT-SLC46A1) associated with hereditary folate malabsorption. Mol Genet Metab 103:33–37

Shinohara Y, Hasegawa H, Ogawa K, Tagoku K, Hashimoto T (2006) Distinct effects of folate and choline deficiency on plasma kinetics of methionine and homocysteine in rats. Metabolism 55:899–906

Sofer Y, Harel L, Sharkia M, Amir J, Schoenfeld T, Straussberg R (2007) Neurological manifestations of folate transport defect: case report and review of the literature. J Child Neurol 22: 783–786

Steinschneider M, Sherbany A, Pavlakis S, Emerson R, Lovelace R, De Vivo DC (1990) Congenital folate malabsorption: reversible clinical and neurophysiologic abnormalities. Neurology 40: 1315

Su PC (1976) Congenital folate deficiency. New Engl J Med 294:1128

Suleiman SA, Spector R, Cancilla P (1981) Partial purification and characterization of a folate binding protein from human choroid plexus. Neurochem Res 6:331–341

Surtees R (2001) Cobalamin and folate responsive disorders. In: Baxter P (ed) Vitamin responsive conditions in pediatric neurology, International review of child neurology series. Mac Keith, London, pp 96–108

Surtees R, Heales S, Bowron A (1993) Biochemical pathogenesis of subacute combined degeneration of the spinal cord and brain. J Inherit Metab Dis 16:762–770

Urbach J, Abrahamov A, Grossowicz N (1987) Congenital isolated folic acid malabsorption. Arch Dis Child 62:78–80

Wang Q, Li X, Ding Y, Liu Y, Qin Y, Yang Y (2014) The first Chinese case report of hereditary folate malabsorption with a novel mutation on SLC46A1. Brain Dev. doi:10.1016/j.braindev.2014.01.010

Whitehead VM (2006) Acquired and inherited disorders of cobalamin and folate in children. Br J Haematol 134(2):125–136

Wright AJ, Finglas PM, Dainty JR et al (2003) Single oral doses of 13C forms of pteroylmonoglutamic acid and 5-formyltetrahydrofolic acid elicit differences in short-term kinetics of labelled and unlabelled folates in plasma: potential problems in interpretation of bioavailability studies. Br J Nutr 90:363–371

Wu D, Pardridge WM (1999) Blood–brain barrier transport of reduced folic acid. Pharm Res 16:415–419

Zhao R, Min SH, Qiu A, Sakaris A, Goldberg GL, Sandoval C, Malatack JJ, Rosenblatt DS, Goldman ID (2007) The spectrum of mutations in the PCFT gene, coding for an intestinal folate transporter, that are the basis for hereditary folate malabsorption. Blood 110:1147–1152

Zhao R, Min SH, Wang Y, Campanella E, Low PS, Goldman ID (2009) A role for the proton-coupled folate transporter (PCFT-SLC46A1) in folate receptor-mediated endocytosis. J Biol Chem 284:4267–4274

Zhao R, Akabas MH, Goldman ID (2012) Identification of a functionally critical GXXG motif and its relationship to the folate binding site of the proto-coupled folate transporter (PCFT-SLC46A1). Am J Physiol Cell Physiol 303(6):C673–C681

Zittoun J, Zittoun R (1999) Modern clinical testing strategies in cobalamin and folate deficiency. Semin Hematol 36:35–46

JIMD Reports
DOI 10.1007/8904_2015_446

CASE REPORT

A Novel Catastrophic Presentation of X-Linked Adrenoleukodystrophy

M.M. Vawter-Lee · B.E. Hallinan · T.A. Burrow · C.G. Spaeth · T.M. Arthur

Received: 19 February 2015 / Revised: 06 April 2015 / Accepted: 21 April 2015 / Published online: 13 May 2015

Abstract *Objective*: We report a novel presentation of childhood cerebral X-linked adrenoleukodystrophy: status epilepticus followed by abrupt and catastrophic neurologic deterioration.

Methods: A description of the clinical presentation, laboratory evaluation, and imaging findings leading to a diagnosis of X-linked adrenoleukodystrophy.

Results: A 3-year-old male with prior history of autism presented with fever, diarrhea, and status epilepticus requiring a pentobarbital coma. Admission labs were notable only for a glucose level of 22 mg/dL, which stabilized after correction. The child never returned to his prior neurologic baseline, with complete loss of gross motor, fine motor, and speech skills. Serial brain magnetic resonance imaging (MRI)/magnetic resonance spectroscopy (MRS) was notable for progressive diffuse cortical signal changes with swelling, diffusion restriction, and ultimately laminar necrosis. Nine months after presentation, CSF (cerebrospinal fluid) protein and MRS lactate were persistently elevated, concerning for a neurodegenerative disorder. This led to testing for mitochondrial disease, followed by lysosomal and peroxisomal disorders. Very long-chain fatty acids were elevated. Identification of a pathogenic ABCD1 mutation confirmed the diagnosis of X-linked adrenoleukodystrophy.

Conclusions: Boys with childhood cerebral X-linked adrenoleukodystrophy typically present with gradual behavioral changes. Rare reports of boys presenting with transient altered mental status or status epilepticus describe a recovery to their pre-presentation baseline. To our knowledge this is the first X-ALD patient to present with status epilepticus with abrupt and catastrophic loss of neurologic function. X-linked adrenoleukodystrophy should be suspected in young males presenting with seizures, acute decline in neurologic function, with persistently elevated CSF protein and MRS lactate.

Introduction

X-linked adrenoleukodystrophy (X-ALD, OMIM 300100) is a disorder of impaired transmembrane transport of very long-chain fatty acids (VLCFA) into the peroxisome. As a result, VLCFAs accumulate in tissues of the body. ALD presents as childhood cerebral ALD, adrenomyeloneuropathy, or Addison's disease. In ALD, patients usually present with several years of progressive cognitive decline and behavioral problems. Findings on neuroimaging usually include MRI FLAIR hyperintensities in the parietal-occipital regions (Engelen et al. 2012). Approximately 9% of patients with childhood cerebral ALD present acutely, usually at a younger age than ALD typically presents (around 5.5 versus 7.2 years old) (Stephenson et al. 2000). We report the case of a 3-year-old male, with a past medical history of autism, who presented with fever, vomiting, diarrhea, and status epilepticus. He had catastrophic loss of developmental milestones post-pentobarbital coma. After extensive testing and imaging, he was found to have

Communicated by: Jutta Gaertner

Competing interests: None declared

M.M. Vawter-Lee (✉) · B.E. Hallinan · T.M. Arthur
Division of Neurology, Cincinnati Children's Hospital Medical Center, 3333 Burnet Avenue, MLC 2015, 45229, Cincinnati, OH, USA
e-mail: Marissa.Vawter@cchmc.org

T.A. Burrow · C.G. Spaeth
Division of Human Genetics, Cincinnati Children's Hospital Medical Center, Cincinnati, OH, USA

X-ALD. This is the first report of a patient with childhood cerebral ALD presenting acutely with status epilepticus and no recovery of prior function.

Case Presentation

A 3-year-old Caucasian male presented to the emergency room with a first-time seizure. The child had been ill with fever, vomiting, and diarrhea for the preceding 12 h. His mother witnessed the onset of a generalized tonic-clonic seizure, which lasted 10 min. In the emergency room he had a seizure of bilateral extremity jerking with eye deviation to the left, which resolved with 0.1 mg/kg lorazepam intravenous. Labs at this time were notable for a glucose of 22 mg/dL, which was corrected with an intravenous dextrose bolus. A head CT was normal. Given the hypoglycemia, fever, and back-to-back seizures, the patient was admitted to the critical care unit for medical management. After admission he had a reassuring lumbar puncture (WBC 0 mm^3, RBC 0 mm^3, glucose 74 mg/dL, protein 21 mg/dL). Serum lactate and pyruvate were 2.3 mmol/L (normal range 1.00–2.40 mmol/L) and 0.11 mmol/L (normal range 0.06–0.17 mmol/L), respectively. His electrolytes, including sodium, and renal function were within normal limits after the initial correction of glucose.

His past medical history was notable for receptive and expressive speech delay. He was in speech therapy and had been diagnosed with autism. His speech had rapidly improved over the prior 6 months, and he was no longer displaying any repetitive behaviors. One week prior to this presentation, he had fallen on stairs and hit his head, with no loss of consciousness.

He was watched overnight in the critical care unit with continuous video electroencephalography (EEG) monitoring. During this time he was lethargic, but no seizures were observed. On the second hospital day, he had a generalized tonic-clonic seizure, after which his EEG showed the development of subclinical status epilepticus. His seizures stopped with initiation of a pentobarbital drip. He remained in burst suppression for 72 h, and then a pentobarbital infusion wean was attempted. He again had clinical and subclinical seizures, and pentobarbital was titrated to a burst suppression pattern for an additional 72 h. On hospital day 8 he was weaned off of pentobarbital and was seizure-free. At that time the patient was minimally responsive: his eyes would spontaneously open and rove, but he had no purposeful movements or speech.

A brain MRI/MRS with and without contrast obtained on hospital day 5 (FLAIR imaging shown in Fig. 1) was strikingly abnormal, with bilateral diffuse cortical swelling, hyperintensities, diffusion restriction, and subtle leptomeningeal enhancement. The MRS of the left frontal white

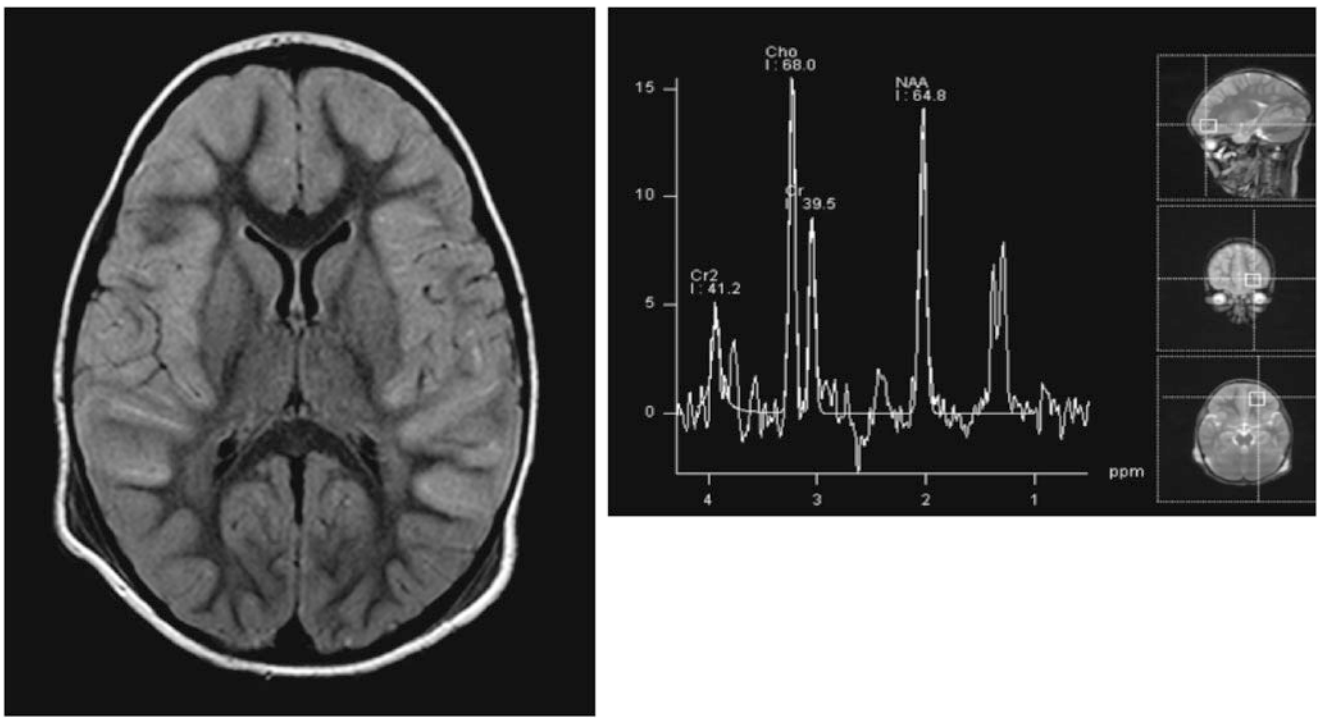

Fig. 1 Brain MRI and MRS 5 days after initial presentation, showing diffuse cortical signal changes, edema, and a lactate peak

matter showed a lactate peak. Though several of these findings can be seen as sequela of status epilepticus (Milligan et al. 2009), the overall MRI pattern was concerning for an underlying metabolic etiology. Extensive testing was performed with normal or nondiagnostic results: initial total and free carnitine were low (repeat testing after carnitine supplementation was normal); urine organic acids; repeat lumbar puncture on hospital day 8 (WBC 4 mm^3, RBC 0 mm^3, glucose 65 mg/dL, protein 46 mg/dL, lactate and pyruvate); neurotransmitter metabolites (pyridoxal 5-phosphate, 5-methyltetrahydrofolate, neopterin, tetrahydrobiopterin, 5-hydroxyindoleacetic acid, homovanillic acid, and 3-0-methyldopa); repeat serum lactate and pyruvate; viral polymerase chain reaction (PCR) testing (CSF, serum, and stool) including HSV, HIV, enterovirus, EBV, CMV, mycoplasma, human metapneumovirus, influenza, parainfluenza, RSV, rhinovirus, West Nile, California encephalitis, St. Louis encephalitis, Eastern equine encephalitis, Western equine encephalitis, JC virus, and rotavirus; serum and CSF paraneoplastic and anti-NMDA receptor antibody panels; serum and CSF amino acids; a third lumbar puncture on hospital day 12 which was notable for high protein (WBC 2 mm^3, RBC 5,550 mm^3, glucose 58 mg/dL, protein 96 mg/dL); inflammatory markers (C-reactive protein and sedimentation rate); and thyroid studies (thyroid-stimulating hormone, free thyroxine, and antithyroid autoantibodies). To evaluate his initial hypoglycemia, he was also evaluated by endocrinology with a reassuring insulin level of 0.8 mcIU/mL (normal fasting level is $<$ 13 mcIU/mL) and reassuring morning cortisol level of 10.9 mcg/dL (normal for his age is 3–21 mcg/dL).

Repeat brain MRI with and without contrast 1 month later (flair imaging shown in Fig. 2) showed progressive and diffuse white matter changes, along with laminar necrosis. Findings were also notable for significant atrophy and contrast enhancement throughout the frontal, parietal, temporal, and left occipital regions. There was a persistent lactate peak on MRS of the frontal white matter in the absence of diffusion restriction.

The following genetic testing was performed and normal: microarray; fragile X; whole mtDNA sequencing, duplication, and deletion; sequencing of POLG1, TYMP, SCN1A, SCN1B, and GABARG2; and TPP1 and PPT1 enzyme activity. Genetic testing for a primary carnitine deficiency syndrome as well as multiple fatty acid oxidation defects revealed a single variant of unknown significance in acyl-CoA dehydrogenase, C-4 to C-12 straight chain (ACADM), felt to be noncontributory. A third brain MRI/MRS with and without contrast was performed on hospital day 60 and was similar to the prior studies, demonstrating laminar necrosis, extensive T2 signal abnormality of white matter diffusely including corticospinal tracts, contrast enhancement, and a lactate peak. Throughout

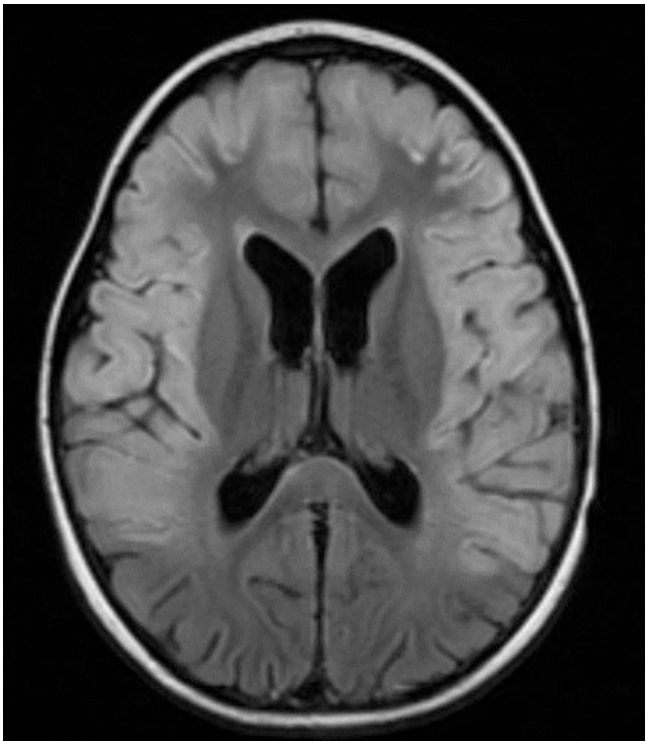

Fig. 2 Brain MRI 30 days after onset showing progression of cortical changes with laminar necrosis

the hospital stay, the patient was seizure-free on a regimen of phenobarbital and lacosamide, but unfortunately his development and level of consciousness did not improve. The patient was discharged home with extensive support.

At 4 years of age, 9 months after presentation, the patient had a repeat lumbar puncture and brain MRI/MRS with and without contrast (flair imaging shown in Fig. 3). The CSF was notable for continued elevation of the protein (WBC 2 mm^3, RBC 1 mm^3, glucose 69 mg/dL, protein 70 mg/dL). The brain MRI/MRS showed progression of cerebral volume loss, signal abnormalities of both white matter and gray matter with extension of abnormalities into the bilateral cerebellar hemispheres, and the development of bilateral subdural fluid collections. Based on the MRI findings of a progressive chronic neurodegenerative disorder and continued protein elevation in the CSF, which though nonspecific is an indicator of a potential neurodegenerative disorder (commonly seen in Krabbe and metachromatic leukodystrophy), the patient had further testing including copper and ceruloplasmin levels (normal), leukocyte lysosomal enzyme-screening assay (normal), and VLCFAs to rule out peroxisomal disorders.

VLCFA profile was notable for elevation of C26:0 at 1.17 ug/mL (normal 0.23 $\pm$ 0.09), elevation of C26:1 at 0.900 ug/mL (normal 0.18 $\pm$ 0.09), elevation of C24/C22 at 1.793 ug/mL (normal 0.84 $\pm$ 0.10), and elevation of

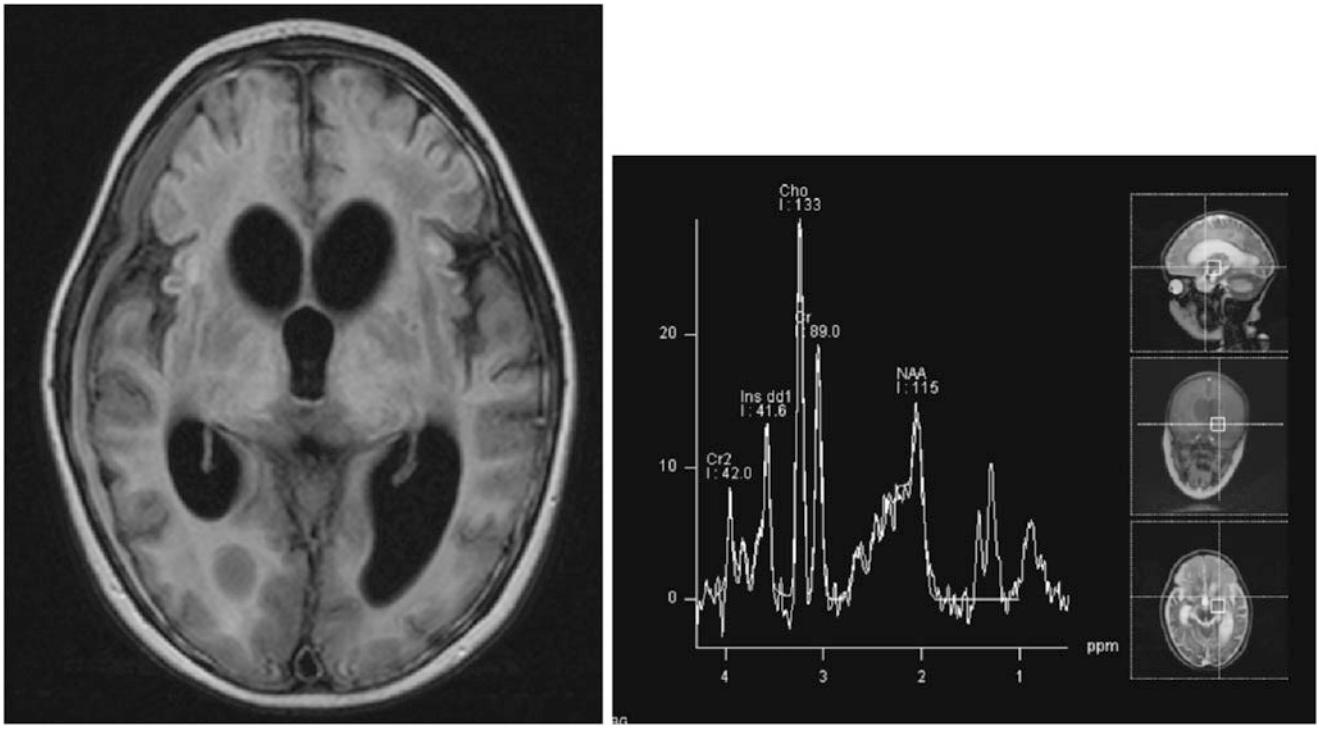

Fig. 3 Brain MRI and MRS 9 months after onset showing extensive cortical signal changes, atrophy, and laminar necrosis, along with a persistent lactate peak on MRS

C26/C22 at 0.109 ug/mL (normal 0.01 ± 0.004). Analysis of the ABCD1 (ATP-binding cassette, subfamily D) gene revealed a novel deletion (c.136*>-AGCGAGCGCA-CAGA; p.X46X.), consistent with a diagnosis of X-linked adrenoleukodystrophy. This frameshift deletion resulted in a premature stop codon. Further testing of the patient with an adrenocorticotropin (ACTH) stimulation test showed that he had adrenal insufficiency (baseline cortisol level was 9.3 mcg/dL, 30 min after stimulation cortisol level was 8.6 mcg/dL, and 60 min after stimulation cortisol level was 9.7 mcg/dL; both renin and aldosterone levels were normal). Given the advanced stage of the patient's disease, he was not a candidate for bone marrow or stem cell transplant, and management transitioned to palliative care. The patient's mother was found to be a carrier of the same deletion. Due to insurance concerns the patient's maternal grandmother was not tested for the mutation, but there were three maternal uncles who were potentially at risk for X-ALD, each of whom had a normal VLCFA profile, ruling out the diagnosis.

Discussion

Childhood cerebral adrenoleukodystrophy classically presents with neuropsychiatric symptoms, including attention-deficit/hyperactivity disorder, followed by slow behavioral decline and developmental regression. Seizures are known to affect patients with X-ALD, typically occurring 2–4 years after onset of other neurological symptoms (Wang et al. 2001). In a retrospective chart review of 485 boys, Stephenson et al. (2000) noted that 9% ($n = 45$) had an acute presentation of adrenal crisis, seizures, or encephalopathy.

Seizures occurred in approximately 44% ($n = 20$) of the children who presented acutely (Stephenson et al. 2000). Of the patients presenting with seizures, four presented in status epilepticus, six presented with focal seizures, and ten presented with generalized tonic-clonic seizures (Stephenson et al. 2000). In Stephenson's study three of the patients had seizures within hours of sustaining a head injury, while our patient had a head injury 1 week prior to presentation. Many of the patients who presented with seizures did not have neuroimaging initially, and the diagnosis of X-ALD was not suspected. All of the patients who presented with seizures, including status epilepticus, had full recovery to prior baseline (Stephenson et al. 2000).

Adrenal crisis occurred in around 44% ($n = 20$) of the children with an acute presentation (Stephenson et al. 2000). Signs and symptoms included vomiting, lethargy, hyponatremia, hypoglycemia, and dehydration. Additionally, half of these patients had fever on presentation, and many were diagnosed with encephalopathy. Several of these boys had been hospitalized multiple times for

dehydration prior to the diagnosis of X-ALD. Ravid et al. (2000) describe one child who presented with fever, vomiting, and subsequent coma found to have adrenal insufficiency (low baseline cortisol level, confirmed with inadequate response of cortisol levels to ACTH stimulation). This patient had minimal improvement in mental status after diagnosis and treatment with steroids (Ravid et al. 2000). Zammarchi et al. (1994) describe another child who presented with symptoms initially thought to be consistent with acute encephalitis (fever, vomiting, and altered mental status), but found on laboratory evaluation to have hyponatremia and adrenal insufficiency (inadequate response to ACTH stimulation). This child's mental status rapidly returned to baseline after steroids were started (Zammarchi et al. 1994). Our patient's initial lack of hyponatremia and normal cortisol level argued against adrenal insufficiency.

A minority of patients ($n = 5$ or 11%) in Stephenson's review had an acute presentation of encephalopathy or coma with no seizures or adrenal dysfunction (Stephenson et al. 2000). Follow-up of these patients was limited. At least one child gradually returned to his neurologic baseline before decline and diagnosis of X-ALD.

Stephenson et al. (2000) provide a cohesive review of the common acute presentations of X-ALD. Of the 20 patients who presented with seizures including status epilepticus, all recovered to their prior level of function (Stephenson et al. 2000). Though there are many reports of children presenting with adrenal insufficiency and full recovery, there is one case report of a child presenting with adrenal insufficiency and no return to prior baseline (Zammarchi et al. 1994; Ravid et al. 2000; Stephenson et al. 2000). Several of the patients with acute presentations had the pathognomonic posterior white matter changes on neuroimaging. However, other patients had head CTs that were interpreted as normal at initial presentation. This highlights the difficulty of making an early diagnosis of ALD.

Our patient's initial imaging findings were not pathognomonic for X-ALD. Status epilepticus can lead to MRI changes such as diffusion restriction in the hippocampus, gyri, and splenium (Milligan et al. 2009). This diffusion restriction may be secondary to hypoxemia or vasogenic and cytotoxic edema. These findings would be expected to improve on repeat imaging after the seizures are controlled (Milligan et al. 2009). Laminar necrosis has been reported in pediatric patients in the setting of status epilepticus with persistent hypoglycemia (Christiaens et al. 2003; Huang et al. 2009). Although our patient was initially hypoglycemic, subsequent serum and CSF glucoses were normal. The progressive nature of our patient's imaging findings, along with the persistence of a lactate peak on MRS, was more consistent with a neurodegenerative disease than with the sequela of status epilepticus.

X-ALD rarely presents acutely. To our knowledge, our patient is the first with an acute status epilepticus presentation and no recovery to prior baseline. The previously reported patients with acute presentations of seizures and coma all returned, some gradually and others quickly, to their baseline level of function. Our patient, on the other hand, did not. He remained neurologically devastated, which correlated with the diffuse and extensive brain injury seen on serial MRIs. X-ALD is a devastating disorder and can be difficult to diagnose. Early diagnosis is vital for both the patient and family members who may be affected yet still asymptomatic.

Conclusion

Boys with childhood cerebral adrenoleukodystrophy typically present with gradual onset of learning and behavioral changes; however, 9% of boys with X-ALD have an acute presentation of altered mental status, adrenal insufficiency, or seizures (Stephenson et al. 2000). With the exception of one boy with adrenal insufficiency, prior reports describe a full recovery to the prior level of function (Ravid et al. 2000). To our knowledge this is the first patient to present with status epilepticus followed by an abrupt, catastrophic, and irreversible loss of neurologic function. X-linked adrenoleukodystrophy should be considered in young males presenting with seizures and acute neurologic deterioration, especially if there is supporting data, such as persistently elevated CSF protein or lactate peaks on serial MRS.

Synopsis

Practitioners should consider the diagnosis of X-linked adrenoleukodystrophy in males presenting with status epilepticus followed by neurologic deterioration, especially if the patient has elevated CSF protein, MRI white matter changes, or a lactate peak on MRS.

Compliance with Ethics Guidelines

Conflict of Interest

Marissa Vawter-Lee, Barbara Hallinan, T. Andrew Burrow, Christine Spaeth, and Todd Arthur declare that they have no conflict of interest.

Informed Consent

All procedures followed were in accordance with the ethical standards of the responsible committee on human experi-

mentation (institutional and national) and with the Helsinki Declaration of 1975, as revised in 2000. Informed consent was obtained from the guardian of the patient included in this study. Proof that informed consent has been obtained is available upon request.

Author Contributorship Statement

Marissa M Vawter-Lee: conception and design, data acquisition, analysis, interpretation of data, writing of the manuscript, final approval of article

Barbara E Hallinan: conception and design, interpretation of data, writing of the manuscript, final approval of article

T. Andrew Burrows: interpretation of data and writing of the manuscript

Christine G Spaeth: interpretation of data and writing of the manuscript

Todd M Arthur: conception and design, interpretation of data, writing of the manuscript, final approval of article

References

Christiaens FJ, Mewasingh LD, Christophe C, Goldman S, Dan B (2003) Unilateral cortical necrosis following status epilepticus with hypoglycemia. Brain Dev 25:107–112

Engelen M, Kemp S, de Visser M et al (2012) X-linked adrenoleukodystrophy (X-ALD): clinical presentation and guidelines for diagnosis, follow-up and management. Orphanet J Rare Dis 7:51

Huang YC, Weng HH, Tsai YT et al (2009) Periictal magnetic resonance imaging in status epilepticus. Epilepsy Res 86:72–81

Milligan TA, Zamani A, Bromfield E (2009) Frequency and patterns of MRI abnormalities due to status epilepticus. Seizure 18:104–108

Ravid S, Diamond AS, Eviatar L (2000) Coma as an acute presentation of adrenoleukodystrophy. Pediatr Neurol 22:237–239

Stephenson DJ, Bezman L, Raymond GV (2000) Acute presentation of childhood adrenoleukodystrophy. Neuropediatrics 31:293–297

Wang PJ, Hwu WL, Shen YZ (2001) Epileptic seizures and electroencephalographic evolution in genetic leukodystrophies. J Clin Neurophysiol 18:25–32

Zammarchi E, Donati MA, Tucci F, Fonda C, Fanelli F, Pazzaglia R (1994) Acute onset of X-linked adrenoleukodystrophy mimicking encephalitis. Brain Dev 16:238–240

JIMD Reports
DOI 10.1007/8904_2015_447

RESEARCH REPORT

High Incidence of Biotinidase Deficiency from a Pilot Newborn Screening Study in Minas Gerais, Brazil

Marilis T. Lara • Juliana Gurgel-Giannetti • Marcos J.B. Aguiar • Roberto V.P. Ladeira • Nara O. Carvalho • Dora M. del Castillo • Marcos B. Viana • José N. Januario

Received: 06 March 2015 / Revised: 12 April 2015 / Accepted: 20 April 2015 / Published online: 13 May 2015

Abstract *Objective*: To assess the incidence of biotinidase deficiency among newborns and their clinical outcome up to one year of age in a large pilot screening study in Minas Gerais, Brazil.

Methods: A prospective cohort study was conducted from September 2007 to June 2008 with heel-prick blood samples collected on filter paper for the purpose of newborn screening. A qualitative colorimetric test was used as the primary screening method. Colorimetric-positive cases were further tested with a serum confirmatory assay. Gene sequencing was performed for eight children suspected with biotinidase deficiency and for some of their parents. Positive cases were daily supplemented with oral biotin and were followed up for approximately six years.

Results: Out of 182,891 newborns screened, 129 were suspected of having biotinidase deficiency. Partial deficiency was confirmed in seven children (one was homozygous for p.D543E) and profound deficiency in one child (homozygous p.H485Q). Thus the incidence was one in 22,861 live births (95% confidence interval 1:13,503 to 1:74,454) for profound and partial biotinidase deficiency combined. Two novel mutations were detected: p.A281V and p.E177K. In silico analysis and estimation of the enzyme activity in the children and their parents showed that p.A281V is pathogenic and p.E177K behaves like p.D444H.

Conclusion: The incidence of biotinidase deficiency in newborn screening in Minas Gerais was higher than several international studies. The sample size should be larger for final conclusions. Oral daily biotin apparently precluded clinical symptoms, but it may have been unnecessary in some newborns.

Communicated by: Georg Hoffmann

Competing interests: None declared

M.T. Lara
UFMG University Hospital, NUPAD – Center for Newborn Screening and Genetic Diagnostics, UFMG Federal University of Minas Gerais, Belo Horizonte, Brazil

J. Gurgel-Giannetti · M.J.B. Aguiar · M.B. Viana
Department of Pediatrics, NUPAD – Center for Newborn Screening and Genetic Diagnostics, UFMG Federal University of Minas Gerais, Belo Horizonte, Brazil

R.V.P. Ladeira · N.O. Carvalho · D.M. del Castillo
NUPAD – Center for Newborn Screening and Genetic Diagnostics, UFMG Federal University of Minas Gerais, Belo Horizonte, Brazil

J.N. Januario (✉)
Department of Medicine, NUPAD – Center for Newborn Screening and Genetic Diagnostics, UFMG Federal University of Minas Gerais, Av. Alfredo Balena 189, sala 1004, 30130-100, Belo Horizonte, Brazil
e-mail: nelio@nupad.medicina.ufmg.br; josenelio@gmail.com

Introduction

Biotinidase (E.C. 3.5.1.12) is the enzyme that recycles biotin. Biotinidase deficiency (BD; OMIM #253260 and *609019) is an autosomal recessive and inherited metabolic disorder with a varied phenotypic expression. The disorder is classified into two types according to the serum enzyme activity relative to a reference value: profound deficiency (up to 10%) and partial deficiency (from 10% to 30%) (Mcvoy et al. 1990; Wolf 2001). The biotinidase gene (*BTD*) has been mapped to the chromosome 3p25. Approximately 200 variants have been recognized (UTAH BTD Database 2013). The most prevalent mutation in the

world (allele frequency around 0.039) is c.1330G>C (p.D444H) that results in half of the activity of the enzyme produced by the wild-type gene (Swango et al. 1998). Most individuals with partial BD are compound heterozygotes, having the c.1330G>C mutation in combination with another mutation that causes severe deficiency of the biotinidase activity (Swango et al. 1998).

Profound BD usually manifests as neurological and skin disorders after the age of seven weeks. Patients who are not treated early enough often have hearing and visual impairments as well as motor and language delays. Simple and low-cost supplementation with oral biotin (5–20 mg daily for life) prevents clinical manifestations if provided early in life (Wolf 2001).

The prevalence of BD in Minas Gerais, Brazil, is unknown. The state has approximately 20 million inhabitants, and 240,000 newborns are tested yearly. The state has been performing newborn screening tests since 1994 for phenylketonuria, congenital hypothyroidism, cystic fibrosis, and sickle cell disease. Only in 2014, BD was included in the mandatory panel of screened diseases.

This pilot study aimed to evaluate the incidence of BD in the Newborn Screening Program of Minas Gerais (NSP-MG). All of the suspected cases were supplemented with daily biotin and were referred for further laboratory and clinical follow-up evaluations.

Methods

A prospective cohort study was conducted on 182,942 newborns from September 2007 to June 2008. Possible partial or profound cases of BD were referred for biotin supplementation therapy (Wolf 2010) before the DNA analysis was available, and they have been maintained on biotin therapy to date. Mutation analyses were performed on DNA from the whole-blood samples of children suspected with BD and on DNA from the whole-blood samples of their parents in 2014–2015. The biochemical and molecular tests were performed at the laboratories of the Center for Newborn Screening and Genetic Diagnostics (Nupad-UFMG).

Dried blood samples (DBS) were collected on filter paper (Schleicher & Schuell 903) when the newborns were approximately five days old, which was in compliance with the NSP-MG protocol. Umtest Biotinidasa Test® (Tecnosuma) was used as the primary qualitative screening test (González et al. 2006). It was repeated on another DBS sample if positive. The quantitative serum test for the biochemical diagnosis was performed on the 120 newborns with positive results in screening tests, as described by Cowan et al. (2010). In 2014–2015, a second and third serum sample was drawn from five newborns and their parents (Table 1), and the biotinidase activity was determined again. The mean reference value at Nupad Laboratory is 7.2 nmol/min/mL. Accordingly, results below 0.8 nmol/min/mL (10% of the mean) were considered to be a profound deficiency; from 0.8 to 2.1 (10–30%), partial deficiency; from 2.2 to 5.1, suggestive of a heterozygous state; and results above 5.1 nmol/min/mL were considered "normal."

Mutation analyses were performed on the DNA of eight newborns with deficient biotinidase activity and on that of the parents of five newborns (see Table 1). Genomic DNA was extracted from peripheral blood lymphocytes with Chelex 100, Molecular Biology Grade Resin, Bio-Rad (Walsh et al. 1991).

DNA Sequencing

Exons 1–4 of the *BTD* gene as well as their flanking regions were amplified by polymerase chain reaction (PCR). Specific primers are available on request and were designed according to published papers (Pomponio et al. 1997; Thodi et al. 2011; Mühl et al. 2001).

Electrophoresis was performed on an ABI Prism 3130XL Genetic Analyzer (Applied Biosystems). Analysis was based on the NCBI Reference Sequence NG_008019.1.

This study was approved by the UFMG institutional review board and the Minas Gerais State Health Administration.

Results

Of the 182,891 newborns who had satisfactory DBS (51 were excluded because the samples were unsatisfactory and the patients could not be found for another blood collection), 129 were suspected of BD based on the qualitative tests. BD was confirmed in ten of them by a quantitative serum test. Two newborns were excluded from the study because their families declined to participate during its molecular phase. Out of these eight cases, seven had partial and one a profound BD. Table 1 shows the quantitative tests and respective mutations.

Thus, the combined incidence of partial and profound BD based on these eight cases was 1:22,861 live births (95% confidence interval 1:13,503 to 1:74,454). The NSP-MG population coverage during the study period was 94.8% of all live births in the state.

Considering the initial group of ten newborns with BD, detected in the first quantitative test, their mean age for the first clinical appointment was 71 days (range, 30–285 days),

Table 1 Biochemical and molecular features of patients detected with biotinidase deficiency

	Sex	BTD activity (nmol/min/ml)	Allele 1 (protein change)	Allele 2 (protein change)	Deficiency classification
Child 1	M	0.7, 0.7	c.1455C>G (p.H485Q)	c.1455C>G (p.H485Q)	Profound
Mother	F	3.6, 3.3	c.1455C>G (p.H485Q)	Wild type	
Child 2	F	1.4, 1.7	c.842 C>T (p.A281V)[a]	c.1330G>C (p.D444H)	Partial
Mother	F	3.4	c.842 C>T (p.A281V)	Wild type	
Father	M	4.8	c.1330G>C (p.D444H)	Wild type	
Child 3	F	1.5, 1.4	c.1330G>C (p.D444H)	Wild (?) type	Partial
Mother	F	5.4	c.1330G>C (p.D444H)	Wild type	
Father	M	4.9	Wild type	Wild (?) type	
Child 4	F	2.0	c.529 G>A (p.E177K)[b]	c.1595C>T (p.T532M)	Partial
Mother	F	3.9	c.1595C>T (p.T532M)	Wild type	
Father	M	5.1	c.529 G>A (p.E177K)	Wild type	
Child 5	M	1.0, 1.2	c.1629C>A (p.D543E)	c.1629C>A (p.D543E)	Partial
Mother	F	3.1	c.1629C>A (p.D543E)	Wild type	
Father	M	4.6	c.1629C>A (p.D543E)	Wild type	
Child 6	F	1.8	c.511G>A;1330G>C (p.A171T; p.D444H)	c.1330G>C (p.D444H)	Partial
Child 7	F	1.8	c.511G>A;1330G>C (p.A171T; p.D444H)	c.1330G>C (p.D444H)	Partial
Child 8	M	1.8, 1.8	c.1489C>T (p.P497S)[c]	c.1330G>C (p.D444H)	Partial

Wild (?) = coding and splicing regions of *BTD* gene corresponded to the wild sequence, but promoter and intronic regions were not completely sequenced

[a] Newly described mutation predicted to affect protein function (see text)

[b] Newly described mutation predicted *not* to affect protein function (see text)

[c] A silent variant [c.1284C>T (Y428Y)] was also detected together with the pathogenic variant p.P497S, as reported by Wolf et al. (2005)

the mean age for diagnosis confirmation was 103 days (range, 38–258 days), and the mean age for starting biotin supplementation was 135 days (range, 60–300 days).

The mutation analysis (Table 1) detected two homozygous newborns: p.D543E/p.D543E with consanguineous parents and p.H485Q/p.H485Q without consanguineous parents. The first child was classified as partially deficient. His enzyme activity corresponded to 17% of the mean reference value. The second child was classified as profoundly deficient (9.7% of the mean reference value). Five double heterozygotes were detected: two patients with p.A171T;D444H/p.D444H, one with p.281V/p.D444H, one with p.P497S/p.D444H, and one with p.E177K/p.T532M. Child #3 (Table 1) was classified as having partial BD on the basis of biotinidase activity of 1.5 and 1.4 nmol/min/mL in the first and second serum samples, respectively. Only p.D444H was detected in the child and her mother. Her father's biotinidase activity was within the heterozygous range of values, although apparently having two wild alleles. Promoter and intronic regions of the *BTD* gene were not completely sequenced, and thus it is possible that he has a "hidden" pathogenic mutation.

Two novel mutations were identified, i.e., p.281V and p.E177K. The first one (child # 2, Table 1) was predicted to be pathogenic by SIFT (http://sift.bii.a-star.edu.sg/) and by estimation of the enzyme activity in the heterozygous mother and in the double heterozygous child (with D444H). The predicted value was zero. The second mutation (p.E177K) was predicted NOT pathogenic by SIFT. The estimated enzyme activity was 42%.

Up to one year of age, all newborns underwent normal clinical and neurological evaluations prior to and after oral biotin supplementation (10 mg daily).

Discussion

The combined incidence of BD in newborns in this pilot study was 1:22,861 live births. The frequency rates of BD reported in the literature are variable. Based on 36 pilot newborn screening programs conducted from January 1984 to December 1990 (Wolf and Heard 1990; Wolf 1991) in a sample of 8,532,617 newborns, the following figures were reported: profound BD, 1:112,271 live births; partial BD, 1:129,282 live births; and combined BD incidence, 1:60,089 live births. The combined incidence of BD was 1:47,486 out of 1,321,989 newborns in nine European countries (Loeber 2007). Thus, the incidence found in the current study was higher than that observed worldwide and in many countries. Nevertheless, pilot newborn screening

studies in isolated regions or selected groups have disclosed higher incidences (1:4,500 to 1:14,000) than that reported in the present research (Thodi et al. 2013; Dunkel et al. 1989; Lawler et al. 1992; Sarafoglou et al. 2009).

In Brazil, the available prevalence rates are divergent. A study in the State of Paraná (South) showed a combined prevalence of BD of 1:62,500 live births and 1:125,000 for partial BD (Pinto et al. 1998). The highest incidence (1:9,000) was reported by a private laboratory study (Neto et al. 2004) that reported the results from samples received from several Brazilian regions. The authors recognized several problems with the samples received for the serum quantitative tests. Although the epidemiological data are quite different, it is possible that regional variations in a large country like Brazil explain such divergent results.

The most common mutation was D444H, which was present in seven of the 16 alleles studied, as has been reported by almost all investigators, including a recent Brazilian genetic study on BD (Borsatto et al. 2014). Two novel mutations were detected. The pA281V mutation was observed in compound heterozygosity with a D444H mutation in a girl. The mutation segregated with the parents. Biotinidase activity of the mutant enzyme was estimated to be zero, according to the activity data from the child and her parents. Furthermore, SIFT analysis also suggested a pathogenic variant. The E177K mutation was described in compound heterozygosity with p.T532M. Allele-independent segregation was also demonstrated in this case. The enzyme activity of T532M, considered to be pathogenic in a homozygous child derived from a newborn screening program (Norrgard et al. 1999; patient No. 415), was reported to be 0.6 nmol/min/mL (8.4% of the mean reference value for the laboratory). The estimated activity for this mutant in the present study was also 0.6 nmol/min/mL (8.3% of the mean reference value in our laboratory). The estimated activity of biotinidase for the E177K was quite similar to that usually estimated for the D444H enzyme. The pathogenic nature of the p.H485Q mutation has been considered to be uncertain (UTAH BTD Database 2013) because no enzyme activity and clinical information were available in a patient with a compound H485Q/A171T_D444 mutation. The homozygous p.H485Q in the present report was associated with a profound BD; thus, it should be considered pathogenic.

The D543E mutation has been previously assigned as pathogenic when compounded with p.Q456H or c.587delC in two Hispanic children (Cowan et al. 2012), both with profound BD. At the UTAH BTD Database (2013), it was compounded with p.D444H and resulted in a biotinidase activity level of 2.4 nmol/min/mL. A Brazilian study also reported a child with the same double heterozygosity and activity level of 2.6 nmol/min/mL (Borsatto et al. 2014; patient No. 18). If a mean reference value of 7.2 nmol/min/mL is adopted and p.D444H is considered to have half the activity of the wild enzyme, the activity of p.D543E would be 16.7% and 22.2%, respectively. The estimated value in the homozygous child in the present report was 16.7%. Thus, the present report confirmed the pathogenicity of p.D543E which should be considered a mutant that leads, when homozygous, to a severe partial biotinidase deficiency.

In conclusion, this study describes a pilot newborn screening study that estimated an incidence rate of 1:22,861 live births for partial and profound BD combined. This incidence rate was higher than that reported in several large studies worldwide. The cases were asymptomatic prior to the start of biotin supplementation and remained so up to one year of follow-up examinations. Two novel mutations were detected: one pathogenic (p.A281V) and the other (p.E177K) with biotinidase activity similar to D444H. Two already registered mutations were confirmed as pathogenic (p.H485Q and p.D543E).

Acknowledgments The authors gratefully acknowledge the technical and scientific staff of the Center for Newborn Screening and Genetic Diagnostics (Nupad/UFMG) for their involvement and logistical support. The contribution of the technologist Daniela Magalhães Nolasco was essential for the standardization of the biotinidase serum analysis. Marcos Antunes Lopes, Lívia Uliana, and their teams collaborated for the successful recall of the families for confirmatory tests. The authors also wish to thank Nupad and Fapemig for their financial support. Marcos Borato Viana received a researcher grant from CNPq (Brazilian National Council for Research).

Synopsis

This extensive pilot study showed a high incidence (1:22,861) of biotinidase deficiency in Brazilian newborns through a three-phase laboratory procedure: a colorimetric screening test, confirmatory determination of serum biotinidase activity, and gene sequencing (two novel mutants were detected).

Compliance with Ethics Guidelines

Conflict of Interest

The authors declare that they have no conflict of interest.

Informed Consent

All procedures followed were in accordance with the ethical standards of the responsible committee on human experimentation (institutional and national) and with the Helsinki Declaration of 1975, as revised in 2000. Informed consent

was obtained from all patients for being included in the study.

Details of the Contributions of Individual Authors

Study concept and design: Januario, Gurgel-Giannetti, Lara; Acquisition of data: Lara, Ladeira; Analysis and interpretation of data: Lara, Januario, Viana, del Castillo; Drafting of the manuscript: Lara, Gurgel-Giannetti; Critical revision of the manuscript for important intellectual content: Januario, Viana, Gurgel-Giannetti, Aguiar; Molecular and Biochemical analysis: Ladeira, Carvalho, del Castillo; Final proofreading: Januario, Viana; Paper Guarantor: Januario

References

Borsatto T, Sperb-Ludwig F, Pinto LL et al (2014) Biotinidase deficiency: clinical and genetic studies of 38 Brazilian patients. BMC Med Genet 15:96

Cowan TM, Blitzer MG, Wolf B, Working Group of the American College of Medical Genetics Laboratory Quality Assurance Committee (2010) Technical standards and guidelines for the diagnosis of biotinidase deficiency. Genet Med 12:464–470

Cowan TM, Kazerouni NN, Dharajiya N et al (2012) Increased incidence of profound biotinidase deficiency among Hispanic newborns in California. Mol Genet Metab 106:485–487

Dunkel G, Scriver CR, Clow CL et al (1989) Prospective ascertainment of complete and partial serum biotinidase deficiency in the newborn. J Inherit Metab Dis 12:131–138

González EC, Marrero N, Frómeta A, Herrera D, Castells E, Pérez PL (2006) Qualitative colorimetric ultramicroassay for the detection of biotinidase deficiency in newborns. Clin Chim Acta 369:35–39

Lawler MG, Frederick DL, Anza SR, Wolf B, Levy HL (1992) Newborn screening for biotinidase deficiency: pilot study and follow-up of identified cases. Screening 1:37–47

Loeber JG (2007) Neonatal screening in Europe: the situation in 2004. J Inherit Metab Dis 30:430–438

McVoy JR, Levy HL, Lawler M et al (1990) Partial biotinidase deficiency: clinical and biochemical features. J Pediatr 116:78–83

Mühl A, Möslinger D, Item CB, Stockler-Ipsiroglu S (2001) Molecular characterisation of 34 patients with biotinidase deficiency ascertained by newborn screening and family investigation. Eur J Hum Genet 9(4):237–243

Neto EC, Schulte J, Rubim R et al (2004) Newborn screening for biotinidase deficiency in Brazil: biochemical and molecular characterizations. Braz J Med Biol Res 37:295–299

Norrgard KJ, Pomponio RJ, Hymes J, Wolf B (1999) Mutations causing profound biotinidase deficiency in children ascertained by newborn screening in the United States occur at different frequencies than in symptomatic children. Pediatr Res 46:20–27

Pinto AL, Raymond KM, Bruck I, Antoniuk SA (1998) Prevalence study of biotinidase deficiency in newborns. Rev Saude Publica 32(2):148–152

Pomponio RJ, Hymes J, Reynolds TR et al (1997) Mutations in the human biotinidase gene that cause profound biotinidase deficiency in symptomatic children: molecular, biochemical, and clinical analysis. Pediatr Res 42:840–848

Sarafoglou K, Bentler K, Gaviglio A et al (2009) High incidence of profound biotinidase deficiency detected in newborn screening blood spots in the Somalian population in Minnesota. J Inherit Metab Dis 32(Suppl 1):S169–S173

Swango KL, Demirkol M, Hüner G et al (1998) Partial biotinidase deficiency is usually due to the D444H mutation in the biotinidase gene. Hum Genet 102:571–575

Thodi G, Molou E, Georgiou V et al (2011) Mutational analysis for biotinidase deficiency of a Greek patients' cohort ascertained through expanded newborn screening. J Hum Genet 56:861–865

Thodi G, Schulpis KH, Molou E et al (2013) High incidence of partial biotinidase deficiency cases in newborns of Greek origin. Gene 524(2):361–362

UTAH BTD Database (2013) http://www.arup.utah.edu/database/BTD/BTD_display.php

Walsh PS, Metzger DA, Higuchi R (1991) Chelex 100 as a medium for simple extraction of DNA for PCR-based typing from forensic material. Biotechniques 10:506–513

Wolf B, Heard GS (1990) Screening for biotinidase deficiency in newborns: worldwide experience. Pediatrics 85:512–517

Wolf B (1991) Worldwide survey of neonatal screening for biotinidase deficiency. J Inherit Metab Dis 14:923–927

Wolf B (2001) Disorders of biotin metabolism. In: Scriver CR, Beaudet AL, Sly WS et al (eds) The metabolic and molecular bases of inherited disease, 8th edn. Mc-Graw-Hill, New York, pp 3935–3962

Wolf B, Jensen KP, Barshop B et al (2005) Biotinidase deficiency: novel mutations and their biochemical and clinical correlates. Hum Mutat 25:413

Wolf B (2010) Clinical issues and frequent questions about biotinidase deficiency. Mol Genet Metab 100:6–13

JIMD Reports
DOI 10.1007/8904_2015_450

RESEARCH REPORT

Dopamine-Responsive Growth-Hormone Deficiency and Central Hypothyroidism in Sepiapterin Reductase Deficiency

Matthias Zielonka · Nawal Makhseed · Nenad Blau · Markus Bettendorf · Georg Friedrich Hoffmann · Thomas Opladen

Received: 03 March 2015 / Revised: 20 April 2015 / Accepted: 28 April 2015 / Published online: 26 May 2015

Abstract Sepiapterin reductase (SR) deficiency is a rare autosomal recessively inherited error of tetrahydrobiopterin (BH_4) biosynthesis, resulting in disturbed dopaminergic and serotonergic neurotransmission. The clinical phenotype is characterized by dopa-responsive movement disorders including muscular hypotonia, dystonia, and parkinsonism. Due to the rarity of the disease, the phenotype of SR deficiency is far from being completely understood. Here, we report a 7-year-old boy, who was referred for diagnostic evaluation of combined psychomotor retardation, spastic tetraplegia, extrapyramidal symptoms, and short stature. Due to discrepancy between motor status and mental condition, analyses of biogenic amines and pterins in CSF were performed, leading to the diagnosis of SR deficiency. The diagnosis was confirmed by a novel homozygous mutation c.530G>C; p.(Arg177Pro) in exon 2 of the *SPR* gene. Because of persistent short stature, systematic endocrinological investigations were initiated. Insufficient growth-hormone release in a severe hypoglycemic episode after overnight fasting confirmed growth-hormone deficiency as a cause of short stature. In addition, central hypothyroidism was present. A general hypothalamic affection could be excluded. Since dopamine is known to regulate growth-hormone excretion, IGF-1, IGF-BP3, and peripheral thyroid hormone levels were monitored under L-dopa/carbidopa supplementation. Both growth-hormone-dependent factors and thyroid function normalized under treatment. This is the first report describing growth-hormone deficiency and central hypothyroidism in SR deficiency. It extends the phenotypic spectrum of the disease and identifies dopamine depletion as cause for the endocrinological disturbances.

Communicated by: Verena Peters

Competing interests: None declared

M. Zielonka · N. Blau · G.F. Hoffmann · T. Opladen (✉)
Division of Neuropediatrics and Metabolic Medicine, Department of General Pediatrics, University Hospital Heidelberg, Im Neuenheimer Feld 430, 69120 Heidelberg, Germany
e-mail: thomas.opladen@med.uni-heidelberg.de

N. Makhseed
Pediatric Department, Jahra Hospital, Qadisiya, Kuwait

M. Bettendorf
Division of Pediatric Endocrinology, Department of General Pediatrics, University Hospital Heidelberg, Heidelberg, Germany

Abbreviations

3-OMD	3-*O*-methyldopa
5-HIAA	5-Hydroxyindoleacetic acid
5-HTP	5-Hydroxytryptophan
BH_2	Dihydrobiopterin
BH_4	Tetrahydrobiopterin
CSF	Cerebrospinal fluid
HVA	Homovanillic acid
L-dopa	Levodopa
Phe	Phenylalanine
SR	Sepiapterin reductase

Introduction

Sepiapterin reductase (SR) deficiency is a rare levodopa-responsive disorder due to an autosomal inherited error in pterin metabolism (Bonafe et al. 2001; Blau et al. 2001). The molecular basis is an inherited deficiency of sepiapterin reductase, which is caused by two disease-causing mutations in the *SPR* gene locus located on chromosome 2p14-p12 (Thöny and Blau 2006). SR catalyzes the last step in

the tetrahydrobiopterin (BH_4) synthesis pathway converting 6-pyruvoyl-tetrahydropterin to BH_4 in a two-step NADPH-dependent reaction (Hyland 1999; Pearl et al. 2004). BH_4 is an essential cofactor necessary for the function of phenylalanine hydroxylase (PAH), tyrosine hydroxylase (TH), tryptophan hydroxylase (TPH), and nitric-oxide synthase. TH and TPH are rate limiting in the biosynthesis of the biogenic amines dopamine and serotonin, which play important roles in the generation and regulation of motor movements, sleep maintenance, learning, memory, and emotional behavior (Hyland 1999; Surtees 1999). Dopamine exerts some of its functional effects via D2 receptors. In recent years, evidence was gathered that D2 receptors are crucial in the regulation of growth-hormone-dependent body growth as well as thyroid hormone secretion (Díaz-Torga et al. 2002; Lewis et al. 1987; Samuels et al. 1992).

Patients with SR deficiency exhibit characteristic symptoms. While the early clinical phenotype is dominated by axial muscular hypotonia or developmental delay, older patients present with cardinal features of dopamine-responsive disorders including dystonia, sleep disorders, and oculogyric crises, most of them with diurnal fluctuations (Friedman et al. 2011). However, due to the rarity of the disease and lack of systematic investigations, the phenotype of SR deficiency is far from being completely understood.

Diagnosis of SR deficiency is depending on the analysis of biogenic amines and pterins in CSF. SR deficiency must be suspected finding an increased dihydrobiopterin (BH_2) concentration combined with low levels of both homovanillic (HVA) and 5-hydroxindolacetic acid (5-HIAA). Diagnosis can be confirmed biochemically by elevated CSF sepiapterin and molecular genetic studies (Blau et al. 2001). Here, we report a 7-year-old boy with newly diagnosed SR deficiency who presented with severe endocrinological disturbances.

Case Summary

History and Examination

The male patient was born spontaneously after an uneventful pregnancy at term to healthy consanguineous parents (1st-degree cousins; target height SDS −1.59) of Kuwaiti ancestry. He is the 6th child of 9 children. There was no history of genetic disorders in the families. Growth parameters at birth were small for gestational age (birth weight 2,500 g, SDS −2.55, birth length 46 cm, SDS −2.83). Perinatal adaption was normal without any signs of neonatal infection or early metabolic decompensation. Newborn screening for inherited metabolic diseases was not performed. At age 6 months, the boy was evaluated for the first time by a neuropediatrician due to developmental delay, axial muscular hypotonia, and short stature without finding a specific underlying diagnosis. In the further course, growth parameters remained under the 3rd centile. During the first year of life, successively increasing limb spasticity, predominantly on the left side, was observed associated with episodes of generalized tonic hyperextensions. The clinical examination at age 12 months was dominated by significantly reduced head control and truncal muscular hypotonia with increased limb stiffness. Hyperreflexia, widened reflex zones and foot clonus led to the initial diagnosis of spastic tetraparesis. Cerebral palsy was suspected. Ocular movements described as frequent uprolling of eyes were regarded as epileptic. Anticonvulsant therapy with valproic acid was initiated, but stopped after a total of 1 month since follow-up EEG examination did not reveal epileptic discharges. Expanded metabolic analyses including blood ammonia level, amino acid and acylcarnitine profiles, biotinidase activity, and analysis of lysosomal enzymes performed at the age of 3 years were all negative. Repeated MRI scans of the brain were unremarkable. An underlying neuropathy was excluded by normal nerve conduction studies. Under regular physical therapy, the boy mildly progressed in his development.

At the time of presentation at the University Children's Hospital, Heidelberg, at the age of 7 years, the patient still had poor head control with severe axial muscular hypotonia, was unable to sit or walk, and did not use spoken language. There was a striking contrast between his motor disabilities and his cognitive capacities. The boy was alert and interactive, exploring his environment attentively. On physical examination, he showed apart from a severe generalized muscular hypotonia extrapyramidal symptoms with rigor and bradykinesia associated with generalized hyperreflexia and pes equinus. Bilateral striatal toe was noted. Typical dystonic movements were absent. Body height, weight, and head circumference were under the 3rd centile (height 99.0 cm, SDS −5.17, weight 11.0 kg, SDS −7.89, head circumference 48.0 cm, SDS −3.52). Because of the marked discrepancy between his motor status and mental condition, analyses of biogenic amines and pterins in CSF were included in the metabolic workup. CSF analysis revealed significantly decreased concentrations of HVA 22 nmol/l (normal range 260–713 nmol/l) and 5-HIAA 27 nmol/l (normal range 110–247 nmol/l). BH_2 and sepiapterin concentrations in CSF were highly elevated (BH_2 91 nmol/l, normal range 0–18 nmol/l; sepiapterin 24 nmol/l, normal range < detection limit), while BH_4 concentration was low at 6 nmol/l (normal range 20–49 nmol/l). Plasma and CSF phenylalanine (Phe) concentrations were within the normal range: plasma, 59 μmol/l (normal range 26–91 μmol/l), and CSF, 8.7 μmol/l (normal range 6.4–11.5 μmol/l). Surprisingly, plasma prolactin concentration was found within the normal

Table 1 Endocrinological data before and during treatment

Biochemical marker	Before therapy	After 2 weeks of therapy (L-dopa/carbidopa 2.7 mg/kg/day)	After 4 weeks of therapy (L-dopa/carbidopa, 4.1 mg/kg/day)	After 8 weeks of therapy (L-dopa/carbidopa, 6.8 mg/kg/day and 5-hydroxytryptophan, 5.5 mg/kg/day)	Control range
IGF-1 (ng/ml)	nd ↓	36 ↓	33 ↓	27 ↓	62–248
IGF-1 (SDS)	na ↓	−3.1 ↓	−3.3 ↓	−3.8 ↓	
IGF-BP3 (mg/l)	1.08 ↓	1.15 ↓	1.36 ↓	1.69	1.66–3.59
IGF-BP3 (SDS)	−3.8 ↓	−3.4 ↓	−2.6 ↓	−1.7	
TSH (mU/l)	0.98	1.33	0.98	1.80	0.7–3.7
T3 (ng/ml)	0.56 ↓	0.92 ↓	0.95 ↓	0.97 ↓	1.18–2.14
fT3 (ng/l)	2.42 ↓	4.14	3.15 ↓	3.95	3.4–6.6
T4 (ng/ml)	65.82	59.55 ↓	65.54	63.63	60.61–117.02
fT4 (ng/l)	10.37	8.88	7.70	9.45	7.5–18.7

nd not detectable, *na* not available, *IGF-1* insulin-like growth factor 1, *IGF-BP3* insulin-like growth factor binding-protein 3, *TSH* thyroid-stimulating hormone, *T3* total triiodothyronine, *fT3* free triiodothyronine, *T4* total thyroxine, *fT4* free thyroxine, ↓ below control range

range. For confirmation of the biochemical findings, genetic analysis of the SR gene (*SPR*) was initiated, which identified a novel homozygous mutation c.530G>C; p.(Arg117Pro) in exon 2. Taking the phenotype into consideration, the mutation has to be judged as functionally relevant, thereby affirming the diagnosis of SR deficiency. Diagnostic workup of short stature (SDS −5.17) showed a strikingly decreased concentration of IGF-1 and IGF-BP3 (Table 1). Growth-hormone deficiency was confirmed by inadequate growth-hormone release (max. 1.31 ng/ml) in hypoglycemia (plasma glucose 27 mg/dl, normal range 45–100 mg/dl) that spontaneously occurred after overnight fasting. Further systematic endocrinological investigations revealed central hypothyroidism (Table 1). The analysis of steroid metabolites in urine, 24-h cortisol–ACTH profile, as well as gonadotropin concentrations were within the normal range, thereby excluding a panhypopituitarism as concomitant disease. Brain MRI was unremarkable, particularly showing no evidence of morphological alteration of hypothalamic–pituitary axis.

Treatment and Follow-Up

Treatment with L-dopa/carbidopa [4:1] was started immediately after diagnosis with a slow dose increase up to a total L-dopa dosage of 6.8 mg/kg body weight per day. After 1 month, 5-hydroxytryptophane was added with doses slowly increased up to 5.5 mg/kg body weight per day. Growth hormone and thyroid function were monitored carefully. L-dopa/carbidopa supplementation led to a prompt increase of the very low IGF-1 and IGF-BP3 concentrations (Table 1). Similarly central hypothyroidism significantly improved. Specific supplementation of L-thyroxin was not necessary. After 2 months of therapy, overall thyroid function was euthyroid (Table 1). Clinically at the 2-month follow-up visit, the boy presented with improved alertness and improved motor function. Prone position was tolerated well; in addition the patient was partially supporting his own weight when held and showed improved hand–hand and hand–mouth contact. However, orofacial dyskinesia as side effect of treatment was noted. On 6-month follow-up examination, laboratory testing showed marked hyperprolactinemia (prolactin 450.9 mIU/l, normal range 57–281 mIU/l).

Discussion

SR deficiency is a rare inherited neurological disease in the biosynthesis of BH_4 leading to monoamine neurotransmission deficiency. Due to the missing hyperphenylalaninemia, SR deficiency fails early identification by newborn screening, which results in a significantly delayed diagnosis (Opladen et al. 2012). Within the inherited BH_4 deficiencies, apart from SR deficiency, only the autosomal dominant and a subgroup of the autosomal recessive inherited GTP cyclohydrolase deficiencies are characterized by normal phenylalanine levels (Opladen et al. 2011; Segawa 2011). The phenotype of SR deficiency is mainly characterized by an affection of the motor and cognitive system. Patients exhibit psychomotor retardation and neurologic symptoms dominated by axial muscular hypotonia, dystonic movements, spasticity, and parkinsonism with diurnal fluctuation (Abeling et al. 2006; Dill et al. 2012; Neville et al. 2005). In infancy, muscular hypotonia and developmental delay are usually the only clinical findings. Therefore, due to mimicking characteristics, infantile cerebral palsy is one of the most important differential diagnoses of SR deficiency (Friedman et al. 2011). The underlying pathophysiological basis of SR deficiency is a defect in the

synthesis of BH_4 leading to severe depletion in monoamines serotonin and dopamine. In the central nervous system, dopamine exerts its effects mainly through the activation of dopamine D2 receptors. Recent in vivo studies, using genetically modified mice that lack dopamine D2 receptors ($Drd2^{-/-}$), revealed dopamine as a crucial regulator of growth-hormone-dependent body growth. $Drd2^{-/-}$ mice exhibit deficiency of pituitary somatotrophs associated with decreased growth hormone and IGF-1 serum levels, ultimately resulting in dwarfism (Díaz-Torga et al. 2002; Noaín et al. 2013). In addition, mice deficient in the *SPR* gene ($Spr^{-/-}$) display a phenotype comparable to $Drd2^{-/-}$ mice with severely reduced concentrations of IGF-1 in serum and growth retardation (Yang et al. 2006). Growth-hormone deficiency is thereby not specific for SR deficiency but related to all primary deficiencies in dopamine synthesis. Mice deficient in the *PTS* gene ($Pts^{-/-}$), coding 6-pyruvoyl-tetrahydropterin synthase, and homozygous DDC knock-in mice (Ddc(IVS6/IVS6)), deficient in aromatic L-amino acid decarboxylase, exhibit dwarfism and low IGF-1 concentration (Elzaouk et al. 2003; Lee et al. 2013). Interestingly, analogous to transgenic $Pts^{-/-}$ and $Spr^{-/-}$ mice, where administration of dopaminergic substances rescued dwarfism and concentration of IGF-1 (Elzaouk et al. 2003; Yang et al. 2006), treatment with L-dopa/carbidopa led to a significant increase of IGF-1 and IGF-BP3 serum levels in our patient. The results demonstrate for the first time that growth-hormone deficiency in human SR deficiency is caused by dopamine depletion and can be sufficiently treated by restoring dopamine concentration in the central nervous system.

While changes of thyroid functions were not documented in either animal models, endocrinological evaluation revealed central hypothyroidism in our SR-deficient patient. Concerning the regulation of hypothalamic–pituitary–thyroid axis by dopamine, evidence was gathered implicating opposite effects of D2 receptor activation on the hypothalamus and the pituitary thyrotroph. Whereas dopamine suppresses TSH pulse amplitude in healthy volunteers (Samuels et al. 1992), in vitro studies illustrated that dopamine stimulates the release of TRH by acting via the same D2 receptors (Lewis et al. 1987). It is appropriate to hypothesize that basal activation of D2 receptors in the hypothalamus is required for sufficient TRH release. Interestingly, it was recently shown that levodopa-induced hyperkinesia is associated with increased TRH expression in the striatum (Cantuti-Castelvetri et al. 2010). Similar to the effect on IGF-1 and IGF-BP3 concentrations, supplementation with L-dopa/carbidopa significantly improved thyroid hormone levels with TSH and fT3 within the normal range. This supports the hypothesis that central hypothyroidism is caused by dopamine depletion in SR deficiency. As hypothyroidism is a known cause for mental retardation in children, central hypothyroidism might contribute to the severe cognitive deficits in patients with SR deficiency. Prolactin concentrations in the periphery are known to inversely correlate with the dopamine levels in the central nervous system and therefore are expected to be elevated in the case of dopamine depletion. The normal prolactin level in our patient, measured once before supplementation with L-Dopa, reflects the diurnal fluctuations of plasma prolactin levels. Recently, it has been shown that prolactin levels in blood range from normal values to severe hyperprolactinemia in the BH_4 biosynthesis disorders 6-pyruvoyl-tetrahydropterin synthase deficiency and dihydropteridine reductase deficiency (Porta et al. 2009; Porta et al. 2012). Follow-up evaluation after 6 months showed marked hyperprolactinemia, emphasizing the fact that repeated examinations of plasma prolactin levels are necessary for the reliable, indirect assessment of dopamine homoeostasis in the central nervous system.

Given their pathophysiological basis, it is likely that growth-hormone deficiency and central hypothyroidism are part of the general phenotype of SR deficiency. The fact that patients with growth-hormone deficiency have a higher risk to develop life-threatening hypoglycemic episodes, as seen in our patient, highlights the importance of an early diagnosis of SR deficiency and immediate start of treatment with dopaminergic substances. As hypoglycemic episodes are known and potentially lethal complications in several inherited neurotransmitter disorders including aromatic L-amino acid decarboxylase (AADC) deficiency (Arnoux et al. 2013; Manegold et al. 2009), analyses of biogenic amines and pterins in CSF should be taken into consideration in children presenting with fasting hypoglycemia and neurologic symptoms.

Conclusion

Analyses of biogenic amines in CSF should be considered in the metabolic workup of children with fasting hypoglycemia and neurologic symptoms.

Synopsis

Systematic endocrinological investigations should be performed in patients with sepiapterin reductase deficiency as dopamine depletion might result in growth-hormone deficiency and central hypothyroidism associated with cognitive impairment and life-threatening hypoglycemic episodes. Analyses of biogenic amines in CSF should be considered in the metabolic workup of children with fasting hypoglycemia and neurologic symptoms.

References to Electronic Databases

Phenylalanine hydroxylase, EC 1.14.16.1; tyrosine hydroxylase, EC 1.14.16.2; tryptophan hydroxylase, EC 1.14.16.4; nitric-oxide synthase, EC 1.14.13.39

Competing Interest Statement

The authors declare no potential conflicts of interest with respect to the research, authorship, and/or publication of this article.

Details of Contributions of Individual Authors

All authors contributed to clinical care and diagnostic evaluation of this patient. The manuscript was prepared and written by Matthias Zielonka and Thomas Opladen. All authors contributed to the critical revision of the manuscript for intellectual content and gave final approval for the version to be published.

Name of One Author Who Serves as Guarantor

Thomas Opladen accepts full responsibility for the work and/or conduct of the study, had access to the data, and controlled the decision to publish.

Ethical Approval

No approval from the institutional review board was necessary as this is a case report without inclusion of any identifying information.

References

Abeling NG, Duran M, Bakker HD et al (2006) Sepiapterin reductase deficiency an autosomal recessive DOPA-responsive dystonia. Mol Genet Metab 89:116–120

Arnoux JB, Damaj L, Napuri S et al (2013) Aromatic L-amino acid decarboxylase deficiency is a cause of long-fasting hypoglycemia. J Clin Endocrinol Metab 98:4279–4284

Blau N, Bonafe L, Thöny B (2001) Tetrahydrobiopterin deficiencies without hyperphenylalaninemia: diagnosis and genetics of dopa responsive dystonia and sepiapterin reductase deficiency. Mol Genet Metab 74:172–185

Bonafe L, Thöny B, Penzien JM et al (2001) Mutations in the sepiapterin reductase gene cause a novel tetrahydrobiopterin dependent monoamine neurotransmitter deficiency without hyperphenylalaninemia. Am J Hum Genet 69:169–177

Cantuti-Castelvetri I, Hernandez LF, Keller-McGandy CE et al (2010) Levodopa-induced dyskinesia is associated with increased thyrotropin releasing hormone in the dorsal striatum of hemiparkinsonian rats. PLoS One 5:e13861

Díaz-Torga G, Feierstein C, Libertun C et al (2002) Disruption of the D2 dopamine receptor alters GH and IGF-1 secretion and causes dwarfism in male mice. Endocrinology 143:1270–1279

Dill P, Wagner M, Sommerville A et al (2012) Child neurology: paroxysmal stiffening, upward gaze and hypotonia: hallmarks of sepiapterin reductase deficiency. Neurology 78: e29–e32

Elzaouk L, Leimbacher W, Turri M et al (2003) Dwarfism and low insulin-like growth factor-1 due to dopamine depletion in $Pts^{-/-}$ mice rescued by feeding neurotransmitter precursors and H4-biopterin. J Biol Chem 278:28303–28311

Friedman J, Roze E, Abdenur JE et al (2011) Sepiapterin reductase deficiency: a treatable mimic of cerebral palsy. Ann Neurol 71:520–530

Hyland K (1999) Neurochemistry and defects of biogenic amine neurotransmitter metabolism. J Inherit Metab Dis 22:353–366

Lee NC, Shieh YD, Chien YH et al (2013) Regulation of the dopaminergic system in a murine model of aromatic L-amino acid decarboxylase deficiency. Neurobiol Dis 52:177–190

Lewis BM, Dieguez C, Lewis MD, Scanlon MF (1987) Dopamine stimulates release of thyrotropin-releasing hormone from perfused intact rat hypothalamus via hypothalamic D2-receptors. J Endocrinol 115:419–424

Manegold C, Hoffmann GF, Degen I et al (2009) Aromatic L-amino acid decarboxylase deficiency: clinical features, drug therapy and follow-up. J Inherit Metab Dis 32:371–380

Neville BGR, Parascandalo R, Farrugia R, Felica A (2005) Sepiapterin reductase deficiency: a congenital dopa responsive motor and cognitive disorder. Brain 128:2291–2296

Noaín D, Pérez-MillÄn M, Bello EP et al (2013) Central dopamine D2 receptors regulate growth-hormone-dependent body growth and pheromone signaling to conspecific males. J Neurosci 33:5834–5842

Opladen T, Hoffmann G, Hörster F et al (2011) Clinical and biochemical characterization of patients with early infantile onset of autosomal recessive GTP cyclohydrolase I deficiency without hyperphenylalaninemia. Mov Disord 26:157–161

Opladen T, Hoffmann GF, Blau N (2012) An international survey of patients with tetrahydrobiopterin deficiencies presenting with hyperphenylalaninaemia. J Inherit Metab Dis 35:963–973

Pearl PL, Wallis DD, Gibson M (2004) Pediatric neurotransmitter diseases. Curr Neurol Neurosci Rep 4:147–152

Porta F, Mussa A, Concolino D et al (2009) Dopamine agonists in 6-pyruvoyl tetrahydropterin synthase deficiency. Neurology 73:633–637

Porta F, Mussa A, Concolino D et al (2012) Dopamine agonists in dihydropteridine reductase deficiency. Mol Genet Metab 105:582–584

Samuels MH, Henry P, Ridgway EC (1992) Effects of dopamine and somatostatin on pulsatile pituitary glycoprotein secretion. J Clin Endocrinol Metab 74:217–222

Segawa M (2011) Hereditary progressive dystonia with marked diurnal fluctuation. Brain Dev 33:195–201

Surtees R (1999) Inborn errors of neurotransmitter receptors. J Inherit Metab Dis 22:374–380

Thöny B, Blau N (2006) Mutations in the BH4-metabolizing genes GTP cyclohydrolase I, 6-pyruvoyl-tetrahydropterin synthase, sepiapterin reductase, carbinolamine-4a-dehydratase, and dihydropteridine reductase. Hum Mutat 27:870–878

Yang S, Lee YJ, Kim JM et al (2006) A murine model for human sepiapterin-reductase deficiency. Am J Hum Genet 78:575–587

JIMD Reports
DOI 10.1007/8904_2015_451

RESEARCH REPORT

Clinical Findings and Natural History in Ten Unrelated Families with Juvenile and Adult GM1 Gangliosidosis

João Stein Kannebley · Laura Silveira-Moriyama · Laís Orrico Donnabella Bastos · Carlos Eduardo Steiner

Received: 07 January 2015 / Revised: 13 April 2015 / Accepted: 27 April 2015 / Published online: 25 June 2015

Abstract We describe 12 subjects of ten unrelated families from the region of Campinas and the southern state of Minas Gerais, Brazil, who presented with juvenile ($n = 4$) and adult ($n = 8$) GM1 gangliosidosis. Data includes clinical history, physical examination, and ancillary exam findings. Six subjects presented initially with skeletal deformities, while the remaining six had neurological manifestations at onset. Over time, all exhibited a combination of osteoarticular and neurologic degeneration with varying degrees of severity. Corneal clouding, angiokeratomas, and inguinal hernia were seen in one individual each. Other features commonly described in lysosomal storage disorders were not found in this series, such as coarse faces, gingival hypertrophy, visceromegaly, and cherry red spot. All subjects presented with short stature, dysostosis multiplex, dysarthria, and impairment of activities of daily living, 10/12 had extrapyramidal signs, 8/12 had pyramidal signs, 8/12 had oculomotor abnormalities, 4/12 had behavioral alterations, and 2/12 had ataxia. None had seizures or Parkinsonism. All female subjects developed severe hip dysplasia and underwent arthroplasty due to chronic pain. A vertebral bone bar and *os odontoideum*, not previously described in this condition, were found in one patient each. There was no clear genotype–phenotype correlation regarding enzyme residual activity and clinical findings, since all subjects were compound heterozygous, but the p.T500A was the most frequent allele in eight families and was associated to Morquio B phenotype. Two sets of siblings allowed intrafamilial comparison revealing consistent features among the families. Interfamilial correlation among unrelated families presenting the same mutations was less consistent.

Communicated by: Pascale de Lonlay

Competing interests: None declared

Electronic supplementary material: The online version of this chapter (doi:10.1007/8904_2015_451) contains supplementary material, which is available to authorized users.

J.S. Kannebley · L.O.D. Bastos · C.E. Steiner (✉)
Postgraduate Research Program in Medical Sciences, School of Medical Sciences, University of Campinas (Unicamp), Rua Tessália Vieira de Camargo 126, 13083-887 Campinas, SP, Brazil
e-mail: steiner@fcm.unicamp.br

L. Silveira-Moriyama
Postgraduate Research Program in Medicine, Universidade Nove de Julho (Uninove), 235/249 Rua Vergueiro, São Paulo, SP 01504-001, Brazil

L. Silveira-Moriyama
Department of Neurology, School of Medical Sciences, University of Campinas (Unicamp), Rua Tessália Vieira de Camargo 126, 13083-887 Campinas, SP, Brazil

L. Silveira-Moriyama
Reta Lila Weston Institute of Neurological Studies, UCL Institute of Neurology, 1 Wakefield Street WC1N 1PJ, London, UK

C.E. Steiner
Department of Medical Genetics, School of Medical Sciences, University of Campinas (Unicamp), Rua Tessália Vieira de Camargo 126, 13083-887 Campinas, SP, Brazil

Introduction

GM1 gangliosidosis is a lysosomal storage disorder caused by deficiency in β-galactosidase (β-gal) activity due to various different mutations in the *GLB1* gene (Suzuki et al. 2014). Patients of various ethnic origins have been reported with an overall incidence estimated in 1:100,000–200,000 live births, thus being considered a rare condition, except for a few ethnic groups (Suzuki et al. 2014). In southern Brazil, incidence has been estimated in 1:17,000 (Severini et al. 1999).

Three forms have been identified: type 1 (infantile, OMIM#230500), type 2 (late infantile or juvenile, OMIM#230600), and type 3 (adult or chronic, OMIM#

230650) (Brunetti-Pierri and Scaglia 2008). As in many other metabolic disorders, they represent a clinical continuum rather than separate entities. Many patients also present as Morquio B disease (OMIM#253010) which is allelic to the various forms of GM1 gangliosidosis (Giugliani et al. 1987; Paschke et al. 2001; Sperb et al. 2013).

Type 1 is characterized by facial dysmorphism, skeletal abnormalities, visceromegaly, cherry red spot, hypotonia, and psychomotor regression, with onset from birth to 7 months of age. Type 2 is characterized by mild skeletal changes, neurologic regression, seizures, muscle weakness, and onset between 7 months and 3 years of age. Type 3 starts between 3 and 30 years of age and is characterized by complex gait and speech abnormalities, florid extrapyramidal features, mild vertebral deformities, and short stature (Suzuki et al. 2014).

It has pan-ethnic distribution, and the infantile form of the disease is described more often than the others, but adult patients have been reported most often in Japan (Suzuki et al. 2014).

Patients and Methods

We describe 12 patients of ten unrelated families from the metropolitan region of Campinas and the southern state of Minas Gerais, Brazil. All were diagnosed with GM1 gangliosidosis confirmed by low enzyme activity of β-galactosidase (β-gal) measurement in leukocytes or fibroblasts using artificial 4-methylumbeliferyl β-galactosidase and by mutation analysis of *GLB1* gene on DNA extracted from lymphocytes following PCR amplification and direct DNA sequencing (Baptista 2013).

Retrospective clinical data was collected from patient's records, and prospective evaluations were performed by the same clinical geneticist and the same neurologist, with especial attention to natural history, somatic features, neurologic signs, and radiological changes.

Results

The sample was composed of seven males and five females. Consanguinity was denied by all families. In two families there was recurrence in the sibship (individuals 3–4 and 11–12). Based on the age of onset, four (subjects 2, 5, 6, and 8) were diagnosed with the juvenile and eight (subjects 1, 3, 4, 5, 7, 9, 10, 11, 12) with the adult form. Onset ranged from 1 to 12 years (mean 4.75 years). Six individuals presented with skeletal deformities, and the remaining six patients presented initially with neurological abnormalities. Over time, all 12 subjects exhibited a combination of neurological and skeletal disease (Table 1).

All patients presented with short stature and variable findings of *dysostosis multiplex*. Unusual skeletal findings comprised congenital clubfeet and a vertebral bone bar in individual 1 and *os odontoideum* in individual 2. Other signs previously described in lysosomal storage diseases included angiokeratoma, inguinal hernia, and corneal clouding, in one individual each. Cholelithiasis, hydronephrosis, nephrolithiasis, horseshoe kidney, and *cutis verticis gyrata* were also seen in one individual each. No patients presented with coarse face, gingival hypertrophy, cherry red spot, visceromegaly, cardiomyopathy, or adrenal calcification (Table 2).

Clinical evaluation revealed impairment in activities of daily living in all subjects due to a mixture of neurological and osteoarticular disease, which was severe in all but one case. Limitations were mainly motor, although cognitive or behavioral abnormalities were seen in five patients and were severe in one pair of siblings. All patients had gait and speech difficulties, including some degree of dysarthria, which was accompanied by symptoms of dysphagia in 8/12. Extrapyramidal signs like facial and limb dystonia were seen in 10/12 patients, and 9/12 of them presented noticeable muscle atrophy. Pyramidal signs were present in 8/12 patients. Abnormal eye movement was seen in 8/12 patients. Signs of ataxia were documented in only one case. No patients presented with seizures or Parkinsonism (Table 3).

Discussion

Large case series with detailed clinical descriptions of GM1 gangliosidosis are rare, and only a few focused on type 3 GM1 gangliosidosis. Muthane et al. (2004), described three patients from India and revised 40 other subjects previously reported, reinforcing that the most frequent clinical findings were generalized dystonia with prominent facial dystonia and severe speech disturbances. Roze et al. (2005) described four new patients and analyzed data from other 44 meticulously selected subjects from 16 Japanese and 15 non-Japanese families. Clinical manifestations occurred before age 20 years in most patients, typically presenting with gait disorders and/or speech disturbances, showing wide variations in severity and progression rate. Considering the ethnic background, both groups showed similar clinical manifestations, but Japanese individuals presented with an older median age at onset and greater frequency of short stature, corneal opacity, and putaminal hyperintensity when compared to non-Japanese subjects. On the other hand, non-Japanese patients had higher frequencies of mental retardation, Parkinsonism, dystonia, and scoliosis. Brunetti-Pierri and Scaglia (2008) revised clinical, molecular, and therapeutic aspects in 209 subjects with all types of

Table 1 Clinical, biochemical, and molecular findings

Patient	Gender Age	β-Gal activity (%)	*GLB1* mutations	Symptom (age)
1	Female 31 years	15 (3.8)[a]	p.T384S/p.T500A	Skeletal deformities (3 years), learning difficulties (7 years), dysarthria and dystonia (17 years), hip dysplasia, wheelchair (19 years), dysphagia (20 years)
2	Male 32 years	6 (7.7)[b]	p.R59H/p.T500A IVS12nt + 8 t > C/-	Development delay (12 months), skeletal deformities (30 months), lumbar spondylolisthesis (14 years), dysarthria and dysphagia (22 years), wheelchair (23 years)
3	Female 29 years	3.3 (4.2)[b] 28 (7.1)[a]	p.R59H/p.R201H IVS12 + 8 t > C/-	Neurologic regression, dysarthria (7 years), gait disorder, hip dysplasia (12 years), wheelchair (17 years), angiokeratomas (22 years)
4	Male 26 years	4 (5.1)[b]	p.R59H/p.R201H IVS12 + 8 t > C/-	Neurologic regression, dysarthria (7 years), skeletal deformities (9 years), hip dysplasia (25 years), wheelchair (27 years)
5	Female 27 years	7.8 (10)[b]	c.1722-1727AinsG/ p.T500A	Skeletal deformities (14 months), gait disorder (2 years), dysarthria (13 years), hip dysplasia, wheelchair (14 years), dysphagia (21 years)
6	Male 23 years	10 (12.8)[b] 21 (5.3)[a]	p.T500A/?	Gait abnormalities (12 months), skeletal deformities (7 years), inguinal hernia (17 years), dysarthria, dysphagia (19 years)
7	Female 23 years	9 (11.5)[b] 32 (8.1)[a]	p.G311R/p.T500A	Gait disorder, development delay (3.5 years), dysarthria (4 years), dystonia (11 years) wheelchair (12 years), dysphagia (18 years)
8	Male 18 years	10 (12.8)[b] 11.7 (2.9)[a]	p.F107L/p.L173P p.P152P/-	Gait abnormalities (12 months), neurologic regression (3 years), dysarthria (7 years), dysphagia (11 years), wheelchair (12 years)
9	Female 21 years	9.3 (11.9)[b] 16 (4.0)[a]	p.I354S/p.T500A	Skeletal deformities (5 years), dysarthria, dysphagia (11 years), hip dysplasia, wheelchair (14 years)
10	Male 21 years	36 (9.1)[b]	c.1722-1727AinsG/ p.T500A	Skeletal deformities (12 years), dysarthria, dysphagia (16 years)
11	Male 35 years	11.7 (15)[b]	NA	Skeletal deformities (6 years), gait disorder (24 years), dysarthria (28 years), dysphagia (34 years), walking frame/wheelchair (34 years)
12	Male 37 years	NA	p.I354S/p.T500A	Short stature, gait disorder (5 years), dysarthria (20 years), dysphagia (36 years), walking frame/wheelchair (36 years)

[a] On fibroblasts, reference value 394–1,440 nmol/h/mg protein
[b] On leukocytes, reference value 78–280 nmol/h/mg protein
NA not available, *?* unknown

GM1 gangliosidosis, comprising 130 infantile, 23 juvenile, and 56 adult patients. Signs and symptoms of the CNS involvement were invariably present in all cases, with a predominance of hypotonia and development delay in the infantile form in contrast with extrapyramidal, gait disturbances, speech difficulties, and dystonia in the adult form. A total of 102 mutations in *GLB1* gene have been also revised showing extensive molecular heterogeneity and hindering a clear genotype–phenotype correlation. In the Brazilian population, Sperb et al. (2013) revised 32 patients with all types of GM1 gangliosidosis from different regions from Brazil who were diagnosed at their reference laboratory, including clinical and molecular analysis. The series included five subjects with the infantile, 15 with the juvenile, and nine with the adult form. Once more, a genotype–phenotype relationship could not be established for most patients. The most frequent mutation, c.1622–1627insG, was associated with cognitive delay and hypertonia in homozygous patients and ophthalmic findings in compound heterozygous patients. Enzyme activity was also highly variable, even for patients with the same genotype.

Our series adds 12 new patients to the literature and further highlights the phenotypic overlap between GM1 and Morquio B, which are allelic variants of various mutations of the *GLB1* gene. Although all patients in our series eventually developed neurological signs, the initial presentation in half of them was skeletal (Table 1). Five subjects were initially diagnosed elsewhere as "Morquio disease" (patients 1, 5, 6, 9, and 10), three as "spondyloepiphyseal dysplasia" (patient 2 and brothers 11 and 12), and the remaining with nonspecific neurological degeneration (3, 4, 7, and 8).

Morquio was the most frequent initial diagnosis made by pediatricians and orthopedists who referred their patients for biochemical investigation. Although suggested that Morquio B disease presents with no primary central nervous system involvement (Bagshaw et al. 2002), previous studies showed that some patients develop progressive neurologic symptoms (Giugliani et al. 1987; Paschke et al. 2001). Corneal clouding is also frequent in

Table 2 Skeletal, somatic, and visceral findings

Patient	1	2	3	4	5	6	7	8	9	10	11	12	Total
Short stature	+	+	+	+	+	+	+	+	+	+	+	+	12/12
Hip dysplasia	+	+	+	+	+	+	+	–	+	+	+	NA	10/11
Epiphyseal dysplasia	+	+	+	+	+	+	+	–	+	+	+	NA	10/11
Platyspondyly	+	+	+	+	+	+	+	+	NA	+	+	NA	10/10
Anterior beaking of L1	+	+	+	+	+	+	+	+	NA	+	–	NA	9/10
Scoliosis	+	+	+	+	–	+	+	+	NA	+	+	NA	9/10
Kyphosis	+	–	–	–	+	–	+	–	NA	NA	+	NA	4/9
Vertebral bone bar	+	–	–	–	–	–	–	–	NA	–	–	NA	1/10
Os odontoideum	–	+	–	–	–	–	–	–	–	–	NA	NA	1/10
Congenital clubfoot	+	–	–	–	–	–	–	–	–	–	–	–	1/12
Cutis verticis gyrata	–	+	–	–	–	–	–	–	–	–	–	–	1/12
Angiokeratomas	–	–	+	–	–	–	–	–	–	–	–	–	1/12
Corneal clouding	–	–	–	–	–	–	–	–	+	–	–	–	1/12
Inguinal hernia	–	–	–	–	–	+	–	–	–	–	–	–	1/12
Cholelithiasis	+	–	–	–	–	–	–	–	–	–	–	–	1/12
Nephrolithiasis	+	–	–	–	–	+	–	–	–	–	–	–	2/12
Hydronephrosis	+	–	–	–	–	–	–	–	–	–	–	–	1/12
Horseshoe kidney	–	–	–	–	–	+	–	–	–	–	–	–	1/12

+ present, – absent, *NA* not available

Table 3 Neurological examination findings

Patient	1	2	3	4	5	6	7	8	9	10	11	12	Total
Impact on ADL	S	S	S	S	S	S	S	S	S	M	S	S	12/12
Dysarthria	+	+	+	+	+	+	+	+	+	+	+	+	12/12
Extrapyramidal signs	+	+	+	+	+	–	+	+	+	–	+	+	10/12
Facial dystonia	+	+	+	+	+	–	+	+	+	–	+	+	10/12
Limb dystonia	+	+	+	+	+	–	+	+	+	–	+	+	10/12
Grimacing face	+	+	+	+	+	–	+	+	+	–	+	+	10/12
Muscular atrophy	+	+	+	–	+	–	+	+	+	–	+	+	9/12
Pyramidal signs	–	+	+	–	+	–	+	+	+	+	–	+	8/12
Dysphagia	+	+	–	–	+	+	+	+	NA	+	–	+	8/12
Abnormal ocular movement	+	+	NA	NA	+	+	+	NA	+	+	NA	+	8/12
Behavioral alterations	–	–	+	+	–	–	+	+	–	–	–	–	4/12
Ataxia	–	–	–	?	–	–	–	+	–	–	–	–	2/12
Parkinsonism	–	–	–	–	–	–	–	–	–	–	–	–	0/12
Seizures	–	–	–	–	–	–	–	–	–	–	–	–	0/12

+ present, – absent, *?* unknown, *ADL* activities of daily living, *M* mild, *NA* not available, *S* severe

Morquio B disease (Suzuki et al. 2014) and was diagnosed only in patient 9 who is a compound heterozygous for the p.T500A mutation.

Among other signs typically described in lysosomal storage diseases, angiokeratomas were seen in patient 3 and inguinal hernia in patient 6. None in this series presented with gingival hypertrophy, visceromegaly, cardiomyopathy, or cherry red spot, which are characteristic of patients with younger onset GM1 (Suzuki et al. 2014).

Short stature was seen in all patients, and signs of dysostosis multiplex were detected in all subjects who underwent complete radiologic evaluation (Table 2). Abnormalities of

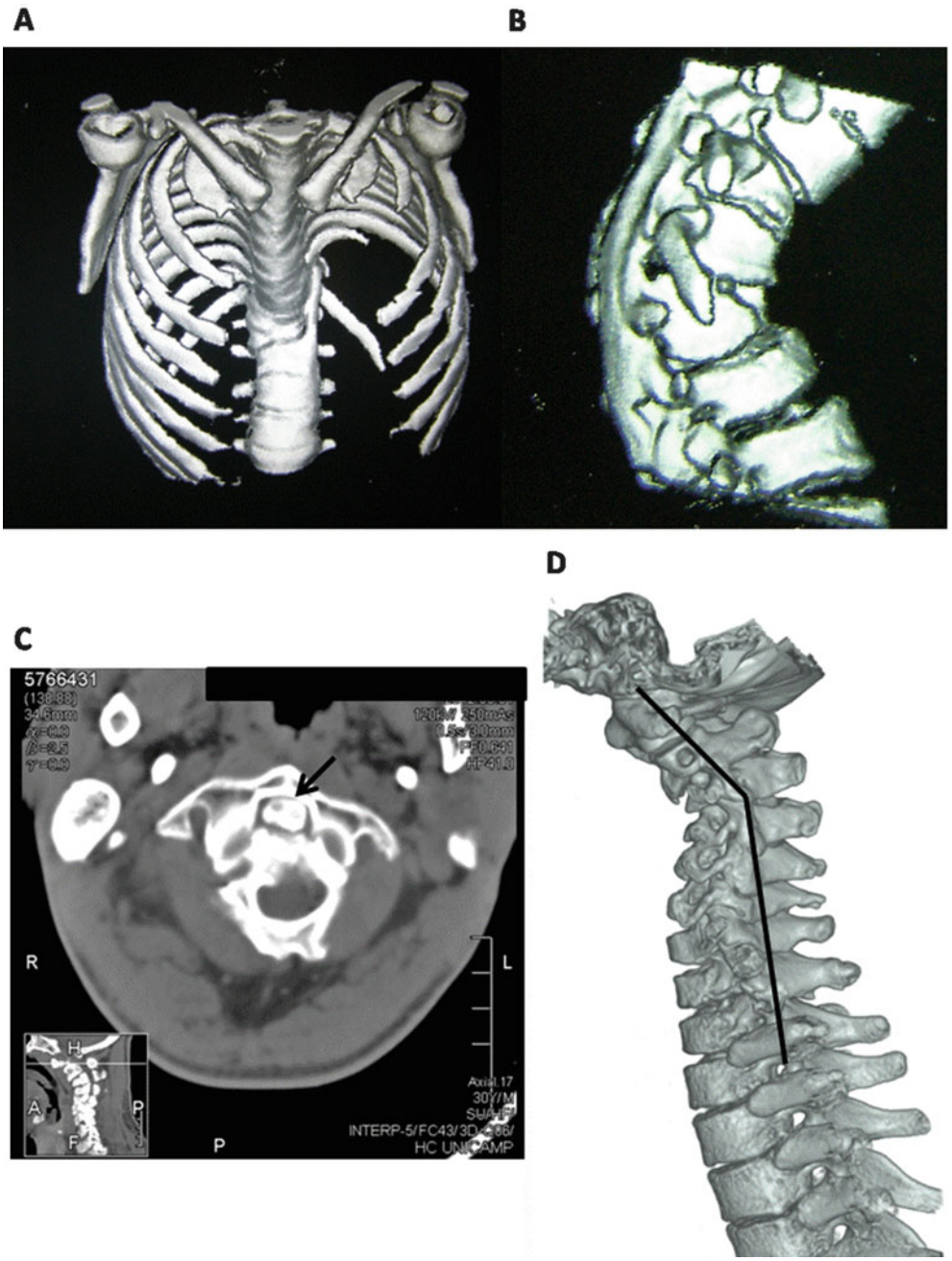

Fig. 1 CT scan showing spine deformity, anterior beaking of L1, and a bone bar in subject 1 (**a**, **b**). Stenosis of cervical spine between C1 and C2 vertebrae and *os odontoideum*; (**c**, *arrow*) and spondylolisthesis with narrowing and deformity of the spinal cord (**d**) seen in subject 2

the craniocervical transition were noted in five out of six subjects submitted to head magnetic resonance imaging, two of them also presenting with cervical spine stenosis. This further shows how the skeletal and neurological also overlap in their pathophysiology: while dystonia is a known cause of chronic skeletal deformities and in particular spine deformities (Wong et al. 2005), the spine deformities caused symptomatic spine chord compression further worsening the neurologic phenotype in these patients. Atypical vertebral abnormalities were found in two individuals (Fig. 1). A vertebral bone bar was seen in patient 1, who also presented with congenital clubfeet, which might represent coincidental findings. Patient 2 presented with *os odontoideum*, a separation of the odontoid process from the body of the axis, which may result in dysfunctional and restraining atlantoaxial joint motion (Rozzelle et al. 2013). It was detected only at the age of 30 years and is not clear whether it is congenital or acquired, and previous reports have

associated it with severe cervical dystonia (Amess et al. 1998).

All individuals in this series had impairment of the activities of daily living, mainly due to the severe motor difficulties. Four subjects presented with noticeable cognitive or behavioral abnormalities including intellectual deficiency in sibs 3 and 4, poor comprehension skills in patient 7, and depression in patient 8. Besides, patient 9 presented with a psychotic episode at age 16 which was considered a side effect of carbamazepine prescribed for chronic pain relief treatment, with complete remission after discontinuation of the drug. Cognitive and behavioral deficit has been rarely reported in adult GM1, but is possible that the severe motor impairment and the frequent finding of anarthria precluded a thorough cognitive evaluation in this and in previous series.

Dysarthria was diagnosed in all patients in our series and is a frequent symptom occurring in over 90% of the individuals with the adult form (Muthane et al. 2004). Dystonia of the face and limbs was described in 10/12 patients. Severe motor disability and significant complaints of dysphagia probably contributed to muscle wasting seen in 9/12 patients. This value is higher than the series of Japanese patients with the adult form where only 3/16 had muscular atrophy (Yoshida et al. 1992), but the socioeconomic conditions present in our sample might explain this discordance, rather than ethnic and genetic factors.

Pyramidal signs were described in 66% in one series of Japanese patients and 62% in non-Japanese patients (Roze et al. 2005). A similar value was seen in our series, where 8/12 subjects (66%) had pyramidal signs, although the neurologic evaluation was compromised because most patients had limitations due to pain or skeletal abnormalities. The same is valid for gait ataxia, which was confirmed only for patient 8, but could not be evaluated in the more severe patients who were wheelchair bound. Abnormal ocular movements were seen in 8/12 patients, who exhibited saccadic impairment. This has been reported previously by Muthane et al. (2004) in one adult GM1 patient. Further reports should endeavor to examine the eye movements and to confirm the frequency and characteristics of oculomotor abnormalities.

Parkinsonism has been reported in case series varying from 7.5% (Muthane et al. 2004) to 48% (Roze et al. 2005) of patients, but was not seen in our series. Epilepsy was also not reported by our patients.

The fact that all subjects were compound heterozygous poses a challenge to the study of genotype–phenotype correlations. The p.T500A was the most frequent allele, and all eight individuals presenting with this codon had an early and pronounced skeletal dysplasia, five of them being referred as having “Morquio disease.” In fact, p.T500A has been previously associated to Morquio B phenotype (Bagshaw et al. 2002; Santamaria et al. 2006; Santamaria et al. 2007; Hofer et al. 2010).

It is interesting to note that two sets of siblings allowed intrafamilial comparison revealing consistent features among the families. That is quite striking for sibs 3 and 4 who showed a very similar and unusual phenotype marked by severe cognitive impairment and also showed low values of residual β-gal activity, although the female exhibited a more pronounced hip dysplasia and the male presented more behavioral abnormalities with agitation and a hyperkinetic disorder with stereotypic movements. For sibs 11 and 12, β-gal activity was measured only in the former and molecular study only in the latter; thus, analysis of the biochemical phenotype was not possible. Concerning clinical features both presented early onset skeletal features (being initially diagnosed as X-linked SED tarda) followed by a slowly progressive neurologic disorder characterized by dysarthria, dysphagia, severe muscle wasting, and normal cognition. They are the eldest subjects in this series, and although one of the siblings became wheelchair bound during this study (he presented with spinal cord compression), the other remains still capable of short-distance walks with the aid of a walking frame, contrasting with other patients in our series that were confined to a wheelchair at a younger age.

An effort of interfamilial genotype–phenotype correlation was made among individuals presenting the same mutations, and we attempted to correlate residual enzyme activity with the phenotype. No clear relationship was visible, but some observations, if corroborated in future studies, might help understand the pleomorphic manifestations of this condition. Patients 5 and 10 present a similar residual enzyme activity, but based on the age of onset, the former was classified as having the juvenile and the latter the adult form, also being the one with the latest onset and the best clinical outcome to date in our sample. Patient 9 has the same genotype as sibs 11 and 12. All presented initially with skeletal features around the age of 5 years and developed dysarthria and dysphagia, but patient 9 had a more incapacitating hip dysplasia, as seen in the all other female subjects. Other details can be obtained from the tables and supplementary materials.

Finally, the frequency of GM1 gangliosidosis in our clinic is similar to another Brazilian case series from Rio Grande do Sul, where the juvenile phenotype was the most common (Sperb et al. 2013). However, there might be a bias in our records because the infantile form is probably underdiagnosed in our population. It is also important to note that consanguinity was denied in all families in this series and patients were in fact compound heterozygous, thus suggesting that gene frequency might be high in our region with a higher frequency of the p.T500A mutation in comparison with other mutations.

Conclusions

The adult form was the most frequent presentation of GM1 gangliosidosis in our service. This might be due to the infantile form being underdiagnosed in Brazil. The absence of consanguinity and the occurrence of compound heterozygous mutations in our series might indicate higher gene frequency in the local population, in line with previous findings from southern Brazil. Clinical presentation is very variable among the individuals, and skeletal deformities and neurologic symptoms occurred in similar frequencies as initial features, but a combination of both was seen in all individuals over time. Hip dysplasia was present in both genders and had a more severe presentation in females. Some considerations on genotype– phenotype correlation support interfamilial variation and intrafamilial homogeneity, but further studies are warranted to better understand the phenotypic pleiotropy in *GLB1*-related disorders.

Acknowledgments The authors would like to thank the Laboratory of Inborn Errors of Metabolism from Hospital de Clínicas de Porto Alegre (LREIM/HCPA), Brazil, for the laboratory support.

Synopsis

Juvenile and adult GM1 gangliosidosis

Compliance with Ethics Guidelines

Conflict of Interest Statement

João Stein Kannebley, Laís Orrico Donnabella Bastos, Laura Silveira-Moriyama, and Carlos Eduardo Steiner declare that they have no conflict of interest.

Informed Consent

All procedures followed were in accordance with the ethical standards of the responsible committee on human experimentation (institutional and national) and with the Helsinki Declaration of 1975, as revised in 2000. Informed consent was obtained from all patients or their guardians for being included in the study. This study was approved by the Research Ethics Committee FCM/Unicamp under protocol no. 236/2011.

Animal Rights

This study did not include laboratory animals.

Details of Author Contributions

João Stein Kannebley planned the work, revised patient's records, performed clinical evaluation, and wrote the manuscript.

Laís Orrico Donnabella Bastos performed neurological examination and revised the manuscript.

Laura Silveira-Moriyama performed neurological examination and revised the manuscript.

Carlos Eduardo Steiner planned the work, performed clinical diagnosis, provided clinical care and follow-up of the patients, and revised the manuscript.

References

Amess P, Chong WK, Kirkham FJ (1998) Acquired spinal cord lesion associated with os odontoideum causing deterioration in dystonic cerebral palsy: case report and review of the literature. Dev Med Child Neurol 40(3):195–198

Bagshaw RD, Zhang S, Hinek A et al (2002) Novel mutations (Asn 484 Lys, Thr 500 Ala, Gly 438 Glu) in Morquio B disease. Biochim Byophy Acta 1588:247–253

Baptista MB (2013) Mutation analysis in *GLB1* gene in patients with GM1 Gangliosidosis, juvenile and chronic types [dissertation]. Campinas (BR): School of Medical Sciences, University of Campinas (Unicamp).

Brunetti-Pierri N, Scaglia F (2008) GM1 gangliosidosis: review of clinical, molecular and therapeutic aspects. Mol Genet Metab 94:391–396

Giugliani R, Jackson M, Skinner SJ et al (1987) Progressive mental regression in siblings with Morquio disease type B (mucopolysaccharidosis IV B). Clin Genet 32(5):313–325

Hofer D, Paul K, Fantur K et al (2010) Phenotype determining alleles in GM1 gangliosidosis patients bearing novel GLB1 mutations. Clin Genet 78:236–246

Muthane U, Kaneski C, Shankar SK et al (2004) Clinical features of adult GM1 Gangliosidosis: report of three Indian patients and review of 40 cases. Movement Disord 19(11):1334–1341

Paschke E, Milos I, Kreimer-Erlacher H et al (2001) Mutation analyses in 17 patients with deficiency in acid beta-galactosidase: three novel point mutations and high correlation of mutation W273L with Morquio disease type B. Hum Genet 109(2): 159–166

Roze E, Paschke E, Lopez N et al (2005) Dystonia and Parkinsonism in GM1 type 3 gangliosidosis. Movement Disord 20(10): 1366–1369

Rozzelle CJ, Aarabi B, Dhall SS et al (2013) Os odontoideum. Neurosurgery 72(Suppl 2):159–169

Santamaria A, Chabás A, Coll MJ et al (2006) Twenty-one novel mutations in the GLB1 gene identified in a large group of GM1-gangliosidosis and Morquio B patients: possible common origin for the prevalent p.R59H mutation among gypsies. Hum Mutat 922:1–11

Santamaria R, Chabas A, Callahan JW et al (2007) Expression and characterization of 14 GLB1 mutant alleles found in GM1-gangliosidosis and Morquio B patients. J Lipid Res 48: 2275–2282

Severini MH, Silva CD, Sopelsa A et al (1999) High frequency of type 1 GM1-gangliosidosis in southern Brazil. Clin Genet 56:168

Sperb F, Vairo F, Burin M (2013) Genotypic and phenotypic characterization of Brazilian patients with GM1 gangliosidosis. Gene 512(1):113–116

Suzuki Y, Nanba E, Matsuda J et al (2014) β-Galactosidase deficiency (β-galactosidosis): GM1 gangliosidosis and morquio B disease. In: Valle D, Beaudet AL, Vogelstein B, Kinzler KW, Antonarakis SE, Ballabio A, Gibson K, Mitchell G (eds) OMMBID-the online metabolic and molecular bases of inherited diseases. McGraw-Hill, New York

Wong AS, Massicotte EM, Fehlings MG (2005) Surgical treatment of cervical myeloradiculopathy associated with movement disorders: indications, technique, and clinical outcome. J Spinal Disord Tech 18(Suppl S):107–114

Yoshida K, Oshima A, Sakubara H et al (1992) GM1 gangliosidosis in adults: clinical and molecular analysis of 16 Japanese patients. Ann Neurol 319(3):328–332

JIMD Reports
DOI 10.1007/8904_2015_452

RESEARCH REPORT

High Incidence of Serologic Markers of Inflammatory Bowel Disease in Asymptomatic Patients with Glycogen Storage Disease Type Ia

Nicole T. Lawrence • Tayoot Chengsupanimit • Laurie M. Brown • David A. Weinstein

Received: 05 March 2015 / Revised: 09 April 2015 / Accepted: 23 April 2015 / Published online: 21 June 2015

Abstract Most patients with glycogen storage disease (GSD) type Ib show features related to inflammatory bowel disease (IBD). The development of IBD seems to be associated with the defect of neutrophil function in GSD Ib. Patients with GSD Ia were not recognized to have similar gastrointestinal complaints until recently and are not associated with a neutrophil defect. Fifty consecutive GSD Ia inpatients over the age of 2 years without a diagnosis of IBD were screened using serologic and genetic markers via the Prometheus IBD sgi Diagnostic test. Eleven patients were tested positive for IBD (22%), with five fitting the pattern for Crohn's disease, five for ulcerative colitis, and one with nonspecific IBD. Only 2 out of the 11 patients had any gastrointestinal complaints. No pattern could be distinguished from individual inflammatory markers, genetics, inflammation antibodies, age, complications, or metabolic control. Of note, 9 out of 11 patients testing positive were female. Patients with GSD Ia were found to have a higher rate of serologically indicated IBD when compared with the general population. While these subjects will need to be followed to determine if these serologic markers correlate with clinical disease, this study supports that IBD may be more common in the GSD Ia population. Further studies are warranted to explain the relationship between IBD and GSD I since it may provide clues regarding the pathogenesis of IBD development in the general population.

Communicated by: Gerard T. Berry, M.D.

Competing interests: None declared

N.T. Lawrence
Division of Pediatric Gastroenterology, Department of Pediatrics, University of Florida College of Medicine, Gainesville, FL, USA

T. Chengsupanimit · L.M. Brown · D.A. Weinstein (✉)
Glycogen Storage Disease Program, Division of Pediatric Endocrinology, Department of Pediatrics, University of Florida College of Medicine, PO Box 100296, Gainesville, FL 32610-0296, USA
e-mail: weinsda@peds.ufl.edu

Background

Glycogen storage disease type Ia (GSD Ia; OMIM 232200) is an autosomal recessive disorder of glycogen metabolism that affects approximately 1 in 100,000 live births (Chen 2001). Mutations of the genes that encode glucose-6-phosphatase (subtype Ia) and glucose-6-phosphate translocase (subtype Ib) have been isolated (Lei et al. 1993, 1995). Diagnosis is suspected in infants with fasting hypoglycemia, lactic acidosis, hyperlipidemia, and hepatomegaly. Other complications include hepatic adenomas, growth retardation, osteoporosis, and nephropathy. GSD Ib is similar to GSD Ia with the added features of neutropenia and phagocyte dysfunction (Gitzelmann and Bosshard 1993). Without immediate recognition of symptoms and appropriate treatment, GSD can be fatal in infancy. Fortunately, much success has been achieved in the management of GSD as blood glucose levels can be sustained with cornstarch and overnight nasogastric feeds (Wolfsdorf and Crigler 1997, 1999). However, the improved mortality rates have been offset by an increase in morbidity as patients reach older ages.

Roe et al. (1986) first described an association between inflammatory bowel disease (IBD) and GSD Ib. Since that time, there have been continued investigations on the causal relationship of these two conditions (Melis et al. 2003). Historically, neutropenia has been used to explain the almost universal development of GSD enterocolitis in patients with GSD Ib. Surprisingly, treatment with granulocyte colony-stimulating factor has led to an improvement of

the symptoms of IBD, but has not resulted in the resolution of the disease (Visser et al. 2002). It is published that up to 77% of GSD Ib patients have serologically, histologically, and clinically confirmed IBD (Visser et al. 2000). A prospective study of 19 asymptomatic patients with GSD Ib also found that 89% of the subjects had elevated anti-CBir1 concentrations and serologic studies consistent with IBD (Davis et al. 2010). Until recently, there have been no definitive connections made between IBD and other types of GSD.

We have recently found a cohort of GSD Ia patients that are endoscopically and/or histologically confirmed to have either enteritis or colitis, two of which had characteristics of Crohn's disease (CD) and three with disease most consistent with ulcerative colitis (UC) (Lawrence et al. 2014). As mentioned previously, IBD in patients with GSD Ib is typically attributed to functional deficiency in neutrophils. However to date, GSD Ia is rarely associated with a quantitative or qualitative defect of neutrophils.

The aim of this study was to determine if there is a genetic or serologic predisposition of patients with GSD Ia to develop IBD.

Methods

Blood samples were obtained from 50 consecutive inpatients with GSD Ia who qualified for the study and did not already have a diagnosis of IBD at UF Health Shands Hospital between January 2014 and October 2014. Informed consent was obtained from all participants to confirm they understood how their sample would be used in an IBD panel. Study protocols conformed to ethical guidelines and was approved by the University of Florida Institutional Review Board (IRB201300312).

This is an observational, nonrandomized prevalence study of patients diagnosed with GSD Ia who did not manifest symptoms of IBD. The Prometheus IBD sgi Diagnostic test (Prometheus Laboratories, San Diego, CA) was used to predict and differentiate IBD based on an algorithm combining serologic, genetic, and inflammatory markers. The serologic markers include antibodies against yeast (ASCA-IgA and –IgG), antibodies against bacteria (Anti-OmpC, Anti-CBir1, Anti-Fla-X, and Anti-A4-Fla2), and autoantibodies (ANCA, pANCA, and DNase-sensitive ANCA). Genetic markers include *ATG16L1*, *NKX2-3*, *STAT3*, and *ECM1*. These are associated with autophagy, cell type specification and differentiation, signal transduction, and the extracellular matrix, respectively. Inflammatory markers include ICAM-1, VCAM-1, VEGF, CRP, and SAA.

To ensure appropriate statistical power, 50 patients were recruited as the total cohort. Means and standard deviations were used to analyze the continuous data. Frequency tables were used to summarize categorical data.

Results

Out of 50 total participants in the study, 11 tested positive for IBD. Five had a pattern consistent with Crohn's disease, five had a pattern consistent with ulcerative colitis, and one had nonspecific IBD. Our prevalence rate is thus 22% within this cohort.

Of note, 9 out of 11 patients testing positive for IBD were female. Sex and panel result were not independent ($\chi^2 = 11.22$, $p = 0.007$). For all other individual variables (age, antibody assays, genetics/genotype, inflammatory markers), either no pattern was discovered or there was no significant difference between patients testing positive for IBD and patients testing negative for IBD (Fig. 1, Table 1). The same patients testing positive do not seem to show a higher complication rate or less optimal metabolic control than the patients testing negative.

Discussion

The management of GSD has markedly improved over the past 40 years. While survival was rare prior to the 1970s, most patients with GSD Ia and Ib are now doing well into adulthood (Rake et al. 2002; Visser et al. 2000). With aging, long-term complications have been appreciated, including the development of hepatic adenomas (Beegle et al. 2015), hepatocellular carcinomas (Limmer et al. 1988), osteoporosis (Minarich et al. 2012), and hepcidin-induced anemia (Wang et al. 2012). IBD may be a

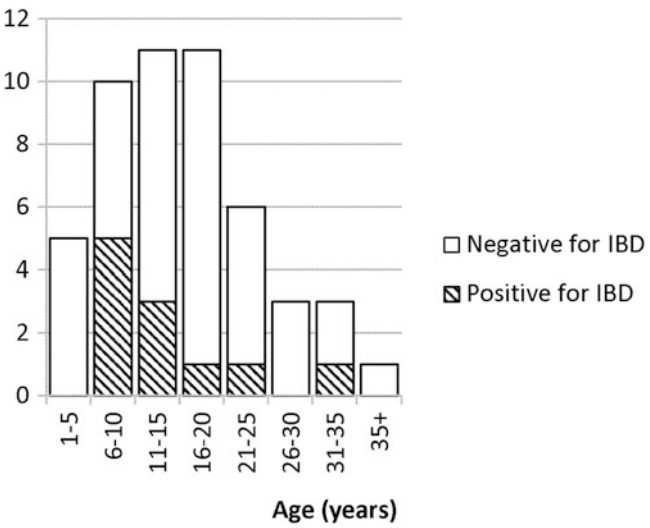

Fig. 1 Inflammatory bowel disease (IBD) panel result of patients by age

Table 1 Serological, genetic, and inflammatory markers of patients who tested positive for inflammatory bowel disease (IBD)

Patient		1	2	3	4	5	6	7	8	9	10	11
Sex		F	F	F	F	F	M	F	F	M	F	F
Age (year)		13	6	7	22	10	18	9	10	13	11	31
Diagnosis	CD	x					x	x	x			x
	UC			x	x	x				x	x	
	Inconclusive for CD vs. UC		x									
Serology	ASCA-IgA ELISA (EU/mL)	4.8	<3.1	<3.1	<3.1	<3.1	<3.1	<3.1	<3.1	<3.1	<3.1	6.1
	ASCA IgG ELISA (EU/mL)	4.8	<3.1	<3.1	12.3	<3.1	7.0	8.4	8.8	6.2	5.1	<3.1
	Anti-OmpC IgA ELISA (EU/mL)	5.0	3.7	<3.1	<3.1	<3.1	11.7	4.9	4.0	3.4	4.9	13.1
	Anti-CBir1 IgG ELISA (EU/mL)	>100.0	94.7	46.3	7.5	34.7	>100.0	>100.0	>100.0	40.0	21.5	63.7
	Anti-A4-Fla2 IgG ELISA (EU/mL)	77.7	55.9	91.9	8.8	48.5	76.6	79.8	36.8	11.9	22.6	82.9
	Anti-FlaX IgG ELISA (EU/mL)	>100.0	78.4	80.3	20.3	59.5	>100.0	>100.0	56.5	15.8	31.4	>100.0
	AutoAntibody ELISA (EU/mL)	18.6	22.1	29.4	34.4	53.0	23.7	6.7	<3.1	21.5	29.1	8.9
	IFA perinuclear pattern detected									x	x	
	DNAse sensitive									x	x	
Genetics	ATG16L1 (rs2241880)	G;G	A;A	G;A	G;G	G;A	G;G	A;G	A;A	G;G	A;A	A;G
	ECM1 (rs3737240)	C;C	C;C	T;C	C;C	T;T	C;C	C;C	C;C	C;T	C;C	C;T
	NKX2-3 (rs10883365)	A;A	A;A	G;G	G;G	G;G	A;G	G;G	G;G	G;G	A;A	A;G
	STAT3 (rs744166)	A;G	A;A	G;G	A;A	A;A	A;A	A;A	G;G	A;A	G;G	A;A
Inflammation	ICAM-1 (μg/mL)	0.47	0.43	0.70	0.55	0.46	0.59	0.45	0.46	0.42	0.66	0.39
	VCAM-1 (μg/mL)	0.52	0.53	1.19	0.40	0.57	0.84	0.45	0.59	0.71	0.68	0.51
	VEGF (pg/mL)	812	244	401	664	844	214	576	171	391	884	553
	CRP (mg/L)	0.3	0.4	1.2	20.9	1.6	8.4	1.9	0.6	0.2	16.4	12.5
	SAA (mg/L)	2.2	1.1	4.6	13.8	2.5	19.4	2.7	1.4	1.4	1.9	11.7

complication of GSD Ia that has been recently uncovered. Our 22% prevalence rate dramatically exceeds the incidence of IBD in the general adult population in the United States, which is 0.91% (Nguyen et al. 2014). A comparable study of pediatric IBD prevalence in Canada found values of 0.02% for ages 0–9 and 0.15% for ages 10–19 (Benchimol et al. 2014). While it seems that there was a trend toward children to test positive for IBD since 9 out of 11 patients were under 20 years old, we were unable to include some GSD Ia adults in this study because they already had a diagnosis of IBD.

While an association between GSD Ib and IBD is well recognized, there are few reports focusing on the presence of diarrhea in the GSD Ia patient and none have linked this symptom to IBD. Unlike in patients with GSD Ib, patients diagnosed with GSD Ia do not have neutropenia to explain this consequence. Patients seen at the University of Florida and managed with cornstarch have frequently complained of adverse gastrointestinal effects, namely, abdominal pain and diarrhea, as has been previously reported at other institutions (Grabitske and Slavin 2009). As such, a possible explanation for our findings is that the IBD is secondary to the effects of cornstarch on the gastrointestinal tract. Cornstarch creates an acidic environment. In general, when the stools of nonhuman subjects consuming diets high in cornstarch are analyzed, they typically demonstrate increased reducing substances and a decreased pH (Kotarski et al. 1992). These findings are consistent with carbohydrate malabsorption. Fermenting bacteria in the colon are responsible for metabolizing carbohydrates that are not absorbed in the small intestine into short-chain fatty acids (SCFA). As a result, these SCFA are absorbed throughout the colon and, in addition, are involved in the reabsorption of water and sodium. The acidification of the stools leads to an alteration in the amount of fermenting bacteria, and thus there is decreased conversion of unabsorbable starches to SCFA. This can lead to significant diarrhea (Treem et al. 1996). While cornstarch may be involved in the pathogenesis of IBD development in GSD I, IBD has not been recognized in other types of GSD which also use this therapy. However, other types of GSD do not have doses of cornstarch therapy as high as in type I. We also have not yet seen a difference between uncooked cornstarch and the slow-release hydrothermally processed cornstarch which has become more popular for overnight use.

A second possible explanation for the development of IBD is that the underlying enzyme defect in GSD causes abnormalities that predispose to the development of IBD. Glucose-6-phosphatase is known to be present in the small intestine, but the function of the intestinal enzyme has not been elucidated. Davis et al. linked antibodies to CBir-1 to all the patients with GSD Ib who have IBD (Davis et al. 2010). The finding is significant because CBir-1 antibodies are found in 50% of all patients with Crohn's disease and more prevalent in small bowel disease. In contrast to the GSD Ib population, colonic disease predominated in the GSD Ia population when compared with the GSD Ib population. This supports that the intestinal abnormality alone is not sufficient to cause the disease. The role of the intestinal defect will likely be elucidated by the studies in the intestinal glucose-6-phosphatase knockout mouse model (Rajas et al. 2014).

A third possibility is that the development of IBD is not directly related to GSD, but instead occurs due to a genetic or epigenetic predisposition of both diseases in certain populations. For example, the Ashkenazi Jewish population has a carrier rate of 1 in 72 for GSD, and this population also has a high risk of IBD (Ekstein et al. 2004). The strongest evidence for a genetic cause of IBD may be found in the human studies of twins (Halfvarson et al. 2003). Patients of Jewish descent are up to four times more likely to develop the disease. Moreover, it has been estimated that the rate of developing IBD is 20 times more likely in first degree relatives of Jewish patients with IBD (Yang et al. 1993). Several of the patients in this cohort carried the classic Jewish mutation for GSD Ia, placing them at higher risk at baseline for developing IBD. While this genetic predisposition should be considered, not all of the patients had Jewish heritage or the mutation associated with this population which supports that this indeed is a complication of GSD.

While the rate of positivity was markedly higher in the GSD population when compared with the general population, it is important to note that there are significant drawbacks to the Prometheus IBD sgi Diagnostic test as outlined previously: three of the least expensive and most available components may account for the entire predictive value of the test, and routine laboratory tests may have higher predictive values (Benor et al. 2010; Shirts et al. 2012). In addition, no endoscopies were performed to confirm the diagnosis of IBD on the patients who tested positive on the IBD panel because they were subclinical, and ethically the risk of the procedure was deemed too high. In GSD, endoscopies are not benign and require the patient to be admitted to the hospital in advance of the procedure to maintain glucose concentrations during the cleanout. During the procedure itself, crises can occur if the patient experiences excessive stress due to increased metabolic load or if the glucose infusion is interrupted. These patients should continue to be followed in the future to determine if they eventually develop IBD.

Conclusions

In light of finding an increased rate of serologic IBD in the GSD Ia population, it is clear that further research is needed

to characterize the relationship between IBD and GSD I. If patients testing positive for IBD develop clinical manifestations of the disease, the confirmation of a higher rate of IBD in GSD Ia may provide important clues to the pathogenesis of IBD in the general population.

Acknowledgment We would like to thank the following nurses of the Clinical Research Center for their assistance: Charles J. Church, Emma B. Labrador, Dorothy G. Nichols, and Elizabeth A. Potocik. This research was supported by philanthropic support provided by the following funds managed through the University of Florida Office of Development: the GSD Ia Research Fund and Charlotte's Cure for Type Ia GSD. This work was also supported in part by the NIH/NCATS Clinical and Translational Science Award UL1 TR000064 granted to the University of Florida. Prometheus Laboratories provided the serological testing used in this study.

Synopsis

Serologic panels suggest inflammatory bowel disease may be a new complication of glycogen storage disease type Ia.

Compliance with Ethics Guidelines

Conflict of Interest

The authors declare that they have no conflict of interest.

Informed Consent

All procedures followed were in accordance with the ethical standards of the responsible committee on human experimentation (institutional and national) and with the Helsinki Declaration of 1975, as revised in 2000. Informed consent was obtained from all patients for being included in the study. The study was approved by the University of Florida Institutional Review Board (IRB201300312).

Details of the Contributions of Individual Authors

NL and DW conceived of and participated in the design of the study. NL, TC, and LB recruited participants for the study. TC performed the data collection and statistical analysis. NL and TC co-drafted the manuscript and LB and DW provided critical review. All authors read and approved the final manuscript.

References

Beegle RD, Brown LM, Weinstein DA (2015) Regression of hepatocellular adenomas with strict dietary therapy in patients with glycogen storage disease type I. JIMD Rep 18:23–32

Benchimol EI, Manuel DG, Guttmann A, Nguyen GC, Mojaverian N, Quach P, Mack DR (2014) Changing age demographics of inflammatory bowel disease in Ontario, Canada: a population-based cohort study of epidemiology trends. Inflamm Bowel Dis 20(10):1761–1769

Benor S, Russell GH, Silver M, Israel EJ, Yuan Q, Winter HS (2010) Shortcomings of the inflammatory bowel disease Serology 7 panel. Pediatrics 125(6):1230–1236

Chen Y-T (2001) Glycogen storage diseases. In: Scriver CR, Beaudet AL, Sly WS, Valle D (eds) The metabolic and molecular bases of inherited disease, 8th edn. McGraw-Hill, New York, pp 1521–1551

Davis MK, Valentine JF, Weinstein DA, Polyak S (2010) Antibodies to CBir1 are associated with glycogen storage disease type Ib. J Pediatr Gastroenterol Nutr 51(1):14–18

Ekstein J, Rubin BY, Anderson SL et al (2004) Mutation frequencies for glycogen storage disease Ia in the Ashkenazi Jewish population. Am J Med Genet A 129A(2):162–164

Gitzelmann R, Bosshard NU (1993) Defective neutrophil and monocyte functions in glycogen storage disease type Ib: a literature review. Eur J Pediatr 152(Suppl 1):S33–S38

Grabitske HA, Slavin JL (2009) Gastrointestinal effects of low-digestible carbohydrates. Crit Rev Food Sci Nutr 49(4):327–360

Halfvarson J, Bodin L, Tysk C, Lindberg E, Järnerot G (2003) Inflammatory bowel disease in a Swedish twin cohort: a long-term follow-up of concordance and clinical characteristics. Gastroenterology 124(7):1767–1773

Kotarski SF, Waniska RD, Thurn KK (1992) Starch hydrolysis by the ruminal microflora. J Nutr 122(1):178–190

Lawrence NT, Chengsupanimit T, Brown LM, Derks TG, Smit GP, Weinstein DA (2014) Inflammatory bowel disease in glycogen storage disease type Ia: a case series. J Pediatr Gastroenterol Nutr. doi:10.1097/MPG.0000000000000592

Lei KJ, Shelly LL, Pan CJ, Sidbury JB, Chou JY (1993) Mutations in the glucose-6-phosphatase gene that cause glycogen storage disease type Ia. Science 262(5133):580–583

Lei KJ, Shelly LL, Lin B et al (1995) Mutations in the glucose-6-phosphatase gene are associated with glycogen storage disease types Ia and IaSP but not Ib and Ic. J Clin Invest 95(1):234–240

Limmer J, Fleig WE, Leupold D, Bittner R, Ditschuneit H, Beger HG (1988) Hepatocellular carcinoma in type I glycogen storage disease. Hepatology 8(3):531–537

Melis D, Parenti G, Della Casa R et al (2003) Crohn's-like ileo-colitis in patients affected by glycogen storage disease Ib: two years' follow-up of patients with a wide spectrum of gastrointestinal signs. Acta Paediatr 92(12):1415–1421

Minarich LA, Kirpich A, Fiske LM, Weinstein DA (2012) Bone mineral density in glycogen storage disease type Ia and Ib. Genet Med. doi:10.1038/gim.2012.36

Nguyen GC, Chong CA, Chong RY (2014) National estimates of the burden of inflammatory bowel disease among racial and ethnic groups in the United States. J Crohns Colitis 8(4):288–295

Rajas F, Clar J, Gautier-Stein A, Mithieux G (2014) Lessons from new mouse models of glycogen storage disease type 1a in relation to the time course and organ specificity of the disease. J Inherit Metab Dis. doi:10.1007/s10545-014-9761-0

Rake JP, Visser G, Labrune P, Leonard JV, Ullrich K, Smit GP (2002) Glycogen storage disease type I: diagnosis, management, clinical course and outcome. Results of the European Study on Glycogen Storage Disease Type I (ESGSD I). Eur J Pediatr 161(Suppl 1): S20–S34

Roe TF, Thomas DW, Gilsanz V, Isaacs H Jr, Atkinson JB (1986) Inflammatory bowel disease in glycogen storage disease type Ib. J Pediatr 109(1):55–59

Shirts B, von Roon AC, Tebo AE (2012) The entire predictive value of the Prometheus IBD sgi diagnostic product may be due to the

three least expensive and most available components. Am J Gastroenterol 107(11):1760–1761

Treem WR, Ahsan N, Kastoff G, Hyams JS (1996) Fecal short-chain fatty acids in patients with diarrhea-predominant irritable bowel syndrome: in vitro studies of carbohydrate fermentation. J Pediatr Gastroenterol Nutr 23(3):280–286

Visser G, Rake JP, Fernandes J et al (2000) Neutropenia, neutrophil dysfunction, and inflammatory bowel disease in glycogen storage disease type Ib: results of the European Study on Glycogen Storage Disease type I. J Pediatr 137(2):187–191

Visser G, Rake JP, Labrune P et al (2002) Granulocyte colony-stimulating factor in glycogen storage disease type 1b. Results of the European Study on Glycogen Storage Disease Type 1. Eur J Pediatr 161(Suppl 1):S83–S87

Wang DQ, Carreras CT, Fiske LM, Austin S, Boree D, Kishnani PS, Weinstein DA (2012) Characterization and pathogenesis of anemia in glycogen storage disease type Ia and Ib. Genet Med 14(9):795–799

Wolfsdorf JI, Crigler JF Jr (1997) Cornstarch regimens for nocturnal treatment of young adults with type I glycogen storage disease. Am J Clin Nutr 65(5):1507–1511

Wolfsdorf JI, Crigler JF Jr (1999) Effect of continuous glucose therapy begun in infancy on the long term clinical course of patients with type I glycogen storage disease. J Pediatr Gastroenterol Nutr 29 (2):136–143

Yang H, McElree C, Roth MP, Shanahan F, Targan SR, Rotter JI (1993) Familial empirical risks for inflammatory bowel disease: differences between Jews and non-Jews. Gut 34(4):517–524